



universität
wien

DISSERTATION

Titel der Dissertation

„Microbial biogeography, carbon degradation, and temperature adaptation: Insights from ecological studies of sulfate-reducing microorganisms in marine sediments“

verfasst von

Mag. Albert Leopold Müller

angestrebter akademischer Grad

Doctor of Philosophy (PhD)

Wien, 2015

Studienkennzahl lt. Studienblatt: A 094 437

Dissertationsgebiet lt. Studienblatt: Biologie

Betreut von: Assoz. Prof. Dipl.-Biol. Dr. Alexander Loy

Table of contents

Chapter I	Introduction	5
Chapter II	Overview of publications/manuscripts	17
Chapter III	Phylogenetic and environmental diversity of DsrAB-type dissimilatory (bi)sulfite reductases	21
Chapter IV	Bacterial community response during degradation of cyanobacterial biomass and acetate in a sulfate-reducing Arctic fjord sediment	67
Chapter V	Endospores of thermophilic bacteria as tracers of microbial dispersal by ocean currents	97
Chapter VI	Activity and community structures of sulfate-reducing microorganisms in polar, temperate and tropical marine sediments	129
Chapter VII	Concluding discussion	153
Chapter VIII	Summary & Zusammenfassung	163
Appendix	Acknowledgements & Curriculum Vitae	169

Chapter I

Introduction

Introduction

Studying the diversity and activity of microorganisms is the core of microbial ecology research. Microorganisms interact with each other and the environment to form complex communities that are able to perform an enormous range of biochemical processes and populate virtually every imaginable habitat on Earth. How microbial communities generate and maintain their diversity is a complex and endlessly fascinating question. Trying to answer it is not only scientifically compelling but also essential for facing major challenges of modern civilization, such as the management of natural ecosystems, the achievement of sustainable agriculture and energy generation, and the mitigation of climate change. In order to get a grasp of the ecology of microorganisms it helps to subdivide microorganisms into groups defined by their function. During my thesis I focused my research on the functional guild of sulfate-reducing microorganisms (SRM) and used this group as a model to examine how passive dispersal, temperature, and defined substrate input impact the composition of microbial communities in marine sediments.

A primer to sulfate-reducing microorganisms

SRM are anaerobic organisms that are ubiquitous in anoxic habitats and at oxic-anoxic interfaces, where they fulfill an important role in the biochemical cycling of sulfur and carbon (Figure 1) (reviewed in Muyzer and Stams, 2008). By using sulfate as terminal electron acceptor in the degradation of organic compounds, they reduce sulfur from an oxidation state of +6 to -2. SRM are of great importance for the oxidation of organic carbon in anoxic habitats where sulfate is available (Pester *et al.*, 2012; Bowles *et al.*, 2014), for example in marine sediments, where sulfate reduction is the primary terminal step in the mineralization of organic matter (Jørgensen, 1982). SRM mainly use the major end-products of fermentation (e.g. acetate, propionate, lactate, butyrate, and hydrogen) as carbon and energy sources (Sørensen *et al.*, 1981; Christensen, 1984; Parkes *et al.*, 1989). However, a great variety of additional substrates are also used by different SRM, ranging from sugars, amino acids, one-carbon compounds, aromatic hydrocarbons to alkanes and alkenes (Muyzer and Stams, 2008). Generally, polymers (e.g. proteins, nucleic acids, lipids, and polysaccharides) are not directly utilized by SRM. Instead, they are usually dependent on other microorganisms to hydrolyze these polymeric substrates and ferment them to suitable substrates (Figure 1). Many organisms are able to reduce sulfate during the assimilation of sulfur into sulfur-containing amino acids, but the ability to use sulfate for dissimilatory energy generation, during which the reduced sulfur is not only assimilated but excreted as hydrogen sulfide, is restricted to certain members of a limited number of bacterial and archaeal phyla. So far, the ability for dissimilatory sulfate reduction has been found in the bacterial phyla *Proteobacteria*, *Firmicutes*, *Nitrospirae*, and *Thermodesulfobacteria* and the archaeal phyla *Euryarchaeota* and *Crenarchaeota*.

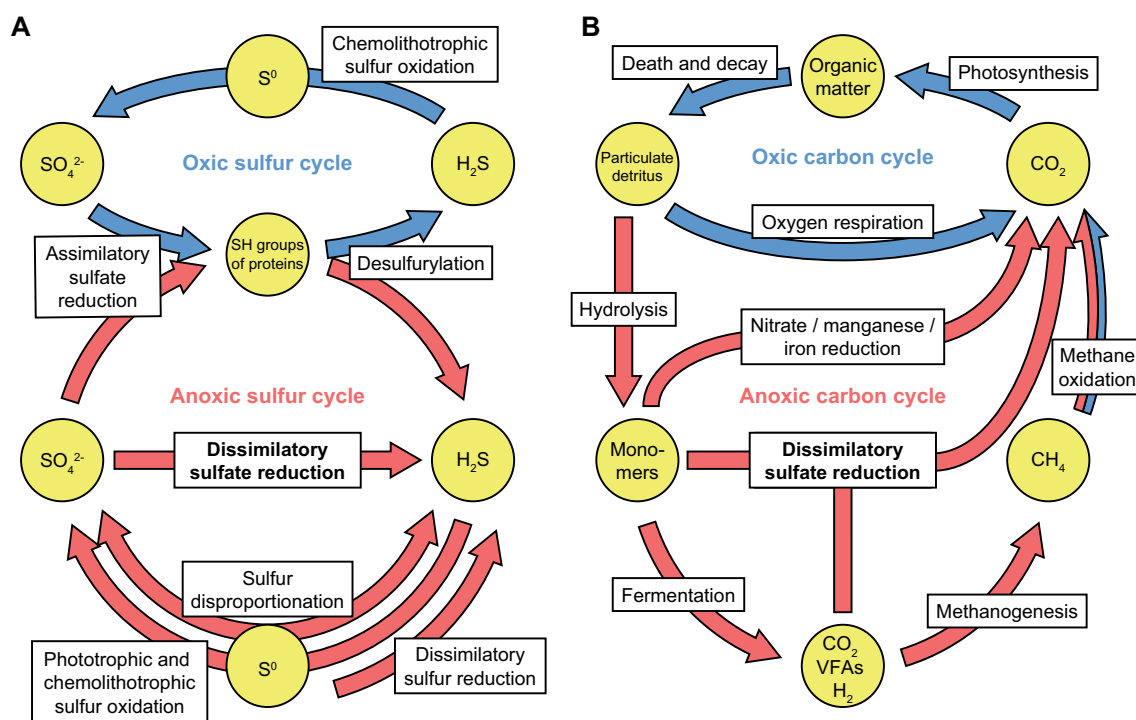


Figure 1. Biochemical cycling of sulfur (A) and carbon (B). A simplified representation highlighting the central position of dissimilatory sulfate reduction in the anoxic part of the sulfur and carbon cycle. SRM use sulfate (SO_4^{2-}) for the oxidation of organic carbon degradation intermediates (e.g. monomers such as amino acids, sugars, and fatty acids), volatile fatty acids (VFAs), and hydrogen (H_2), thereby producing hydrogen sulfide (H_2S) and carbon dioxide (CO_2). CH_4 , methane; S^0 , elemental sulfur.

DsrAB as a phylogenetic marker for SRM?

The phylogenetic heterogeneity of SRM does not allow for easy identification of SRM by using typical phylogenetic marker genes such as the 16S rRNA gene. Therefore, the genes coding for the dissimilatory (bi)sulfite reductase (DsrAB) are commonly used as functional markers for SRM (Wagner *et al.*, 2005). DsrAB catalyzes the reduction of sulfite to sulfide, which is the main energy-conserving step during the dissimilatory reduction of sulfate (Figure 2). DsrAB phylogeny closely reflects phylogenetic relationships reconstructed with 16S rRNA gene sequences, except for a few cases of putative lateral gene transfer among major taxa (Klein *et al.*, 2001; Zverlov *et al.*, 2005; Loy *et al.*, 2009). A disadvantage of using *dsrAB* as functional markers for SRM is the fact that they can also be present in some sulfite-reducing, sulfur-disproportionating, and organosulfonate-utilizing microorganisms (Finster, 2008; Devkota *et al.*, 2012; Simon and Kroneck, 2013), as well as in anaerobic syntrophs that are incapable of reducing sulfite, sulfate or organosulfonates (Brauman *et al.*, 1998; Imachi *et al.*, 2006), all of which are phylogenetically related to SRM. DsrAB is also present in some sulfur-oxidizing bacteria, where it catalyzes the reverse reaction during sulfide oxidation, but the oxidative type of *dsrAB* is phylogenetically clearly distinguishable from the reductive type (Molitor *et al.*, 1998; Zverlov *et al.*, 2005; Loy *et al.*, 2009). Another potential caveat is that some

SRM may employ a DsrAB-independent pathway for sulfate reduction that is yet biochemically and genetically unresolved, but was suggested to operate in a syntrophic microbial consortium that mediated the anaerobic oxidation of methane coupled to sulfate reduction and polysulfide disproportionation (Milucka *et al.*, 2012; Milucka *et al.*, 2013). However, of the three key enzymes in the canonical dissimilatory sulfate reduction pathway (Figure 2), DsrAB genes are the most suitable genetic markers, since the ATP sulfurylase is also present in assimilatory sulfate reducers (Lengeler *et al.*, 1999), whereas the APS reductase, which is also present in sulfur-oxidizing bacteria (Hipp *et al.*, 1997), was possibly impacted by more lateral gene transfer events than *dsrAB* (Friedrich, 2002; Meyer and Kuever, 2007).

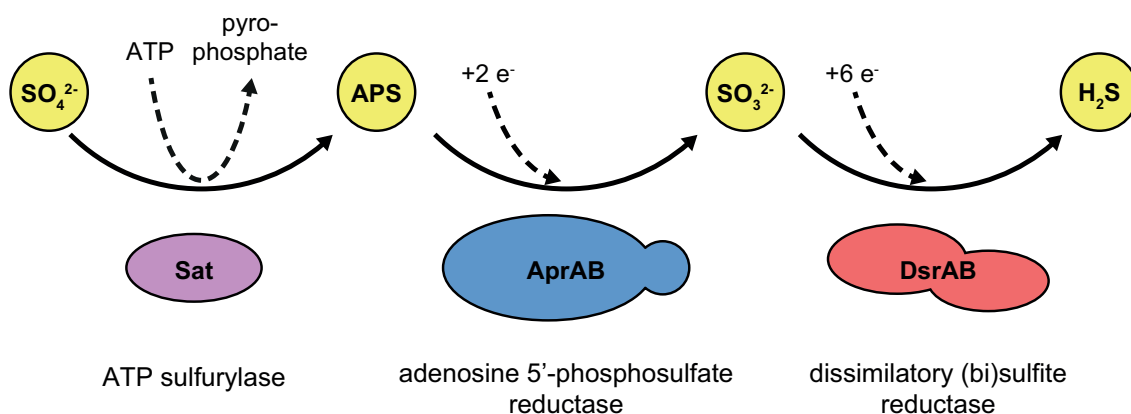


Figure 2. The canonical pathway of dissimilatory sulfate reduction. The ATP sulfurylase (Sat) activates sulfate (SO_4^{2-}) with ATP to form adenosine 5'-phosphosulfate (APS), the adenosine 5'-phosphosulfate reductase (Apr) reduces APS to sulfite (SO_3^{2-}), which in turn is reduced by the dissimilatory (bi)sulfite reductase (Dsr) to hydrogen sulfide (H_2S).

DsrAB is a heterotetrameric protein with an $\alpha_2\beta_2$ structure that possesses iron-sulfur clusters and siroheme prosthetic groups (Dahl *et al.*, 1993). Since DsrAB is conserved in bacteria and archaea and its phylogeny is congruent with 16S rRNA phylogeny, it is considered to be an evolutionary ancient enzyme that might have been present even before the separation of the domains *Bacteria* and *Archaea* and might have played a fundamental role in the metabolism of some of the first microorganisms living in the anoxic, reduced atmosphere environments of the primordial Earth (Wagner *et al.*, 1998; Canfield and Raiswell, 1999; Dhillon *et al.*, 2005). Sequencing of *dsrAB* of microbial communities from many different environments has led to the discovery of an extensive hidden diversity of *dsrAB* sequences not closely related to *dsrAB* from any cultivated organisms. Because the currently available set of environmental *dsrAB* sequences is largely uncharacterized and because next generation sequencing techniques provide opportunities for large-scale alpha- and beta-diversity studies of *dsrAB*, one of the main goals of this thesis was to compile a reference database and to establish a comprehensive classification framework for streamlined computational analyses of *dsrAB* sequences. This database was made publically available and was used for systematic classification and quantification of the known *dsrAB* sequence diversity across various environments and for the evaluation of all published *dsrAB*-targeted primers. Results of the

characterization of the phylogenetic and environmental diversity of DsrAB enzymes are presented in chapter III.

Ecophysiology of psychrophiles: carbon degradation in Arctic marine sediments

Arctic marine sediments are characterized by permanently cold temperatures. Since over 70% of the Earth's surface is covered by oceans and 90% of the sea floor has temperatures below 4°C (Levitus and Boyer, 1994), permanently cold marine sediments are one of the largest microbial ecosystems on our planet. Psychrophilic microorganisms are able to thrive at low temperatures and survive and even maintain metabolic activity at subzero temperatures (reviewed in Margesin and Miteva, 2011). Unique features in their proteins, membranes and genetic responses (reviewed in Deming, 2002) allow cold-adapted microorganisms to be physiologically and ecologically successful in cold environments. Microbial activity in permanently cold habitats has been found to be comparable to the activity in temperate and even tropical environments at ambient temperature (Nedwell *et al.*, 1993; Rivkin *et al.*, 1996; Arnosti *et al.*, 1998; Glud *et al.*, 1998; Sagemann *et al.*, 1998). However, in temperate environments microbial activity is commonly found to be lower during cold seasons (reviewed in Rivkin *et al.*, 1996) and mesophiles predominate even in winter, possibly because psychrophiles grow too slowly to develop a winter community even if they would be better adapted during the cold season (Robador *et al.*, 2009).

Microbial activity in marine sediments is fuelled by gradual degradation and respiration of organic material that reaches the seafloor (reviewed in Arndt *et al.*, 2013). Briefly, extracellular enzymes of hydrolytic bacteria break down polymeric macromolecules into monomers, fermentative bacteria subsequently use these monomers and produce a broad range of fermentation products that are finally mineralized to carbon dioxide (Figure 1). Carbon degradation in Arctic marine sediments has been studied extensively on a functional level, e.g. by determining rates of hydrolysis, sulfate reduction, or denitrification (Rysgaard *et al.*, 2004; Arnosti *et al.*, 2005; Arnosti and Jørgensen, 2006; Finke *et al.*, 2007) and some efforts have been taken to characterize the sulfate-reducing community in Arctic marine sediments (Knoblauch *et al.*, 1999; Sahm *et al.*, 1999; Ravensschlag *et al.*, 2000). However, in order to understand how carbon compounds are degraded in Arctic marine sediments, it is necessary to directly link specific organisms to the processes that they perform. So far, the identities and activities of members of the psychrophilic microbial food chains are for the most part unknown.

In order to link identities of microorganisms to their function in carbon degradation in Arctic marine sediments, we performed anoxic incubations of a Svalbard fjord sediment with stable isotope-labeled substrates. We used ¹³C-labeled acetate as a substrate to selectively target SRM, as acetate was shown to be the most important electron donor accounting for up to 40% of sulfate reduction in this sediment (Finke *et al.*, 2007), and ¹³C-labeled freeze dried spirulina as a complex substrate in order to track its degradation, which likely involves a broad range of functionally interdependent microorganisms. Chapter IV summarizes the results from this incubation experiment based on data from bacterial 16S rRNA gene and cDNA amplicon pyrosequencing, as well as sulfate reduction and volatile fatty acid measurements.

Biogeography of thermophiles: distribution of dormant endospores in marine sediments

While the presence of cold-adapted microorganism in Arctic marine sediments is hardly surprising, the presence of thermophilic microorganisms in permanently cold sediments seems less intuitive. Nevertheless, thermophilic microbes have repeatedly been isolated from cold marine sediments (Egerova, 1938; McBee and McBee, 1956; Bartholomew and Paik, 1966; Lee *et al.*, 2005). During temperature gradient incubations of cold marine sediments from Aarhus Bay, Isaksen *et al.* (1994) discovered high numbers of thermophilic SRM that showed maximum rates of sulfate reduction at ~60°C. Similar temperature profiles were also found in Arctic marine sediments, for example in sediment of Smeerenburgfjorden, Svalbard (Hubert *et al.*, 2009) (Figure 3A). The disappearance of the psychrophilic, but not the thermophilic SRM community after pasteurization (Figure 3B) suggested that these SRM are present in the sediment as dormant spores that germinate and become active only after a significant increase in temperature. Vandieken *et al.* (2006) were able to isolate a member of these spore-forming SRM, the moderately thermophilic *Desulfotomaculum arcticum*, from Svalbard fjord sediment.

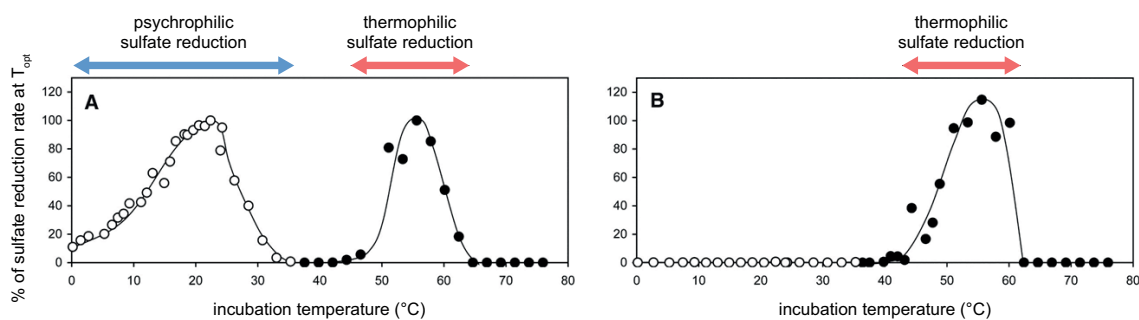


Figure 3. Sulfate reduction rates in temperature-gradient incubations with sediment from Smeerenburgfjorden, Svalbard (modified from Hubert *et al.*, 2009). Sediment was either untreated (A) or pasteurized for 1 hour at 80°C (B) prior to incubation. Two different temperature-activity profiles with temperature optima of 22°C and 56°C represent a psychrophilic (open circles) and a thermophilic (filled circles) SRM community, respectively.

The thermophilic endospore community present in cold marine sediments does not only consist of SRM, but represents a diverse population that, after spore germination induced by high temperature, mirrors the general metabolic potential of the microbial communities *in situ* (Hubert *et al.*, 2009; Hubert *et al.*, 2010). It catalyzes the degradation of organic matter via extracellular enzymatic hydrolysis, fermentation and sulfate reduction (Hubert *et al.*, 2010). Phylogenetically, these Arctic thermophiles were identified as members of the order *Clostridiales* (phylum *Firmicutes*) related to fermentative *Clostridiaceae* and sulfate-reducing *Desulfotomaculum* species (Hubert *et al.*, 2009; Hubert *et al.*, 2010; de Rezende *et al.*, 2013). These endospore formers presumably originate from warm, anoxic habitats that support their growth and arrive in cold marine sediments via passive transport and sedimentation. The supply of dormant endospores of thermophilic bacteria into permanently cold Arctic marine sediments of West Svalbard has been estimated to exceed 10^8 spores per square meter per year (Hubert *et al.*, 2009).

Since these endospores are assumed to be metabolically inert and can be easily selected for in high temperature germination experiments, they are natural indicators for studying the impact of passive dispersal on microbial biogeography. Microbial biogeography is a relatively new field of research, but the biogeographic patterns of microorganisms have recently gained considerable attention (reviewed in Foissner, 2006; Green and Bohannan, 2006; Lindstrom and Langenheder, 2012; Martiny *et al.*, 2006; Ramette and Tiedje, 2007). These patterns are shaped by a combination of four fundamental processes – selection, drift, dispersal, and mutation (Hanson *et al.*, 2012), but the influences of the individual factors are difficult to unravel. Surveying the distribution of endospores of thermophilic bacteria makes it possible to selectively investigate passive dispersal without the confounding influence of environmental selection. Any observed non-random spatial distribution patterns should be directly attributable to the influence of dispersal. There is still controversy regarding the existence of physical dispersal barriers for microorganisms. It was hypothesized that due to their large population sizes and short generation times microorganisms possess unlimited dispersal capabilities and that environmental factors (e.g. temperature, pH, substrate availability, competition) are the sole determinants of observed microbial distribution patterns (Baas Becking, 1934; Finlay, 2002; Fenchel and Finlay, 2004). However, evidence for dispersal limitation by geographic distance among microorganisms is mounting (Papke *et al.*, 2003; Whitaker *et al.*, 2003; Green *et al.*, 2004; Reche *et al.*, 2005; Martiny *et al.*, 2006; Ghiglione *et al.*, 2012; Sul *et al.*, 2013). Since bacterial endospores are metabolically inert, highly stress resistant, and able to survive unfavorable condition for long periods (Nicholson *et al.*, 2000), their dispersal represents an upper boundary for the dispersal capabilities of vegetative cells. This makes them an interesting model to investigate the existence of geographical dispersal barriers of microorganisms.

In order to investigate the biogeography of thermophilic endospores, marine sediment samples were collected from 81 globally distributed locations. We kept our focus on marine sediments from the Arctic with two regional sampling sets with higher spatial coverage: the Baffin Bay between Canada and Greenland and the archipelago of Svalbard. The sediment samples were subjected to high temperature incubations after pasteurization of the vegetative community of mesophilic or psychrophilic microorganisms. We monitored the germination and growth of thermophilic endospores by amplicon pyrosequencing of bacterial 16S rRNA gene amplicons and by measuring of sulfate reduction rates in order to analyze the richness, phylogeny, and distribution of endospores of thermophilic bacteria in marine sediments. Chapter V investigates whether thermophilic spores show signs of dispersal limitation and how local hydrography, sedimentation, and major ocean currents impact their distribution.

Temperature adaptation in marine sediments: activity and composition of SRM communities

In contrast to endospores of thermophilic bacteria, biogeographic patterns of vegetative cells are in large part shaped by environmental selection, as microorganisms that are best adapted to the prevailing environmental conditions will predominate (Prosser *et al.*, 2007). Temperature is one of the most important environmental factors for microorganisms, since it has a direct impact on their ecological and biochemical function by greatly influencing their metabolic rates. The rates of microbial sulfate reduction strongly correlate with changes in sediment temperature over short,

seasonal time scales (Jørgensen, 1977; Aller and Yingst, 1980; Moeslundi *et al.*, 1994; Kristensen *et al.*, 2000) and the thermal response of sulfate reduction seems to be related to metabolic temperature adaptations of SRM populations (Robador *et al.*, 2009; Sawicka *et al.*, 2012). Indeed, SRM at high latitudes in Arctic and Antarctic marine sediments were shown to be predominantly psychrophilic (Isaksen and Jørgensen, 1996; Sagemann *et al.*, 1998), whereas SRM in temperate sediments were shown to be mostly mesophilic (Isaksen *et al.*, 1994). In order to investigate the temperature-dependent distribution of SRM, we determined the thermal response and community composition of natural SRM communities in sediment samples from selected geographic regions with different prevailing temperatures. We explored how temperature controls the respiration rate in short-term thermal gradient incubation experiments and inferred the composition of the bacterial SRM community from presence of sequences related to known SRM lineages in 16S rRNA gene amplicon pyrosequencing libraries. Chapter VI presents our results of the temperature characterization of sulfate reduction and the diversity and co-localization analysis of putative SRM phylotypes in nine polar, temperate and tropical marine sediments.

References

- Aller R, Yingst J (1980). Relationships between microbial distributions and the anaerobic decomposition of organic matter in surface sediments of Long Island Sound, USA. *Mar Biol* **56**: 29-42.
- Arndt S, Jørgensen BB, LaRowe DE, Middelburg JJ, Pancost RD, Regnier P (2013). Quantifying the degradation of organic matter in marine sediments: A review and synthesis. *Earth-Sci Rev* **123**: 53-86.
- Arnosti C, Jørgensen BB, Sagemann J, Thamdrup B (1998). Temperature dependence of microbial degradation of organic matter in marine sediments: polysaccharide hydrolysis, oxygen consumption, and sulfate reduction. *Mar Ecol Prog Ser* **165**: 59-70.
- Arnosti C, Finke N, Larsen O, Ghobrial S (2005). Anoxic carbon degradation in Arctic sediments: Microbial transformations of complex substrates. *Geochim Cosmochim Acta* **69**: 2309-2320.
- Arnosti C, Jørgensen BB (2006). Organic carbon degradation in arctic marine sediments, Svalbard: A comparison of initial and terminal steps. *Geomicrobiol J* **23**: 551-563.
- Baas Becking LGM (1934). *Geobiologie of inleiding tot de milieukunde*. W.P. Van Stockum & Zoon N.V.: The Hague, the Netherlands.
- Bartholomew JW, Paik G (1966). Isolation and Identification of Obligate Thermophilic Sporeforming Bacilli from Ocean Basin Cores. *J Bacteriol* **92**: 635-638.
- Bowles MW, Mogollon JM, Kasten S, Zabel M, Hinrichs KU (2014). Global rates of marine sulfate reduction and implications for sub-sea-floor metabolic activities. *Science* **344**: 889-891.
- Brauman A, Müller JA, Garcia JL, Brune A, Schink B (1998). Fermentative degradation of 3-hydroxybenzoate in pure culture by a novel strictly anaerobic bacterium, *Sporotomaculum hydroxybenzoicum* gen. nov., sp. nov. *Int J Syst Bacteriol* **48 Pt 1**: 215-221.
- Canfield DE, Raiswell R (1999). The evolution of the sulfur cycle. *Am J Sci* **299**: 697-723.
- Christensen D (1984). Determination of Substrates Oxidized by Sulfate Reduction in Intact Cores of Marine-Sediments. *Limnol Oceanogr* **29**: 189-192.
- Dahl C, Kredich NM, Deutzmann R, Trüper HG (1993). Dissimilatory sulphite reductase from *Archaeoglobus fulgidus*: physico-chemical properties of the enzyme and cloning, sequencing and analysis of the reductase genes. *J Gen Microbiol* **139**: 1817-1828.
- de Rezende JR, Kjeldsen KU, Hubert CRJ, Finster K, Loy A, Jørgensen BB (2013). Dispersal of thermophilic *Desulfotomaculum* endospores into Baltic Sea sediments over thousands of years. *ISME J* **7**: 72-84.
- Deming JW (2002). Psychrophiles and polar regions. *Curr Opin Microbiol* **5**: 301-309.
- Devkota S, Wang Y, Musch MW, Leone V, Fehlner-Peach H, Nadimpalli A *et al.* (2012). Dietary-fat-induced taurocholic acid promotes pathobiont expansion and colitis in IL10^{-/-} mice. *Nature* **487**: 104-108.
- Dhillon A, Goswami S, Riley M, Teske A, Sogin M (2005). Domain evolution and functional diversification of sulfite reductases. *Astrobiology* **5**: 18-29.

- Egerova AA (1938). Thermophilic bacteria in Arctic areas. *C R (Dokl) Acad Sci USSR* **19**: 649-650.
- Fenchel T, Finlay BJ (2004). The ubiquity of small species: Patterns of local and global diversity. *Bioscience* **54**: 777-784.
- Finke N, Vandieken V, Jørgensen BB (2007). Acetate, lactate, propionate, and isobutyrate as electron donors for iron and sulfate reduction in Arctic marine sediments, Svalbard. *FEMS Microbiol Ecol* **59**: 10-22.
- Finlay BJ (2002). Global dispersal of free-living microbial eukaryote species. *Science* **296**: 1061-1063.
- Finster K (2008). Microbiological disproportionation of inorganic sulfur compounds. *J Sulfur Chem* **29**: 281-292.
- Foissner W (2006). Biogeography and dispersal of micro-organisms: A review emphasizing protists. *Acta Protozool* **45**: 111-136.
- Friedrich MW (2002). Phylogenetic analysis reveals multiple lateral transfers of adenosine-5'-phosphosulfate reductase genes among sulfate-reducing microorganisms. *J Bacteriol* **184**: 278-289.
- Ghiglione JF, Galand PE, Pommier T, Pedrós-Alió C, Maas EW, Bakker K *et al.* (2012). Pole-to-pole biogeography of surface and deep marine bacterial communities. *Proc Natl Acad Sci U S A* **109**: 17633-17638.
- Glud RN, Holby O, Hoffmann F, Canfield DE (1998). Benthic mineralization and exchange in Arctic sediments (Svalbard, Norway). *Mar Ecol Prog Ser* **173**: 237-251.
- Green J, Bohannan BJ (2006). Spatial scaling of microbial biodiversity. *Trends Ecol Evol* **21**: 501-507.
- Green JL, Holmes AJ, Westoby M, Oliver I, Briscoe D, Dangerfield M *et al.* (2004). Spatial scaling of microbial eukaryote diversity. *Nature* **432**: 747-750.
- Hanson CA, Fuhrman JA, Horner-Devine MC, Martiny JBH (2012). Beyond biogeographic patterns: processes shaping the microbial landscape. *Nat Rev Microbiol* **10**: 497-506.
- Hipp WM, Pott AS, Thum-Schmitz N, Faath I, Dahl C, Trüper HG (1997). Towards the phylogeny of APS reductases and sirohaem sulfite reductases in sulfate-reducing and sulfur-oxidizing prokaryotes. *Microbiology* **143**: 2891-2902.
- Hubert C, Loy A, Nickel M, Arnosti C, Baranyi C, Brüchert V *et al.* (2009). A Constant Flux of Diverse Thermophilic Bacteria into the Cold Arctic Seabed. *Science* **325**: 1541-1544.
- Hubert C, Arnosti C, Brüchert V, Loy A, Vandieken V, Jørgensen BB (2010). Thermophilic anaerobes in Arctic marine sediments induced to mineralize complex organic matter at high temperature. *Environ Microbiol* **12**: 1089-1104.
- Imachi H, Sekiguchi Y, Kamagata Y, Loy A, Qiu YL, Hugenholtz P *et al.* (2006). Non-sulfate-reducing, syntrophic bacteria affiliated with desulfotomaculum cluster I are widely distributed in methanogenic environments. *Appl Environ Microbiol* **72**: 2080-2091.
- Isaksen M, Jørgensen B (1996). Adaptation of psychrophilic and psychrotrophic sulfate-reducing bacteria to permanently cold marine environments. *Appl Environ Microbiol* **62**: 408-414.
- Isaksen MF, Bak F, Jørgensen BB (1994). Thermophilic Sulfate-Reducing Bacteria in Cold Marine Sediment. *FEMS Microbiol Ecol* **14**: 1-8.
- Jørgensen BB (1977). The sulfur cycle of a coastal marine sediment (Limfjorden, Denmark). *Limnol Oceanogr* **22**: 814-831.
- Jørgensen BB (1982). Mineralization of Organic-Matter in the Sea Bed - the Role of Sulfate Reduction. *Nature* **296**: 643-645.
- Klein M, Friedrich M, Roger AJ, Hugenholtz P, Fishbain S, Abicht H *et al.* (2001). Multiple lateral transfers of dissimilatory sulfite reductase genes between major lineages of sulfate-reducing prokaryotes. *J Bacteriol* **183**: 6028-6035.
- Knoblauch C, Sahm K, Jørgensen BB (1999). Psychrophilic sulfate-reducing bacteria isolated from permanently cold arctic marine sediments: description of *Desulfofrigus oceanense* gen. nov., sp. nov., *Desulfofrigus fragile* sp. nov., *Desulfofaba gelida* gen. nov., sp. nov., *Desulfotalea psychrophila* gen. nov., sp. nov. and *Desulfotalea arctica* sp. nov. *Int J Syst Bacteriol* **49 Pt 4**: 1631-1643.
- Kristensen E, Bodenbender J, Jensen MH, Rennenberg H, Jensen KM (2000). Sulfur cycling of intertidal Wadden Sea sediments (Konigshafen, Island of Sylt, Germany): sulfate reduction and sulfur gas emission. *J Sea Res* **43**: 93-104.
- Lee Y-J, Wagner ID, Brice ME, Kevbrin VV, Mills GL, Romanek CS *et al.* (2005). *Thermosediminibacter oceani* gen. nov., sp. nov. and *Thermosediminibacter litoriperuensis* sp. nov., new anaerobic thermophilic bacteria isolated from Peru Margin. *Extremophiles* **9**: 375-383.
- Lengeler JW, Drews G, Schlegel HG (1999). *Biology of the Prokaryotes*. Georg Thieme Verlag.
- Levitus S, Boyer T (1994). World Ocean Atlas 1994. Volume 4. Temperature. National Environmental Satellite, Data, and Information Service, Washington, DC (United States).
- Lindstrom ES, Langenheder S (2012). Local and regional factors influencing bacterial community assembly. *Env Microbiol Rep* **4**: 1-9.

- Loy A, Duller S, Baranyi C, Musmann M, Ott J, Sharon I *et al.* (2009). Reverse dissimilatory sulfite reductase as phylogenetic marker for a subgroup of sulfur-oxidizing prokaryotes. *Environ Microbiol* **11**: 289-299.
- Margesin R, Miteva V (2011). Diversity and ecology of psychophilic microorganisms. *Res Microbiol* **162**: 346-361.
- Martiny JBH, Bohannan BJM, Brown JH, Colwell RK, Fuhrman JA, Green JL *et al.* (2006). Microbial biogeography: putting microorganisms on the map. *Nat Rev Microbiol* **4**: 102-112.
- McBee R, McBee VH (1956). The incidence of thermophilic bacteria in arctic soils and waters. *J Bacteriol* **71**: 182.
- Meyer B, Kuever J (2007). Phylogeny of the alpha and beta subunits of the dissimilatory adenosine-5'-phosphosulfate (APS) reductase from sulfate-reducing prokaryotes—origin and evolution of the dissimilatory sulfate-reduction pathway. *Microbiology* **153**: 2026-2044.
- Milucka J, Ferdelman TG, Polerecky L, Franzke D, Wegener G, Schmid M *et al.* (2012). Zero-valent sulphur is a key intermediate in marine methane oxidation. *Nature* **491**: 541-546.
- Milucka J, Widdel F, Shima S (2013). Immunological detection of enzymes for sulfate reduction in anaerobic methane-oxidizing consortia. *Environ Microbiol* **15**: 1561-1571.
- Moeslund L, Thamdrup B, Jørgensen BB (1994). Sulfur and iron cycling in a coastal sediment: radiotracer studies and seasonal dynamics. *Biogeochemistry* **27**: 129-152.
- Molitor M, Dahl C, Molitor I, Schäfer U, Speich N, Huber R *et al.* (1998). A dissimilatory sirohaem-sulfite-reductase-type protein from the hyperthermophilic archaeon *Pyrobaculum islandicum*. *Microbiology* **144** (Pt 2): 529-541.
- Muyzer G, Stams AJ (2008). The ecology and biotechnology of sulphate-reducing bacteria. *Nat Rev Microbiol* **6**: 441-454.
- Nedwell DB, Walker TR, Ellisevans JC, Clarke A (1993). Measurements of Seasonal Rates and Annual Budgets of Organic-Carbon Fluxes in an Antarctic Coastal Environment at Signy Island, South Orkney Islands, Suggest a Broad Balance between Production and Decomposition. *Appl Environ Microbiol* **59**: 3989-3995.
- Nicholson WL, Munakata N, Horneck G, Melosh HJ, Setlow P (2000). Resistance of *Bacillus* endospores to extreme terrestrial and extraterrestrial environments. *Microbiol Mol Biol Rev* **64**: 548-572.
- Papke RT, Ramsing NB, Bateson MM, Ward DM (2003). Geographical isolation in hot spring cyanobacteria. *Environ Microbiol* **5**: 650-659.
- Parkes RJ, Gibson GR, Muellerharvey I, Buckingham WJ, Herbert RA (1989). Determination of the Substrates for Sulfate-Reducing Bacteria within Marine and Estuarine Sediments with Different Rates of Sulfate Reduction. *J Gen Microbiol* **135**: 175-187.
- Pester M, Knorr KH, Friedrich MW, Wagner M, Loy A (2012). Sulfate-reducing microorganisms in wetlands - fameless actors in carbon cycling and climate change. *Front Microbiol* **3**: 72.
- Prosser JI, Bohannan BJ, Curtis TP, Ellis RJ, Firestone MK, Freckleton RP *et al.* (2007). The role of ecological theory in microbial ecology. *Nat Rev Microbiol* **5**: 384-392.
- Ramette A, Tiedje JM (2007). Biogeography: an emerging cornerstone for understanding prokaryotic diversity, ecology, and evolution. *Microb Ecol* **53**: 197-207.
- Ravenschlag K, Sahm K, Knoblauch C, Jørgensen BB, Amann R (2000). Community structure, cellular rRNA content, and activity of sulfate-reducing bacteria in marine arctic sediments. *Appl Environ Microbiol* **66**: 3592-3602.
- Reche I, Pulido-Villena E, Morales-Baquero R, Casamayor EO (2005). Does ecosystem size determine aquatic bacterial richness? *Ecology* **86**: 1715-1722.
- Rivkin R, Anderson M, Lajzerowicz C (1996). Microbial processes in cold oceans. I. Relationship between temperature and bacterial growth rate. *Aquat Microb Ecol* **10**: 243-254.
- Robador A, Brüchert V, Jørgensen BB (2009). The impact of temperature change on the activity and community composition of sulfate-reducing bacteria in arctic versus temperate marine sediments. *Environ Microbiol* **11**: 1692-1703.
- Rysgaard S, Glud RN, Risgaard-Petersen N, Dalsgaard T (2004). Denitrification and anammox activity in Arctic marine sediments. *Limnol Oceanogr* **49**: 1493-1502.
- Sagemann J, Jørgensen BB, Greeff O (1998). Temperature dependence and rates of sulfate reduction in cold sediments of Svalbard, Arctic Ocean. *Geomicrobiol J* **15**: 85-100.
- Sahm K, Knoblauch C, Amann R (1999). Phylogenetic affiliation and quantification of psychophilic sulfate-reducing isolates in marine Arctic sediments. *Appl Environ Microbiol* **65**: 3976-3981.
- Sawicka JE, Jørgensen BB, Brüchert V (2012). Temperature characteristics of bacterial sulfate reduction in continental shelf and slope sediments. *Biogeosci Discuss* **9**: 673-700.

- Simon J, Kroneck P (2013). Microbial sulfite respiration. *Adv Microb Physiol* **62**: 45-117.
- Sørensen J, Christensen D, Jørgensen BB (1981). Volatile Fatty-Acids and Hydrogen as Substrates for Sulfate-Reducing Bacteria in Anaerobic Marine Sediment. *Appl Environ Microbiol* **42**: 5-11.
- Sul WJ, Oliver TA, Ducklow HW, Amaral-Zettler LA, Sogin ML (2013). Marine bacteria exhibit a bipolar distribution. *Proc Natl Acad Sci U S A* **110**: 2342-2347.
- Vandieken V, Knoblauch C, Jørgensen BB (2006). Desulfotomaculum arcticum sp. nov., a novel spore-forming, moderately thermophilic, sulfate-reducing bacterium isolated from a permanently cold fjord sediment of Svalbard. *Int J Syst Evol Microbiol* **56**: 687-690.
- Wagner M, Roger AJ, Flax JL, Brusseau GA, Stahl DA (1998). Phylogeny of dissimilatory sulfite reductases supports an early origin of sulfate respiration. *J Bacteriol* **180**: 2975-2982.
- Wagner M, Loy A, Klein M, Lee N, Ramsing NB, Stahl DA *et al.* (2005). Functional marker genes for identification of sulfate-reducing prokaryotes. *Method Enzymol* **397**: 469-489.
- Whitaker RJ, Grogan DW, Taylor JW (2003). Geographic barriers isolate endemic populations of hyperthermophilic archaea. *Science* **301**: 976-978.
- Zverlov V, Klein M, Lückner S, Friedrich MW, Kellermann J, Stahl DA *et al.* (2005). Lateral gene transfer of dissimilatory (bi)sulfite reductase revisited. *J Bacteriol* **187**: 2203-2208.

Chapter II

Overview of publications/manuscripts

Chapter III

Manuscript title:

Phylogenetic and environmental diversity of DsrAB-type dissimilatory (bi)sulfite reductases

Author names:

Albert Leopold Müller, Kasper Urup Kjeldsen, Thomas Rattei, Michael Pester, Alexander Loy.

Reference:

The ISME Journal advance online publication 24 October 2014; doi:10.1038/ismej.2014.208

Author contributions:

ALM, MP, and AL designed the research. ALM performed all analyses except tblastx analysis. ALM, KUK, and MP constructed the comprehensive *dsrAB*/DsrAB reference database and TR performed tblastx analysis. ALM and AL wrote the paper. KUK, TR, and MP revised draft versions and approved the final version of the paper.

Chapter IV

Manuscript title:

Bacterial community response during degradation of cyanobacterial biomass and acetate in a sulfate-reducing Arctic fjord sediment

Author names:

Albert Leopold Müller, Júlia Rosa de Rezende, Martina Putz, Kasper Urup Kjeldsen, Bo Barker Jørgensen, Alexander Loy.

Reference:

This manuscript is not yet submitted.

Author contributions:

ALM and AL designed the research. ALM and MP performed the incubations. JRR measured sulfate reduction rates. KUK measured volatile fatty acid concentrations. BBJ provided access to samples and essential research infrastructure. ALM performed the 16S rRNA sequence analyses and prepared the draft manuscript, which was revised by AL.

Chapter V

Manuscript title:

Endospores of thermophilic bacteria as tracers of microbial dispersal by ocean currents

Author names:

Albert Leopold Müller, Júlia Rosa de Rezende, Casey Hubert, Kasper Urup Kjeldsen, Ilias Lagkouravdos, David Berry, Bo Barker Jørgensen, Alexander Loy.

Reference:

The ISME Journal (2014) 8, 1153-1165; doi:10.1038/ismej.2013.225

Author contributions:

ALM, CH, BBJ, KUK, and AL designed the research. ALM, CH, and JRR performed incubation experiments and sulfate reduction rate measurements. ALM performed 16S rRNA sequence analyses. ALM, DB, and IL analyzed the data. ALM and AL wrote the paper. JRR, CH, KUK, IL, DB, and BBJ revised draft versions and approved the final version of the paper.

Chapter VI

Manuscript title:

Activity and community structures of sulfate-reducing microorganisms in polar, temperate and tropical marine sediments

Author names:

Alberto Robador, Albert Leopold Müller, Joanna E. Sawicka, David Berry, Casey Hubert, Alexander Loy, Bo Barker Jørgensen, Volker Brüchert.

Reference:

Submitted to The ISME Journal on December 18th, 2014

Author contributions:

AR designed and performed experiments, analyzed data and wrote the paper. ALM, DB, and AL performed and analyzed 16S rRNA gene pyrosequencing data. JES contributed to the measurement of index properties and the elemental analysis of sediments, interpreted the data and contributed to the preparation of the manuscript. CH helped to interpret the data and contributed to the preparation of the manuscript. BBJ and VB conceived and supported the study. All authors discussed the results and implications and commented on the manuscript at all stages.

Chapter III

**Phylogenetic and environmental diversity
of DsrAB-type dissimilatory (bi)sulfite
reductases**

ORIGINAL ARTICLE

Phylogenetic and environmental diversity of DsrAB-type dissimilatory (bi)sulfite reductases

Albert Leopold Müller^{1,2}, Kasper Urup Kjeldsen³, Thomas Rattei⁴, Michael Pester⁵ and Alexander Loy^{1,2}

¹Department of Microbiology and Ecosystem Science, Division of Microbial Ecology, Faculty of Life Sciences, University of Vienna, Vienna, Austria; ²Austrian Polar Research Institute, Vienna, Austria; ³Center for Geomicrobiology, Department of Bioscience, Aarhus University, Aarhus, Denmark; ⁴Division of Computational Systems Biology, Department of Microbiology and Ecosystem Science, Faculty of Life Sciences, University of Vienna, Vienna, Austria and ⁵Department of Biology, University of Konstanz, Konstanz, Germany

The energy metabolism of essential microbial guilds in the biogeochemical sulfur cycle is based on a DsrAB-type dissimilatory (bi)sulfite reductase that either catalyzes the reduction of sulfite to sulfide during anaerobic respiration of sulfate, sulfite and organosulfonates, or acts in reverse during sulfur oxidation. Common use of *dsrAB* as a functional marker showed that *dsrAB* richness in many environments is dominated by novel sequence variants and collectively represents an extensive, largely uncharted sequence assemblage. Here, we established a comprehensive, manually curated *dsrAB*/DsrAB database and used it to categorize the known *dsrAB* diversity, reanalyze the evolutionary history of *dsrAB* and evaluate the coverage of published *dsrAB*-targeted primers. Based on a DsrAB consensus phylogeny, we introduce an operational classification system for environmental *dsrAB* sequences that integrates established taxonomic groups with operational taxonomic units (OTUs) at multiple phylogenetic levels, ranging from DsrAB enzyme families that reflect reductive or oxidative DsrAB types of bacterial or archaeal origin, superclusters, uncultured family-level lineages to species-level OTUs. Environmental *dsrAB* sequences constituted at least 13 stable family-level lineages without any cultivated representatives, suggesting that major taxa of sulfite/sulfate-reducing microorganisms have not yet been identified. Three of these uncultured lineages occur mainly in marine environments, while specific habitat preferences are not evident for members of the other 10 uncultured lineages. In summary, our publically available *dsrAB*/DsrAB database, the phylogenetic framework, the multilevel classification system and a set of recommended primers provide a necessary foundation for large-scale *dsrAB* ecology studies with next-generation sequencing methods.

The ISME Journal advance online publication, 24 October 2014; doi:10.1038/ismej.2014.208

Introduction

The DsrAB-type dissimilatory (bi)sulfite reductase is a key microbial enzyme in both the reductive and the oxidative steps of the biogeochemical sulfur cycle. Utilized by microorganisms that catalyze redox reactions involving sulfur-containing compounds as components of energy metabolism, it catalyzes the reduction of sulfite to sulfide during anaerobic respiration with sulfate, sulfite or organosulfonates as terminal electron acceptor, and functions in reverse during sulfide oxidation. DsrAB

enzymes are heterotetramer proteins with an $\alpha_2\beta_2$ structure and possess iron-sulfur clusters and siroheme prosthetic groups (Dahl *et al.*, 1993). The α and β subunits are encoded by the paralogous genes *dsrA* and *dsrB*, respectively, which are organized in a single copy operon with *dsrA* preceding *dsrB* (Dahl *et al.*, 1993; Karkhoff-Schweizer *et al.*, 1995; Wagner *et al.*, 1998; Larsen *et al.*, 1999; Pereira *et al.*, 2011). Given the presumed antiquity of siroheme and the proposed existence of DsrAB before the separation of the domains *Bacteria* and *Archaea* (Wagner *et al.*, 1998; Dhillon *et al.*, 2005; Loy *et al.*, 2009), DsrAB enzymes are considered very ancient and might have had a fundamental role in mediating biological conversions of sulfur compounds by some of the first microorganisms in the anoxic, reduced atmosphere environments of the primordial Earth (Wagner *et al.*, 1998; Canfield and Raiswell, 1999; Huston and Logan, 2004).

Correspondence: A Loy, Department of Microbiology and Ecosystem Science, Division of Microbial Ecology, Faculty of Life Sciences, University of Vienna, Althanstrasse 14, Wien 1090, Austria.

E-mail: loy@microbial-ecology.net

Received 30 June 2014; revised 13 September 2014; accepted 23 September 2014

It is now recognized that the distribution of *dsrAB* among extant microorganisms was driven by a combination of divergence through speciation, functional diversification and lateral gene transfer (LGT) between unrelated taxa (Loy *et al.*, 2008b).

DsrAB enzymes are best known from sulfate-reducing microorganisms (SRMs) because of their global relevance for biogeochemical cycling of sulfur and carbon (Pester *et al.*, 2012; Bowles *et al.*, 2014). DsrAB catalyzes the last and main energy-conserving step in the dissimilatory sulfate reduction pathway that is conserved in all cultivated SRM, which are distributed in four bacterial (*Proteobacteria*—class *Deltaproteobacteria*, *Nitrospirae*, *Firmicutes*, *Thermodesulfobacteria*) and two archaeal phyla (*Euryarchaeota*, *Crenarchaeota*). The canonical pathway essentially consists of the enzymes ATP sulfurylase (Sat), adenosine 5'-phosphosulfate reductase (Apr) and dissimilatory (bi)sulfite reductase (Dsr). However, a new, yet unresolved pathway for sulfate reduction was suggested to operate in a syntrophic microbial consortium that mediated the anaerobic oxidation of methane coupled to sulfate reduction and polysulfide disproportionation (Milucka *et al.*, 2012). Surprisingly, sulfate was reduced by an unknown mechanism in the archaeal partner resulting in the formation of disulfide and not by the deltaproteobacterial partner that harbors the canonical DsrAB-based pathway.

DsrAB genes are also present in some microorganisms that are unable to use sulfate as a terminal electron acceptor including sulfite-reducing microorganisms (e.g., *Desulfitobacterium*, *Desulfitibacter* and *Pyrobaculum*) (Simon and Kroneck, 2013), sulfur-disproportionating bacteria (e.g., *Desulfocapsa sulfexigens*) (Finster, 2008) and in organisms that metabolize organosulfonates to internally produce sulfite for respiration (e.g., the taurine-consuming gut bacterium *Bilophila wadsworthia*) (Devkota *et al.*, 2012). The physiological role of DsrAB in anaerobic syntrophs of the spore-forming *Firmicutes* genera *Pelotomaculum* and *Sporotomaculum*, which possess and transcribe *dsrAB* but are incapable of reducing sulfite, sulfate or organosulfonates (Brauman *et al.*, 1998; Imachi *et al.*, 2006), is unknown.

Some but not all sulfur-oxidizing bacteria (SOB) carry a reversely operating DsrAB that is homologous, yet phylogenetically clearly distinct from DsrAB enzymes that function in sulfite reduction (Schedel and Trüper, 1979; Loy *et al.*, 2009). Unlike most SRM, SOB do not share a common sulfur metabolism pathway, but exploit various, partially redundant enzyme systems for the oxidation of a range of reduced sulfur compounds with intermediate oxidation states (Kelly *et al.*, 1997; Kletzin *et al.*, 2004; Friedrich *et al.*, 2005). DsrAB is essential for the oxidation of sulfur globule repositories (Pott and Dahl, 1998; Dahl *et al.*, 2005) and might thus provide these SOB with an advantageous backup sulfur metabolism in environments with varying

concentrations of reduced sulfur compounds. Thus far, *dsrAB* have been detected in free-living and symbiotic sulfur-storing SOB of the phyla *Proteobacteria* (classes *Alpha*-, *Beta*-, *Gamma*- and *Delta*-*proteobacteria*) and *Chlorobi* (Loy *et al.*, 2009; Swan *et al.*, 2011; Sheik *et al.*, 2014).

With a few significant exceptions that are indicative of LGT of *dsrAB* among major SRM taxa, DsrAB and 16S rRNA phylogenies are largely congruent (Klein *et al.*, 2001; Zverlov *et al.*, 2005; Loy *et al.*, 2009). Consequently, *dsrAB* have been frequently exploited as phylogenetic marker genes in amplicon sequencing-based environmental studies (Dhillon *et al.*, 2003; Nakagawa *et al.*, 2004; Leloup *et al.*, 2006; Loy *et al.*, 2009; Moreau *et al.*, 2010; Mori *et al.*, 2010; Pester *et al.*, 2010; Lenk *et al.*, 2011). Application of the *dsrAB* approach (Wagner *et al.*, 2005) in diverse environments has uncovered an extensive hidden diversity of *dsrAB* sequences that are not closely related to *dsrAB* from any recognized organisms. New sequencing techniques have opened up opportunities for large-scale α - and β -diversity studies of *dsrAB*. However, the currently available *dsrAB* sequence set is largely uncharacterized, which poses considerable problems in identifying and classifying newly obtained environmental sequences. A comprehensive classification framework for streamlined computational analyses of large *dsrAB* sequence data sets is thus urgently needed. A first step toward a *dsrAB* classification system has been made by a meta-analysis of *dsrAB* diversity that focused on freshwater wetland SRM (Pester *et al.*, 2012). This study highlighted the existence of at least 10 major monophyletic lineages that were only composed of environmental sequences and similar in intralinear diversity to known SRM families. Furthermore, several primers targeting reductive and oxidative *dsrAB* types have been published and applied for PCR-based environmental monitoring of the diversity and abundance of sulfur-cycling microorganisms (Wagner *et al.*, 1998; Kondo *et al.*, 2004; Geets *et al.*, 2005; Loy *et al.*, 2009; Mori *et al.*, 2010; Lenk *et al.*, 2011; Steger *et al.*, 2011; Lever *et al.*, 2013), but it is unclear how well these primers cover the currently known *dsrAB* diversity and thus how suitable they are for such purposes.

In the present study, we established a comprehensive, manually aligned and curated database of nucleic acid and inferred amino-acid sequences of *dsrAB* that are available in public sequence repositories, and provided a robust, taxonomically and phylogenetically informed classification system for the entire environmental *dsrAB* diversity. This allowed us to classify and systematically quantify the uncharted dimensions of *dsrAB* diversity and to reveal its distribution across various environments. We further used the database to determine the *in silico* coverage of all published *dsrA*- or *dsrB*-targeted primers to provide guidance for future PCR-based studies.

Materials and methods

Construction of a comprehensive dsrAB/DsrAB reference database

A *dsrAB/DsrAB* reference database (Zverlov *et al.*, 2005; Loy *et al.*, 2009), implemented with the ARB software package (Ludwig *et al.*, 2004), was updated to contain all publicly available *dsrAB* sequences (status August 2013). Sequences were retrieved by manually searching the NCBI nucleotide and genome databases using appropriate keywords (e.g., 'dsrAB', 'dsrA', 'dsrB', 'dissimilatory (bi) sulfite reductase', 'dissimilatory sulfite reductase', 'dissimilatory sulfite reductase') and by tblastx analysis (Supplementary Materials and methods) (Camacho *et al.*, 2009). Of more than 13 000 retrieved sequences, we retained 7695 sequences with <1% ambiguous nucleotides. This sequence assemblage represents a core data set of 1292 sequences that fully covered the ~1.9 kb region amplified by the most widely used primer variants DSR1F and DSR4R (which corresponds to ~77% of the entire ~2.5 kb-long *dsrAB*) and 6403 shorter sequences that covered at least 300 nucleotides in this region. Sequences were assigned to broad environmental categories (Supplementary Materials and methods). Alignments of nucleotide and inferred amino-acid sequences were manually corrected. The curated and annotated *dsrAB/DsrAB* database (Supplementary File S1) is available as ARB database in the download section at <http://www.microbial-ecology.net> and additionally provided as FASTA files of classified and environmentally annotated nucleotide (Supplementary File S2) and amino-acid sequences (Supplementary File S3).

Comparative sequence analyses and classification of dsrAB diversity

DsrAB phylogeny was calculated based on core data set sequences and by using alignment filters that exclude sequence regions with insertions and deletions (indel filters). Maximum-likelihood, maximum parsimony and neighbor-joining trees were used to construct consensus trees (Supplementary Materials and methods). Shorter *dsrAB* sequences (300 to <1590 nucleotides in the region used for treeing) were phylogenetically classified by adding each inferred amino-acid sequence separately to the consensus tree using the EPA algorithm (Berger *et al.*, 2011) in RAXML-HPC 7.5.6 (Stamatakis, 2006).

Environmental DsrAB sequences of the core data set that were not affiliated with recognized taxonomic families were assigned into individual lineages of approximate family-level diversity (Supplementary Materials and methods). Lineages were further summarized to superclusters if two or more known families and/or uncultured DsrAB lineages formed a monophyletic cluster with a bootstrap support of >70% in at least one treeing method.

Indications for LGT were obtained using a phylogenetic approach (Klein *et al.*, 2001; Koonin *et al.*, 2001). DsrAB and 16S rRNA consensus trees were manually compared for topological inconsistencies under the assumption that 16S rRNA genes were not subject to LGT and thus are markers for inferring the phylogeny of the analyzed species.

In silico coverage and specificity of dsrA- and dsrB-targeted primers

To obtain comparable coverage values and to avoid basing coverage estimates of primers on sequences that were obtained with the very same primers, we used a data set comprised of 177 full-length *dsrAB* sequences (the majority of which derive from genomes; 115 reductive and 62 oxidative bacterial-type *dsrAB*) for the evaluation of primers that bind at the (r)DSR1F or (r)DSR4R primer target region, and primer pairs that use at least one such primer. To test primers that target the region amplified by the (r)DSR1F/(r)DSR4R primer pair, we additionally used 1110 reductive- and 159 oxidative bacterial-type *dsrAB* sequences of the core data set that completely cover this region (Supplementary Tables S1–S4). Primer coverage was determined with the ARB Probe Match tool using perfect match and one weighted mismatch (standard base-pairing and positional weight settings in ARB). Target positions of primers are numbered relative to the *Desulfovibrio vulgaris* Hildenborough DSM 644 *dsrAB* sequence (NC_002937, 449 888...452 365) for reductive bacterial-type *dsrAB* sequences and the *Allochromatium vinosum* DSM 180 *dsrAB* sequence (NC_013851, 1 439 735...1 442 113) for oxidative bacterial-type *dsrAB* sequences.

Results and discussion

The DsrAB consensus tree provides a robust phylogenetic framework for environmental studies

For a *dsrAB* census, we created a comprehensive database of 7695 sequences with ≥300 nucleotides length and sufficient quality that derived from 530 amplicon sequencing, metagenome or genome studies. For more reliable phylogenetic inferences, we constructed a DsrAB consensus tree using a core data set of 1292 sequences with ~1.9 kb length (Figure 1 and Supplementary Figures S1–S3). The DsrAB tree has four main basal branches that delineate three major DsrAB protein families, namely the reductive bacterial type, the oxidative bacterial type and the reductive archaeal type. The fourth branch is so far only represented by the second *dsrAB* copy of *Moorella thermoacetica* (Pierce *et al.*, 2008; Loy *et al.*, 2009). Through paralogous rooting analysis, we show that this copy and the reductive archaeal-type DsrAB family represent the deepest branches in the DsrAB tree and add support to the previously proposed early evolution of DsrAB as a reductive enzyme

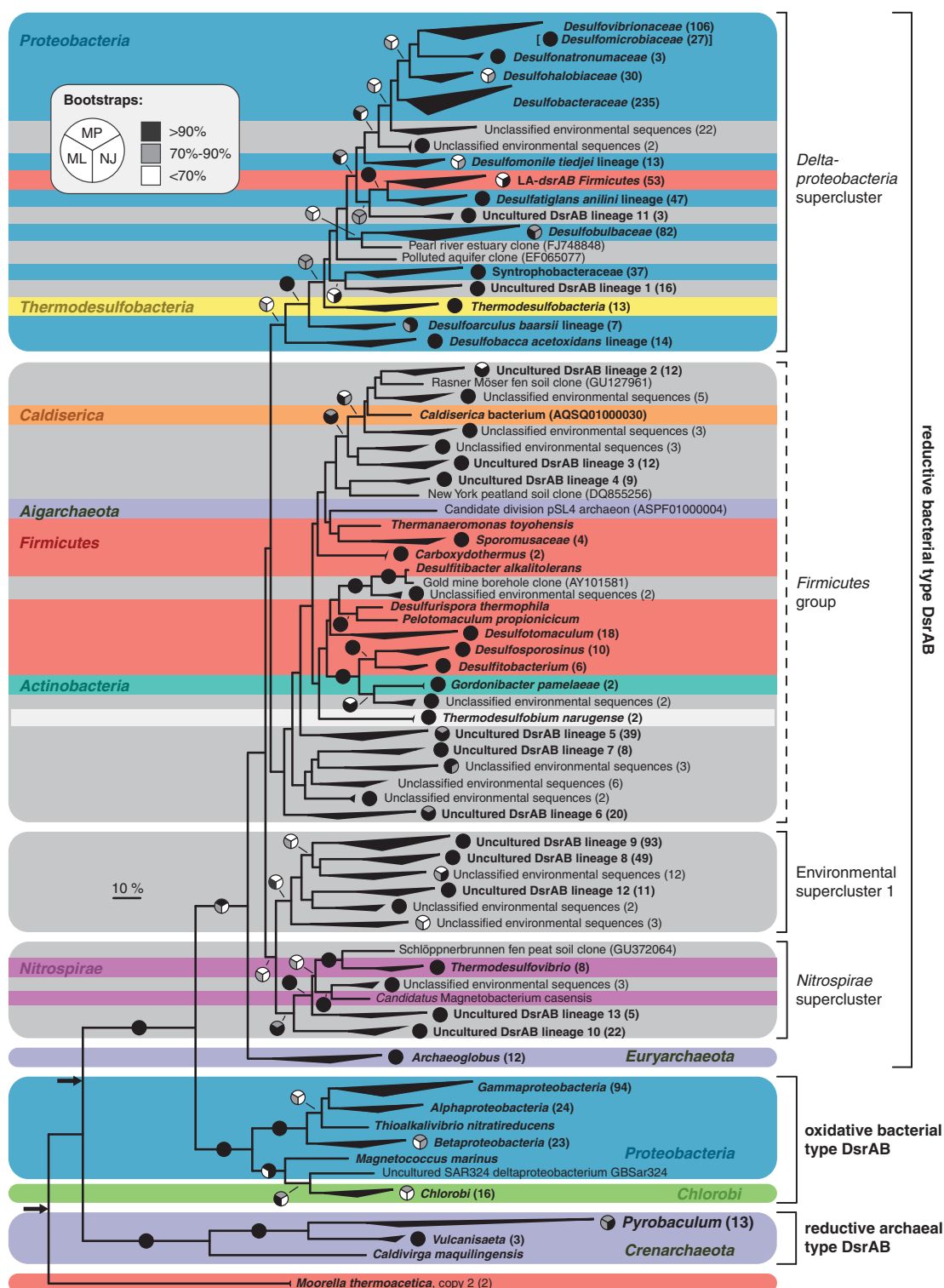


Figure 1 Consensus phylogeny of DsrAB sequences. Trees for reconstruction of the consensus tree (extended majority rule) were calculated using an alignment of 911 representative DsrAB sequences (clustered at 97% amino-acid identity) and an indel filter covering 530 amino-acid positions between the target sites of the most commonly used DSR1F and DSR4R primer variants. Remaining core sequences ($n = 378$) of the clusters were subsequently added to the consensus tree without changing its topology. Scale bar indicates 10% sequence divergence. Bootstrap support (100 resamplings) is shown by split circles (top: maximum parsimony; bottom left: maximum likelihood; bottom right: neighbor joining) at the respective branches, with black, gray and white/absence indicating $\geq 90\%$, $70\%–90\%$ and $<70\%$ support, respectively. DsrAB-carrying phyla are labeled in different background colors; gray background represents lineages with no closely related cultured representatives. Black arrows indicate the possible locations for the root of the tree according to paralogous rooting analysis. LA-dsrAB, laterally acquired dsrAB. *Moorella thermoacetica* dsrAB copy 1 clustered with the LA-dsrAB Firmicutes group.

(Wagner *et al.*, 1998) (Supplementary Results and discussion and Supplementary Figure S4).

To assess the minimum number of *dsrAB*-containing species that are currently represented in the 1292 sequence core data set, we initially inferred a species-level sequence identity cutoff from the linear regression in a plot of corresponding pairs of 16S rRNA gene and non-laterally acquired reductive- and oxidative bacterial-type *dsrAB* identities (Supplementary Figure S5) (Kjeldsen *et al.*, 2007). A *dsrAB* nucleic acid sequence identity of 92% over the ~1.9 kb fragment is equivalent to a 16S rRNA sequence identity of 99%, which is a frequently used threshold for delineating species-level OTUs (Stackebrandt and Ebers, 2006). We recommend using a more conservative threshold of 90% *dsrAB* sequence identity, because two organisms with <90% *dsrAB* identity generally have <99% 16S rRNA identity (Supplementary Figure S5) and will likely represent two different species, given that *dsrAB* is usually present as a single copy per genome. Application of the 90% threshold showed that already the core data set represents a minimum of 779 species-level OTUs, of which 647 are of the reductive and 118 of the oxidative bacterial DsrAB type. For comparison, ~240 species of SRM are currently present in the List of Bacterial Names with Standing in Nomenclature (Euzéby, 1997).

The reductive bacterial-type DsrAB family cluster mostly contains bacteria that use sulfate, sulfite or organosulfonates as terminal electron acceptors (Loy *et al.*, 2008b), and also from sulfate/sulfite-reducing archaea that received *dsrAB* via LGT from ancestral bacterial donors (see section below). Two hundred and ninety-nine environmental sequences of the core data set were not affiliated with members of described taxonomic families and clustered in 13 stable, monophyletic lineages, which were designated ‘uncultured DsrAB lineages 1 to 13’ (note that lineages 1 to 10 were defined previously; Pester *et al.*, 2012) using a combination of *dsrAB* sequence identity-based and phylogenetic criteria (Figure 1, Supplementary Figure S1 and Supplementary Materials and methods). Each of these 13 lineages could represent a taxonomic family whose members are yet uncultured or not known to possess *dsrAB*, illustrating the enormous unexplored diversity of *dsrAB*-harboring microorganisms in the environment. Our phylogenetic analysis even provided indications for further lineages of environmental *dsrAB* sequences (Figure 1), but these did not meet our conservative criteria to label them as an ‘uncultured family-level DsrAB lineage’. Importantly, only very few sequences ($n=4$) of the uncultured family-level lineages contain internal stop codons, which are not confirmed and might result from sequencing errors. Furthermore, non-synonymous/synonymous substitution rate ratios of the branches that lead to the 13 uncultured family-level lineages are clearly below one ($\omega = 0.05\text{--}0.37$), which highlights strong purifying selection and

suggests that these *dsrAB* variants are being expressed as functionally active proteins (Yang, 1997; Yang *et al.*, 2000). Although a very recent loss of function will not be evident in the DsrAB sequence record, it is nevertheless unlikely that this vast environmental *dsrAB* diversity is primarily caused by uncontrolled mutation rates owing to the lack of or reduced selective pressure, for example, in viruses (Anantharaman *et al.*, 2014) or microorganisms that received *dsrAB* via LGT yet do not make use of them.

At a higher phylogenetic level, we could reproduce three previously described ‘superclusters’ (Pester *et al.*, 2012), namely the *Deltaproteobacteria* supercluster, the *Nitrospirae* supercluster, which was previously named *Thermodesulfovibrio* supercluster (Supplementary Results and discussion), and the environmental supercluster 1, which each comprise at least two uncultured DsrAB family-level lineages and/or known SRM families (Figure 1). DsrAB of the euryarchaeal genus *Archaeoglobus* and related sequences from thermophilic environments form a separate branch in the reductive bacterial-type DsrAB family tree. All remaining sequences, namely those that are not affiliated with the three superclusters and the *Archaeoglobus* cluster, did not group consistently at a higher phylogenetic level (Steger *et al.*, 2011; Pester *et al.*, 2012), and we have thus not designated them as a supercluster but as the *Firmicutes* group *sensu lato*. These high-order groups/superclusters are named after the main phylum/class that they affiliate with but do not necessarily imply a taxonomic affiliation. Similar to the *Deltaproteobacteria* supercluster, the highly diverse *Firmicutes* group contains *dsrAB* from cultivated members of different phyla and many environmental sequences (Supplementary Results and discussion).

Oxidative-type DsrAB sequences from SOB form a monophyletic enzyme family that is phylogenetically distinct from all other DsrAB sequences (Figure 1 and Supplementary Figure S4). The branching pattern of the tree suggests that oxidative DsrAB evolved by an ancient functional adaptation from an ancestral reductive DsrAB before the diversification into extant DsrAB-carrying phyla. Sequences from known SOB of the classes *Alpha*-, *Beta*- and *Gammaproteobacteria* and the phylum *Chlorobi* form separate clusters in the DsrAB tree that are generally in accordance with the organismal taxonomy (Figure 1, Supplementary Figure S2 and Supplementary Materials and methods). Only *Thioalkalivibrio nitratireducens* branches outside the *Gammaproteobacteria* cluster. Its DsrAB sequence is remarkably different (67–71% amino-acid identity) from the DsrAB of three other *Thioalkalivibrio* species (as opposed to 87–95% DsrAB identity among these three species). Metagenomic (Sheik *et al.*, 2014) and single-cell genome (Swan *et al.*, 2011) analyses have recently identified reverse *dsrAB* and accessory genes for sulfur

oxidation in members of the deltaproteobacterial SAR324 clade. These deltaproteobacterial reverse DsrAB branch with DsrAB of *Chlorobi* and *Magnetococcus marinus*, a species that has been provisionally included in the *Alphaproteobacteria* (Bazylnski et al., 2013). Interestingly, the root of the oxidative-type DsrAB branch is not located between the *Proteobacteria* and the *Chlorobi*. Instead, *Chlorobi* form a monophyletic cluster with *M. marinus* and the putative sulfur-oxidizing deltaproteobacterium (Figure 1), which provides phylogenetic support for the acquisition of *dsrAB* by *Chlorobi* via LGT from a sulfide-oxidizing proteobacterial donor. Such a scenario has been previously postulated based on the absence of *dsrAB* in the deep-branching *Chlorobi* member *Chloroherpeton thalassium* (Frigaard and Bryant, 2008).

Archaeal-type *dsrAB* sequence diversity is mainly represented by sequenced genomes and metagenomes because PCR primers commonly used for amplification of *dsrAB* do not bind to archaeal-type *dsrAB*. So far, three genera within the hyperthermophilic family *Thermoproteaceae* (order *Thermoproteales*) of the phylum *Crenarchaeota*, namely species of *Pyrobaculum* ($n = 7$), *Vulcanisaeta* ($n = 2$) and *Caldivirga* ($n = 1$), are known to harbor this type of *dsrAB*, and each genus is represented by a distinct monophyletic group in the archaeal DsrAB tree (Figure 1 and Supplementary Figure S3). Members of all three genera of archaeal-type DsrAB-carrying organisms are able to reduce thiosulfate and elemental sulfur (Molitor et al., 1998; Itoh et al., 1999, 2002). So far, sulfate reduction has been shown only for *Caldivirga maquilingensis* (Itoh et al., 1999); however, *Vulcanisaeta* species might also be capable of sulfate reduction (Itoh et al., 2002), as genes for the complete canonical sulfate reduction pathway are present in the genomes of *Vulcanisaeta distributa* (Mavromatis et al., 2010) and *V. moutnovskia* (Gumerov et al., 2011).

dsrAB are robust phylogenetic marker genes for sulfur compound-dissimilating microorganisms

Phylogenetic signal is blurred in genes that are subject to (i) frequent LGT between unrelated organisms and (ii) duplication and subsequent functional diversification (Koonin et al., 2001; Gogarten et al., 2002). The identification of *dsrAB* in members of bacterial (*Actinobacteria*, *Caldiclerica*, oxidative-type *dsrAB* in *Deltaproteobacteria*) and archaeal (*Aigarchaeota*; formerly known as pSL4 or hot water crenarchaeotic group I candidate division (Nunoura et al., 2011); note that it is under debate whether *Aigarchaeota* members represent their own phylum or belong to the *Thaumarchaeota* (Brochier-Armanet et al., 2011)) phyla previously not known to harbor these genes necessitates the re-evaluation of *dsrAB* as phylogenetic markers. Using an established phylogenetic approach (Zverlov et al., 2005; Loy et al., 2009), we directly compared

consensus trees of DsrAB and 16S rRNA sequences originating from 254 pure cultures and genome sequences for topological incongruences that are indicative of LGT. Owing to the apparent functional adaptation of DsrAB, this analysis was carried out separately for organisms using the reductive (Figure 2) and the oxidative sulfur energy metabolism (Figure 3). Our analysis confirms that reductive-type DsrAB and 16S rRNA branching patterns are generally similar and reproduces known topological inconsistencies regarding (i) a group of *Firmicutes* that most likely acquired *dsrAB* from deltaproteobacterial ancestors of the *Desulfatiglans anilini* (formerly *Desulfobacterium anilini*; Suzuki et al., 2014) lineage (Figure 2) (Klein et al., 2001; Zverlov et al., 2005), (ii) members of the phylum *Thermodesulfobacteria* and (iii) members of the euryarchaeotal genus *Archaeoglobus* that possess bacterial-type *dsrAB*. Besides these documented cases, we have obtained evidence for further possible *dsrAB* LGT events (Supplementary Results and discussion and Supplementary Figure S6). The *Aigarchaeota* member clearly has a reductive-type *dsrAB* that was received either directly by LGT from a bacterial donor, possibly a member of the phylum *Firmicutes*, or indirectly from a yet unknown, bacterial *dsrAB*-containing archaeon (Figures 1 and 2). The presence of bacterial *dsrAB* in the *Aigarchaeota* member and members of the genus *Archaeoglobus* seems to be the result of at least two independent LGT events. The stable monophyletic grouping of the actinobacterium *Gordonibacter pamelaiae* with the *Firmicutes* genera *Desulfosporosinus* and *Desulfotobacterium* in the DsrAB tree (Figures 1 and 2) suggests LGT from an unknown donor. Although the deep, independent position of the *Caldiclerica* phylum member in both the DsrAB tree and the 16S rRNA tree is inconclusive regarding LGT, complementary analyses also indicate a foreign origin of its *dsrAB* (Supplementary Results and discussion and Supplementary Figure S6). These results provide a first view into the possible evolutionary paths that led to the presence of a reductive bacterial-type *dsrAB* in the bacterial phyla *Actinobacteria* and *Caldiclerica*, and the archaeal candidate phylum *Aigarchaeota*, but in-depth insights can only be obtained when more *dsrAB* sequences from members of these phyla are available.

Based on larger sequence data sets, we confirm that branching patterns of DsrAB and 16S rRNA trees of SOB are largely congruent (Loy et al., 2009), with one exception (Figure 3). In the DsrAB tree, *T. nitratireducens* is not related to three other species of the genus *Thioalkalivibrio*, but branches independently from other *Proteobacteria*. One possible explanation for the phylogenetic position of DsrAB of *T. nitratireducens* is xenologous replacement of its orthologous *dsrAB* with *dsrAB* from an unknown and unrelated proteobacterial donor.

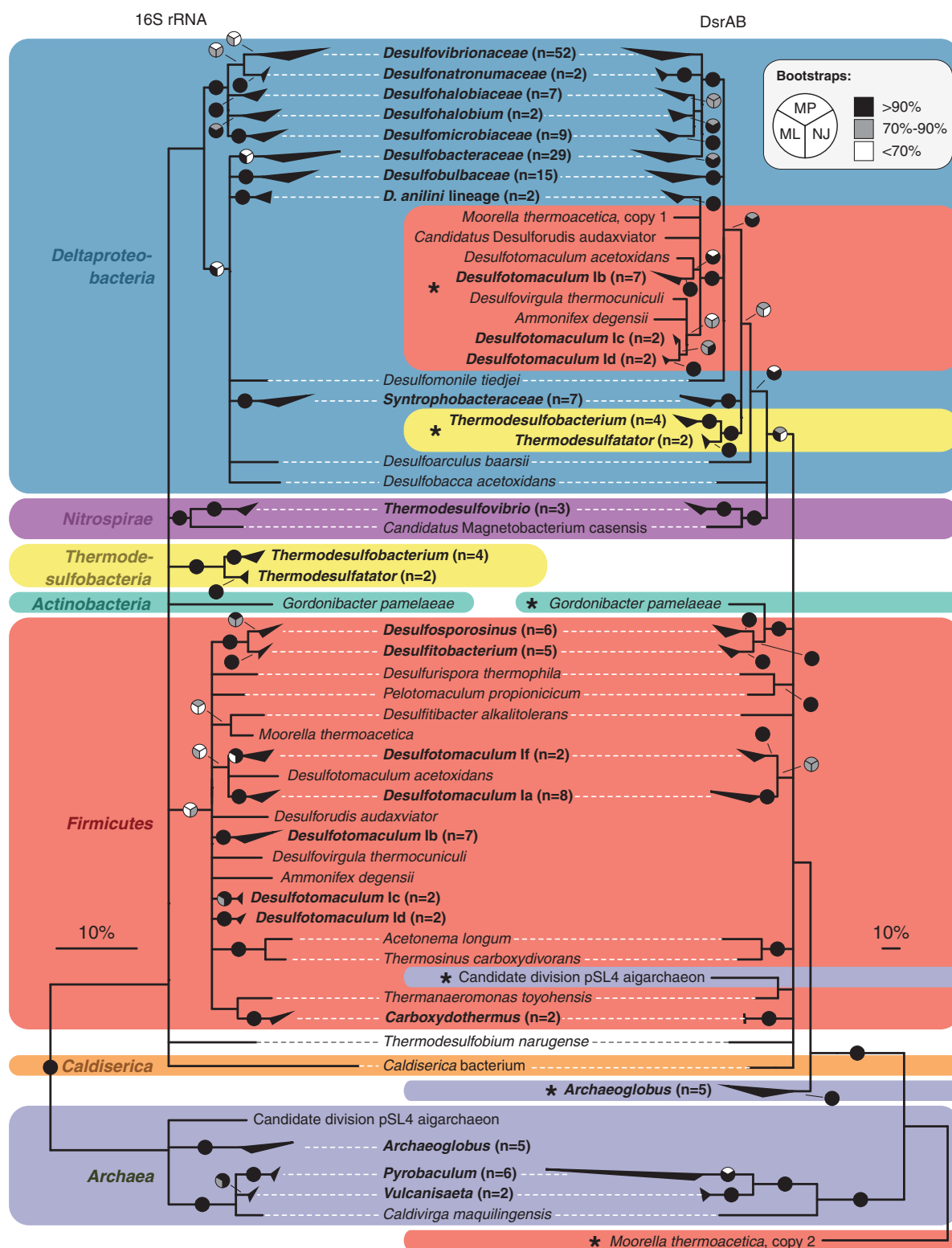


Figure 2 Comparison of 16S rRNA and reductive DsrAB trees. The strict consensus trees are based on corresponding sequence pairs of 16S rRNA and reductive DsrAB from 254 pure cultures and genomes. 16S rRNA and DsrAB trees were calculated using a 50% conservation filter for bacteria (1222 nucleotide positions) and an indel filter for reductive-type DsrAB (530 amino-acid positions), respectively. Scale bars indicate 10% sequence divergence. Both trees are collapsed at the family, genus or (in case of *Desulfotomaculum*) subcluster level. Sequences that branch inconsistently between the trees are marked with an asterisk. Bootstrap support (100 resamplings) is shown by split circles (top: maximum parsimony; bottom left: maximum likelihood; bottom right: neighbor joining) at the respective branches, with black, gray and white/absence indicating $\geq 90\%$, 70%–90% and $< 70\%$ support, respectively.

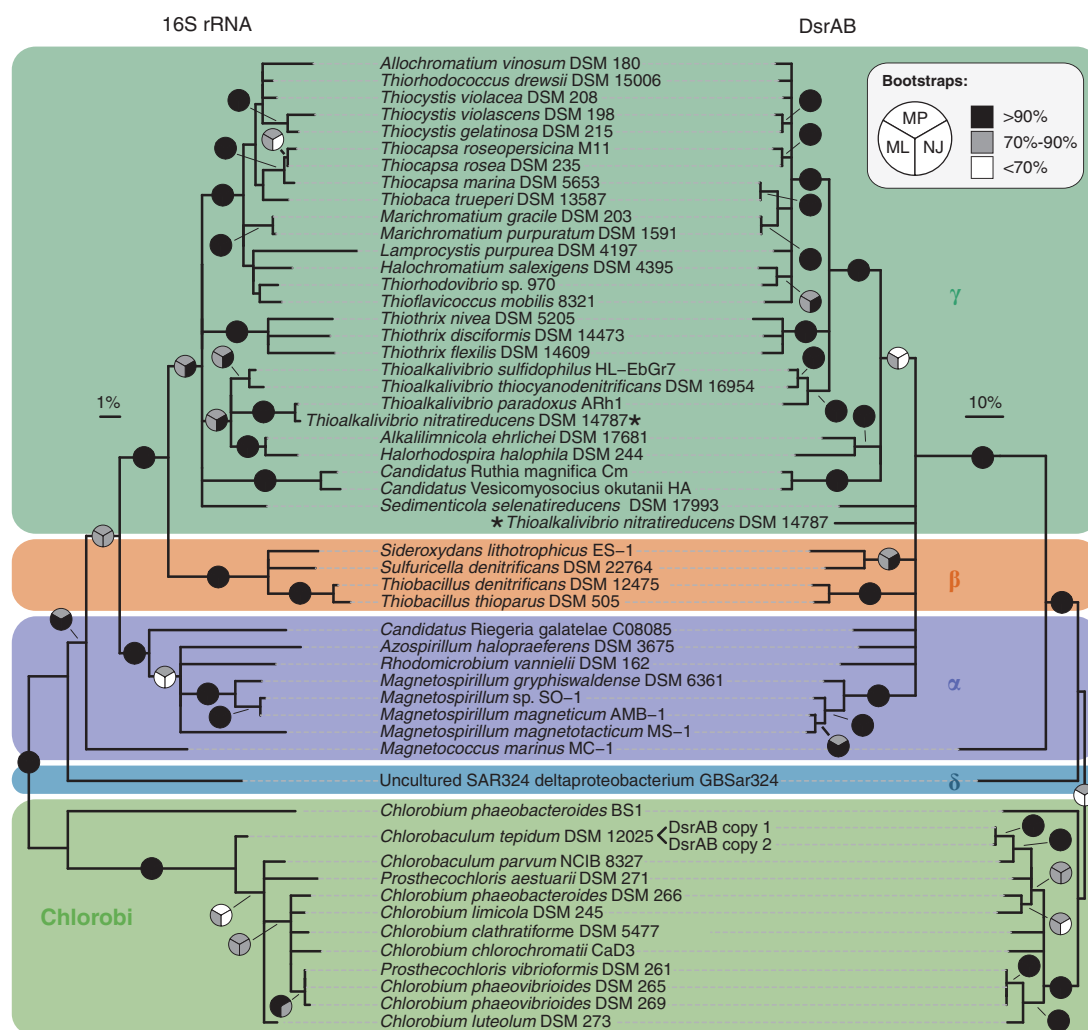


Figure 3 Comparison of 16S rRNA and oxidative DsrAB trees. The strict consensus trees are based on corresponding sequence pairs of 16S rRNA and oxidative DsrAB from 51 pure cultures and genomes. 16S rRNA and DsrAB trees were calculated using a 50% conservation filter for bacteria (1222 nucleotide positions) and an indel filter for oxidative-type DsrAB (552 amino-acid positions), respectively. Scale bars indicate 10% sequence divergence. Sequences that branch inconsistently between the trees are marked with an asterisk. Bootstrap support (1000 resamplings) is shown by split circles (top: maximum parsimony; bottom left: maximum likelihood; bottom right: neighbor joining) at the respective branches, with black, gray and white/absence indicating $\geq 90\%$, $70\%–90\%$ and $< 70\%$ support, respectively.

A robust DsrAB consensus tree and knowing the discrepancies in 16S rRNA and DsrAB-based phylogenies of described taxa are important for a phylogenetically well-informed interpretation of *dsrAB* diversity in environmental samples. The detection of reverse *dsrAB* in a metagenome bin (Sheik *et al.*, 2014) and single-cell genomes (Swan *et al.*, 2011) of the deltaproteobacterial SAR324 clade, whose sulfide-oxidizing members are related to deltaproteobacterial SRM in the 16S rRNA tree, illustrates that inferring general physiological traits such as sulfate/sulfite reduction or sulfur oxidation from 16S rRNA phylogeny can be problematic. In contrast, DsrAB phylogeny clearly distinguishes oxidative versus reductive sulfur metabolism. Despite some limitations, *dsrAB* also remain useful phylogenetic markers because an environmental

dsrAB sequence is identified with high certainty as a member of a recognized taxon if it clusters unambiguously within this taxon. In contrast, the taxonomic identity of an organism represented by an environmental *dsrAB* sequence that branches outside a recognized taxon, such as members of the 13 uncultured family-level DsrAB lineages, is uncertain.

Environmental distribution of *dsrAB*-carrying organisms

We further examined the environmental distribution of the 1292 core *dsrAB* sequences and of 6403 partial *dsrA* or *dsrB* sequences with a minimum length of 300 nucleotides. Owing to the many non-overlapping sequences, partial *dsrA* and *dsrB* sequences could not be jointly clustered into sequence

identity-based species-level OTUs. Instead, they were phylogenetically placed into the consensus tree (Figure 1) without changing its topology (Figure 4). The majority of the 6403 shorter sequences is affiliated with described families and uncultured family-level lineages ($n=5893$; 92%) or unclassified environmental sequences of the core data set ($n=409$; 6%) (Figure 1). Only few sequences ($n=101$; 2%) do not branch within sequence clusters defined by the core data set. A large proportion ($n=2349$; 35%) of the 6686 sequences on the reductive bacterial DsrAB branch are not affiliated with known taxa (i.e., families, genera) that are represented by cultured organisms. For example, uncultured family-level lineage 9 ($n=559$) contains a similar number of sequences as the family *Desulfovibrionaceae* ($n=531$) that harbors many, taxonomically well-described *Desulfovibrio* species (Loy *et al.*, 2002; Muyzer and Stams, 2008).

We additionally grouped the 7695 *dsrAB* sequences into eight broad environmental categories

(i.e., marine, estuarine, freshwater, soil, industrial, thermophilic, alkali-/halophilic and symbiotic) (Supplementary Materials and methods) to gain insights into the environmental distribution patterns of members of major phylogenetic DsrAB lineages. Most sequences derive from marine environments (31%), followed by freshwater (24%), industrial (16%) and soil environments (11%). Members of most major DsrAB lineages are widely distributed among various environments with starkly contrasting biogeochemical properties, which provides limited indications of the possible ecological factors that gave rise to evolution of the many, phylogenetically distinct lineages at the approximate taxonomic rank of families (Figure 4). However, there are notable exceptions that are indicative of environmental preference. Members of the uncultured family-level lineages 2, 3 and 4 are almost exclusively found in marine environments. Not surprisingly, sequences affiliated with the deltaproteobacterial families *Desulfobalobiaceae*

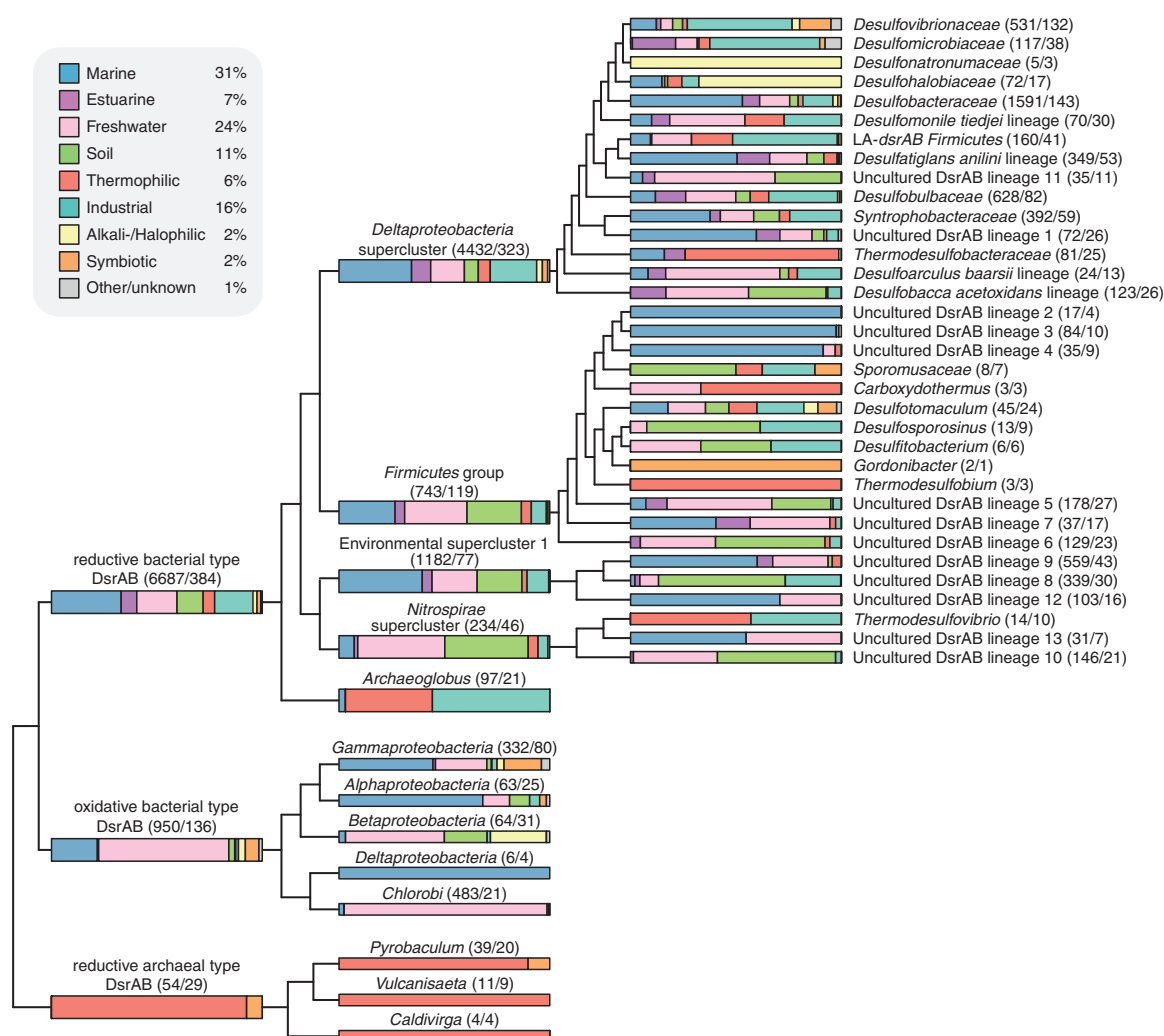


Figure 4 Environmental distribution of *dsrAB* diversity. Environmental classification of 7695 *dsrAB* sequences from 530 amplicon sequencing, metagenome or genome studies. Numbers within parentheses indicate the number of sequences/number of studies per lineage. Unclassified environmental sequences ($n=594$) are only shown as part of DsrAB types/superclusters.

and *Desulfonatronumaceae*, which include known halophilic and alkaliphilic SRM (Ollivier *et al.*, 1991; Pikuta *et al.*, 2003; Jakobsen *et al.*, 2006; Sorokin *et al.*, 2008), derive predominately from high-salt and/or high-pH environments. Oxidative bacterial-type *dsrAB* sequences of *Chlorobi* are most often detected in freshwater habitats. This is, however, possibly a biased representation, as two studies of freshwater environments have provided 94% of all available *Chlorobi* *dsrAB* sequences. Microorganisms with archaeal-type *dsrAB* seem to be restricted to hot environments, but this also needs to be interpreted with caution, because of the low number of available environmental sequences from this DsrAB enzyme family.

Analogous to marker genes for other functional guilds (Mussmann *et al.*, 2011), detection of reductive and oxidative *dsrAB* or their transcripts in an environmental sample is not to be mistaken with the actual physiological capability for dissimilatory sulfate/sulfite reduction and sulfur oxidation, respectively (Pester *et al.*, 2012). In addition to the presence of *dsrAB* in syntrophic bacteria, which are

apparently incapable of using sulfate, sulfite or organosulfonates, environmental fragments of *dsrAB* might derive from viruses or virus-like particles that infect SRM (Rapp and Wall, 1987; Walker *et al.*, 2006; Stanton, 2007) or SOB (Anantharaman *et al.*, 2014), and thus possibly serve as vectors for LGT or supplement the sulfur metabolism of their microbial hosts. Although DsrAB has thus far been shown to function exclusively in dissimilation, it is conceivable that some organisms use it for detoxification of sulfite (Johnson and Mukhopadhyay, 2005; Lukat *et al.*, 2008).

A list of in silico-evaluated primers allows selection of best primer combinations for future environmental dsrAB surveys

We evaluated the *in silico* coverage (i.e., the fraction of sequences in the target group that is matched by the primer) of 103 published, individual *dsrAB*-targeted primers and primer mixtures and 28 primer pairs against the updated *dsrAB* sequence database (Supplementary Results and discussion and Supplementary Tables S1–S4).

Table 1 Recommended primers/primer pairs for the amplification of *dsrAB*

Name ^a	Target gene	Position ^b	Deg. ^c	Full-length dsrAB ^d (%)		Core data set dsrAB ^e (%)		Reference
				0 MM	1 wMM	0 MM	1 wMM	
Primers targeting reductive bacterial-type dsrAB								
DSR1Fmix/DSR4Rmix (1943 nt)	dsrAB	187–2129		47	92	NA	NA	Pester <i>et al.</i> (2010)
DSR1Fmix	dsrA	187–202	11	53	98	NA	NA	Pester <i>et al.</i> (2010)
DSR4Rmix	dsrB	2113–2129	10	77	94	NA	NA	Pester <i>et al.</i> (2010)
DSR67F/DSR698R (1941 nt)	dsrAB	189–2129		37	91	NA	NA	Suzuki <i>et al.</i> (2005)
DSR67F	dsrA	189–203	4	43	100	NA	NA	Suzuki <i>et al.</i> (2005)
DSR698R	dsrB	2113–2129	8	71	91	NA	NA	Suzuki <i>et al.</i> (2005)
dsrB F1a–h/4RSI1a–f (362 nt)	dsrB	1762–2123		27	83	NA	NA	Lever <i>et al.</i> (2013)
dsrB F1a–h	dsrB	1762–1776	8	35	86	44	89	Lever <i>et al.</i> (2013)
dsrB 4RSI1a–f	dsrB	2107–2123	1	62	97	NA	NA	Lever <i>et al.</i> (2013)
DSR1728mix/DSR4Rmix (368 nt)	dsrB	1762–2129		70	94	NA	NA	Steger <i>et al.</i> (2011)
DSR1728Fmix	dsrB	1762–1776	77	90	100	91	100	Steger <i>et al.</i> (2011)
Primers targeting oxidative bacterial-type dsrAB								
rDSR1Fmix/rDSR4Rmix (1865 nt)	dsrAB	169–2033		97	100	NA	NA	Loy <i>et al.</i> (2009)
rDSR1Fmix	dsrA	169–184	80	97	100	NA	NA	Loy <i>et al.</i> (2009)
rDSR4Rmix	dsrB	2017–2033	96	100	100	NA	NA	Loy <i>et al.</i> (2009)
rDSRA240F/rDSRB808R (1856 nt)	dsrAB	172–2027		69	79	NA	NA	Lenk <i>et al.</i> (2011)
rDSRA240F	dsrA	172–188	64	97	100	NA	NA	Lenk <i>et al.</i> (2011)
rDSRB808R	dsrB	2011–2027	144	69	79	NA	NA	Lenk <i>et al.</i> (2011)
DSR874F/rDSR4Rmix (1175 nt)	dsrAB	859–2033		71	100	NA	NA	Loy <i>et al.</i> (2009)
DSR874F	dsrA	859–877	96	71	100	70	100	Loy <i>et al.</i> (2009)
DSR1728mix/rDSR4Rmix (350 nt)	dsrB	1684–2033		90	100	NA	NA	Steger <i>et al.</i> (2011)
DSR1728Fmix	dsrB	1684–1698	77	90	100	95	99	Steger <i>et al.</i> (2011)
dsrB F1a–h/4RSI2a–h (344 nt)	dsrB	1684–2027		29	82	NA	NA	Lever <i>et al.</i> (2013)
dsrB F1a–h	dsrB	1684–1698	8	47	90	43	89	Lever <i>et al.</i> , 2013
dsrB 4RSI2a–h	dsrB	2011–2027	1	44	90	NA	NA	Lever <i>et al.</i> (2013)

Abbreviations: 0 MM, no mismatches; 1 wMM, one weighted mismatch; NA, not applicable for primers binding at the target sites or outside the amplification region of (r)DSR1F/(r)DSR4R; nt, nucleotide.

^aExpected length of the PCR amplicon for primer pairs is given within parentheses. For primer sequences please refer to Supplementary Tables S1 and 2.

^bPosition is relative to *Desulfovibrio vulgaris* Hildenborough *dsrAB* (NC_002937, 449 888...452 365) for reductive bacterial-type and *Allochromatium vinosum* *dsrAB* (NC_013851, 1 439 735...1 442 113) for oxidative-type *dsrAB* sequences.

^cDegeneracy is given as the number of oligonucleotides that comprise the primer.

^dData indicate primer coverage of all full-length reductive bacterial-type ($n = 115$) and oxidative-type ($n = 62$) *dsrAB* sequences.

^eData indicate primer coverage of all reductive bacterial-type ($n = 1110$) and oxidative-type ($n = 159$) *dsrAB* sequences of the core data set.

Although most primers are highly specific for *dsrAB* sequences, only few primers or primer mixes target $\geq 50\%$ (coverage of perfectly matched sequences) and/or $\geq 90\%$ (coverage of sequences with up to one weighted mismatch) of reductive- or oxidative bacterial-type *dsrAB* sequences (Supplementary Tables S1 and S2 and Supplementary Figure S7). The forward primers DSR1Fmix a–h, DSR1728Fmix A–E, DSR67F, *dsrB* F2a–i and reverse primers DSR4Rmix a–g, DSR698R, *dsrB* 4RSI1a–f have highest coverage values for reductive bacterial-type *dsrAB* and are recommended for future use. Reverse *dsrAB* sequences are best covered by forward primers rDSR1Fmix a–c, rDSRA240F, DSR1728Fmix A–E, DSR874F, *dsrB* F1a–h and reverse primers rDSR4Rmix a–b, rDSRB808R, PGdsrAR and *dsrB* 4RSI2a–h. It is noteworthy that DSR1728Fmix A–E and *dsrB* F1a–h have relatively high coverage for both reductive- and oxidative bacterial-type *dsrAB*.

Of the 28 previously published primer pair combinations (Supplementary Tables S3 and S4), only nine have a good coverage of $> 75\%$ when hits with up to one weighted mismatch are considered (Table 1) and are recommended for further use. Primer pairs DSR1Fmix a–h/DSR4Rmix a–g (~ 1.9 kb *dsrAB* PCR product) and DSR1728Fmix A–E/DSR4Rmix a–g (~ 0.4 kb *dsrB* PCR product) have highest perfect-match coverage of 47% and 70%, respectively, for reductive bacterial-type *dsrAB*. Primer pairs rDSR1Fmix a–c/rDSR4Rmix a–b and DSR1728Fmix A–E/rDSR4Rmix a–b, which amplify the homologous regions in SOB, have even higher coverage of 97% and 90%, respectively. Separate coverage values obtained for the five major groups within the reductive bacterial-type DsrAB tree indicate that the DSR1F/DSR4R primer pair mix is biased against sequences of the *Firmicutes* group *sensu lato* and the *Nitrospirae* supercluster. While new primer variants should be designed to improve *in silico* coverage, already many environmental sequences belonging to these two groups were obtained by using the DSR1F/DSR4R primer variants (Kaneko *et al.*, 2007; Martinez *et al.*, 2007; Leloux *et al.*, 2009; Wu *et al.*, 2009).

For an improved coverage of the environmentally occurring *dsrAB* diversity by amplicon sequencing, it is therefore recommended to apply the aforementioned primer pairs at low stringency (e.g., low annealing temperature) to allow for binding of non-perfectly matching target sequences. This also promotes more uniform amplification by the different primers in a degenerate primer mixture (Higuchi *et al.*, 1993). Amplification of complex environmental DNA extracts with highly degenerate primers (Supplementary Tables S1–S4) at low stringency unfortunately increases the likelihood for unspecific PCR products (Wagner *et al.*, 2005). This is particularly a problem if degenerate primers are applied for denaturing gradient gel electrophoresis, terminal restriction fragment length

polymorphism or real-time PCR analyses. Hence, PCR performance/biases must be carefully evaluated for each primer combination individually, and specificity of amplification should additionally be confirmed by sequencing of the environmental PCR product or the extracted denaturing gradient gel electrophoresis bands.

To assist researchers during the evaluation of existing and development of new *dsrAB*-targeted oligonucleotides, we have incorporated our database into the probeCheck webserver for straightforward *in silico* testing of primer specificity and coverage (Loy *et al.*, 2008a).

Conflict of Interest

The authors declare no conflict of interest.

Acknowledgements

We honor the pioneering work of Dave Stahl and Michael Wagner on the evolutionary history of DsrAB and are grateful for the inspiring discussions we had over the years. We further thank the former master/PhD students Ivan Barisic, Norbert Bittner, Christina Braunegger, Stephan Duller, Diana Lebherz-Eichinger, Sebastian Lückner, Doris Steger and Cecilia Wentrup for their contributions in updating and maintaining our in-house *dsrAB* database. Craig Herbold and Kenneth Wasmund are acknowledged for critically revising the manuscript. This work was financially supported by the Austrian Science Fund (FWF, P23117-B17 to MP and AL; P25111-B22 to AL), the Danish National Research Foundation (to KUK), the German Research Foundation (DFG PE 2147/1-1 to MP) and the Zukunftskolleg of the University of Konstanz (to MP).

References

- Anantharaman K, Duhaime MB, Breier JA, Wendt KA, Toner BM, Dick GJ. (2014). Sulfur oxidation genes in diverse deep-sea viruses. *Science* **344**: 757–760.
- Bazylinski DA, Williams TJ, Lefevre CT, Berg RJ, Zhang CLL, Bowser SS *et al.* (2013). *Magnetococcus marinus* gen. nov., sp. nov., a marine, magnetotactic bacterium that represents a novel lineage (Magnetococcaceae fam. nov., Magnetococcales ord. nov.) at the base of the Alpha-proteobacteria. *Int J Syst Evol Microbiol* **63**: 801–808.
- Berger SA, Krompass D, Stamatakis A. (2011). Performance, accuracy, and web server for evolutionary placement of short sequence reads under maximum likelihood. *Syst Biol* **60**: 291–302.
- Bowles MW, Mogollon JM, Kasten S, Zabel M, Hinrichs KU. (2014). Global rates of marine sulfate reduction and implications for sub-sea-floor metabolic activities. *Science* **344**: 889–891.
- Brauman A, Müller JA, Garcia JL, Brune A, Schink B. (1998). Fermentative degradation of 3-hydroxybenzoate in pure culture by a novel strictly anaerobic bacterium, *Sporotomaculum hydroxybenzoicum* gen. nov., sp. nov. *Int J Syst Bacteriol* **48**(Part 1): 215–221.

- Brochier-Armanet C, Forterre P, Gribaldo S. (2011). Phylogeny and evolution of the Archaea: one hundred genomes later. *Curr Opin Microbiol* **14**: 274–281.
- Camacho C, Coulouris G, Avagyan V, Ma N, Papadopoulos J, Bealer K *et al.* (2009). BLAST+: architecture and applications. *BMC Bioinform* **10**: 421.
- Canfield DE, Raiswell R. (1999). The evolution of the sulfur cycle. *Am J Sci* **299**: 697–723.
- Dahl C, Kredich NM, Deutzmann R, Trüper HG. (1993). Dissimilatory sulphite reductase from *Archaeoglobus fulgidus*: physico-chemical properties of the enzyme and cloning, sequencing and analysis of the reductase genes. *J Gen Microbiol* **139**: 1817–1828.
- Dahl C, Engels S, Pott-Sperling AS, Schulte A, Sander J, Lübke Y *et al.* (2005). Novel genes of the *dsr* gene cluster and evidence for close interaction of Dsr proteins during sulfur oxidation in the phototrophic sulfur bacterium *Allochromatium vinosum*. *J Bacteriol* **187**: 1392–1404.
- Devkota S, Wang Y, Musch MW, Leone V, Fehlner-Peach H, Nadimpalli A *et al.* (2012). Dietary-fat-induced taurocholic acid promotes pathobiont expansion and colitis in *Il10^{-/-}* mice. *Nature* **487**: 104–108.
- Dhillon A, Teske A, Dillon J, Stahl DA, Sogin ML. (2003). Molecular characterization of sulfate-reducing bacteria in the Guaymas Basin. *Appl Environ Microbiol* **69**: 2765–2772.
- Dhillon A, Goswami S, Riley M, Teske A, Sogin M. (2005). Domain evolution and functional diversification of sulfite reductases. *Astrobiology* **5**: 18–29.
- Euzéby JP. (1997). List of Bacterial Names with Standing in Nomenclature: a folder available on the Internet. *Int J Syst Bacteriol* **47**: 590–592.
- Finster K. (2008). Microbiological disproportionation of inorganic sulfur compounds. *J Sulfur Chem* **29**: 281–292.
- Friedrich CG, Bardischewsky F, Rother D, Quentmeier A, Fischer J. (2005). Prokaryotic sulfur oxidation. *Curr Opin Microbiol* **8**: 253–259.
- Frigaard N-U, Bryant D. (2008). Genomic and evolutionary perspectives on sulfur metabolism in green sulfur bacteria. In: Dahl C, Friedrich C (eds) *Microbial Sulfur Metabolism*. Springer: Berlin, Heidelberg, Germany, pp 60–76.
- Geets J, Borremans B, Vangronsveld J, Diels L, van der Lelie D. (2005). Molecular monitoring of SRB community structure and dynamics in batch experiments to examine the applicability of in situ precipitation of heavy metals for groundwater remediation. *J Soils Sedim* **5**: 149–163.
- Gogarten JP, Doolittle WF, Lawrence JG. (2002). Prokaryotic evolution in light of gene transfer. *Mol Biol Evol* **19**: 2226–2238.
- Gumerov VM, Mardanov AV, Beletsky AV, Prokofeva MI, Bonch-Osmolovskaya EA, Ravin NV *et al.* (2011). Complete genome sequence of ‘*Vulcanisaeta moutnovskia*’ strain 768-28, a novel member of the hyperthermophilic crenarchaeal genus *Vulcanisaeta*. *J Bacteriol* **193**: 2355–2356.
- Higuchi R, Fockler C, Dollinger G, Watson R. (1993). Kinetic PCR analysis: real-time monitoring of DNA amplification reactions. *Biotechnology (NY)* **11**: 1026–1030.
- Huston DL, Logan GA. (2004). Barite, BIFs and bugs: evidence for the evolution of the Earth’s early hydrosphere. *Earth Planet Sci Lett* **220**: 41–55.
- Imachi H, Sekiguchi Y, Kamagata Y, Loy A, Qiu YL, Hugenholtz P *et al.* (2006). Non-sulfate-reducing, syntrophic bacteria affiliated with desulfotomaculum cluster I are widely distributed in methanogenic environments. *Appl Environ Microbiol* **72**: 2080–2091.
- Itoh T, Suzuki K, Sanchez PC, Nakase T. (1999). *Caldivirga maquilensis* gen. nov., sp. nov., a new genus of rod-shaped crenarchaeote isolated from a hot spring in the Philippines. *Int J Syst Bacteriol* **49**(Pt 3): 1157–1163.
- Itoh T, Suzuki K, Nakase T. (2002). *Vulcanisaeta distributa* gen. nov., sp. nov., and *Vulcanisaeta souniana* sp. nov., novel hyperthermophilic, rod-shaped crenarchaeotes isolated from hot springs in Japan. *Int J Syst Evol Microbiol* **52**: 1097–1104.
- Jakobsen TF, Kjeldsen KU, Ingvorsen K. (2006). *Desulfohalobium utahense* sp. nov., a moderately halophilic, sulfate-reducing bacterium isolated from Great Salt Lake. *Int J Syst Evol Microbiol* **56**: 2063–2069.
- Johnson EF, Mukhopadhyay B. (2005). A new type of sulfite reductase, a novel coenzyme F420-dependent enzyme, from the methanarchaeon *Methanocaldococcus jannaschii*. *J Biol Chem* **280**: 38776–38786.
- Kaneko R, Hayashi T, Tanahashi M, Naganuma T. (2007). Phylogenetic diversity and distribution of dissimilatory sulfite reductase genes from deep-sea sediment cores. *Mar Biotechnol (NY)* **9**: 429–436.
- Karkhoff-Schweizer RR, Huber DP, Voordouw G. (1995). Conservation of the genes for dissimilatory sulfite reductase from *Desulfovibrio vulgaris* and *Archaeoglobus fulgidus* allows their detection by PCR. *Appl Environ Microbiol* **61**: 290–296.
- Kelly DP, Shergill JK, Lu WP, Wood AP. (1997). Oxidative metabolism of inorganic sulfur compounds by bacteria. *Antonie Van Leeuwenhoek* **71**: 95–107.
- Kjeldsen KU, Loy A, Jakobsen TF, Thomsen TR, Wagner M, Ingvorsen K. (2007). Diversity of sulfate-reducing bacteria from an extreme hypersaline sediment, Great Salt Lake (Utah). *FEMS Microbiol Ecol* **60**: 287–298.
- Klein M, Friedrich M, Roger AJ, Hugenholtz P, Fishbain S, Abicht H *et al.* (2001). Multiple lateral transfers of dissimilatory sulfite reductase genes between major lineages of sulfate-reducing prokaryotes. *J Bacteriol* **183**: 6028–6035.
- Kletzin A, Urich T, Muller F, Bandejas TM, Gomes CM. (2004). Dissimilatory oxidation and reduction of elemental sulfur in thermophilic archaea. *J Bioenerg Biomembr* **36**: 77–91.
- Kondo R, Nedwell DB, Purdy KJ, Silva SD. (2004). Detection and enumeration of sulphate-reducing bacteria in estuarine sediments by competitive PCR. *Geomicrobiol J* **21**: 145–157.
- Koonin EV, Makarova KS, Aravind L. (2001). Horizontal gene transfer in prokaryotes: quantification and classification. *Annu Rev Microbiol* **55**: 709–742.
- Larsen O, Lien T, Birkeland NK. (1999). Dissimilatory sulfite reductase from *Archaeoglobus profundus* and *Desulfohalobium thermocisternum*: phylogenetic and structural implications from gene sequences. *Extremophiles* **3**: 63–70.
- Leloup J, Quillet L, Berthe T, Petit F. (2006). Diversity of the *dsrAB* (dissimilatory sulfite reductase) gene sequences retrieved from two contrasting mudflats of the Seine estuary, France. *FEMS Microbiol Ecol* **55**: 230–238.

- Leloup J, Fossing H, Kohls K, Holmkvist L, Borowski C, Jørgensen BB. (2009). Sulfate-reducing bacteria in marine sediment (Aarhus Bay, Denmark): abundance and diversity related to geochemical zonation. *Environ Microbiol* **11**: 1278–1291.
- Lenk S, Arnds J, Zerjatke K, Musat N, Amann R, Mussmann M. (2011). Novel groups of Gamma-proteobacteria catalyse sulfur oxidation and carbon fixation in a coastal, intertidal sediment. *Environ Microbiol* **13**: 758–774.
- Lever MA, Rouxel O, Alt JC, Shimizu N, Ono S, Coggon RM *et al.* (2013). Evidence for microbial carbon and sulfur cycling in deeply buried ridge flank basalt. *Science* **339**: 1305–1308.
- Loy A, Lehner A, Lee N, Adamczyk J, Meier H, Ernst J *et al.* (2002). Oligonucleotide microarray for 16S rRNA gene-based detection of all recognized lineages of sulfate-reducing prokaryotes in the environment. *Appl Environ Microbiol* **68**: 5064–5081.
- Loy A, Arnold R, Tischler P, Rattei T, Wagner M, Horn M. (2008a). probeCheck—a central resource for evaluating oligonucleotide probe coverage and specificity. *Environ Microbiol* **10**: 2894–2898.
- Loy A, Duller S, Wagner M. (2008b). Evolution and ecology of microbes dissimilating sulfur compounds: insights from siroheme sulfite reductases. In: Dahl C (ed) *Microbial Sulfur Metabolism*. Springer: Berlin, Germany, pp 46–59.
- Loy A, Duller S, Baranyi C, Mussmann M, Ott J, Sharon I *et al.* (2009). Reverse dissimilatory sulfite reductase as phylogenetic marker for a subgroup of sulfur-oxidizing prokaryotes. *Environ Microbiol* **11**: 289–299.
- Ludwig W, Strunk O, Westram R, Richter L, Meier H, Yadhukumar *et al.* (2004). ARB: a software environment for sequence data. *Nucleic Acids Res* **32**: 1363–1371.
- Lukat P, Rudolf M, Stach P, Messerschmidt A, Kroneck PM, Simon J *et al.* (2008). Binding and reduction of sulfite by cytochrome *c* nitrite reductase. *Biochemistry* **47**: 2080–2086.
- Martinez CE, Yanez C, Yoon SJ, Bruns MA. (2007). Biogeochemistry of metalliferous peats: sulfur speciation and depth distributions of dsrAB genes and Cd, Fe, Mn, S, and Zn in soil cores. *Environ Sci Technol* **41**: 5323–5329.
- Mavromatis K, Sikorski J, Pabst E, Teshima H, Lapidus A, Lucas S *et al.* (2010). Complete genome sequence of *Vulcanisaeta distributa* type strain (IC-017). *Stand Genom Sci* **3**: 117–125.
- Milucka J, Ferdelman TG, Polerecky L, Franzke D, Wegener G, Schmid M *et al.* (2012). Zero-valent sulphur is a key intermediate in marine methane oxidation. *Nature* **491**: 541–546.
- Molitor M, Dahl C, Molitor I, Schäfer U, Speich N, Huber R *et al.* (1998). A dissimilatory sirohaem-sulfite-reductase-type protein from the hyperthermophilic archaeon *Pyrobaculum islandicum*. *Microbiology* **144**(Pt 2): 529–541.
- Moreau JW, Zierenberg RA, Banfield JF. (2010). Diversity of dissimilatory sulfite reductase genes (dsrAB) in a salt marsh impacted by long-term acid mine drainage. *Appl Environ Microbiol* **76**: 4819–4828.
- Mori Y, Purdy KJ, Oakley BB, Kondo R. (2010). Comprehensive detection of phototrophic sulfur bacteria using PCR primers that target reverse dissimilatory sulfite reductase gene. *Microbes Environ* **25**: 190–196.
- Mussmann M, Brito I, Pitcher A, Sinnighe Damste JS, Hatzepichler R, Richter A *et al.* (2011). Thaumarchaeotes abundant in refinery nitrifying sludges express amoA but are not obligate autotrophic ammonia oxidizers. *Proc Natl Acad Sci USA* **108**: 16771–16776.
- Muyzer G, Stams AJ. (2008). The ecology and biotechnology of sulphate-reducing bacteria. *Nat Rev Microbiol* **6**: 441–454.
- Nakagawa T, Nakagawa S, Inagaki F, Takai K, Horikoshi K. (2004). Phylogenetic diversity of sulfate-reducing prokaryotes in active deep-sea hydrothermal vent chimney structures. *FEMS Microbiol Lett* **232**: 145–152.
- Nunoura T, Takaki Y, Kakuta J, Nishi S, Sugahara J, Kazama H *et al.* (2011). Insights into the evolution of Archaea and eukaryotic protein modifier systems revealed by the genome of a novel archaeal group. *Nucleic Acids Res* **39**: 3204–3223.
- Ollivier B, Hatchikian C, Prensier G, Guezennec J, Garcia J-L. (1991). *Desulfohalobium retbaense* gen. nov., sp. nov., a halophilic sulfate-reducing bacterium from sediments of a hypersaline lake in Senegal. *Int J Syst Bacteriol* **41**: 74–81.
- Pereira IA, Ramos AR, Grein F, Marques MC, da Silva SM, Venceslau SS. (2011). A comparative genomic analysis of energy metabolism in sulfate reducing bacteria and archaea. *Front Microbiol* **2**: 69.
- Pester M, Bittner N, Deevong P, Wagner M, Loy A. (2010). A 'rare biosphere' microorganism contributes to sulfate reduction in a peatland. *ISME J* **4**: 1591–1602.
- Pester M, Knorr KH, Friedrich MW, Wagner M, Loy A. (2012). Sulfate-reducing microorganisms in wetlands—fameless actors in carbon cycling and climate change. *Front Microbiol* **3**: 72.
- Pierce E, Xie G, Barabote RD, Saunders E, Han CS, Detter JC *et al.* (2008). The complete genome sequence of *Moorella thermoacetica* (f. *Clostridium thermoaceticum*). *Environ Microbiol* **10**: 2550–2573.
- Pikuta EV, Hoover RB, Bej AK, Marsic D, Whitman WB, Cleland D *et al.* (2003). *Desulfonatronum thiodismutans* sp. nov., a novel alkaliphilic, sulfate-reducing bacterium capable of lithoautotrophic growth. *Int J Syst Evol Microbiol* **53**: 1327–1332.
- Pott AS, Dahl C. (1998). Sirohaem sulfite reductase and other proteins encoded by genes at the dsr locus of *Chromatium vinosum* are involved in the oxidation of intracellular sulfur. *Microbiology* **144**(Part 7): 1881–1894.
- Rapp BJ, Wall JD. (1987). Genetic transfer in *Desulfovibrio desulfuricans*. *Proc Natl Acad Sci USA* **84**: 9128–9130.
- Schedel M, Trüper HG. (1979). Purification of *Thiobacillus denitrificans* siroheme sulfite reductase and investigation of some molecular and catalytic properties. *Biochim Biophys Acta* **568**: 454–466.
- Sheik CS, Jain S, Dick GJ. (2014). Metabolic flexibility of enigmatic SAR324 revealed through metagenomics and metatranscriptomics. *Environ Microbiol* **16**: 304–317.
- Simon J, Kroneck P. (2013). Microbial sulfite respiration. *Adv Microb Physiol* **62**: 45–117.
- Sorokin DY, Tourova TP, Henstra AM, Stams AJ, Galinski EA, Muyzer G. (2008). Sulfidogenesis under extremely haloalkaline conditions by *Desulfonatronospira thiodismutans* gen. nov., sp. nov., and *Desulfonatronospira delicata* sp. nov.—a novel lineage of Deltaproteobacteria from hypersaline soda lakes. *Microbiology* **154**: 1444–1453.

- Stackebrandt E, Ebers J. (2006). Taxonomic parameters revisited: tarnished gold standards. *Microbiol Today* **33**: 152–155.
- Stamatakis A. (2006). RAxML-VI-HPC: maximum likelihood-based phylogenetic analyses with thousands of taxa and mixed models. *Bioinformatics* **22**: 2688–2690.
- Stanton TB. (2007). Prophage-like gene transfer agents-novel mechanisms of gene exchange for *Methanococcus*, *Desulfovibrio*, *Brachyspira*, and *Rhodobacter* species. *Anaerobe* **13**: 43–49.
- Steger D, Wentrup C, Braunegeer C, Deevong P, Hofer M, Richter A *et al.* (2011). Microorganisms with novel dissimilatory (bi)sulfite reductase genes are widespread and part of the core microbiota in low-sulfate peatlands. *Appl Environ Microbiol* **77**: 1231–1242.
- Suzuki Y, Kelly SD, Kemner KM, Banfield JF. (2005). Direct microbial reduction and subsequent preservation of uranium in natural near-surface sediment. *Appl Environ Microbiol* **71**: 1790–1797.
- Suzuki D, Li Z, Cui X, Zhang C, Katayama A. (2014). Reclassification of *Desulfobacterium anilini* as *Desulfatiglans anilini* comb. nov. within *Desulfatiglans* gen. nov., and description of a 4-chlorophenol-degrading sulfate-reducing bacterium, *Desulfatiglans parachlorophenolica* sp. nov. *Int J Syst Evol Microbiol* **64**(Part 9): 3081–3086.
- Swan BK, Martinez-Garcia M, Preston CM, Sczyrba A, Woyke T, Lamy D *et al.* (2011). Potential for chemolithoautotrophy among ubiquitous bacteria lineages in the dark ocean. *Science* **333**: 1296–1300.
- Wagner M, Roger AJ, Flax JL, Brusseau GA, Stahl DA. (1998). Phylogeny of dissimilatory sulfite reductases supports an early origin of sulfate respiration. *J Bacteriol* **180**: 2975–2982.
- Wagner M, Loy A, Klein M, Lee N, Ramsing NB, Stahl DA *et al.* (2005). Functional marker genes for identification of sulfate-reducing prokaryotes. *Methods Enzymol* **397**: 469–489.
- Walker CB, Stolyar SS, Pinel N, Yen HC, He Z, Zhou J *et al.* (2006). Recovery of temperate *Desulfovibrio vulgaris* bacteriophage using a novel host strain. *Environ Microbiol* **8**: 1950–1959.
- Wu XJ, Pan JL, Liu XL, Tan J, Li DT, Yang H. (2009). Sulfate-reducing bacteria in leachate-polluted aquifers along the shore of the East China Sea. *Can J Microbiol* **55**: 818–828.
- Yang Z. (1997). PAML: a program package for phylogenetic analysis by maximum likelihood. *Comput Appl Biosci* **13**: 555–556.
- Yang Z, Nielsen R, Goldman N, Pedersen AM. (2000). Codon-substitution models for heterogeneous selection pressure at amino acid sites. *Genetics* **155**: 431–449.
- Zverlov V, Klein M, Lückner S, Friedrich MW, Kellermann J, Stahl DA *et al.* (2005). Lateral gene transfer of dissimilatory (bi)sulfite reductase revisited. *J Bacteriol* **187**: 2203–2208.



This work is licensed under a Creative Commons Attribution-NonCommercial-ShareAlike 3.0 Unported License. The images or other third party material in this article are included in the article's Creative Commons license, unless indicated otherwise in the credit line; if the material is not included under the Creative Commons license, users will need to obtain permission from the license holder to reproduce the material. To view a copy of this license, visit <http://creativecommons.org/licenses/by-nc-sa/3.0/>

Supplementary Information accompanies this paper on The ISME Journal website (<http://www.nature.com/ismej>)

SUPPLEMENTARY INFORMATION

Phylogenetic and environmental diversity of DsrAB-type dissimilatory (bi)sulfite reductases

Albert Leopold Müller, Kasper Urup Kjeldsen, Thomas Rattei, Michael Pester, and Alexander Loy

SUPPLEMENTARY MATERIALS AND METHODS

Recovery of *dsrAB* sequences from public databases using tblastx analysis

A bit score threshold for retrieving *dsrAB* sequences from public databases was defined by blasting entries of a *dsrAB* in-house ‘seed’ database (n=998) against each other with archaeal type *dsrAB* sequences serving as the outgroup for bacterial type *dsrAB* sequences and vice versa. The highest bit score of the outgroup entries + 10% (to make the search more conservative) was then used as a bit score threshold for each *dsrAB* seed entry. Subsequently, each *dsrAB* seed entry with its own threshold was blasted against NCBI’s non-redundant and environmental databases (Benson *et al.*, 2014), the IMG/M database (Markowitz *et al.*, 2012) and the Camera database (Sun *et al.*, 2011). Metagenomic databases were filtered to exclude short single reads (<400 bp) in order to enhance search speed. Since we aimed at recovering continuous nucleic acid sequences of *dsrAB* with the intergenic region in addition to partial *dsrA* and *dsrB* sequences, we did not use the FunGene database (Fish *et al.*, 2013) that only collects individual *dsrA* and *dsrB* sequences from GenBank based on a Hidden Markov Model.

Ecological classification of *dsrAB* sequences

To analyze general habitat patterns, *dsrAB* sequences were assigned to broad environmental categories based on the qualitative description submitted with the sequence and/or the information in the publication. Categories based on the environmental origin of the sample (marine, estuarine, freshwater, soil, and industrial) were complemented by categories denoting special microbial lifestyles (thermophilic, alkali-/halophilic, and symbiotic). Sequences were not assigned to multiple categories, in case of sequences fitting in two or more categories, lifestyle categories were given precedence (i.e. a sequence from a marine thermophile would be classified as thermophilic and not as marine).

Tree calculations

Maximum likelihood (RAxML (Stamatakis, 2006), Dayhoff amino acid substitution model) and maximum parsimony (PHYLP PROTPARS) trees were calculated in ARB. Neighbor joining trees (PHYLP NEIGHBOR) were calculated in the PHYLP software package (Felsenstein, 1989) based on the JTT matrix model (Jones *et al.*, 1992). The three trees were combined into a consensus tree by using the extended majority rule in PHYLP CONSENSE. Branch lengths of the consensus tree were inferred by using the JTT matrix model (PHYLP PROML). Bootstrap analysis was performed with all three methods with 100 or 1,000 re-samplings, depending on the size of the tree. In order to save computation time, sequences were clustered at 97% amino acid identity using the average neighbor algorithm in mother (Schloss *et al.*, 2009) and only a representative sequence of each cluster was used for calculation of the larger trees. The other sequences were subsequently added to the consensus tree using the ARB Parsimony interactive tool using the same alignment filter as for tree calculation. Trees were visualized using iTOL (Letunic & Bork, 2007).

For comparison of tree topologies, DsrAB and 16S rRNA trees were based on corresponding data sets, that is, the same number of organisms, to avoid sampling artifacts. Consensus trees were constructed using the strict consensus rule setting to allow for more polytomies and thus conservative, but more robust phylogenies (Ludwig *et al.*, 2004). DsrAB trees were calculated as mentioned previously. 16S rRNA trees were calculated using maximum likelihood (RAxML), maximum parsimony (PHYLP DNAPARS), and neighbor joining (PHYLP NEIGHBOR) methods and branch lengths in the 16S rRNA consensus tree were adjusted using PHYLP DNAML.

Uncultured family-level DsrAB lineages

By adapting previously established criteria (Pester *et al.*, 2012), environmental DsrAB sequences were assigned into uncultured family-level lineages. First, sequences sharing $\geq 64\%$ amino acid identity were clustered into groups using the furthest neighbor algorithm in mothur (Schloss *et al.*, 2009). This very conservative threshold was based on minimum intra-family amino acid sequence identities of known families of sulfate-reducing microorganisms (SRM), which range from 64% to 89%. Second, a $\geq 64\%$ DsrAB sequence identity cluster was only designated as an “uncultured DsrAB lineage” if it consisted of at least three sequences and formed a monophyletic group in the extended majority rule-based consensus tree with a bootstrap support of $>70\%$ in at least two treeing methods. CodeML (PAML 4.8) (Yang, 2007) was used to determine non-synonymous/synonymous substitution rate ratios for the uncultured DsrAB lineages.

Comparisons between *dsrAB* and 16S rRNA gene identities

Gene identity plots of *dsrAB* and 16S rRNA genes of organisms for which both genes are known were performed in R (R Development Core Team, 2008) using nucleic acid distance matrices calculated in ARB without an alignment filter. A nucleotide identity species-level threshold for bacterial type *dsrAB* was inferred from a *dsrAB*/16S rRNA gene identity plot of organisms with non-laterally acquired bacterial type *dsrAB*. A 99% nucleotide similarity was used as a threshold for approximate species level assignment on 16S rRNA level (Stackebrandt & Ebers, 2006).

SUPPLEMENTARY RESULTS AND DISCUSSION

The four families and root of the DsrAB tree

Since *dsrA* and *dsrB* originated from an ancient gene duplication event that likely preceded the divergence of the bacterial and archaeal domains of life (Dahl *et al.*, 1993; Wagner *et al.*, 1998), it is possible to determine the root of the DsrAB tree by paralogous rooting (Iwabe *et al.*, 1989). An alignment of DsrA to DsrB based on 163 conserved homologous amino acid positions supports a nearly bilaterally symmetrical tree in which DsrA and DsrB sequences form mirrored branches converging at the root (Supplementary Figure S4). The family of oxidative DsrAB sequences from sulfide-oxidizing bacteria (SOB) branches off after the split between bacterial type and archaeal type sequences and thus likely represents a secondary, functional diversification. Hence, the branching pattern suggests that ancestral DsrAB functioned in the reductive direction, a finding that is corroborated by geochemical data that suggests that sulfite reduction occurred very early in Earth's history and possibly predated the evolution of sulfate reduction (Skyring & Donnelly, 1982). It is not possible to conclusively determine the root of the DsrAB tree with respect to the fourth type of DsrAB family, constituted by the exceptional second DsrAB copy of *Moorella thermoacetica*, because its position differs in the DsrA and DsrB branches of the tree (Supplementary Figure S4). The basal placement of the *M. thermoacetica* DsrAB copy 2 subunits in the DsrA/DsrB paralog tree might be a treeing artifact caused by long-branch attraction (Bergsten, 2005) between the two subunits. We thus performed long-branch extraction (Siddall & Whiting, 1999) by repeating the tree calculation and by either omitting the DsrA or the DsrB subunit of *M. thermoacetica* DsrAB copy 2 in any one calculation. Erroneous phylogenetic placement of *M. thermoacetica* DsrAB copy 2 is unlikely because the phylogenetic position of the respective subunit in both test trees was identical to the position in the tree calculated with both subunits (data not shown). We thus conclude that the root of the DsrAB tree is either between *M. thermoacetica* DsrAB copy 2 and all other DsrAB sequences or between the *M. thermoacetica* DsrAB copy 2/reductive archaeal type DsrAB branch and the oxidative/reductive bacterial type DsrAB branch.

DsrAB consensus phylogeny and members of main lineages

Reductive bacterial type DsrAB. The *Deltaproteobacteria* supercluster contains the majority of known bacterial type DsrAB sequences, including *dsrAB* from all deltaproteobacterial SRM, *Deltaproteobacteria*-related *dsrAB* from (mostly) thermophilic sulfate and/or sulfite-reducing members of the phyla *Firmicutes* (i.e., members of *Desulfotomaculum* subclusters Ib, Ic, Id, and Ie, *Ammonifex degensii*, *Candidatus Desulforudis audaxviator*, *Desulfoviregula thermocuniculi*, *Sporotomaculum hydroxybenzoicum*, and *Moorella thermoacetica dsrAB* copy 1) and *Thermodesulfobacteria* (*Thermodesulfobacterium* and *Thermodesulfatator*), uncultured DsrAB lineages 1 and 11 and other environmental sequences (Figure 1, Supplementary Figure S1). We have renamed the *Thermodesulfobacterium* supercluster into *Nitrospirae* supercluster because it now comprises *dsrAB* from two taxa within the phylum *Nitrospirae*, namely the genus *Thermodesulfobacterium* and *Candidatus Magnetobacterium casensis* (Lin *et al.*, 2014). The *Nitrospirae* supercluster additionally contains uncultured DsrAB lineage 10 and 13, and other environmental sequences. The environmental supercluster 1 does so far not contain *dsrAB* from any cultured organism and includes uncultured DsrAB lineages 8, 9, and 12, and other environmental *dsrAB* sequences. Most sequences from cultured organisms in the *Firmicutes* group belong to the phylum *Firmicutes* (i.e., the SRM genera *Desulfotomaculum*, *Desulfosporosinus*, and *Desulfurispora*, the non-SRM genera *Desulfitobacterium*, *Carboxydotherrmus*, *Desulfitibacter*, and *Thermanaeromonas* that are able to reduce other sulfur compounds, the syntroph *Pelotomaculum propionicum*, and members of the family *Sporomusaceae* (Yutin & Galperin, 2013), the acetogen *Acetonebma longum* and the thiosulfate-utilizing *Thermosinus carboxydivorans*) yet these do not form a monophyletic DsrAB cluster. Instead, they are phylogenetically intermingled with members of the taxonomically uncertain genus *Thermodesulfobium* (Mori *et al.*, 2003), *dsrAB*-carrying members of the phyla *Actinobacteria*, *Aigarchaeota* and *Caldiserica*, uncultured DsrAB lineages 2 to 7, and other environmental *dsrAB* sequences (Figure 1, Supplementary Figure S1). Continuous genomic analysis of cultured microorganisms or single microbial cells has led to the discovery of *dsrAB* in members of phyla previously not known to possess these genes. Hence, DsrAB-coding genes were detected on amplified genomes of individual cells belonging to the bacterial phylum *Caldiserica* (JGI_0000059-M03, accession AQSQ01000030) and the archaeal candidate phylum *Aigarchaeota* (pSL4 archaeon JGI_0000106-J15, accession ASPF01000004) (Rinke *et al.*, 2013) (Figure 1). The phylum *Caldiserica* (formerly known as candidate phylum OP5) so far contains only one characterized species, *Caldisericum exile*, which uses thiosulfate, sulfite, and elemental sulfur, but not sulfate, as electron acceptors, yet its genome (NC_017096) does not contain *dsrAB* (Mori *et al.*, 2009). The genome of the intestinal actinobacterium *Gordonibacter pamelaee* (NC_021021) (Würdemann *et al.*, 2009) also contains *dsrAB* that consistently cluster with the *Firmicutes* sister genera *Desulfosporosinus* and *Desulfitobacterium*. Importantly, *G. pamelaee*

lacks further genes of the canonical dissimilatory sulfate reduction pathway in its genome and is thus likely not an SRM.

Oxidative bacterial type DsrAB. The majority of oxidative DsrAB sequences belong to the *Gammaproteobacteria* cluster that contains cultivated members of families *Chromatiaceae* (nine genera), *Ectothiorhodospiraceae* (genera *Alkalilimnicola*, *Halorhodospira*, and *Thioalkalivibrio*) and *Thiotrichaceae* (genus *Thiothrix*) (Figure 1, Supplementary Figure S2). Interestingly, DsrAB of *Thioalkalivibrio nitratreducens* does not fall into this *Gammaproteobacteria* cluster, in contrast to sequences of the other members of the genus, *T. sulfidophilus*, *T. thiocyanodenitrificans*, and *T. paradoxus* [the genome sequence of *T. paradoxus*, NZ_AGFB01000003 was wrongly published as *T. thioicyanoxidans* (D.Y. Sorokin, personal communication) and has since been removed]. The second largest oxidative DsrAB cluster, the *Alphaproteobacteria* cluster, is subdivided into two main branches, one harbors members of the genera *Magnetospirillum* and *Azospirillum* (family *Rhodospirillaceae*, order *Rhodospirillales*), and the other contains *Rhodomicrobium vannielii* (family *Hyphomicrobiaceae*, order *Rhizobiales*) and environmental sequences. The *Betaproteobacteria* cluster contains *dsrAB* from members of the genus *Thiobacillus*, from *Sulfuricella denitrificans* (both family *Hydrogenophilaceae*, order *Hydrogenophilales*), and from *Sideroxydans lithotrophicus* (family *Gallionellaceae*, order *Gallionellales*). The *Chlorobi* cluster contains *dsrAB* from members of the family *Chlorobiaceae*. *Magnetococcus marinus* (family *Magnetococcaceae*, order *Magnetococcales*) has been provisionally included in the *Alphaproteobacteria* (Bazylinski *et al.*, 2013), but its DsrAB is very dissimilar from other alphaproteobacterial DsrAB and instead clusters with DsrAB of *Chlorobi* and the *deltaproteobacterial* SAR324 clade.

Reductive archaeal type DsrAB. This type of DsrAB is present in three genera of hyperthermophilic *Crenarchaeota* (*Pyrobaculum*, *Vulcanisaeta* and *Caldivirga*). Each of these three genera represents a distinct monophyletic group in the archaeal DsrAB tree with *Caldivirga maquilingensis*, an organism capable of reducing sulfate, thiosulfate and sulfur (Itoh *et al.*, 1999), occupying the deepest branch (Figure 1, Supplementary Figure S3). *C. maquilingensis* is the only organism in which the neighboring genes *dsrA* and *dsrB* are arranged in different directions. *Vulcanisaeta distributa* (Itoh *et al.*, 2002) and *V. moutnovskia* (Prokofeva *et al.*, 2005) utilize elemental sulfur and thiosulfate for growth. However, both species might also be capable of sulfate reduction (Itoh *et al.*, 2002) since genes for the complete canonical sulfate reduction pathway are present in their genomes (Mavromatis *et al.*, 2010; Gumerov *et al.*, 2011). All *Pyrobaculum* species seem to be capable of using thiosulfate as an electron acceptor (Völkl *et al.*, 1993; Molitor *et al.*, 1998; Huber *et al.*, 2000; Sako *et al.*, 2001; Amo *et al.*, 2002) and some were also shown to use elemental sulfur (*P. arsenaticum* (Huber *et al.*, 2000), *P. islandicum* (Molitor *et*

al., 1998), *P. neutrophilum* (Fischer *et al.*, 1983), *P. oguniense* (Sako *et al.*, 2001)) as a terminal electron acceptor whereas other species are inhibited by elemental sulfur (*P. aerophilum* (Völkl *et al.*, 1993), *P. caldifontis* (Amo *et al.*, 2002)). *P. islandicum* was also shown to utilize other sulfur compounds like sulfite, L-cysteine and oxidized glutathione (Molitor *et al.*, 1998). Interestingly, some but not all *Pyrobaculum* genomes harbor multiple *dsrAB* copies with a phylogeny that indicates a complex evolutionary history of *dsrAB* in members of this genus involving gene duplications, gene losses, and/or intra-genus LGT. Some *Pyrobaculum* species thus possess two (*P. aerophilum*, *P. caldifontis*) or three (*P. arsenaticum*, *P. oguniense*) *dsrAB* copies, all of which have intact reading frames and conserved siroheme binding sites. These multiple copies do not cluster together according to species affiliation (Supplementary Figure S3). No reports exist on function of specific copies of *dsrAB* in *Pyrobaculum* genomes and there is no obvious pattern regarding copy number and/or type and metabolic potential of *Pyrobaculum* species. Gene duplications can be a source of new protein functions because one (or both) of the now functionally redundant paralogs experience a period of relaxed selection and accelerated evolution (Ohno, 1970) in enzymes leading, for example, to different substrate affinities or specificities (Baani & Liesack, 2008). Presence of multiple *dsrAB* in some *Pyrobaculum* species is very unusual as *dsrAB* are mostly present as single-copy genes. The only other organisms known to possess more than one copy of *dsrAB* is *Moorella thermoacetica* with its two significantly different copies of *dsrAB*, and the SOB *Chlorobaculum tepidum*, which possesses two nearly identical *dsrAB* copies, but one has an authentic frameshift in *dsrB* and is likely not functional (Eisen *et al.*, 2002).

Moorella thermoacetica DsrAB copy 2. The unusual second *dsrAB* copy of *M. thermoacetica* is the only representative of this type of DsrAB. The two strains of *M. thermoacetica* for which genome sequences are available, strain ATCC 39073 (Pierce *et al.*, 2008) and strain Y72 (Tsukahara *et al.*, 2014), are the only bacteria known to possess two significantly different copies of *dsrAB*. The first copy (NC_007644, 1634923..1637803; BARR01000003, 15717..18335) is a bacterial DsrAB related to *Firmicutes* sequences within the *Deltaproteobacteria* supercluster, whereas the second copy (NC_007644, 1664993..1667213; BARR01000005, 9074..11294) is not closely related to other DsrAB sequences (Pierce *et al.*, 2008). *M. thermoacetica* can reduce thiosulfate and dimethylsulfoxide (Drake & Daniel, 2004) but nothing specific is known about the individual functions of its DsrAB copies.

Putative lateral gene transfers of *dsrAB*

Consensus trees of corresponding DsrAB and 16S rRNA sequences were compared for topological incongruences as signs of LGT (Figures 2 and 3). Additionally, we plotted identity values of 16S rRNA and *dsrAB* genes of pairs of pure cultures and genomes against each other

(Supplementary Figure S6). 16S rRNA gene and *dsrAB* identities are highly correlated, which indicates that these genes generally evolve in parallel at constant mutation rates. Considerable deviations from linear regression in such a plot thus indicate changes in the standard evolutionary mechanism. In comparisons of the major DsrAB families (Supplementary Figure S6), deviations towards the top left of the plot (*dsrAB* identity > 16S rRNA identity) is indicative of laterally acquired *dsrAB* (LA-*dsrAB*), while deviation towards the bottom right of the plot (*dsrAB* identity < 16S rRNA identity) might have multiple causes such as LGT, diversification of *dsrAB* through accelerated mutation or a combination of these processes with gene duplication/loss events.

DsrAB and 16S rRNA branching patterns are generally similar but show previously recognized and newly identified topological inconsistencies. Acquisition of *dsrAB* of a group of *Firmicutes* from deltaproteobacterial ancestors of the *Desulfatiglans anilini* (formerly *Desulfobacterium anilini*) (Suzuki et al., 2014)) lineage (Figure 2) (Klein et al., 2001; Zverlov et al., 2005) is confirmed by the *dsrAB*-16S rRNA gene identity plot. When compared with all organisms carrying “standard” vertically inherited bacterial *dsrAB*, non-LA-*dsrAB* *Firmicutes* cluster along the linear regression, while LA-*dsrAB* *Firmicutes* show slightly higher *dsrAB* gene identity (Supplementary Figure S6 B). Additionally, *dsrAB* of the latter organisms possess characteristic insertions that are typical for deltaproteobacterial *dsrAB* and provide further independent evidence of a deltaproteobacterial origin (Klein et al., 2001). It has been proposed that members of the phylum *Thermodesulfobacteria* (genera *Thermodesulfobacterium* and *Thermodesulfatator*) also have LA-*dsrAB* (Klein et al., 2001). *Thermodesulfobacteria* form a monophyletic branch within the *Deltaproteobacteria* cluster in the DsrAB tree (Figure 2) and possess the characteristic deltaproteobacterial *dsrAB* insertions, but, in contrast to *Firmicutes* with LA-*dsrAB*, show no deviations in the *dsrAB*-16S rRNA gene identity plot when compared to non-LA bacterial *dsrAB* (Supplementary Figure S6 C). Notably, it has recently been suggested that the phylogenetic inconsistency between 16S rRNA and DsrAB is due to incorrect placement of the phylum *Thermodesulfobacteria* in the 16S rRNA tree (Lang et al., 2013). Phylogenetic analysis of a set of 24 concatenated phylogenetic marker genes identified the *Thermodesulfobacteria* as a sister-group of the deltaproteobacterial order *Desulfovibrionales* (Lang et al., 2013). However, *Thermodesulfobacteria* were clearly unrelated to *Deltaproteobacteria* in another whole genome tree based on 38 concatenated marker genes (Rinke et al., 2013). Because of these conflicting findings, it currently remains unresolved if *Thermodesulfobacteria* received *dsrAB* via LGT.

All evidence points to a bacterial origin of *dsrAB* in members of the archaeal genus *Archaeoglobus*. *Archaeoglobus* DsrAB branches unambiguously in the reductive bacterial type DsrAB family (Klein et al., 2001) (Figure 2). Furthermore, *Archaeoglobus* species (*Euryarcheota*)

are more similar to bacteria on *dsrAB* level than to *Crenarchaeota* and thus deviate considerably from the linear regression of *dsrAB*-16S rRNA sequence identities, whereas *Crenarchaeota* do not (Supplementary Figure S6 C). This is consistent with paralogous rooting analysis and confirms an archaeal origin of *dsrAB* in *Crenarchaeota* members.

Analogous to *Archaeoglobus*, DsrAB in the *Aigarchaeota* member clearly belongs to the reductive bacterial type DsrAB family (Figures 1 and 2). Substantial differences in GC content between host genomes and acquired genes can be used to infer LGT events (Lawrence & Ochman, 1997) and a difference of more than 10% was previously used as an additional indication of LA-*dsrAB* (Klein et al., 2001). The GC content of the *dsrAB* sequence (44%) of the aigarchaeon is more than 10% different from the whole genome (38%), whereas the most closely related *dsrAB* sequences have GC contents between 51 and 55%, suggesting that *dsrAB* was relatively recently acquired from a donor with a higher genomic GC content and is currently undergoing evolutionary adaptation into the new genome (Lawrence & Ochman, 1997). The *Aigarchaeota* member also shows a deviation pattern in the *dsrAB*-16S rRNA gene identity plot that is similar to *Archaeoglobus*, with its *dsrAB* being much more similar to bacterial sequences than its 16S rRNA sequence (Supplementary Figure S6 C).

DsrAB of the actinobacterium *G. pamelaee* forms a stable monophyletic group with DsrAB of the *Firmicutes* genera *Desulfosporosinus* and *Desulfitobacterium* (Figures 1 and 2), which suggests that *G. pamelaee dsrAB* were laterally acquired from a *Firmicutes* member. However, there is no evidence that this potential LGT event occurred recently, since the GC content of *dsrAB* (65.3%, the highest value of any known organisms with a bacterial type DsrAB) is similar to the GC content of the whole genome (64%) of *G. pamelaee*, but considerably higher than the GC content of *dsrAB* and genome sequences of *Desulfosporosinus* and *Desulfitobacterium* species (41-49%). Furthermore, *dsrAB* of *G. pamelaee* lack a characteristic insertion at position 1053 that is shared by all *Desulfosporosinus* and *Desulfitobacterium* species. The *dsrAB*-16S rRNA gene identity plot does not suggest LGT (Supplementary Figure S6 C). So far *G. pamelaee* is the only member of the phylum *Actinobacteria* with *dsrAB* and there are no closely related environmental *dsrAB* sequences with a similar, high GC content that might hint at the presence of further actinobacterial *dsrAB* sequences in the database.

The branching patterns of the only known *dsrAB*-carrying member of the phylum *Caldiseirica* do not suggest LGT of its *dsrAB* as it branches deeply in both the DsrAB tree and the 16S rRNA tree (Figure 2). However, the GC content is >10% different between *dsrAB* (44.1%) and genome (35%) and more similar to phylogenetically related *dsrAB* sequences, hinting to lateral

acquisition. Furthermore, in the *dsrAB*-16S rRNA gene identity plot it shows considerable deviation from other bacterial *dsrAB* sequences (Supplementary Figure S6 C).

Primers targeting *dsrA* and *dsrB*

The very first *dsrAB*-targeted primers were designed on the basis of nucleotide sequence homologies of only two sequences, namely *dsrAB* from *Archaeoglobus fulgidus* and *Desulfovibrio vulgaris* (Karkhoff-Schweizer *et al.*, 1995). Shortly after, first versions of the now widely used DSR1F and DSR4R primers were published (Wagner *et al.*, 1998). They target highly conserved sequence regions of *dsrAB* and amplify a ~1.9kb fragment that covers approximately 85% of *dsrA*, 70% of *dsrB* and the intergenic spacer region between the two genes (Supplementary Figure S7). These degenerated primers were repeatedly updated by introducing additional primer variants (Loy *et al.*, 2004; Zverlov *et al.*, 2005; Pester *et al.*, 2010) and were modified (Kondo *et al.*, 2004; Suzuki *et al.*, 2005; Schmalenberger *et al.*, 2007; Loy *et al.*, 2009; Lenk *et al.*, 2011; Lever *et al.*, 2013) to adjust their coverage or improve PCR efficiency (Supplementary Tables S1 and S3). Also, several primers were developed that bind within the region amplified by DSR1F/DSR4R primer variants and were applied to amplify shorter fragments of either *dsrA* or *dsrB* for denaturing gradient gel electrophoresis (Geets *et al.*, 2005; Steger *et al.*, 2011), terminal restriction fragment length polymorphism analysis (Santillano *et al.*, 2010), quantitative real-time PCR (Kondo *et al.*, 2004; Ben-Dov *et al.*, 2007; Chin *et al.*, 2008; Gittel *et al.*, 2009; Pereyra *et al.*, 2010) or (nested) PCR (Dhillon *et al.*, 2003; Giloteaux *et al.*, 2010; Akob *et al.*, 2012; Lever *et al.*, 2013). Analogous to primers targeting the reductive bacterial type *dsrAB*, primers were also developed for oxidative bacterial type *dsrAB* of SOB (Loy *et al.*, 2009; Mori *et al.*, 2010; Lenk *et al.*, 2011; Luo *et al.*, 2011; Lever *et al.*, 2013) (Supplementary Tables S2 and S4). Primers for amplification of reductive, archaeal type *dsrAB* sequences or the second *dsrAB* copy of *M. thermoacetica* are not yet available.

REFERENCES

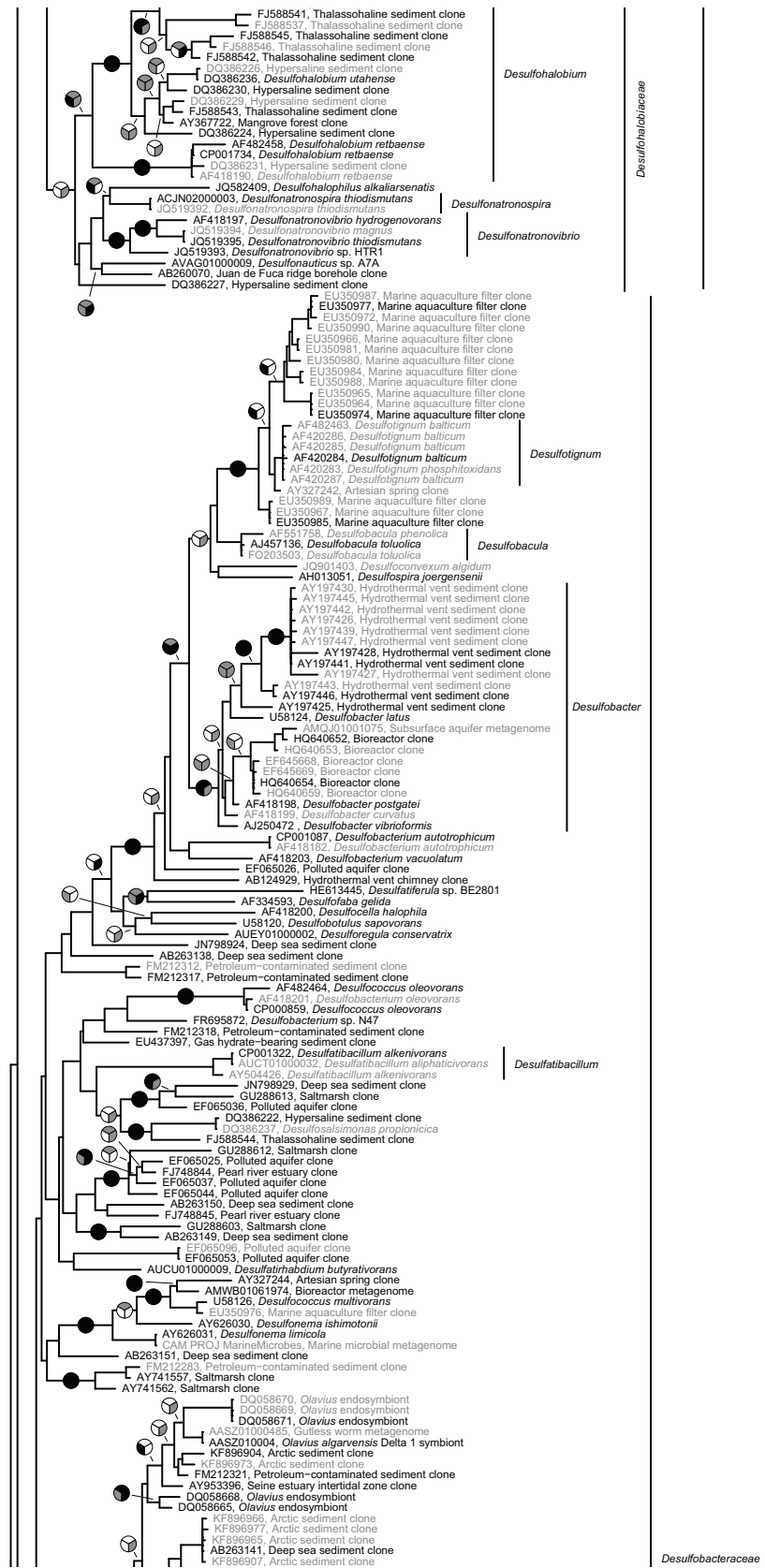
- Akob DM, Lee SH, Sheth M, Küsel K, Watson DB, Palumbo AV *et al.* (2012). Gene Expression Correlates with Process Rates Quantified for Sulfate- and Fe(III)-Reducing Bacteria in U(VI)-Contaminated Sediments. *Front Microbiol* **3**: 280.
- Amo T, Paje ML, Inagaki A, Ezaki S, Atomi H, Imanaka T. (2002). *Pyrobaculum calidifontis* sp. nov., a novel hyperthermophilic archaeon that grows in atmospheric air. *Archaea* **1**: 113-121.
- Baani M, Liesack W. (2008). Two isozymes of particulate methane monooxygenase with different methane oxidation kinetics are found in *Methylocystis* sp. strain SC2. *Proc Natl Acad Sci U S A* **105**: 10203-10208.
- Bazylinski DA, Williams TJ, Lefevre CT, Berg RJ, Zhang CLL, Bowser SS *et al.* (2013). *Magnetococcus marinus* gen. nov., sp. nov., a marine, magnetotactic bacterium that represents a novel lineage (Magnetococcaceae fam. nov., Magnetococcales ord. nov.) at the base of the Alphaproteobacteria. *Int J Syst Evol Microbiol* **63**: 801-808.

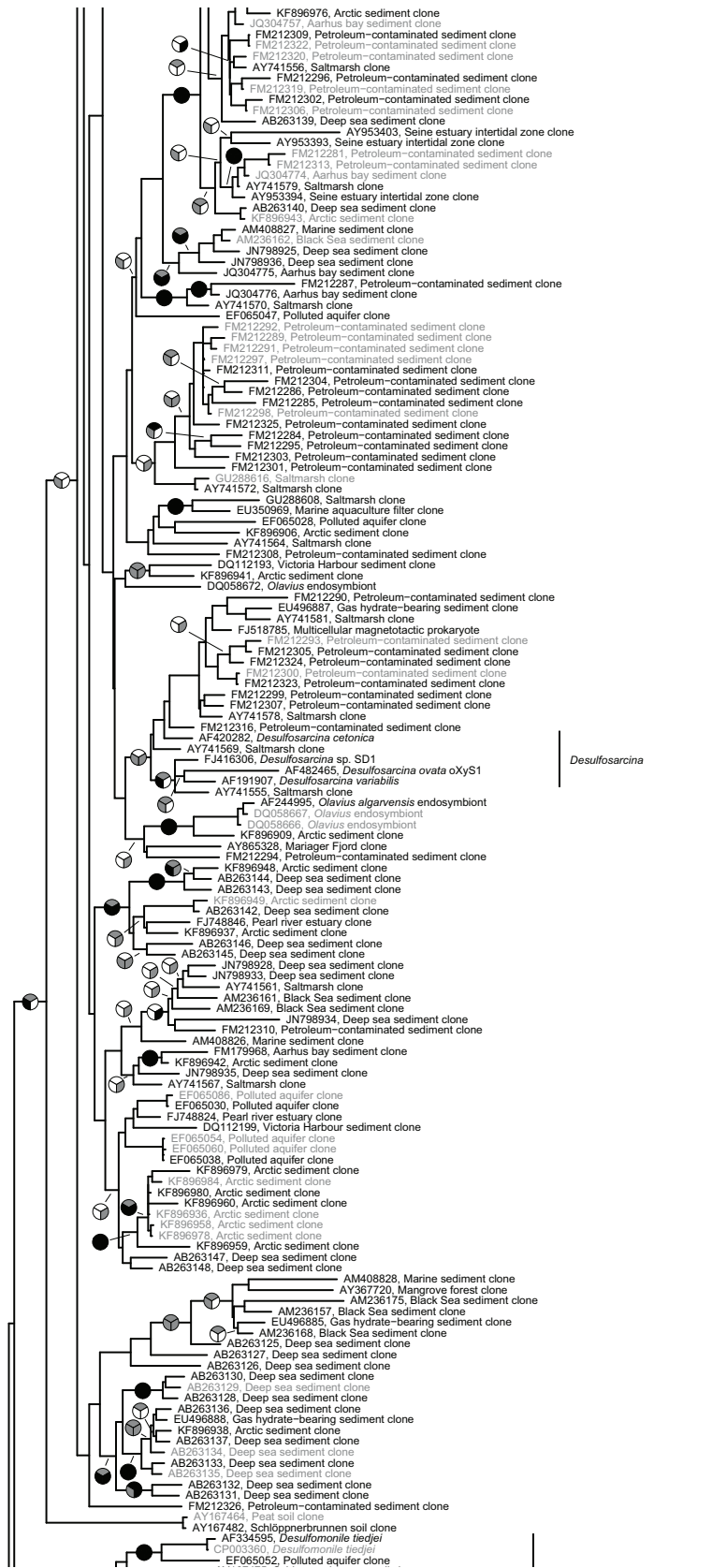
- Ben-Dov E, Brenner A, Kushmaro A. (2007). Quantification of sulfate-reducing bacteria in industrial wastewater, by real-time polymerase chain reaction (PCR) using *dsrA* and *apsA* genes. *Microb Ecol* **54**: 439-451.
- Benson DA, Clark K, Karsch-Mizrachi I, Lipman DJ, Ostell J, Sayers EW. (2014). GenBank. *Nucleic Acids Res* **42**: D32-37.
- Bergsten J. (2005). A review of long-branch attraction. *Cladistics* **21**: 163-193.
- Chin KJ, Sharma ML, Russell LA, O'Neill KR, Lovley DR. (2008). Quantifying expression of a dissimilatory (bi) sulfite reductase gene in petroleum-contaminated marine Harbor Sediments. *Microb Ecol* **55**: 489-499.
- Dahl C, Kredich NM, Deutzmann R, Trüper HG. (1993). Dissimilatory sulphite reductase from *Archaeoglobus fulgidus*: physico-chemical properties of the enzyme and cloning, sequencing and analysis of the reductase genes. *J Gen Microbiol* **139**: 1817-1828.
- Dhillon A, Teske A, Dillon J, Stahl DA, Sogin ML. (2003). Molecular characterization of sulfate-reducing bacteria in the Guaymas Basin. *Appl Environ Microbiol* **69**: 2765-2772.
- Drake HL, Daniel SL. (2004). Physiology of the thermophilic acetogen *Moorella thermoacetica* (vol 155, pg 422, 2004). *Res Microbiol* **155**: 868-883.
- Eisen JA, Nelson KE, Paulsen IT, Heidelberg JF, Wu M, Dodson RJ *et al.* (2002). The complete genome sequence of *Chlorobium tepidum* TLS, a photosynthetic, anaerobic, green-sulfur bacterium. *Proc Natl Acad Sci U S A* **99**: 9509-9514.
- Felsenstein J. (1989). PHYLIP-phylogeny inference package. *Cladistics* **5**: 163-166.
- Fischer F, Zillig W, Stetter KO, Schreiber G. (1983). Chemolithoautotrophic metabolism of anaerobic extremely thermophilic archaeobacteria. *Nature* **301**: 511-513.
- Fish JA, Chai B, Wang Q, Sun Y, Brown CT, Tiedje JM *et al.* (2013). FunGene: the functional gene pipeline and repository. *Front Microbiol* **4**: 291.
- Geets J, Borremans B, Vangronsveld J, Diels L, van der Lelie D. (2005). Molecular monitoring of SRB community structure and dynamics in batch experiments to examine the applicability of in situ precipitation of heavy metals for groundwater remediation. *J Soils Sediments* **5**: 149-163.
- Giloteaux L, Goni-Urriza M, Duran R. (2010). Nested PCR and new primers for analysis of sulfate-reducing bacteria in low-cell-biomass environments. *Appl Environ Microbiol* **76**: 2856-2865.
- Gittel A, Sørensen KB, Skovhus TL, Ingvorsen K, Schramm A. (2009). Prokaryotic Community Structure and Sulfate Reducer Activity in Water from High-Temperature Oil Reservoirs with and without Nitrate Treatment. *Appl Environ Microbiol* **75**: 7086-7096.
- Gumerov VM, Mardanov AV, Beletsky AV, Prokofeva MI, Bonch-Osmolovskaya EA, Ravin NV *et al.* (2011). Complete genome sequence of "Vulcanisaeta moutnovskia" strain 768-28, a novel member of the hyperthermophilic crenarchaeal genus *Vulcanisaeta*. *J Bacteriol* **193**: 2355-2356.
- Huber R, Sacher M, Vollmann A, Huber H, Rose D. (2000). Respiration of arsenate and selenate by hyperthermophilic archaea. *Syst Appl Microbiol* **23**: 305-314.
- Itoh T, Suzuki K, Sanchez PC, Nakase T. (1999). *Caldivirga maquilingsensis* gen. nov., sp. nov., a new genus of rod-shaped crenarchaeote isolated from a hot spring in the Philippines. *Int J Syst Bacteriol* **49 Pt 3**: 1157-1163.
- Itoh T, Suzuki K, Nakase T. (2002). *Vulcanisaeta distributa* gen. nov., sp. nov., and *Vulcanisaeta souniana* sp. nov., novel hyperthermophilic, rod-shaped crenarchaeotes isolated from hot springs in Japan. *Int J Syst Evol Microbiol* **52**: 1097-1104.
- Iwabe N, Kuma K, Hasegawa M, Osawa S, Miyata T. (1989). Evolutionary relationship of archaeobacteria, eubacteria, and eukaryotes inferred from phylogenetic trees of duplicated genes. *Proc Natl Acad Sci U S A* **86**: 9355-9359.
- Jones DT, Taylor WR, Thornton JM. (1992). The rapid generation of mutation data matrices from protein sequences. *Comput Appl Biosci* **8**: 275-282.
- Karkhoff-Schweizer RR, Huber DP, Voordouw G. (1995). Conservation of the genes for dissimilatory sulfite reductase from *Desulfovibrio vulgaris* and *Archaeoglobus fulgidus* allows their detection by PCR. *Appl Environ Microbiol* **61**: 290-296.
- Klein M, Friedrich M, Roger AJ, Hugenholtz P, Fishbain S, Abicht H *et al.* (2001). Multiple lateral transfers of dissimilatory sulfite reductase genes between major lineages of sulfate-reducing prokaryotes. *J Bacteriol* **183**: 6028-6035.
- Kondo R, Nedwell DB, Purdy KJ, Silva SD. (2004). Detection and enumeration of sulphate-reducing bacteria in estuarine sediments by competitive PCR. *Geomicrobiol J* **21**: 145-157.
- Lang JM, Darling AE, Eisen JA. (2013). Phylogeny of bacterial and archaeal genomes using conserved genes: supertrees and supermatrices. *PLoS one* **8**: e62510.
- Lawrence JG, Ochman H. (1997). Amelioration of bacterial genomes: rates of change and exchange. *J Mol Evol* **44**: 383-397.

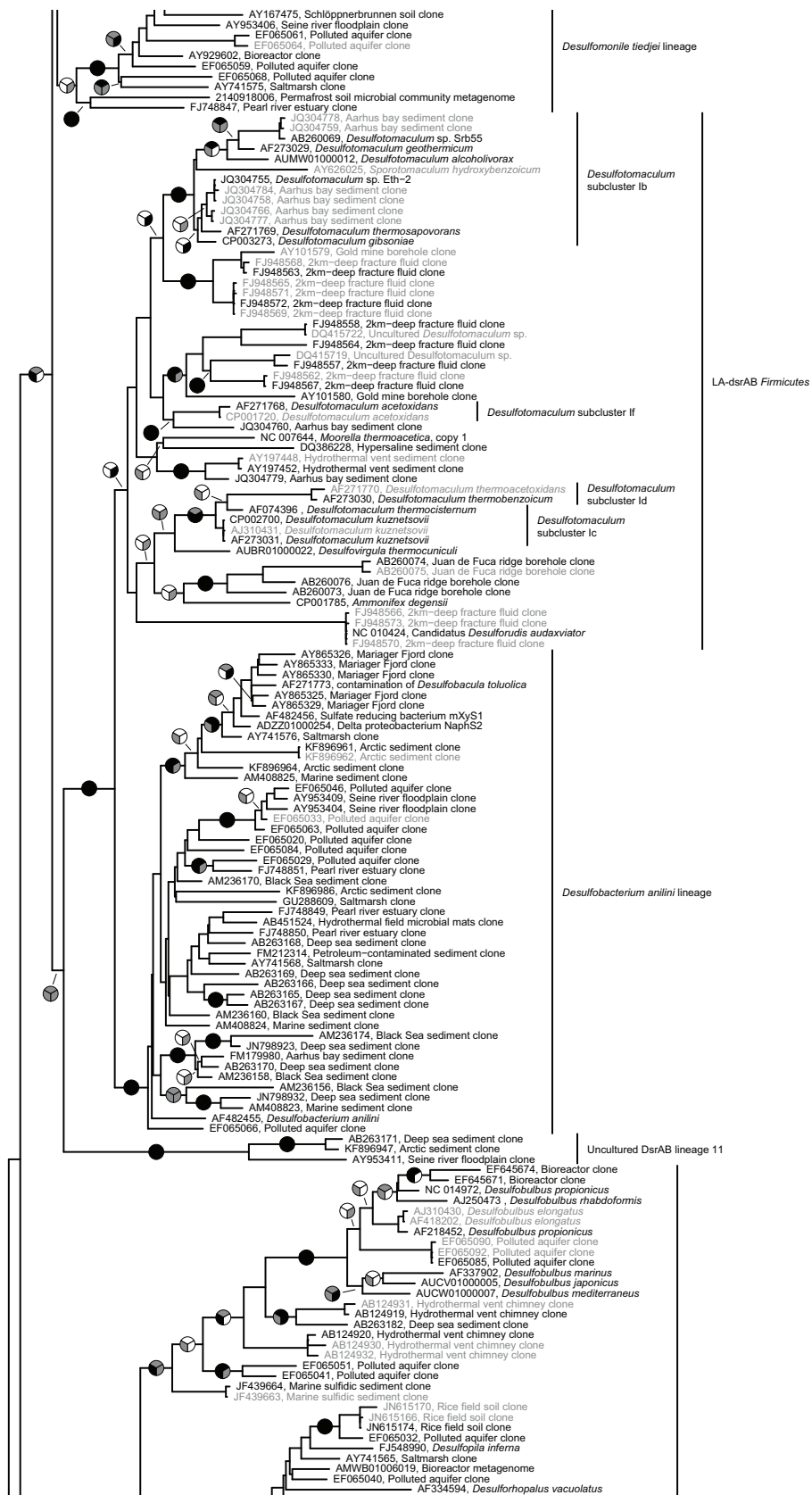
- Lenk S, Arnds J, Zerjatke K, Musat N, Amann R, Musmann M. (2011). Novel groups of Gammaproteobacteria catalyze sulfur oxidation and carbon fixation in a coastal, intertidal sediment. *Environ Microbiol* **13**: 758-774.
- Letunic I, Bork P. (2007). Interactive Tree Of Life (iTOL): an online tool for phylogenetic tree display and annotation. *Bioinformatics* **23**: 127-128.
- Lever MA, Rouxel O, Alt JC, Shimizu N, Ono S, Coggon RM *et al.* (2013). Evidence for microbial carbon and sulfur cycling in deeply buried ridge flank basalt. *Science* **339**: 1305-1308.
- Lin W, Deng A, Wang Z, Li Y, Wen T, Wu LF *et al.* (2014). Genomic insights into the uncultured genus 'Candidatus Magnetobacterium' in the phylum Nitrospirae. *ISME J.*
- Loy A, Küsel K, Lehner A, Drake HL, Wagner M. (2004). Microarray and functional gene analyses of sulfate-reducing prokaryotes in low-sulfate, acidic fens reveal cooccurrence of recognized genera and novel lineages. *Appl Environ Microbiol* **70**: 6998-7009.
- Loy A, Duller S, Baranyi C, Musmann M, Ott J, Sharon I *et al.* (2009). Reverse dissimilatory sulfite reductase as phylogenetic marker for a subgroup of sulfur-oxidizing prokaryotes. *Environ Microbiol* **11**: 289-299.
- Ludwig W, Strunk O, Westram R, Richter L, Meier H, Yadhukumar *et al.* (2004). ARB: a software environment for sequence data. *Nucleic Acids Res* **32**: 1363-1371.
- Luo JF, Lin WT, Guo Y. (2011). Functional genes based analysis of sulfur-oxidizing bacteria community in sulfide removing bioreactor. *Appl Microbiol Biotechnol* **90**: 769-778.
- Markowitz VM, Chen IM, Chu K, Szeto E, Palaniappan K, Grechkin Y *et al.* (2012). IMG/M: the integrated metagenome data management and comparative analysis system. *Nucleic Acids Res* **40**: D123-129.
- Mavromatis K, Sikorski J, Pabst E, Teshima H, Lapidus A, Lucas S *et al.* (2010). Complete genome sequence of *Vulcanisaeta distributa* type strain (IC-017). *Stand Genomic Sci* **3**: 117-125.
- Molitor M, Dahl C, Molitor I, Schäfer U, Speich N, Huber R *et al.* (1998). A dissimilatory sirohaem-sulfite-reductase-type protein from the hyperthermophilic archaeon *Pyrobaculum islandicum*. *Microbiology* **144** (Pt 2): 529-541.
- Mori K, Kim H, Kakegawa T, Hanada S. (2003). A novel lineage of sulfate-reducing microorganisms: *Thermodesulfobiaceae* fam. nov., *Thermodesulfobium narugense*, gen. nov., sp. nov., a new thermophilic isolate from a hot spring. *Extremophiles* **7**: 283-290.
- Mori K, Yamaguchi K, Sakiyama Y, Urabe T, Suzuki K. (2009). *Caldisericum exile* gen. nov., sp. nov., an anaerobic, thermophilic, filamentous bacterium of a novel bacterial phylum, *Caldiserica* phyl. nov., originally called the candidate phylum OP5, and description of *Caldiseriaceae* fam. nov., *Caldisericales* ord. nov. and *Caldisericia* classis nov. *Int J Syst Evol Microbiol* **59**: 2894-2898.
- Mori Y, Purdy KJ, Oakley BB, Kondo R. (2010). Comprehensive Detection of Phototrophic Sulfur Bacteria Using PCR Primers That Target Reverse Dissimilatory Sulfite Reductase Gene. *Microbes Environ* **25**: 190-196.
- Ohno S. (1970). *Evolution by gene duplication*. London: George Alien & Unwin Ltd. Berlin, Heidelberg and New York: Springer-Verlag.
- Pereyra LP, Hiibel SR, Riquelme MVP, Reardon KF, Pruden A. (2010). Detection and Quantification of Functional Genes of Cellulose-Degrading, Fermentative, and Sulfate-Reducing Bacteria and Methanogenic Archaea. *Appl Environ Microbiol* **76**: 2192-2202.
- Pester M, Bittner N, Deevong P, Wagner M, Loy A. (2010). A 'rare biosphere' microorganism contributes to sulfate reduction in a peatland. *ISME J* **4**: 1591-1602.
- Pester M, Knorr KH, Friedrich MW, Wagner M, Loy A. (2012). Sulfate-reducing microorganisms in wetlands - fameless actors in carbon cycling and climate change. *Front Microbiol* **3**: 72.
- Pierce E, Xie G, Barabote RD, Saunders E, Han CS, Detter JC *et al.* (2008). The complete genome sequence of *Moorella thermoacetica* (f. *Clostridium thermoaceticum*). *Environ Microbiol* **10**: 2550-2573.
- Prokofeva MI, Kublanov IV, Nercessian O, Tourova TP, Kolganova TV, Lebedinsky AV *et al.* (2005). Cultivated anaerobic acidophilic/acidotolerant thermophiles from terrestrial and deep-sea hydrothermal habitats. *Extremophiles* **9**: 437-448.
- R Development Core Team. (2008). R: A language and environment for statistical computing.: R Foundation for Statistical Computing, Vienna, Austria. ISBN 3-900051-07-0, URL <http://www.R-project.org>.
- Rinke C, Schwientek P, Sczyrba A, Ivanova NN, Anderson IJ, Cheng JF *et al.* (2013). Insights into the phylogeny and coding potential of microbial dark matter. *Nature* **499**: 431-437.
- Sako Y, Nunoura T, Uchida A. (2001). *Pyrobaculum oguniense* sp. nov., a novel facultatively aerobic and hyperthermophilic archaeon growing at up to 97 degrees C. *Int J Syst Evol Microbiol* **51**: 303-309.
- Santillano D, Boetius A, Ramette A. (2010). Improved *dsrA*-Based Terminal Restriction Fragment Length Polymorphism Analysis of Sulfate-Reducing Bacteria. *Appl Environ Microbiol* **76**: 5308-5311.

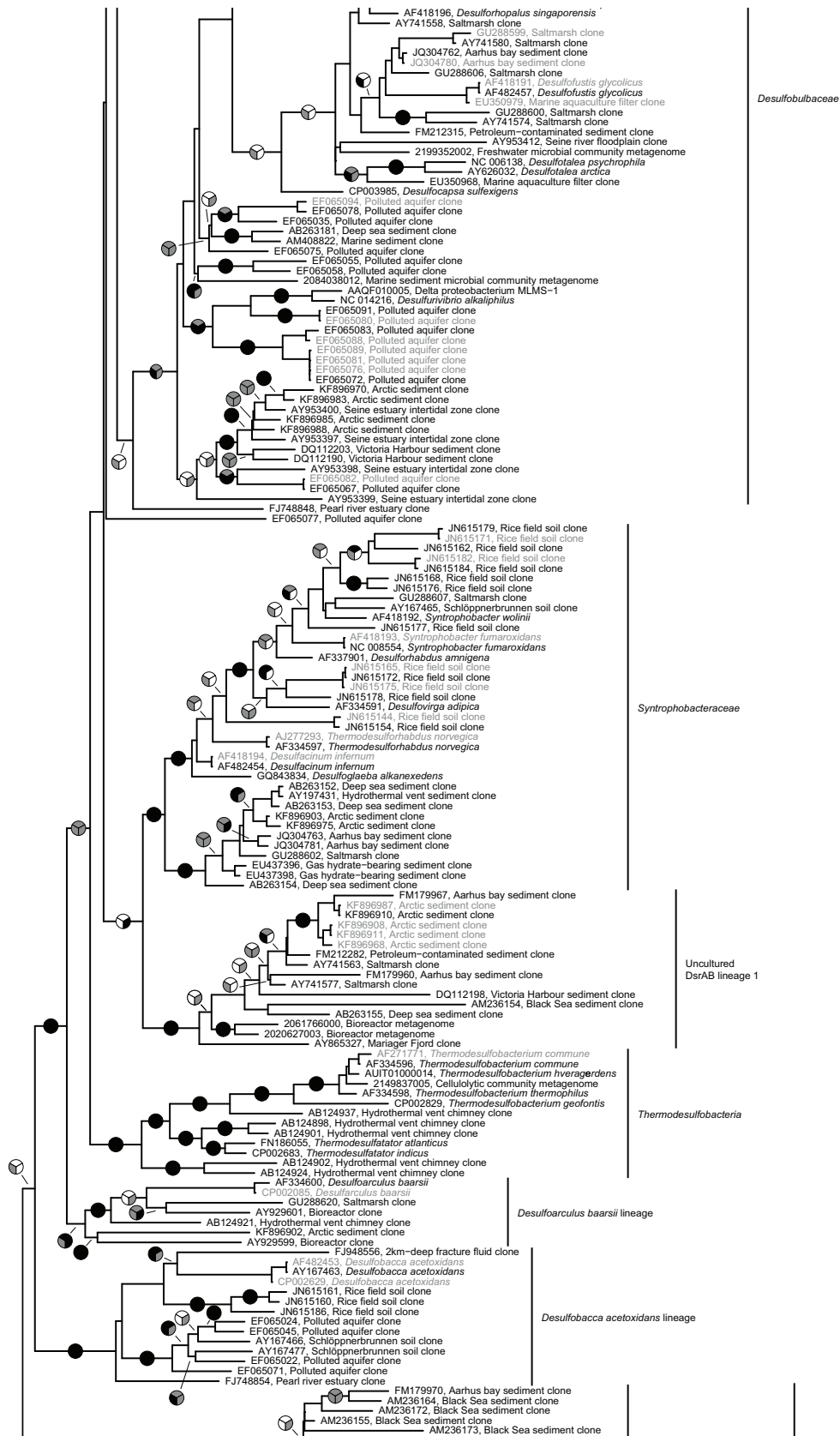
- Schloss PD, Westcott SL, Ryabin T, Hall JR, Hartmann M, Hollister EB *et al.* (2009). Introducing mothur: open-source, platform-independent, community-supported software for describing and comparing microbial communities. *Appl Environ Microbiol* **75**: 7537-7541.
- Schmalenberger A, Drake HL, Kusel K. (2007). High unique diversity of sulfate-reducing prokaryotes characterized in a depth gradient in an acidic fen. *Environ Microbiol* **9**: 1317-1328.
- Siddall ME, Whiting MF. (1999). Long-branch abstractions. *Cladistics* **15**: 9-24.
- Skyring GW, Donnelly TH. (1982). Precambrian Sulfur Isotopes and a Possible Role for Sulfite in the Evolution of Biological Sulfate Reduction. *Precambrian Res* **17**: 41-61.
- Stackebrandt E, Ebers J. (2006). Taxonomic parameters revisited: tarnished gold standards. *Microbiol Today* **33**: 152.
- Stamatakis A. (2006). RAxML-VI-HPC: maximum likelihood-based phylogenetic analyses with thousands of taxa and mixed models. *Bioinformatics* **22**: 2688-2690.
- Steger D, Wentrup C, Braunegger C, Deevong P, Hofer M, Richter A *et al.* (2011). Microorganisms with Novel Dissimilatory (Bi)Sulfite Reductase Genes Are Widespread and Part of the Core Microbiota in Low-Sulfate Peatlands. *Appl Environ Microbiol* **77**: 1231-1242.
- Sun S, Chen J, Li W, Altintas I, Lin A, Peltier S *et al.* (2011). Community cyberinfrastructure for Advanced Microbial Ecology Research and Analysis: the CAMERA resource. *Nucleic Acids Res* **39**: D546-551.
- Suzuki D, Cui X, Li Z, Zhang C, Katayama A. (2014). Reclassification of *Desulfobacterium anilini* as *Desulfatiglans anilini* comb. nov. to *Desulfatiglans* gen. nov., and description of a 4-chlorophenol-degrading sulfate-reducing bacterium-*Desulfatiglans parachlorophenolica* sp. nov. *Int J Syst Evol Microbiol*: ijs-0.
- Suzuki Y, Kelly SD, Kemner KM, Banfield JF. (2005). Direct microbial reduction and subsequent preservation of uranium in natural near-surface sediment. *Appl Environ Microbiol* **71**: 1790-1797.
- Tsukahara K, Kita A, Nakashimada Y, Hoshino T, Murakami K. (2014). Genome-guided analysis of transformation efficiency and carbon dioxide assimilation by *Moorella thermoacetica* Y72. *Gene* **535**: 150-155.
- Völkl P, Huber R, Drobner E, Rachel R, Burggraf S, Trincone A *et al.* (1993). *Pyrobaculum aerophilum* sp. nov., a novel nitrate-reducing hyperthermophilic archaeum. *Appl Environ Microbiol* **59**: 2918-2926.
- Wagner M, Roger AJ, Flax JL, Brusseau GA, Stahl DA. (1998). Phylogeny of dissimilatory sulfite reductases supports an early origin of sulfate respiration. *J Bacteriol* **180**: 2975-2982.
- Würdemann D, Tindall BJ, Pukall R, Lunsdorf H, Strompl C, Namuth T *et al.* (2009). *Gordonibacter pamelaee* gen. nov., sp. nov., a new member of the Coriobacteriaceae isolated from a patient with Crohn's disease, and reclassification of *Eggerthella hongkongensis* Lau *et al.* 2006 as *Paraeggerthella hongkongensis* gen. nov., comb. nov. *Int J Syst Evol Microbiol* **59**: 1405-1415.
- Yang Z. (2007). PAML 4: phylogenetic analysis by maximum likelihood. *Mol Biol Evol* **24**: 1586-1591.
- Yutin N, Galperin MY. (2013). A genomic update on clostridial phylogeny: Gram-negative spore formers and other misplaced clostridia. *Environ Microbiol* **15**: 2631-2641.
- Zverlov V, Klein M, Lückner S, Friedrich MW, Kellermann J, Stahl DA *et al.* (2005). Lateral gene transfer of dissimilatory (bi)sulfite reductase revisited. *J Bacteriol* **187**: 2203-2208.

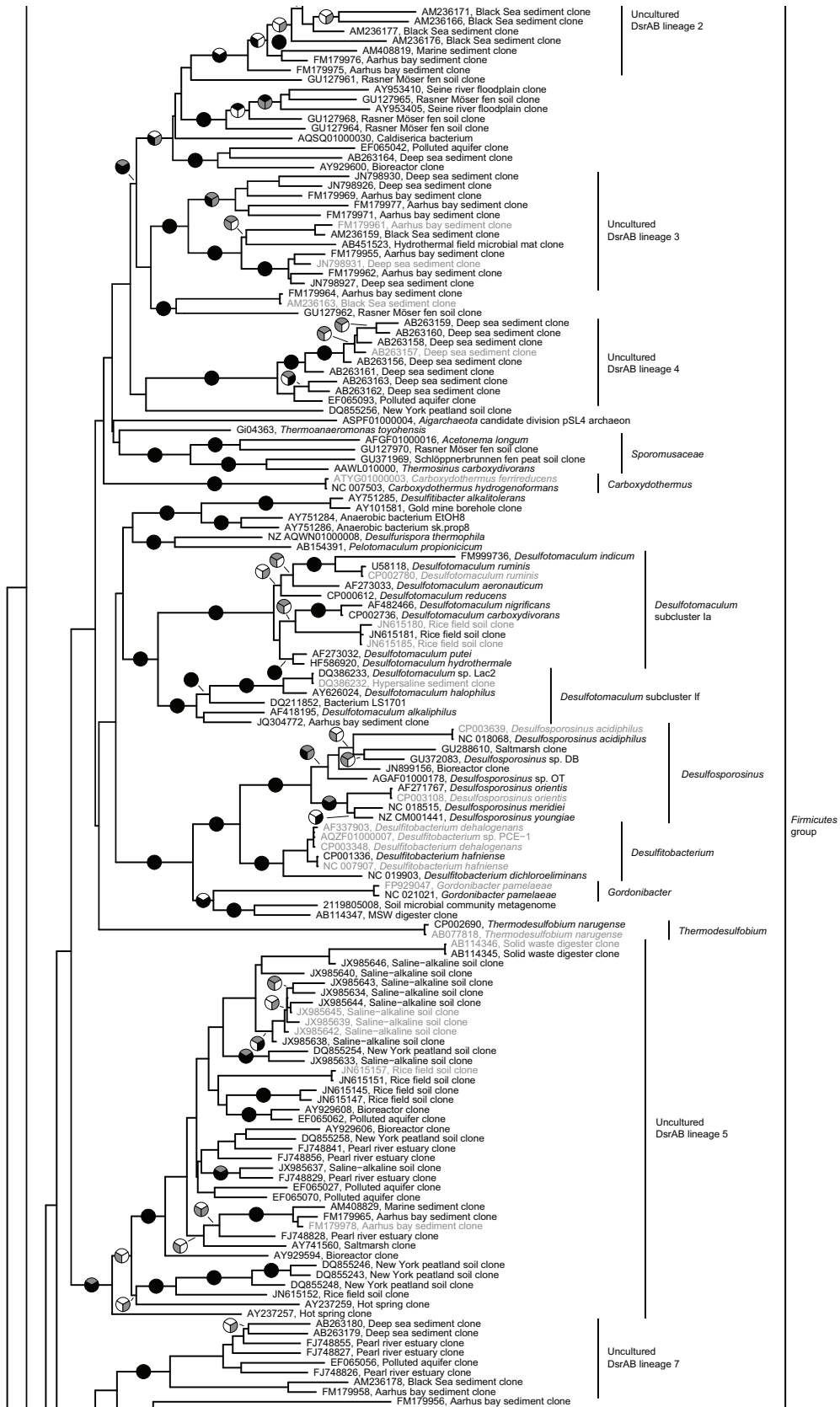




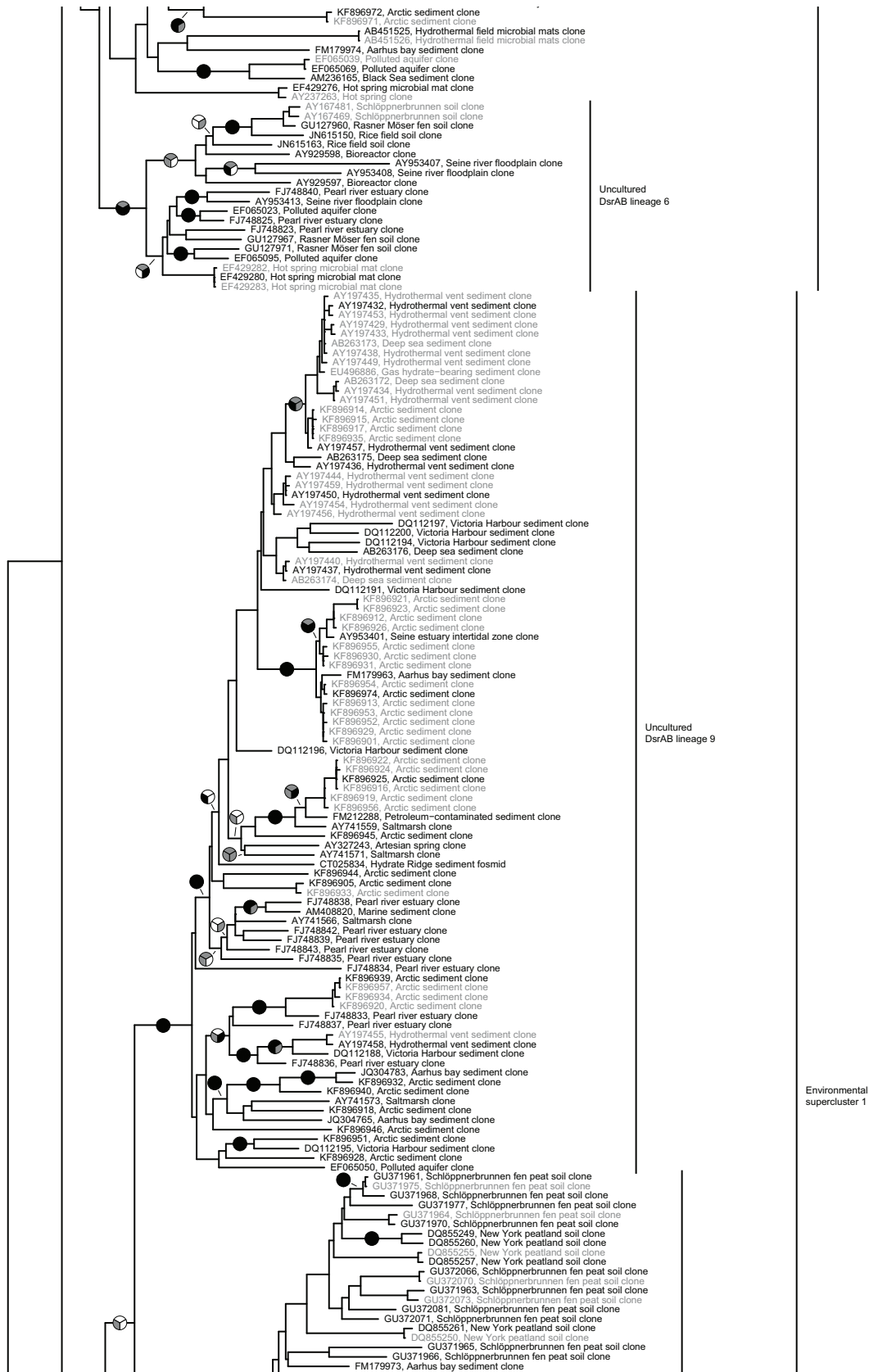


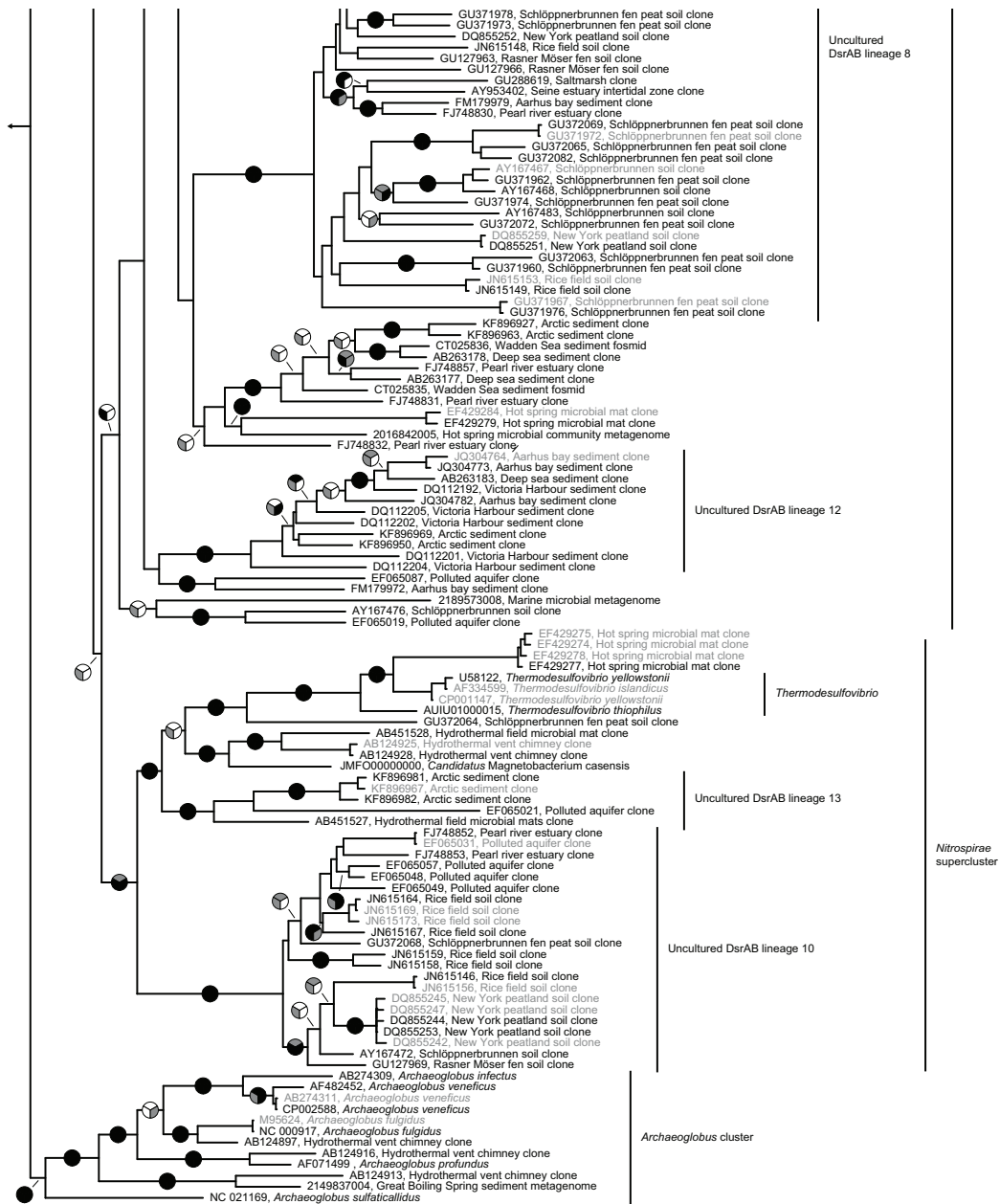




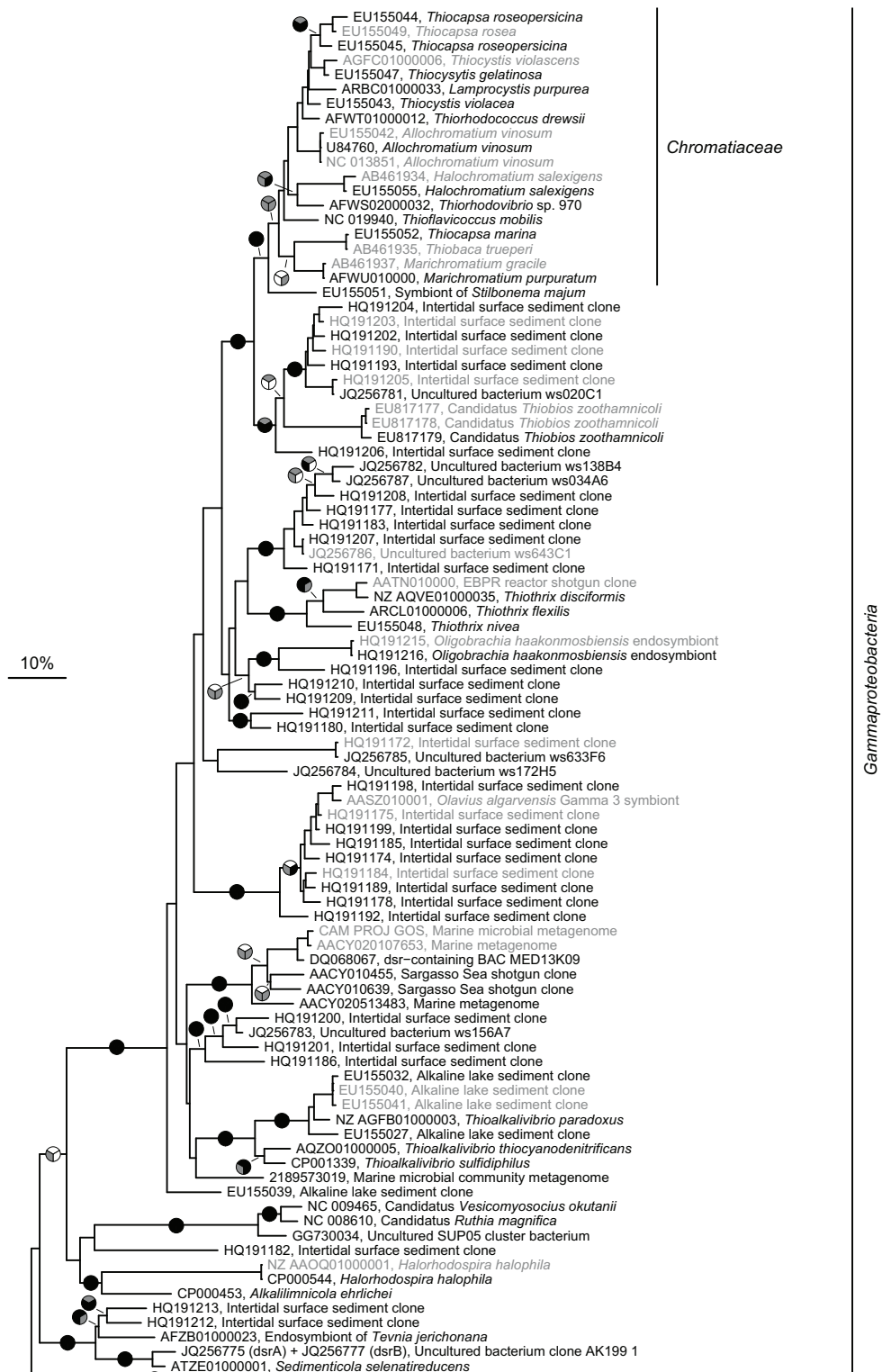


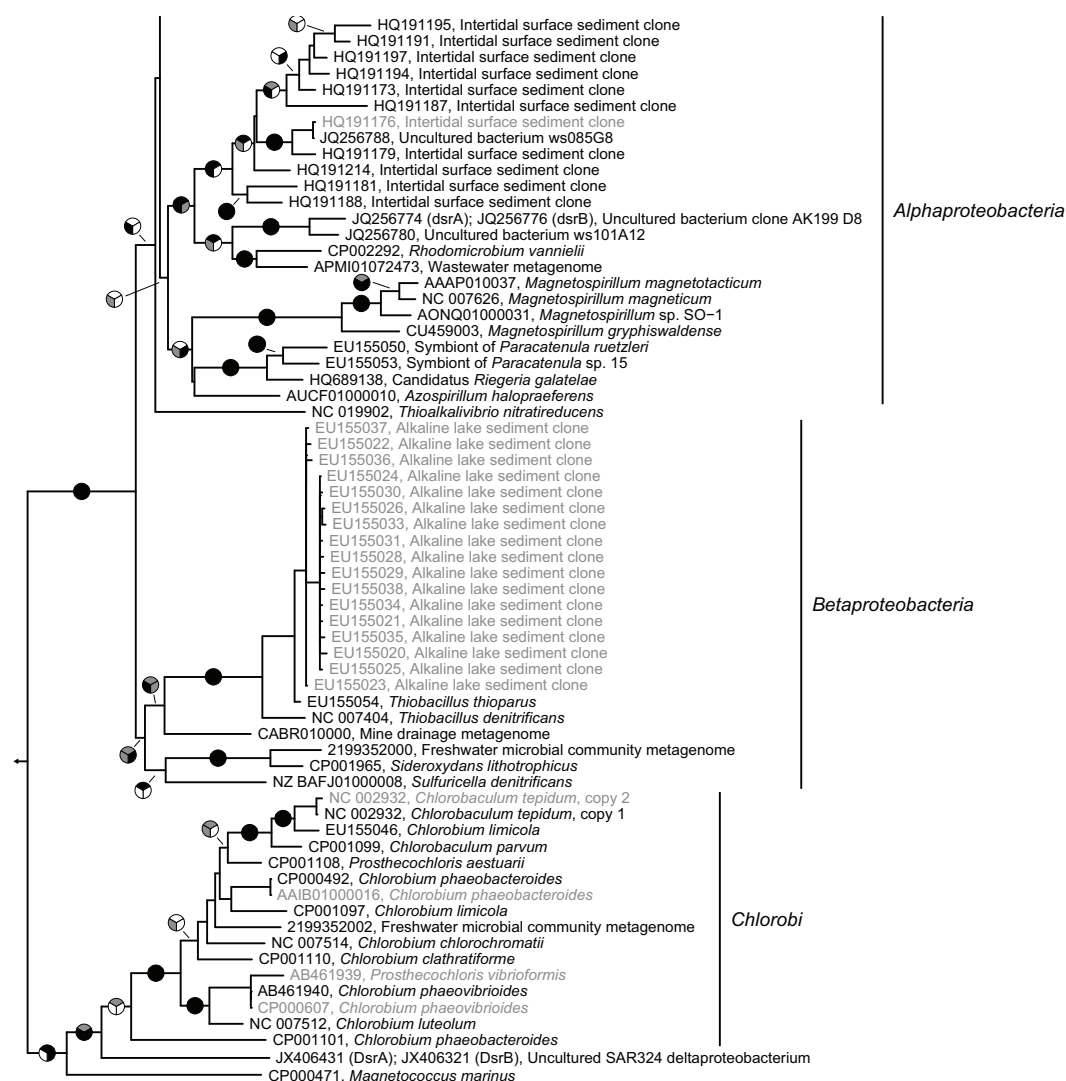
Chapter III - Supplementary Information



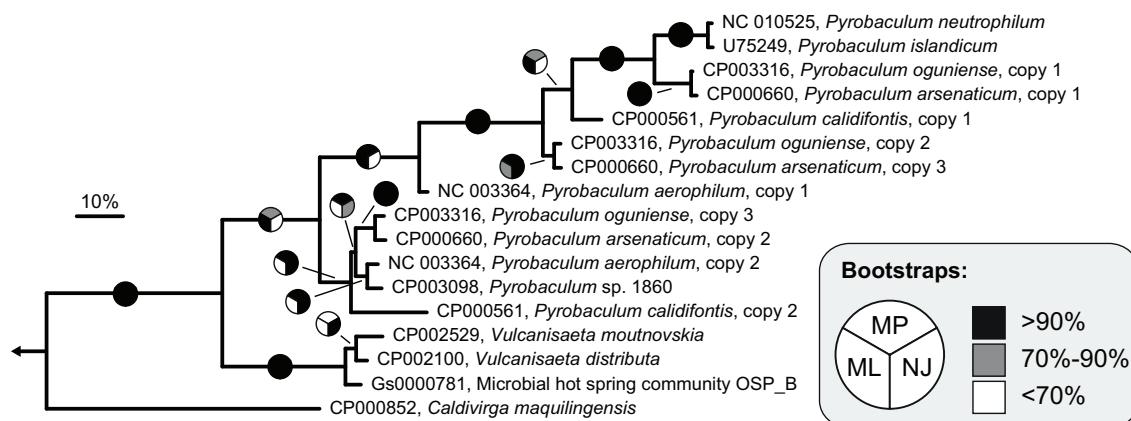


Supplementary Figure S1. Consensus phylogeny of reductive bacterial type DsrAB sequences. This figure shows an un-collapsed version of the consensus tree shown in Figure 1 depicting only reductive bacterial type DsrAB. Sequences in grey were subsequently added to the consensus tree without changing its topology. Scale bar indicates 10% sequence divergence.

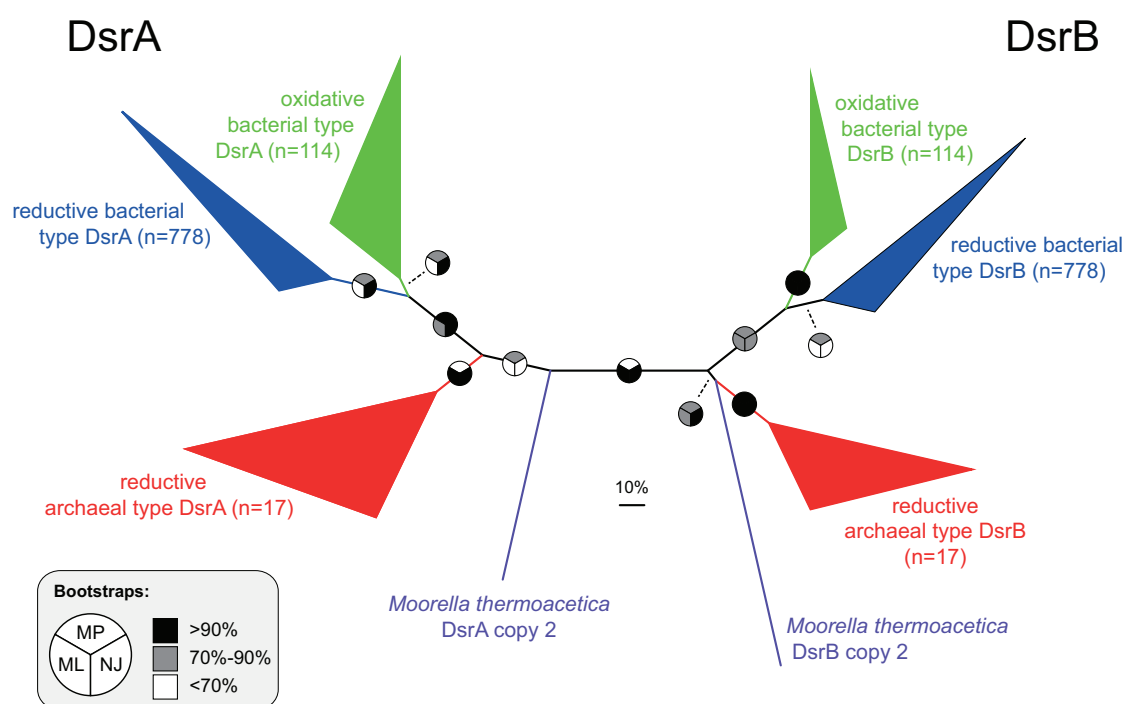




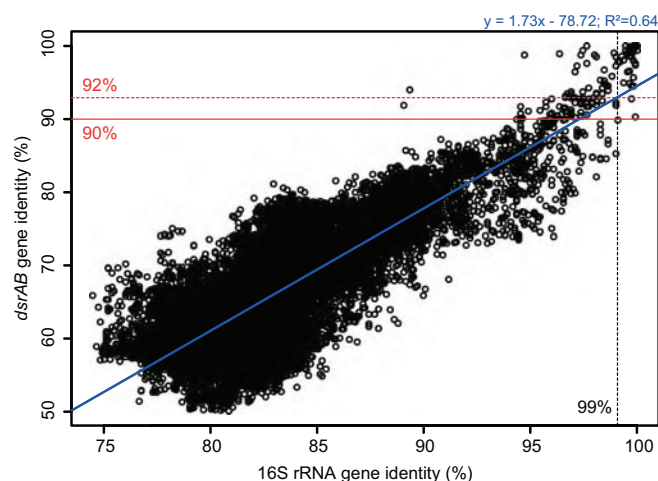
Supplementary Figure S2. Consensus phylogeny of oxidative bacterial type DsrAB sequences. Trees for reconstruction of the consensus tree (extended majority rule) were calculated using an amino acid alignment of 115 representative oxidative DsrAB sequences (clustered at 97% amino acid identity) and a filter covering 552 amino acid positions (omitting insertions/deletions). The tree was rooted with reductive bacterial type DsrAB sequences as outgroup. Sequences in grey (n=45) were subsequently added to the consensus tree without changing its topology. Scale bar indicates 10% sequence divergence. Bootstrap support (1000 re-samplings) is shown by split circles (top: maximum parsimony, bottom left: maximum likelihood, bottom right: neighbor joining) at the respective branches; with black, grey, and white/absence indicating $\geq 90\%$, 70%-90%, and $< 70\%$ support, respectively.



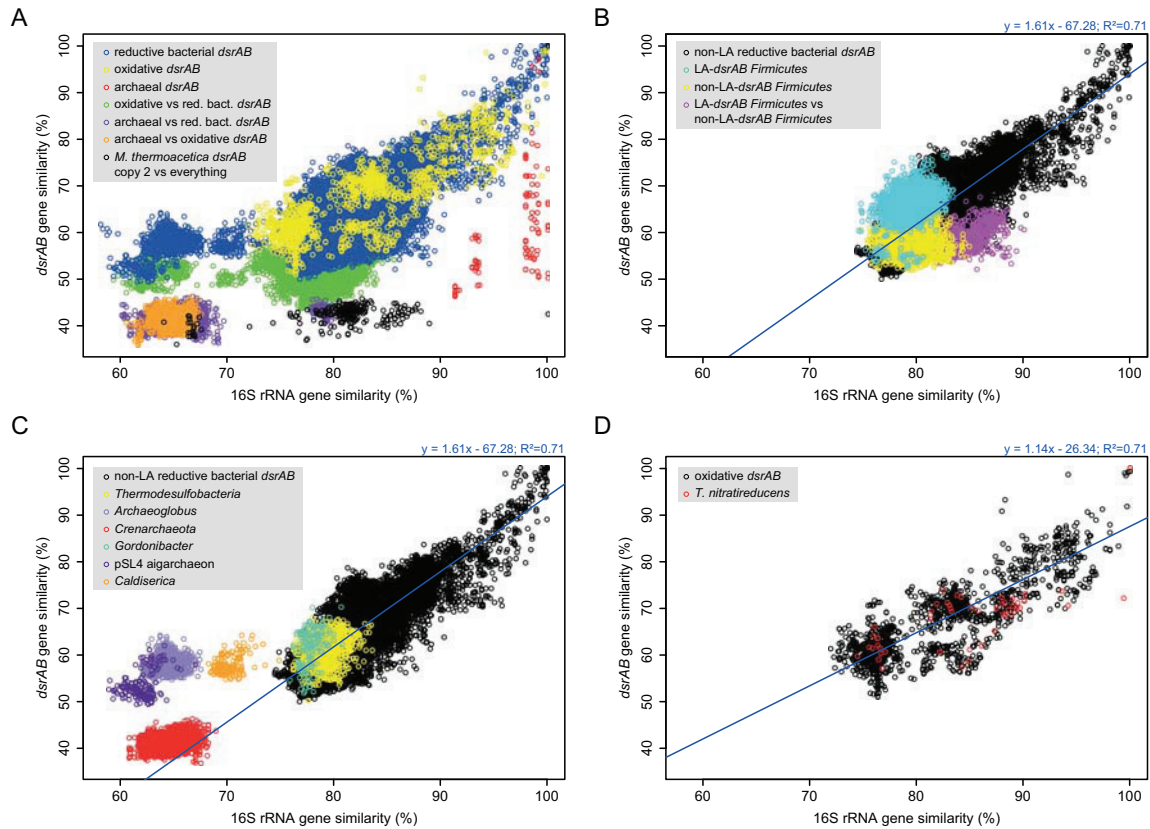
Supplementary Figure S3. Consensus phylogeny of reductive archaeal type DsrAB sequences. Trees for reconstruction of the consensus tree (extended majority rule) were calculated using an amino acid alignment of 17 archaeal type DsrAB sequences and a filter covering 629 amino acid positions (omitting insertions/deletions). The tree was rooted with bacterial DsrAB sequences as outgroup. Scale bar indicates 10% sequence divergence. Bootstrap support (1000 re-samplings) is shown by split circles (top: maximum parsimony, bottom left: maximum likelihood, bottom right: neighbor joining) at the respective branches; with black, grey, and white indicating $\geq 90\%$, 70%-90%, and $< 70\%$ support, respectively.



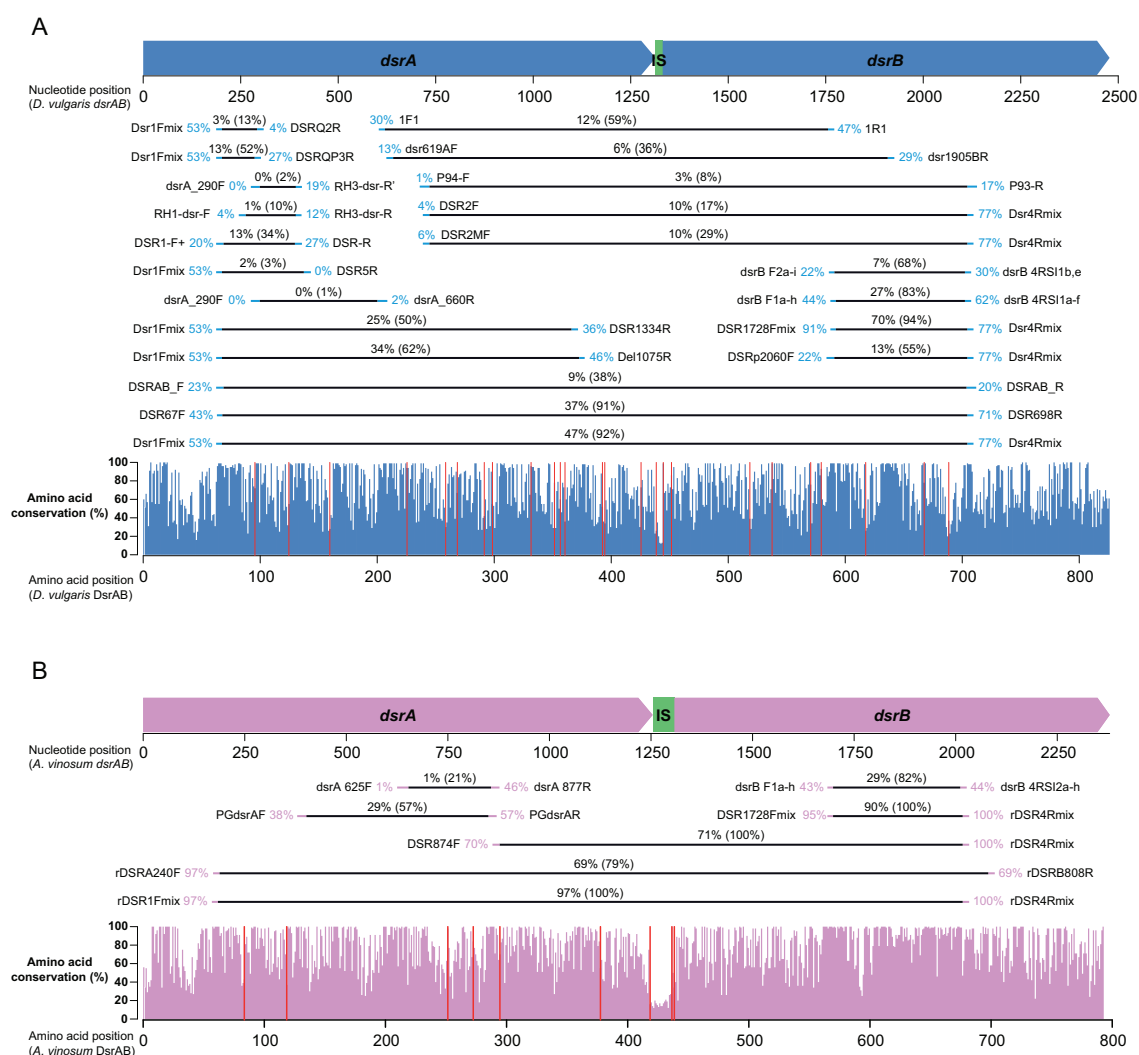
Supplementary Figure S4. Revealing the root in the DsrAB tree by paralogous rooting. Trees for reconstruction of the consensus tree (extended majority rule) were calculated using an alignment of 910 DsrA to corresponding DsrB sequences and a filter covering 163 amino acid positions that are conserved and homologous between DsrA and DsrB subunits. Scale bar indicates 10% sequence divergence. Bootstrap support (100 re-samplings) is shown by split circles (top: maximum parsimony, bottom left: maximum likelihood, bottom right: neighbor joining) at the respective branches; with black, grey, and white indicating ≥90%, 70%-90%, and <70% support, respectively.



Supplementary Figure S5. Species-level threshold for *dsrAB* nucleotide identity inferred from a gene identity plot on non-laterally acquired bacterial *dsrAB*-carrying organisms using 99% nucleotide identity on 16S rRNA level as threshold for species level.



Supplementary Figure S6. Gene identity plot of *dsrAB* against 16S rRNA. Sequence identities of *dsrAB* and 16S rRNA for pairs of organisms for which both genes are known (mostly pure cultures and genomes) were plotted against each other. A) Pairwise comparisons between 259 corresponding *dsrAB*-16S rRNA pairs. Comparisons within and among the three main DsrAB enzyme families as well as comparisons with *M. thermoacetica dsrAB* copy 2 are highlighted in different colors. B) Comparisons of *Firmicutes* with laterally acquired and vertically inherited *dsrAB* with all organisms that have vertically inherited *dsrAB*. Linear regression of comparisons between organisms with non-laterally acquired reductive bacterial type *dsrAB* is shown for reference. C) Comparisons between organisms with laterally acquired *dsrAB* and organisms with vertically inherited *dsrAB*. Linear regression of comparisons between organisms with non-laterally acquired reductive bacterial type *dsrAB* is shown for reference. D) Comparisons of *T. nitratireducens* with reverse *dsrAB*-carrying organisms. Linear regression of comparisons between organisms with oxidative type *dsrAB* is shown for reference.



Supplementary Figure S7. Binding sites and *in silico* coverages of reductive (A) and oxidative (B) bacterial type *dsrAB*-targeted primers. Perfect-match coverage values are displayed for individual primers (blue or pink) and primer pairs (black), coverage values using one weighted mismatch are additionally indicated in parentheses for primer pairs. Displayed coverage values for primers binding at the target sites or outside the amplification region of (r)DSR1F/(r)DSR4R are based on full length datasets of reductive (n=115) and oxidative (n=62) bacterial type *dsrAB* sequences, whereas coverage values for primers binding within the region amplified by (r)DSR1F/(r)DSR4R are based on a core dataset of reductive (n=1110) and oxidative (n=159) bacterial type *dsrAB* sequences that completely cover this region. Bar charts show positional amino acid sequence variability (calculated in ARB using the ARB_PHYLO 'filter by base frequency' method and indicated in blue or pink bars) and regions with deletions/insertions (red bars) in *DsrAB*. Sequence numbering and primer binding positions correspond to *dsrAB*/*DsrAB* of *Desulfovibrio vulgaris* (NC_002937, 449880..452365) or *Allochromatium vinosum* (NC_013851, 1439735..1442113).

Supplementary Table S1

Primers targeting reductive bacterial type <i>dsrAB</i> ^a					full length <i>dsrAB</i> ^b (%)		core dataset <i>dsrAB</i> ^c (%)		Phylogenetic clusters ^d (%)					Reference
Name	Sequence (5'-3')	Target gene	Position ^e	Deg. ^f	0 MM	1 wMM	0 MM	1 wMM	DpS	Fg	ES1	NsS	AgC	
DSR1F	ACSCACTGGAAGCAGC	<i>dsrA</i>	187-202	2	25	49	<i>n.a.</i>	<i>n.a.</i>	35	0	0	0	60	Wagner <i>et al.</i> , 1998
DSR1Fmix (+a-b)		<i>dsrA</i>	187-202	5	38	90	<i>n.a.</i>	<i>n.a.</i>	52	7	0	0	60	Loy <i>et al.</i> , 2004
DSR1Fa	ACCCAYTGGAAACACG	<i>dsrA</i>	187-202	2	11	87	<i>n.a.</i>	<i>n.a.</i>	17	0	0	0	0	Loy <i>et al.</i> , 2004
DSR1Fb	GGCCACTGGAAGCAGC	<i>dsrA</i>	187-202	1	2	26	<i>n.a.</i>	<i>n.a.</i>	0	7	0	0	0	Loy <i>et al.</i> , 2004
DSR1Fmix (+a-d)		<i>dsrA</i>	187-202	7	49	90	<i>n.a.</i>	<i>n.a.</i>	68	7	0	0	60	Zverlov <i>et al.</i> , 2005
DSR1Fc	ACCCATTGGAAACATG	<i>dsrA</i>	187-202	1	3	11	<i>n.a.</i>	<i>n.a.</i>	4	0	0	0	0	Zverlov <i>et al.</i> , 2005
DSR1Fd	ACTCACTGGAAGCAGC	<i>dsrA</i>	187-202	1	8	43	<i>n.a.</i>	<i>n.a.</i>	12	0	0	0	0	Zverlov <i>et al.</i> , 2005
DSR1Fmix (+a-h)		<i>dsrA</i>	187-202	11	53	98	<i>n.a.</i>	<i>n.a.</i>	68	14	60	0	60	Pester <i>et al.</i> , 2010
DSR1Fe	GTTCACTGGAACACG	<i>dsrA</i>	187-202	1	2	37	<i>n.a.</i>	<i>n.a.</i>	0	7	0	0	0	Pester <i>et al.</i> , 2010
DSR1Ff	AGCCACTGGAACACG	<i>dsrA</i>	187-202	1	1	72	<i>n.a.</i>	<i>n.a.</i>	0	0	20	0	0	Pester <i>et al.</i> , 2010
DSR1Fg	GGCCACTGGAACATG	<i>dsrA</i>	187-202	1	1	24	<i>n.a.</i>	<i>n.a.</i>	0	0	20	0	0	Pester <i>et al.</i> , 2010
DSR1Fh	GGCTATTGGAAGCAG	<i>dsrA</i>	187-202	1	1	2	<i>n.a.</i>	<i>n.a.</i>	0	0	20	0	0	Pester <i>et al.</i> , 2010
DSR1-F+	ACSCACTGGAAGCAGCGGG	<i>dsrA</i>	187-206	2	20	41	<i>n.a.</i>	<i>n.a.</i>	31	0	0	0	0	Kondo <i>et al.</i> , 2004
DSRAB_F	ACSCACTGGAAGCAGGCGG	<i>dsrA</i>	187-206	4	23	42	<i>n.a.</i>	<i>n.a.</i>	35	0	0	0	20	Schmalenberger <i>et al.</i> , 2007
DSR67F	SCACTGGAARACG	<i>dsrA</i>	189-203	4	43	100	<i>n.a.</i>	<i>n.a.</i>	53	21	20	0	60	Suzuki <i>et al.</i> , 2005
RH1-dsr-F	GCCGTTACTGTGACCAGCC	<i>dsrA</i>	245-263	1	9	21	4	13	6	0	0	0	0	Ben-Dov <i>et al.</i> , 2007
dsrA_290F	CGGCGTTGGCGATTTCYACVVT	<i>dsrA</i>	276-299	36	0	1	0	3	0	0	0	0	0	Pereyra <i>et al.</i> , 2010
DSRQP3R	CGCATGGTRTGRAARTG	<i>dsrA</i>	286-302	8	17	52	27	60	40	9	3	0	0	Akob <i>et al.</i> , 2012
DSRQ2R	GTTGAYACGATGGTRTG	<i>dsrA</i>	292-309	4	5	13	4	17	6	0	1	0	0	Chin <i>et al.</i> , 2007
DSR-R	GTGGMRCCGTGCAKRTTGG	<i>dsrA</i>	389-407	16	33	67	27	71	36	18	10	5	0	Kondo <i>et al.</i> , 2004
RH3-dsr-R'	gGTGGAGCGCTGCATGTT	<i>dsrA</i>	391-408	1	15	40	12	49	15	15	1	3	0	Ben-Dov <i>et al.</i> , 2007
RH3-dsr-R'	GTGGMGCCGTGCATGTT	<i>dsrA</i>	392-408	2	22	49	19	56	24	3	22	3	0	Pereyra <i>et al.</i> , 2010
DSR5R	TGCCGAGGAACGATGTC	<i>dsrA</i>	412-430	1	2	3	0	2	1	0	0	0	0	Wagner <i>et al.</i> , 1998
dsrA_660R	GCCGGACGATGCAHGTCTCTGRWA	<i>dsrA</i>	601-626	24	2	9	2	13	4	0	0	0	0	Pereyra <i>et al.</i> , 2010
1F1	CAGGAYGARTCTKACCG	<i>dsrA</i>	604-620	8	36	61	30	66	34	39	14	0	0	Dhillon <i>et al.</i> , 2003
dsr619AF	GYCCGCVTTCCSTACAA	<i>dsrA</i>	623-641	12	15	38	13	44	18	8	0	8	0	Giloteaux <i>et al.</i> , 2010
P94-F	ATCGGWACCTGGAAGAGYACATCAA	<i>dsrA</i>	709-734	4	3	8	1	6	1	0	0	0	17	Karkhoff-Schweizer <i>et al.</i> , 1995
DSR2F	CTGGAAGGAYGACATCAA	<i>dsrA</i>	717-734	2	10	17	4	15	6	0	0	0	17	Wagner <i>et al.</i> , 1998
DSR2MF	CTGGAAGGAYGACATCAA	<i>dsrA</i>	717-734	4	11	30	6	34	10	0	0	0	17	Akob <i>et al.</i> , 2012
DSR1334R	TYTTCATCACCARTCC	<i>dsrA</i>	1098-1115	4	37	50	36	50	56	0	1	0	0	Santillano <i>et al.</i> , 2010
Del1075R	GYTCVCGGTTCTTDC	<i>dsrA</i>	1118-1132	18	45	63	46	61	66	15	2	49	0	Gittel <i>et al.</i> , 2009
DSRp2060F	CAACATCTGYCAYACCCAGGG	<i>dsrB</i>	1752-1772	4	14	56	22	65	23	39	8	0	0	Geets <i>et al.</i> , 2005
1R1	CCCTGGGTRTGRAYAT	<i>dsrB</i>	1756-1772	16	29	74	47	87	55	54	19	0	50	Dhillon <i>et al.</i> , 2003
dsrB F2a-i		<i>dsrB</i>	1758-1772	9	16	81	22	93	20	40	13	0	25	Lever <i>et al.</i> , 2013
dsrB F2a	CGTCCACACCCAGGG	<i>dsrB</i>	1758-1772	1	10	50	17	69	14	39	9	0	8	Lever <i>et al.</i> , 2013
dsrB F2b	TGTGCATACCCAGGG	<i>dsrB</i>	1758-1772	1	0	7	2	9	2	1	1	0	0	Lever <i>et al.</i> , 2013
dsrB F2c	CATTACATCCAGGG	<i>dsrB</i>	1758-1772	1	0	25	1	27	1	0	0	0	0	Lever <i>et al.</i> , 2013
dsrB F2d	TGTTACACCCAGGG	<i>dsrB</i>	1758-1772	1	1	43	1	61	2	0	0	0	0	Lever <i>et al.</i> , 2013
dsrB F2e	CGTGACACGCGAGGG	<i>dsrB</i>	1758-1772	1	3	3	1	5	1	1	3	0	0	Lever <i>et al.</i> , 2013
dsrB F2f	CGTTACATACAGGG	<i>dsrB</i>	1758-1772	1	1	16	0	12	0	0	0	0	0	Lever <i>et al.</i> , 2013
dsrB F2g	TGTCCACATCCAGGG	<i>dsrB</i>	1758-1772	1	1	11	0	11	0	0	0	0	17	Lever <i>et al.</i> , 2013
dsrB F2h	CGTGACATACGAGGG	<i>dsrB</i>	1758-1772	1	0	3	0	2	0	0	1	0	0	Lever <i>et al.</i> , 2013
dsrB F2i	CATCTACATCAGGG	<i>dsrB</i>	1758-1772	1	0	14	0	11	0	0	0	0	0	Lever <i>et al.</i> , 2013
DSR1728Fmix		<i>dsrB</i>	1762-1776	77	90	100	91	100	88	98	95	100	100	Steger <i>et al.</i> , 2011
DSR1728FmixA	CAYACCCAGGNTGG	<i>dsrB</i>	1762-1776	8	43	77	65	89	71	66	42	56	50	Steger <i>et al.</i> , 2011
DSR1728FmixB	CAYACBCAAGNTGG	<i>dsrB</i>	1762-1776	24	17	90	7	89	2	9	26	0	0	Steger <i>et al.</i> , 2011
DSR1728FmixC	CATACDCAGGGHTGG	<i>dsrB</i>	1762-1776	9	15	43	6	37	3	2	12	33	0	Steger <i>et al.</i> , 2011
DSR1728FmixD	CACACDCAGGNTGG	<i>dsrB</i>	1762-1776	12	12	58	10	62	6	21	16	10	50	Steger <i>et al.</i> , 2011
DSR1728FmixE	CATACHCAGGNTAY	<i>dsrB</i>	1762-1776	24	3	80	4	92	6	0	0	0	0	Steger <i>et al.</i> , 2011
dsrB F1a-h		<i>dsrB</i>	1762-1776	8	35	86	44	89	45	54	31	49	42	Lever <i>et al.</i> , 2013
dsrB F1a	CACACCCAGGGCTGG	<i>dsrB</i>	1762-1776	1	22	59	30	74	30	46	17	21	42	Lever <i>et al.</i> , 2013
dsrB F1b	CATACCTAGGGCTGG	<i>dsrB</i>	1762-1776	1	3	27	1	21	1	1	2	0	0	Lever <i>et al.</i> , 2013
dsrB F1c	CATACCCAGGGCTGG	<i>dsrB</i>	1762-1776	1	8	53	11	65	14	4	6	21	0	Lever <i>et al.</i> , 2013
dsrB F1d	CACACTCAAGTTGG	<i>dsrB</i>	1762-1776	1	1	26	0	11	0	1	2	0	0	Lever <i>et al.</i> , 2013
dsrB F1e	CACACACAGGGATGG	<i>dsrB</i>	1762-1776	1	0	6	0	10	0	0	0	8	0	Lever <i>et al.</i> , 2013
dsrB F1f	CACACGACGGATGG	<i>dsrB</i>	1762-1776	1	0	4	1	5	0	0	3	0	0	Lever <i>et al.</i> , 2013
dsrB F1g	CACACGACGGGTTGG	<i>dsrB</i>	1762-1776	1	1	3	1	4	0	2	1	0	0	Lever <i>et al.</i> , 2013
dsrB F1h	CATACGCAAGTTGG	<i>dsrB</i>	1762-1776	1	0	3	0	3	0	1	0	0	0	Lever <i>et al.</i> , 2013
dsr1905BR	RTGHGSCGCCGCACAT	<i>dsrB</i>	1909-1926	12	25	52	29	69	33	31	13	36	0	Giloteaux <i>et al.</i> , 2010
dsrB 4RS1a-f		<i>dsrB</i>	2107-2123	1	62	97	<i>n.a.</i>	<i>n.a.</i>	73	39	60	50	20	Lever <i>et al.</i> , 2013
dsrB 4RS1a	CAGTTACCGCAGTACAT	<i>dsrB</i>	2107-2123	1	17	58	<i>n.a.</i>	<i>n.a.</i>	19	11	0	50	20	Lever <i>et al.</i> , 2013
dsrB 4RS1b	CAGTTACCGCAGACAT	<i>dsrB</i>	2107-2123	1	12	61	<i>n.a.</i>	<i>n.a.</i>	19	0	0	0	0	Lever <i>et al.</i> , 2013
dsrB 4RS1c	CAGTTGCCGCGAGTACAT	<i>dsrB</i>	2107-2123	1	15	63	<i>n.a.</i>	<i>n.a.</i>	12	25	20	0	0	Lever <i>et al.</i> , 2013
dsrB 4RS1d	CAGTTTCCGCGAGTACAT	<i>dsrB</i>	2107-2123	1	1	37	<i>n.a.</i>	<i>n.a.</i>	0	4	0	0	0	Lever <i>et al.</i> , 2013
dsrB 4RS1e	CAGTTGCCGCGAGACAT	<i>dsrB</i>	2107-2123	1	17	60	<i>n.a.</i>	<i>n.a.</i>	24	0	40	0	0	Lever <i>et al.</i> , 2013
dsrB 4RS1f	CAGTTTCCACAGACAT	<i>dsrB</i>	2107-2123	1	0	14	<i>n.a.</i>	<i>n.a.</i>	0	0	0	0	0	Lever <i>et al.</i> , 2013
DSRAB_R	GTAGCAGTWCAGCAGWACATG	<i>dsrB</i>	2111-2136	4	20	82	<i>n.a.</i>	<i>n.a.</i>	25	11	0	0	20	Schmalenberger <i>et al.</i> , 2007
DSR4R	GTGTAGCAGTTACCGCA	<i>dsrB</i>	2113-2129	1	28	80	<i>n.a.</i>	<i>n.a.</i>	31	29	0	0	20	Wagner <i>et al.</i> , 1998
DSR4Rmix (+a-c)		<i>dsrB</i>	2113-2129	5	57	94	<i>n.a.</i>	<i>n.a.</i>	67	46	20	0	40	Loy <i>et al.</i> , 2004
DSR4Ra	GTGTAACAGTTTCCACA	<i>dsrB</i>	2113-2129	1	1	6	<i>n.a.</i>	<i>n.a.</i>	0	0	0	0	20	Loy <i>et al.</i> , 2004
DSR4Rb	GTGTAACAGTTACCGCA	<i>dsrB</i>	2113-2129	1	2	37	<i>n.a.</i>	<i>n.a.</i>	3	0	0	0	0	Loy <i>et al.</i> , 2004
DSR4Rc	GTGTAGCAGTTKCCGCA	<i>dsrB</i>	2113-2129	2	27	83	<i>n.a.</i>	<i>n.a.</i>	33	18	20	0	0	Loy <i>et al.</i> , 2004
DSR4Rmix (+a-e)		<i>dsrB</i>	2113-2129	7	70	94	<i>n.a.</i>	<i>n.a.</i>	80	54	20	0	100	Zverlov <i>et al.</i> , 2005
DSR4Rd	GTGTAGCAGTTACCGCA	<i>dsrB</i>	2113-2129	1	9	51	<i>n.a.</i>	<i>n.a.</i>	11	7	0	0	0	Zverlov <i>et al.</i> , 2005
DSR4Re	GTGTAACAGTTACCGCA	<i>dsrB</i>	2113-2129	1	4	17	<i>n.a.</i>	<i>n.a.</i>	3	0	0	0	60	Zverlov <i>et al.</i> , 2005
DSR4Rmix (+a-g)		<i>dsrB</i>	2113-2129	10	77	94	<i>n.a.</i>	<i>n.a.</i>	83	68	60	0	100	Pester <i>et al.</i> , 2010
DSR4Rf	GTATAGCARTTCCCGCA	<i>dsrB</i>	2113-2129	2	5	42	<i>n.a.</i>	<i>n.a.</i>	3	14	0	0	0	Pester <i>et al.</i> , 2010
DSR4Rg	GTGAAGCAGTTGCCGCA	<i>dsrB</i>	2113-2129	1	2	34	<i>n.a.</i>	<i>n.a.</i>	0	0	40	0	0	Pester <i>et al.</i> , 2010
DSR698R	GTGTARCACTTCCRCRA	<i>dsrB</i>	2113-2129	8	71	91	<i>n.a.</i>	<i>n.a.</i>	83	50	40	0	80	Suzuki <i>et al.</i> , 2005
P93-R	GGGCACATSGTGTACGAGTTACCGCA	<i>dsrB</i>	2113-2138	2	17	61	<i>n.a.</i>	<i>n.a.</i>	20	11	0	0	20	Karkhoff-Schweizer <i>et al.</i> , 1995

^a Recommended primers are highlighted in gray.^b Data indicate primer coverage of all full length reductive bacterial type *dsrAB* sequences (n=115); 0 MM, no mismatches; 1 wMM, one weighted mismatch.^c Data indicate primer coverage of all core reductive bacterial type *dsrAB* sequences (n=1110); 0 MM, no mismatches; 1 wMM, one weighted mismatch; *n.a.*, not applicable for primers binding at the target sites or outside the amplification region of DSR1F/DSR4R.^d Primer coverage of full length/core dataset *dsrAB* sequences in higher taxonomic clusters. DpS, *Deltaproteobacteria* supercluster (n=75/709); Fg, *Firmicutes* group (n=28/180); ES1, Environmental supercluster 1 (n=5/170); NsS, *Nitrospirae* supercluster (n=2/39); AgC, *Archaeoglobus* cluster (n=5/12). The larger core dataset is used for primers binding within the DSR1F/DSR4R region.^e Position is relative to *Desulfotomaculum vulgare* Hildenborough *dsrAB* (NC_002937, 449888..452365).^f Degeneracy is given as the number of oligonucleotides that comprise the primer.

Supplementary Table S2

Primers targeting oxidative bacterial type <i>dsrAB</i> ^a					full length <i>dsrAB</i> ^b (%)		core dataset <i>dsrAB</i> ^c (%)		Reference
Name	Sequence (5'-3')	Target gene	Position ^d	Deg. ^e	0 MM	1 wMM	0 MM	1 wMM	
rDSR1Fmix		<i>dsrA</i>	169-184	80	97	100	<i>n.a.</i>	<i>n.a.</i>	Loy <i>et al.</i> , 2009
rDSR1Fa	AARGNTAYTGAARG	<i>dsrA</i>	169-184	32	69	98	<i>n.a.</i>	<i>n.a.</i>	Loy <i>et al.</i> , 2009
rDSR1Fb	TTYGGNTAYTGAARG	<i>dsrA</i>	169-184	32	0	69	<i>n.a.</i>	<i>n.a.</i>	Loy <i>et al.</i> , 2009
rDSR1Fc	ATGGGNTAYTGAARG	<i>dsrA</i>	169-184	16	27	71	<i>n.a.</i>	<i>n.a.</i>	Loy <i>et al.</i> , 2009
rDSRA240F	GGNTAYTGAARGGNGG	<i>dsrA</i>	172-188	64	97	100	<i>n.a.</i>	<i>n.a.</i>	Lenk <i>et al.</i> , 2011
PGdsrAF	CAYGGBCAGACCGGBRAYATYATG	<i>dsrA</i>	379-402	144	39	56	38	61	Mori <i>et al.</i> , 2010
dsrA 625F	TTCAAGTTCTCCGGCTGCSCNAAYGACTG	<i>dsrA</i>	625-653	16	2	26	1	21	Luo <i>et al.</i> , 2011
PGdsrAR	RCAGTGCAATRCACGHAACRCA	<i>dsrA</i>	850-870	48	60	81	57	89	Mori <i>et al.</i> , 2010
dsrA 877R	CGTTSANRCAGTGCATGCAGCG	<i>dsrA</i>	856-877	16	39	79	46	86	Luo <i>et al.</i> , 2011
DSR874F	TGYATGCAYTGYTVAAYG	<i>dsrA</i>	859-877	96	71	100	70	100	Loy <i>et al.</i> , 2009
DSR1728Fmix		<i>dsrB</i>	1684-1698	77	90	100	95	99	Steger <i>et al.</i> , 2011
DSR1728FmixA	CAYACCCAGGGNTGG	<i>dsrB</i>	1684-1698	8	56	74	65	82	Steger <i>et al.</i> , 2011
DSR1728FmixB	CAYACBCAAGGNTGG	<i>dsrB</i>	1684-1698	24	18	97	14	98	Steger <i>et al.</i> , 2011
DSR1728FmixC	CATACDCAGGGHTGG	<i>dsrB</i>	1684-1698	9	6	27	6	28	Steger <i>et al.</i> , 2011
DSR1728FmixD	CACACDCAGGGNTGG	<i>dsrB</i>	1684-1698	12	10	63	9	68	Steger <i>et al.</i> , 2011
DSR1728FmixE	CATACHCAGGGNTAY	<i>dsrB</i>	1684-1698	24	0	74	0	82	Steger <i>et al.</i> , 2011
dsrB F1a-h		<i>dsrB</i>	1684-1698	8	47	90	43	89	Lever <i>et al.</i> , 2013
dsrB F1a	CACACCCAGGGCTGG	<i>dsrB</i>	1684-1698	1	35	63	32	70	Lever <i>et al.</i> , 2013
dsrB F1b	CATACTCAGGGCTGG	<i>dsrB</i>	1684-1698	1	0	18	1	13	Lever <i>et al.</i> , 2013
dsrB F1c	CATACCCAGGGCTGG	<i>dsrB</i>	1684-1698	1	10	53	9	61	Lever <i>et al.</i> , 2013
dsrB F1d	CACACTCAAGGTTGG	<i>dsrB</i>	1684-1698	1	0	21	1	11	Lever <i>et al.</i> , 2013
dsrB F1e	CACACACAGGGATGG	<i>dsrB</i>	1684-1698	1	0	11	0	13	Lever <i>et al.</i> , 2013
dsrB F1f	CACACGCAAGGATGG	<i>dsrB</i>	1684-1698	1	2	8	1	7	Lever <i>et al.</i> , 2013
dsrB F1g	CACACGCAAGGGTGG	<i>dsrB</i>	1684-1698	1	0	6	0	5	Lever <i>et al.</i> , 2013
dsrB F1h	CATACGCAAGGTTGG	<i>dsrB</i>	1684-1698	1	0	8	0	5	Lever <i>et al.</i> , 2013
dsrB 4RSI2a-h		<i>dsrB</i>	2011-2027	1	44	90	<i>n.a.</i>	<i>n.a.</i>	Lever <i>et al.</i> , 2013
dsrB 4RSI2a	CAGGCGCCGAGCAGAT	<i>dsrB</i>	2011-2027	1	23	60	<i>n.a.</i>	<i>n.a.</i>	Lever <i>et al.</i> , 2013
dsrB 4RSI2b	CAGGCGCCGAGCACAC	<i>dsrB</i>	2011-2027	1	8	15	<i>n.a.</i>	<i>n.a.</i>	Lever <i>et al.</i> , 2013
dsrB 4RSI2c	CATGCTCCGAGCAGAT	<i>dsrB</i>	2011-2027	1	2	13	<i>n.a.</i>	<i>n.a.</i>	Lever <i>et al.</i> , 2013
dsrB 4RSI2d	CACGCGCCGAAGCCAC	<i>dsrB</i>	2011-2027	1	3	3	<i>n.a.</i>	<i>n.a.</i>	Lever <i>et al.</i> , 2013
dsrB 4RSI2e	CATGCACCAACAAAT	<i>dsrB</i>	2011-2027	1	2	13	<i>n.a.</i>	<i>n.a.</i>	Lever <i>et al.</i> , 2013
dsrB 4RSI2f	CAGGCACCAAGCAGAT	<i>dsrB</i>	2011-2027	1	0	18	<i>n.a.</i>	<i>n.a.</i>	Lever <i>et al.</i> , 2013
dsrB 4RSI2g	CAGGCTCCGAGCAGAT	<i>dsrB</i>	2011-2027	1	5	44	<i>n.a.</i>	<i>n.a.</i>	Lever <i>et al.</i> , 2013
dsrB 4RSI2h	CAGGCGCCGAGTACAT	<i>dsrB</i>	2011-2027	1	2	42	<i>n.a.</i>	<i>n.a.</i>	Lever <i>et al.</i> , 2013
rDSR4Rmix		<i>dsrB</i>	2017-2033	96	100	100	<i>n.a.</i>	<i>n.a.</i>	Loy <i>et al.</i> , 2009
rDSR4Ra	CCRAARCAIGCNCCRCA	<i>dsrB</i>	2017-2033	32	23	50	<i>n.a.</i>	<i>n.a.</i>	Loy <i>et al.</i> , 2009
rDSR4Rb	GGRWARCAIGCNCCRCA	<i>dsrB</i>	2017-2033	64	77	100	<i>n.a.</i>	<i>n.a.</i>	Loy <i>et al.</i> , 2009
rDSRB808R	CCCCNACCCADATNGC	<i>dsrB</i>	2011-2027	144	69	79	<i>n.a.</i>	<i>n.a.</i>	Lenk <i>et al.</i> , 2011

^a Recommended primers are highlighted in gray.^b Data indicate primer coverage of all full length oxidative bacterial type *dsrAB* sequences (n=62); 0 MM, no mismatches; 1 wMM, one weighted mismatch.^c Data indicate primer coverage of core dataset oxidative bacterial type *dsrAB* sequences (n=159); 0 MM, no mismatches; 1 wMM, one weighted mismatch; *n.a.*, not applicable for primers binding at the target sites or outside the amplification region of rDSR1F/rDSR4R.^d Position is relative to *Allochroaetium vinosum dsrAB* (NC_013851, 1439735..1442113).^e Degeneracy is given as the number of oligonucleotides that comprise the primer.

Supplementary Table S3

Primer pairs targeting reductive bacterial type <i>dsrAB</i> ^a				full length <i>dsrAB</i> ^b (%)		core dataset <i>dsrAB</i> ^c (%)		Phylogenetic clusters ^d (%)					Reference
Primers	Target gene	Position ^e	Length ^f	0 MM	1 wMM	0 MM	1 wMM	DpS	Fg	ES1	NsS	AgC	
DSR1Fmix/DSR1334R	<i>dsrA</i>	187-1115	929	25	50	n.a.	n.a.	39	0	0	0	0	Santillano <i>et al.</i> , 2010
DSR1Fmix/De11075R	<i>dsrA</i>	187-1132	946	34	62	n.a.	n.a.	51	0	20	0	0	Gittel <i>et al.</i> , 2009
DSR1Fmix/DSR4Rmix	<i>dsrAB</i>	187-2129	1943	47	92	n.a.	n.a.	39	7	0	0	40	Pester <i>et al.</i> , 2010
DSRAB_F/DSRAB_R	<i>dsrAB</i>	187-2136	1950	9	38	n.a.	n.a.	13	0	0	0	0	Schmalenberger <i>et al.</i> , 2007
DSR1Fmix/DSRQP3R	<i>dsrA</i>	187-302	116	13	52	n.a.	n.a.	19	0	20	0	0	Akob <i>et al.</i> , 2012
DSR1Fmix/DSRQ2R	<i>dsrA</i>	187-309	123	3	13	n.a.	n.a.	5	0	0	0	0	Chin <i>et al.</i> , 2007
DSR1-F+/DSR-R	<i>dsrA</i>	187-407	221	13	34	n.a.	n.a.	20	0	0	0	0	Kondo <i>et al.</i> , 2004
DSR1Fmix/DSR5R	<i>dsrA</i>	187-430	244	2	3	n.a.	n.a.	3	0	0	0	0	Wagner <i>et al.</i> , 1998
DSR67F/DSR698R	<i>dsrAB</i>	189-2129	1941	37	91	n.a.	n.a.	45	18	20	0	40	Suzuki <i>et al.</i> , 2005
RH1-dsr-F/RH3-dsr-R	<i>dsrAB</i>	245-408	164	3	18	1	10	2	0	0	0	0	Ben-Dov <i>et al.</i> , 2007
dsr_290F/RH3-dsr-R'	<i>dsrAB</i>	276-408	133	0	1	0	2	0	0	0	0	0	Pereyra <i>et al.</i> , 2010
dsr_290F/dsrA_660R	<i>dsrAB</i>	276-626	351	0	0	0	1	0	0	0	0	0	Pereyra <i>et al.</i> , 2010
1F1/1R1	<i>dsrAB</i>	604-1778	1175	13	47	12	59	34	39	14	0	0	Dhillon <i>et al.</i> , 2003
dsr619AF/dsr1905BR	<i>dsrAB</i>	623-1926	1304	10	36	6	36	8	4	0	3	0	Giloteaux <i>et al.</i> , 2010
P94-F/P93-R	<i>dsrAB</i>	709-2138	1430	3	8	n.a.	n.a.	4	0	0	0	20	Karkhoff-Schweizer <i>et al.</i> , 1995
DSR2MF/DSR4Rmix	<i>dsrAB</i>	717-2129	1413	10	29	n.a.	n.a.	15	0	0	0	20	Akob <i>et al.</i> , 2012
DSR2F/DSR4Rmix	<i>dsrAB</i>	717-2129	1413	10	17	n.a.	n.a.	13	0	0	0	20	Wagner <i>et al.</i> , 1998
DSRp2060F/DSR4Rmix	<i>dsrB</i>	1752-2129	378	13	55	n.a.	n.a.	20	0	0	0	0	Geets <i>et al.</i> , 2005
dsrB F2a-i/4RSI1b,e	<i>dsrB</i>	1758-2123	366	7	68	n.a.	n.a.	11	0	0	0	0	Lever <i>et al.</i> , 2013
dsrB F1a-h/4RSI1a-f	<i>dsrB</i>	1762-2123	362	27	83	n.a.	n.a.	36	14	0	0	0	Lever <i>et al.</i> , 2013
DSR1728mix/DSR4Rmix	<i>dsrB</i>	1762-2129	368	70	94	n.a.	n.a.	72	64	60	0	100	Steger <i>et al.</i> , 2011

^a Coverage values for primer pairs published using DSR1F or DSR4R are calculated using the most up to date version of the primer mix. Recommended primer pairs are highlighted in gray.

^b Data indicate primer coverage of all full length reductive bacterial type *dsrAB* sequences (n=115); 0 MM, no mismatches; 1 wMM, one weighted mismatch.

^c Data indicate primer coverage of all core reductive bacterial type *dsrAB* sequences (n=1110); 0 MM, no mismatches; 1 wMM, one weighted mismatch; n.a., not applicable for primers binding at the target sites or outside the amplification region of DSR1F/DSR4R.

^d Primer coverage of full length/core dataset *dsrAB* sequences in higher taxonomic clusters. DpS, *Deltaproteobacteria* supercluster (n=75/709); Fg, *Firmicutes* group (n=28/180); ES1, Environmental supercluster 1 (n=5/170); NsS, Nitrospirae supercluster (n=2/39); AgC, *Archaeoglobus* cluster (n=5/12). The larger core dataset is used for primers binding within the DSR1F/DSR4R region.

^e Position is relative to *Desulfovibrio vulgaris* Hildenborough *dsrAB* (NC_002937, 449888..452365).

^f Expected length of the PCR amplicon.

Supplementary Table S4

Primer pairs targeting oxidative bacterial type <i>dsrAB</i> ^a				full length <i>dsrAB</i> ^b (%)		core dataset <i>dsrAB</i> ^c (%)		Reference
Name	Target gene	Position ^d	Length ^e	0 MM	1 wMM	0 MM	1 wMM	
rDSR1Fmix/rDSR4Rmix	<i>dsrAB</i>	169-2033	1865	97	100	n.a.	n.a.	Loy <i>et al.</i> , 2009
rDSRA240F/rDSRB808R	<i>dsrAB</i>	172-2027	1856	69	79	n.a.	n.a.	Lenk <i>et al.</i> , 2011
PGdsrAF/PGdsrAR	<i>dsrA</i>	379-870	492	32	53	29	57	Mori <i>et al.</i> , 2010
dsrA 625F/dsrA 877R	<i>dsrA</i>	625-877	253	2	26	1	21	Luo <i>et al.</i> , 2011
DSR874F/rDSR4Rmix	<i>dsrAB</i>	859-2033	1175	71	100	n.a.	n.a.	Loy <i>et al.</i> , 2009
dsrB F1a-h/4RSI2a-h	<i>dsrB</i>	1684-2027	344	29	82	n.a.	n.a.	Lever <i>et al.</i> , 2013
DSR1728mix/rDSR4Rmix	<i>dsrB</i>	1684-2033	350	90	100	n.a.	n.a.	Steger <i>et al.</i> , 2011

^a Recommended primer pairs are highlighted in gray.

^b Data indicate primer coverage of all full length reverse *dsrAB* sequences (n=62); 0 MM, no mismatches; 1 wMM, one weighted mismatch.

^c Data indicate primer coverage of core dataset reverse *dsrAB* sequences (n=159); 0 MM, no mismatches; 1 wMM, one weighted mismatch; n.a., not applicable for primers binding at the target sites or outside the amplification region of rDSR1F/rDSR4R.

^d Position is relative to *Allochrocatium vinosum dsrAB* (NC_013851, 1439735..1442113).

^e Expected length of the PCR amplicon.

Chapter IV

**Bacterial community response during
degradation of cyanobacterial biomass and
acetate in a sulfate-reducing Arctic fjord
sediment**

Bacterial community response during degradation of cyanobacterial biomass and acetate in a sulfate-reducing Arctic fjord sediment

Müller A.L., de Rezende J.R., Putz M., Kjeldsen K.U., Jørgensen B.B., and Loy A.

Biogeochemical processes in marine sediments are primarily responsible for the remineralization of organic matter in the ocean and are therefore a crucial part of the global carbon cycle. Since 90% of the sea floor has temperatures below 4°C, psychrophilic organisms adapted to these temperatures are of yet underappreciated importance. The aim of this study was to gain novel insights into the ecophysiology of organic matter degradation in an Arctic marine sediment and the impact of sulfate-reducing microorganisms on this process by using cyanobacterial biomass as a model substrate mixture for complex organic matter input and acetate as a typical degradation intermediate. Here we show the response of individual phylotypes in cold, anoxic sediment incubations as determined by relative increases in 16S rRNA gene and cDNA abundance via pairwise comparisons of amplicon libraries with and without added substrate. Measurement of volatile fatty acid concentrations and sulfate reduction rates revealed that acetate, formate, and propionate were the main degradation products of cyanobacterial biomass and that consumption of acetate, propionate, butyrate, and valerate was selectively impacted by sulfate-reducing microorganisms in the sediment. Bacterial 16S rRNA phylotype dynamics suggested that phylotypes classified as *Psychrilyobacter*, *Colwellia*, *Marinifilum*, and *Psychromonas* were the primary degraders of cyanobacterial biomass and phylotypes classified as *Desulfobacteraceae*, *Desulfobulbaceae*, and *Arcobacter* were the main acetate utilizers. Additionally, we identified several putative sulfate-reducing phylotypes among the deltaproteobacterial families *Desulfobacteraceae* and *Desulfobulbaceae*. In summary, our findings provide a step forward in understanding the dynamics of psychrophilic degradation of organic matter in Arctic marine sediments and provide a solid basis for further studies aiming to directly link identity and function of carbon degrading bacteria in these sediments.

Note: This is a preliminary manuscript of a study that was designed as a stable isotope probing experiment. The manuscript has been written by Albert Müller and provisionally revised by Alexander Loy but not by the other co-authors. We present data from sulfate reduction and volatile fatty acid measurements as well as bacterial 16S rRNA gene and cDNA amplicon pyrosequencing data from the incubations. Results from this study will be published at a later time point, together with data confirming the incorporation of the labeled substrate by methods like Raman microspectroscopy combined with fluorescence in situ hybridization.

Introduction

Organic material that reaches the sea floor is gradually degraded and respired (reviewed in Arndt *et al.* (2013)). Oxidation of organic matter is coupled to the sequential utilization of terminal electron acceptors, typically in the order of oxygen, nitrate, manganese, iron and sulfate. Oxygen respiration dominates in deep sea sediments, whereas in continental shelf sediments equal parts of organic carbon are oxidized by sulfate reduction and oxic respiration (Jørgensen, 1982; Canfield, 1989). In

continental shelf sediments, which typically have higher sedimentation rates, the more favorable electron acceptors are quickly depleted in the uppermost few centimeters and sulfate reduction becomes the most important oxidative process (Jørgensen, 1982). In anoxic subsurface marine sediments, polymeric macromolecules, such as proteins, nucleic acids, lipids or polysaccharides, are broken down by hydrolytic bacteria into monomers that subsequently serve as substrates for fermentative bacteria. These organisms then produce a broad range of fermentation products

that are further mineralized by sulfate reducing microorganisms (SRM) to carbon dioxide in the presence of sulfate or by methanogens to methane in the absence of sulfate (Muyzer & Stams, 2008).

Arctic marine sediments are characterized by permanently cold temperatures. Since 90% of the sea floor has temperatures below 4°C (Levitus & Boyer, 1994), permanently cold marine sediments represent one of the largest microbial habitats. While microbial activity in temperate environments is generally reduced during cold seasons (reviewed in Rivkin *et al.* (1996)), microbial activity in permanently cold habitats is comparable to the activity in temperate environments during the warm season (Nedwell *et al.*, 1993; Rivkin *et al.*, 1996; Arnosti *et al.*, 1998; Glud *et al.*, 1998; Sagemann *et al.*, 1998). These observations suggest that these permanently cold sediments are inhabited by genuine psychrophiles, i.e. organisms that are well adapted to cold temperatures by unique features in their proteins (e.g. reduced activation energy and enhanced structural flexibility) and membranes (e.g. incorporation of specific lipid constituents that maintain fluidity) (reviewed in Deming (2002)). The degradation of organic material in Arctic marine sediments has been studied in Svalbard fjords by determining rates of enzymatic hydrolysis, sulfate reduction, or denitrification (Rysgaard *et al.*, 2004; Arnosti *et al.*, 2005; Arnosti & Jørgensen, 2006; Finke *et al.*, 2007). Despite the cold temperatures, the transformation of particulate to dissolved organic matter and the turnover of carbon through the dissolved pool occur quite rapidly (Arnosti & Jørgensen, 2006). Microbial abundance and cellular rRNA content in Svalbard sediments are comparable to temperate sediments and show a steep decrease with increasing sediment depth (Sahm & Berninger, 1998). Svalbard sediments harbor highly diverse microbial communities that were shown to be dominated by *Deltaproteobacteria*, *Gammaproteobacteria*, and *Bacteroidetes* by rRNA slot blot hybridization and fluorescence *in situ* hybridization (Ravenschlag *et al.*, 1999; Ravenschlag *et al.*, 2000; Ravenschlag *et al.*, 2001). These communities are particularly adapted to low temperature and are substrate limited, rather than temperature limited (Arnosti *et al.*, 1998; Sagemann *et al.*, 1998; Kostka *et al.*, 1999; Arnosti & Jørgensen, 2003). Identities of members of the microbial community in Svalbard sediments have been determined by 16S rRNA sequencing (Park *et al.*, 2011; Teske *et al.*, 2011), but in order to understand carbon degradation in Arctic marine sediments, it is necessary to directly link processes to the specific organisms performing them. So far, specific members of the SRM community have been isolated (Knoblauch *et al.*, 1999; Sahm *et al.*, 1999), but the identities and

activities of other members of the microbial food chain are largely unknown.

We performed a stable isotope probing approach in order to unravel carbon degradation processes in Arctic marine sediments in Smeerenburgfjorden, Svalbard, and directly link them with the organisms performing these processes. Smeerenburgfjorden Station J is a comparatively well-studied sampling location for which a large amount of data is available (Ravenschlag *et al.*, 2000; Ravenschlag *et al.*, 2001; Finke *et al.*, 2007; Teske *et al.*, 2011). Sulfate reduction was shown to be the sole terminal mineralization process in the sulfidic layer between 5 cm and 10 cm depth (Finke *et al.*, 2007). Sediment taken from this layer was incubated at 0°C with ¹³C-labeled substrates in order to identify the members of the bacterial community that are responsible for their degradation. Acetate was chosen as a substrate to specifically target members of the SRM community, since it was shown to be the most important electron donor accounting for 40% of sulfate reduction in this sediment layer (Finke *et al.*, 2007), whereas freeze-dried cyanobacterial cells were used in order to track the degradation of a natural complex substrate mixture. Changes in volatile fatty acid (VFA) concentrations and sulfate reduction rates were measured to monitor organic carbon degradation, while corresponding bacterial phylotype dynamics were analyzed by pyrosequencing of bacterial 16S rRNA gene and cDNA amplicons. We thereby identified phylotypes that (i) responded to acetate and/or cyanobacterial biomass addition and (ii) were associated with sulfate reduction.

Materials and Methods

Marine sediment samples

Arctic marine sediment samples were collected from Smeerenburgfjorden, Svalbard (Station J; 79°43'N, 11°05'E; water depth 216 m). The 5 to 10-cm sediment depth interval, which generally corresponds to the zone of maximal sulfate reduction at this station (Finke *et al.*, 2007), was collected from several HAPS cores (KC Denmark A/S, Silkeborg, Denmark) (Kannevorff & Nicolaisen, 1972) after removing the top 5 cm surface layer, transferred to gas-tight plastic bags (Hansen *et al.*, 2000) and stored on ice at 0°C for 2.5 months prior to incubation.

Sediment incubation

Approximately 8 l of sediment slurry were prepared by homogenizing sediment with anoxic Station J bottom water at a 1:1 (w/w) ratio under constant flow of N₂ gas to maintain anoxic conditions. Slurries

were distributed to 200 ml serum bottles under N_2 , amended with different substrates and incubated at 0°C (Figure 1). Incubations were performed in two replicates with two different substrates, acetate and “spirulina” (Sigma-Aldrich, Steinheim, Germany), which consists of freeze-dried cells of the cyanobacterium *Arthrospira platensis*. Two different substrate concentrations (50 μM and 1 mM acetate, 50 $\mu\text{g l}^{-1}$ and 1 mg l^{-1} spirulina) were used; a low concentration mimicking concentrations that the organisms could realistically encounter *in situ*, as well as a higher concentration in order to enhance labeling efficiency and possibly stimulate growth of organisms able to utilize the respective substrate. Spirulina was added as a one-time pulse in the beginning of the experiment, whereas acetate was continuously added every 4-7 days in order to compensate for the acetate turnover (Figure 1B). Each incubation was performed with ^{13}C -labeled acetate or ^{13}C -labeled spirulina (both Sigma Aldrich, 99 atom % ^{13}C), a ^{12}C substrate (“unlabeled control”), a ^{13}C -labeled substrate in combination with a sulfate reduction inhibitor (“inhibited control”) and a control incubation to which no substrate was added (“no substrate control”). 5 mM molybdate was used as an inhibitor of sulfate reduction and replenished

after 3 weeks. 6.5 ml samples were taken 0, 4, 8, 13, 20, 25, 32, and 39 days after the start of the incubation and frozen at -80°C . Concentrations of eight VFAs (formate, acetate, propionate, butyrate, valerate, lactate, pyruvate, and succinate) were measured in the supernatant by 2-dimensional ion chromatography-mass spectrometry (IC-IC-MS; Dionex ICS-3000-MSQ, with AS 11 HC as the first column to separate the VFAs from chloride, and AS 24 as the second column) (Glombitza *et al.*, 2014). Parallel incubations were set up with ^{35}S -labeled carrier-free sulfate tracer and sulfate reduction rates were determined using a single-step cold chromium distillation method (Kallmeyer *et al.*, 2004).

Nucleic acid extraction

Total RNA was extracted by a protocol modified from Lueders *et al.* (2004). Approximately 500 μl of sediment slurry were homogenized by bead beating with 750 μl of sodium phosphate buffer and 250 μl of a sodium dodecyl sulfate solution (Henckel *et al.*, 1999) and centrifuged. Nucleic acids were extracted from the supernatant consecutively with equal volumes of phenol/chloroform/isoamyl alcohol (P/C/I, 25:24:1, pH 5.2, Fisher Scientific, Fair Lawn, NJ, USA) and chloroform/isoamyl alcohol (C/I, 24:1,

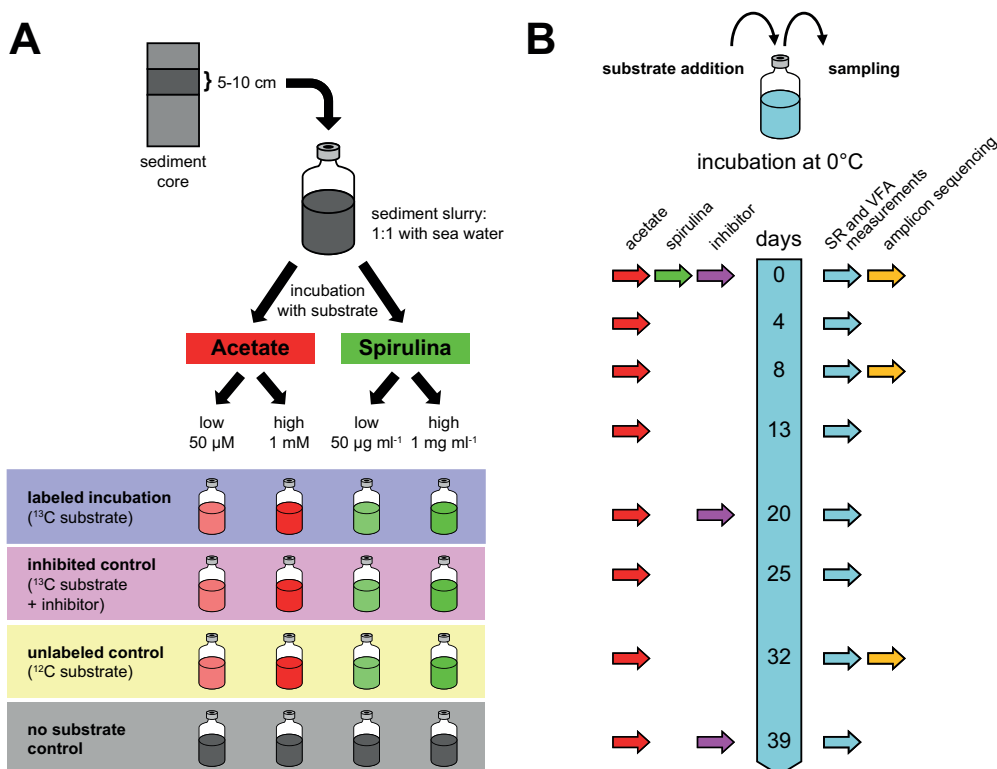


Figure 1. Sediment slurry incubations at 0°C . A) Overview of the incubation setup showing used substrates, substrate concentrations and control incubations. B) Incubation timeline showing time points of substrate addition and sampling.

Carl Roth, Karlsruhe, Germany) and were precipitated from the aqueous phase with two volumes of polyethylene glycol 8000 (Sigma-Aldrich, Steinheim, Germany) (Griffiths *et al.*, 2000). After centrifugation (20,000 g, 4°C, 30 min), the pellets were washed with 70% ethanol and resuspended in 100 µl H₂O. Co-extracted DNA was digested with the TURBO DNA-free™ kit (Ambion, Austin, TX, USA) according to the manufacturer's instructions and RNA was re-extracted with TRIzol (Invitrogen, Darmstadt, Germany) according to the manufacturer's instructions. Extraction of total DNA was performed using PowerSoil®DNA isolation kit (MO BIO Laboratories, Inc., Carlsbad, CA, USA) according to manufacturer's instructions.

PCR and multiplex amplicon pyrosequencing

PCR amplicon libraries were constructed from DNA and RNA extracted from each incubation at days 0, 8, and 32 using a two-step PCR approach with low cycle numbers (20+5 cycles) and triplicate PCR reactions were pooled to reduce variability associated with barcoded pyrosequencing primers (Berry *et al.*, 2011). For the RNA extractions the Access RT-PCR System (Promega, Madison, WI, USA) was used instead of the first PCR steps according to the manufacturer's instructions (but with only 20 PCR cycles). PCR products were purified using the Agencourt® Ampure® XP system (Beckman Coulter, Vienna, Austria) and the DNA concentration was determined using a Quant-iT™ PicoGreen® dsDNA Assay (Invitrogen, Darmstadt, Germany). Amplicons were then pooled and sequencing was performed on a GS FLX+ instrument using Titanium chemistry (Roche, Mannheim, Germany) by Eurofins MWG Operon (Ebersberg, Germany). Sequencing reads were filtered using the PyroNoise implementation in mothur (Quince *et al.*, 2009; Schloss *et al.*, 2009). A 97% identity threshold was used for clustering reads into phylotypes of approximate species-level resolution with UCLUST (Edgar, 2010) and representative sequences were aligned with mothur using default settings (Schloss *et al.*, 2009). Chimeras were detected using Chimera Slayer (Haas *et al.*, 2011) and excluded from further analysis.

Alpha and beta diversity analyses

Alpha diversity metrics (observed phylotype richness, Chao1 richness, Simpson index, Shannon index, and equitability index) were calculated (Caporaso *et al.*, 2010) with re-sampling (100 re-samples) at 3,250 reads to avoid sample based artifacts (Lozupone *et al.*, 2011). Principle coordinates analysis (PCoA) was performed based on Bray-Curtis dissimilarities using QIIME (Caporaso *et al.*, 2010) with re-sampling (100 re-samples) at the size of the smallest library (210 reads).

Identification of phylotypes associated with substrate utilization and sulfate reduction

Pairwise comparisons of incubations with ¹³C-labeled substrate to the no substrate controls and inhibited controls (¹³C-labeled substrate plus molybdate) at any given time point were used to identify phylotypes associated with the utilization of the added substrate and sulfate reduction, respectively. Significant enrichment of phylotypes in an incubation with ¹³C-labeled substrate compared to the respective control was determined using a two-proportion T-test and P-values were corrected for multiple comparisons using the false discovery rate method in R (Benjamini & Hochberg, 1995) to account for uncertainty due to sequence sampling depth. Corrected P-values less than or equal to 0.01 were considered significant.

Phylogenetic tree calculation

Representative sequences of phylotypes that were present with a relative abundance of ≥1% of the community in at least one incubation sample were aligned using the online aligner SINA (Pruesse *et al.*, 2012). A phylogenetic consensus tree was calculated using a manually curated alignment of the three most closely related sequences for each phylotype determined by SINA as well as closely related cultivated organisms from the non-redundant SILVA database (SSU Ref NR 119) (Quast *et al.*, 2013) and/or the NCBI RefSeq database (Tatusova *et al.*, 2014) for reference. Three trees were calculated using a 50% conservation filter for bacteria covering 1,222 nucleotide positions using maximum likelihood (RAxML) and maximum parsimony (PHYLIP DNAPARS) in ARB (Ludwig *et al.*, 2004) and neighbor joining (PHYLIP NEIGHBOR) in the PHYLIP software package (Felsenstein, 1989). A consensus tree was constructed using the extended majority rule (PHYLIP CONSENSE) and branch lengths of the consensus tree were adjusted using PHYLIP DNAML. The short amplicon sequences were subsequently added to the consensus tree using the EPA algorithm (Berger *et al.*, 2011) in RAxML-HPC 7.5.6 (Stamatakis, 2006). Taxonomy was assigned to phylotypes according to SILVA taxonomy (Yilmaz *et al.*, 2014) in case no closely related cultivated organisms were available. Trees were visualized using iTOL (Letunic & Bork, 2007).

Results

16S rRNA gene and cDNA amplicon pyrosequencing

We performed pyrosequencing of bacterial 16S rRNA gene and cDNA amplicons in order to identify the organisms that responded to substrate addition

during psychrophilic incubations (Figure 1). Altogether, we obtained 344,867 high quality reads (4,732 reads per sample on average) with an average length of 220 nucleotides that clustered into 11,715 phylotypes (of which 4,338 were singletons). Coverage of the bacterial community and alpha diversity estimates were comparable across most incubation samples and were not influenced by incubation time, substrate addition, substrate type, substrate concentration, or the type of nucleic acid analyzed (Table S1). PCoA indicated that beta diversity remained largely unchanged during the incubations, by showing no clear separation by incubation time or substrate addition for both 16S rRNA gene and cDNA libraries (Figure 2). The only exceptions were samples from incubations with high concentration of ^{13}C -labeled spirulina, which clustered separately from all other incubations samples (Figure 2). This indicates that a high concentration of this substrate led to substantial changes in the composition of the bacterial community. Samples from incubations with a high concentration of unlabeled spirulina, however, did not cluster with these samples.

The bacterial 16S rRNA gene and cDNA amplicon libraries retrieved at the start of the experiment were dominated by *Deltaproteobacteria* (28%/31% of all sequences on DNA/RNA level), *Bacteroidetes* (18%/15%), *Gammaproteobacteria* (16%/16%), *Verrucomicrobia* (4%/7%), and *Planctomycetes* (5%/5%) (Figure 3A). 3,824 phylotypes were found in day 0 samples with the most abundant phylotype constituting 3.1% and 6.8% of all sequences at

DNA/RNA level. At DNA level, 33 phylotypes showed an abundance of $\geq 0.5\%$, together comprising 44.6% of all sequences. Figure 3B shows rank abundance plots for DNA and RNA samples at day 0 of the incubation. 89 phylotypes were present with $\geq 1\%$ of the community at any incubation time point (Figure S1). 25 of those 89 phylotypes showed an average abundance of $\geq 1\%$ in DNA and/or RNA samples at day 0 (Table S2, Figure 3B).

Deltaproteobacteria accounted for almost a third of all 16S rRNA gene and cDNA sequences at day 0 and were mostly represented by phylotypes that were affiliated with sulfate-reducing bacteria of the families *Desulfobacteraceae* and *Desulfobulbaceae* (Table S2, Figure S1). The most abundant phylotypes at day 0 were *Desulfobacteraceae* phylotypes 2011, 11380, and 4982, *Desulfobulbus* phylotypes 6023 and 10263, *Desulfuromonas* phylotype 3714, and *Desulfobacteraceae* phylotype 10184. *Gammaproteobacteria* were mostly represented by members of the orders *Alteromonadales*, *Chromatiales* and *Oceanospirillales*, the most abundant gammaproteobacterial phylotypes at day 0 were *Marinicella* phylotype 62, *Acidiferrobacter* phylotype 2799, BD7-8 marine group phylotype 9245, and *Colwellia* phylotype 7234 (Table S2, Figure S1). *Bacteroidetes* were mostly represented by phylotypes of the families *Marinilabiliaceae* and *Flavobacteriaceae* (Table S2, Figure S1). The most abundant *Bacteroidetes* phylotypes at day 0 were *Marinifilum* phylotype 4400 (*Marinilabiliaceae*), *Lutimonas* phylotype 1270 and *Lutibacter* phylotype 10972 (both *Flavobacteriaceae*).

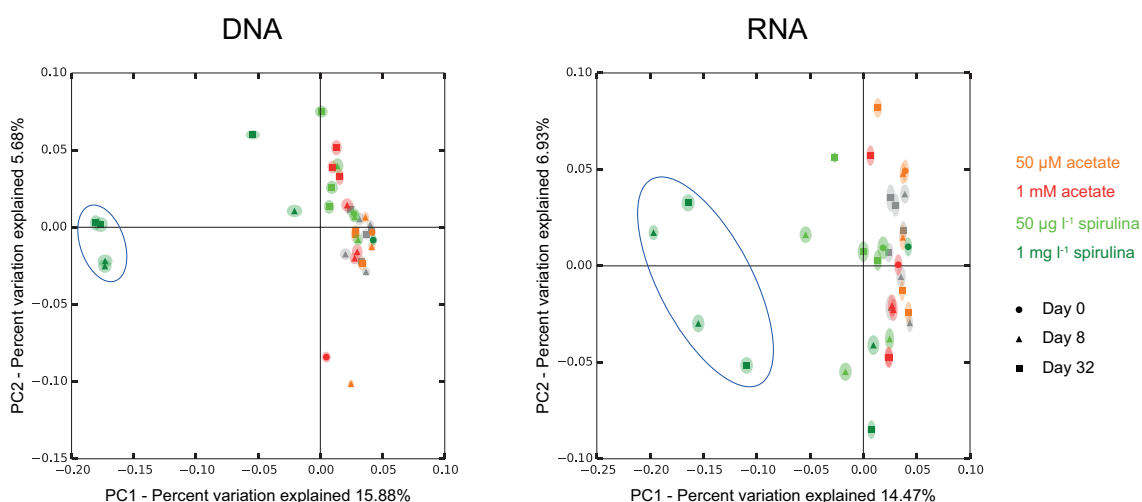


Figure 2. Principal coordinates analysis (PCoA) of the bacterial community based on the Bray-Curtis dissimilarity metric. Incubation samples are colored by type and concentration of the used substrate: 1 mg l^{-1} spirulina (dark green), 50 $\mu\text{g l}^{-1}$ spirulina (light green), 1 mM acetate (red), 50 μM acetate (orange), no substrate controls (gray). Samples from day 0 are colored in black. The blue circle indicates clustering of samples that were incubated with 1 mg l^{-1} ^{13}C -labeled spirulina.

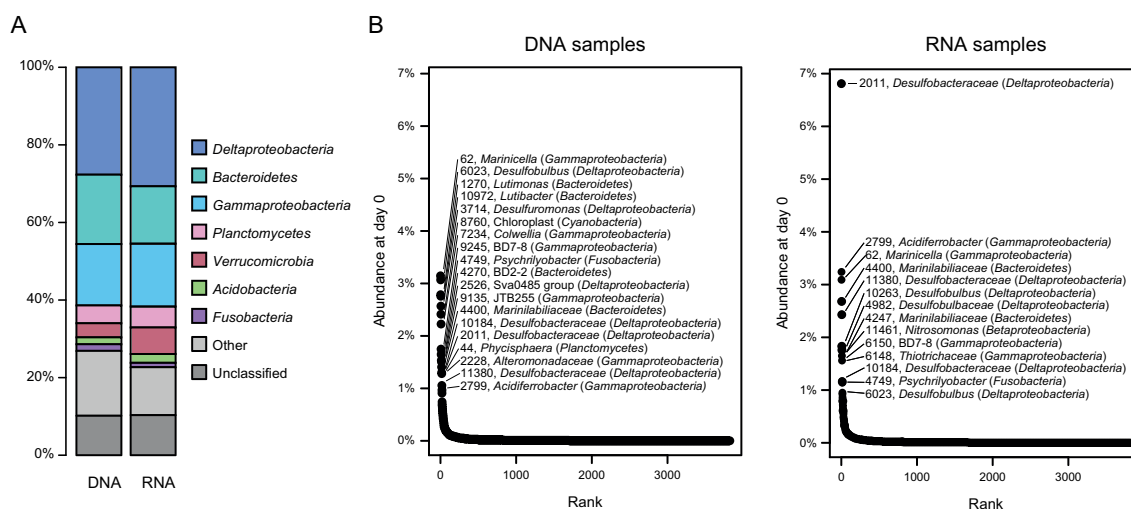


Figure 3. Microbial community composition based on sequencing of bacterial 16S rRNA amplicons in DNA and RNA samples from day 0. A) Composition on phylum level (class level for *Proteobacteria*). B) Rank abundance plots of phylotypes (97% identity). Phylotypes with $\geq 1\%$ of total sequences are labeled.

Sulfate reduction rates

Sulfate reduction rates were measured over the course of the incubation (Figure 4). The background sulfate reduction rates of the no substrate control varied between 9 and 18 $\text{nmol cm}^{-3} \text{d}^{-1}$. Sulfate reduction rates in the inhibited control did not exceed background level. Addition of acetate (Figure 4A) generally resulted in increased rates of 12-40 $\text{nmol cm}^{-3} \text{d}^{-1}$ compared to the no substrate control. Generally, sulfate reduction rates were higher when a higher concentration of acetate was added. However, an acetate addition increase by a factor of

20 led only to an average increase in sulfate reduction of 38%. The trends were similar when spirulina was used as a substrate (Figure 4B). Addition of spirulina clearly stimulated sulfate reduction to rates of 12-64 $\text{nmol cm}^{-3} \text{d}^{-1}$ and increasing the substrate concentration from 50 $\mu\text{g l}^{-1}$ to 1 mg l^{-1} only led to an increase of 55% in average sulfate reduction rates. While sulfate reduction rates remained constant over the course of the incubation in the acetate incubations they increased markedly from day 0 to day 4 and day 8 in the spirulina incubations.

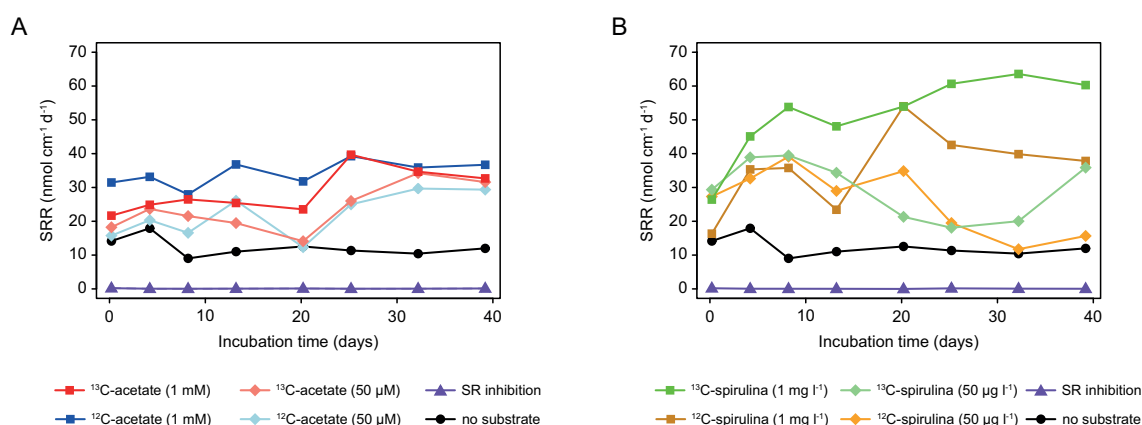


Figure 4. Sulfate reduction rates (in $\text{nmol cm}^{-3} \text{d}^{-1}$) measured in incubations where acetate (A) and spirulina (B) were added as substrates.

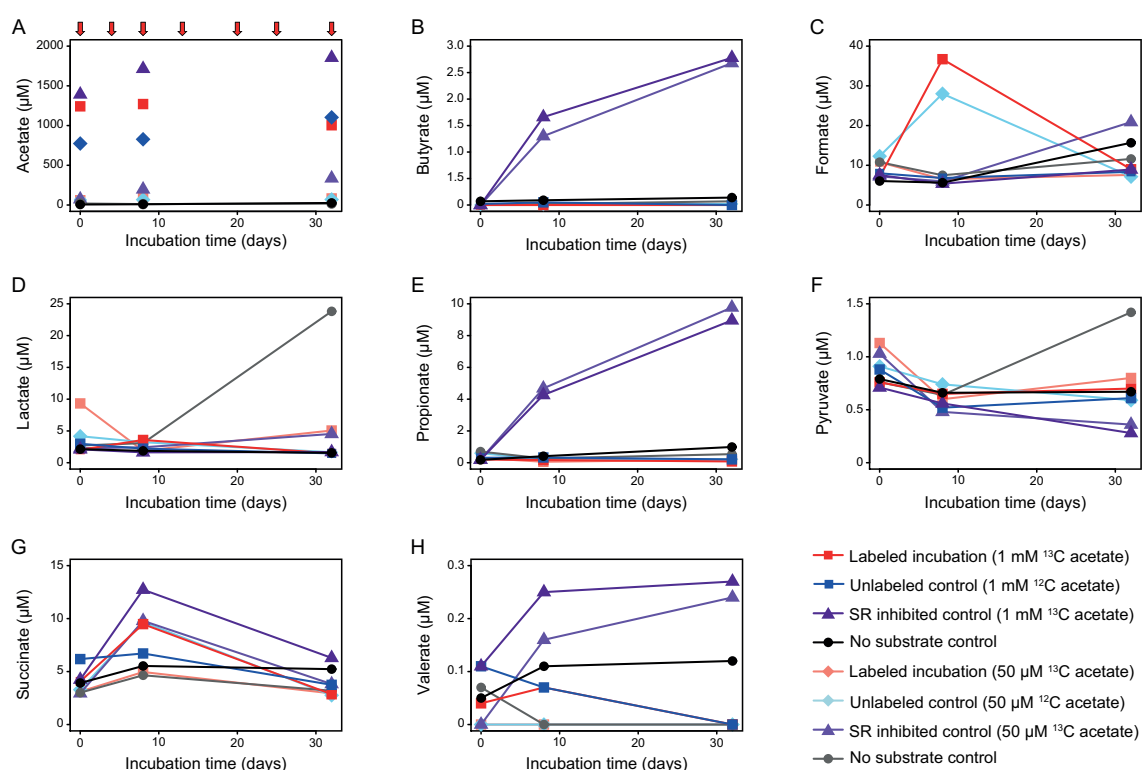


Figure 5. Concentration (in μM) of volatile fatty acids measured in incubations where acetate was added as a substrate: acetate (A; note that acetate was added (red arrows) right before the measurement so changes due to consumption of acetate are not visible in the graph), butyrate (B), formate (C), lactate (D), propionate (E), pyruvate (F), succinate (G), and valerate (H).

Volatile fatty acids

VFA concentrations were monitored over the course of the incubations (Figures 5 and 6). The VFAs with the highest background concentration (average concentration in the no substrate controls) were acetate ($12 \mu\text{M}$), formate ($9 \mu\text{M}$), succinate ($5 \mu\text{M}$), and lactate ($4 \mu\text{M}$), whereas the other measured VFAs were present at average concentrations of $<1 \mu\text{M}$ (propionate, 411 nM ; pyruvate, 756 nM ; butyrate, 44 nM ; valerate, 41 nM).

In the incubations where acetate was added as a substrate (Figure 5), acetate was consumed and repeatedly replenished to the desired level (1 mM and $50 \mu\text{M}$) by addition of $^{13}\text{C}/^{12}\text{C}$ acetate to the respective incubations (Figure 5A). With the exception of a few outliers (formate in the incubations with $1 \text{ mM } ^{13}\text{C}$ -acetate and the $50 \mu\text{M } ^{12}\text{C}$ acetate at day 8 (Figure 5C) and lactate and pyruvate in a no substrate control at day 32 (Figure 5D and F)), concentrations of other VFAs remained similar after acetate addition. However, inhibition of sulfate reduction led to an accumulation over time of acetate, butyrate, propionate, and valerate (Figure 5A, B, E, and H). Such a buildup indicates that under uninhibited conditions sulfate reduction is

responsible for removing the excess of these VFAs from the substrate pool, suggesting that acetate, propionate, butyrate, and valerate are substrates of SRM in this sediment.

In the incubations with spirulina we observed differences in VFA concentrations between incubations with labeled and unlabeled substrate, possibly caused by different properties of ^{13}C - and ^{12}C -spirulina substrates (substrate solutions were visibly different in regards to color and homogeneity) (Figure 6). In contrast to acetate, spirulina was only added in the beginning as a pulse labeling. At day 0, all measured VFA levels in the incubations with ^{13}C -labeled spirulina are similar to the no substrate control, indicating that the ^{13}C -spirulina substrate does not contain significant amounts of these VFAs. Acetate, formate, and propionate increased in concentration at day 8 and decreased again at day 32 of the incubation, whereas concentrations of butyrate, lactate, pyruvate, succinate, and valerate did not change substantially in the incubations with ^{13}C -labeled spirulina and were comparable to the no substrate controls (Figure 6). An increase and subsequent decrease in concentration of acetate, formate, and propionate indicates that these VFAs

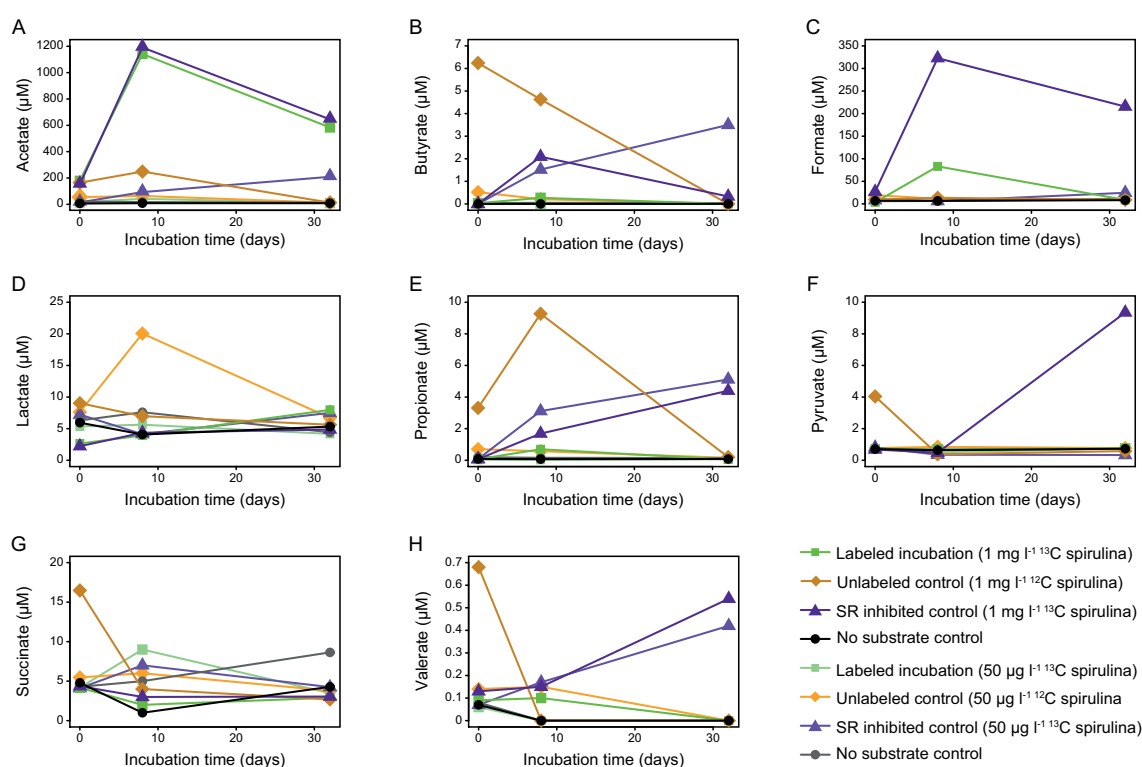


Figure 6. Concentration (in μM) of volatile fatty acids measured in incubations where spirulina was added as a substrate: acetate (A), butyrate (B), formate (C), lactate (D), propionate (E), pyruvate (F), succinate (G), and valerate (H).

are first produced from the added organic matter and later consumed. Analogous to the acetate incubations, inhibition of sulfate reduction led to the accumulation of acetate, butyrate, propionate, and valerate, as well as formate and pyruvate (though in the latter case only at high spirulina concentration). Again, indicating that these VFAs are normally consumed during sulfate reduction. The additional accumulation of formate and pyruvate suggests that these VFAs primarily derive from the added spirulina substrate, which in case of formate is supported by its increased levels in the incubation with ^{13}C -labeled spirulina compared to the no substrate control.

Phylotypes responding to substrate addition

We compared incubations with supplemented substrate to the no substrate control of the same time point to reveal which phylotypes responded to substrate addition. 18 phylotypes were significantly enriched in 16S rRNA gene or cDNA libraries when acetate was added (Table 1). Most phylotypes stimulated by acetate addition were affiliated with *Deltaproteobacteria* (n=6) and *Lentisphaerae* (n=4). *Desulfobacteraceae* phylotype 2011, which is highly abundant at day 0 with 1.3% of all bacterial 16S rRNA gene and 6.8% of all bacterial 16S cDNA

sequences, was significantly enriched in two incubation samples and generally increased in abundance in incubations where sulfate reduction was not inhibited and generally decreased in the inhibited controls (Table 1). *Desulfobulbaceae* phylotype 4982, *Desulfobulbus* phylotype 10263 (both *Deltaproteobacteria*), and *Colwellia* phylotype 7234 (*Gammaproteobacteria*) were the only other acetate stimulated phylotypes that were highly abundant at day 0. Significant enrichments of these four phylotypes were only observed in cDNA libraries, indicating that they mainly responded to acetate addition with increased transcriptional activity but not growth. Most of the other phylotypes were detected in low sequence numbers at day 0 and were generally only significantly enriched at a single incubation time point. The one exception was *Arcobacter* phylotype 10615 (*Epsilonproteobacteria*) that was present at day 0 with <0.02% of sequences but was consistently enriched when acetate was added; with the extent of enrichment scaling with both incubation time and amount of substrate added (Table 1). It was also the only phylotype that showed clear signs of growth in response to acetate addition, as its abundance increased to up to 6.7% of all 16S rRNA gene

sequences after 32 days of incubation with 1 mM acetate.

When spirulina was added as a substrate, 24 phylotypes were significantly enriched in at least one incubation time point (Table 2) with multiple phylotypes among *Deltaproteobacteria* (n=7), *Bacteroidetes* (n=6), *Firmicutes* (n=3), and *Gamma-proteobacteria* (n=2). *Marinifilum* phylotype 4400, *Psychrobacter* phylotype 4749, and *Psychromonas* phylotype 7435 responded with massive abundance increases in both 16S rRNA gene and cDNA libraries (especially after 32 days of incubation with a high spirulina concentration) of up to 28%, 14%, and 36% of all sequences at one incubation time point, respectively (Table 2). Other phylotypes that were consistently enriched (in ≥ 7 of 24 samples) compared to the no substrate control were *Colwellia* phylotype 7234 (*Gammaproteobacteria*), *Fusibacter* phylotype 1452 (*Firmicutes*), *Marinilabiliaceae* phylotype

9869 (*Bacteroidetes*) and *Arcobacter* phylotype 10615 (*Epsilonproteobacteria*) (Table 2). All of these phylotypes showed significant enrichment in both 16S rRNA gene and cDNA amplicon libraries (Table 2).

Given that acetate was the main fermentation product of spirulina degradation it is not surprising that the phylotypes that showed a strong response to the addition of acetate were also enriched in the spirulina incubations (Table 2). The four acetate-utilizing phylotypes with the highest abundances at day 0 (*Desulfobacteraceae* phylotype 2011, *Desulfobulbaceae* phylotype 4982, *Colwellia* phylotype 7234, and *Desulfobulbus* phylotype 10263) were all enriched in at least one spirulina incubation time point compared to the respective no substrate control. Also *Arcobacter* phylotype 10615 responded similarly to spirulina as to acetate addition.

Table 1. Relative abundance of phylotypes that were significantly enriched following addition of acetate^a compared to the no substrate control

OTU ID	Phylogenetic affiliation	sample type	d0	50 μ M acetate						1 mM acetate						Legend ^b
				d8			d32			d8			d32			
				¹³ C	¹² C	¹³ C inh.	¹³ C	¹² C	¹³ C inh.	¹³ C	¹² C	¹³ C inh.	¹³ C	¹² C	¹³ C inh.	
2011	<i>Desulfobacteraceae</i> (<i>Deltaproteobacteria</i>)	DNA	1.3%	0.2%	2.7%	1.3%	1.2%	2.2%	1.0%	1.2%	1.3%	1.3%	1.0%	1.0%	1.1%	5.0%
		RNA	6.8%	7.3%	n.d. ^c	3.3%	9.1%	7.7%	1.6%	9.4%	6.2%	n.d. ^b	9.7%	7.9%	2.5%	2.5%
4982	<i>Desulfobulbaceae</i> (<i>Deltaproteobacteria</i>)	DNA	0.7%	0.7%	2.3%	0.3%	1.1%	1.1%	0.3%	0.8%	0.9%	0.5%	1.1%	0.6%	0.9%	1.0%
		RNA	1.8%	3.0%	n.d.	1.3%	2.7%	4.4%	0.6%	2.5%	3.4%	n.d.	2.8%	2.8%	1.2%	0.5%
7234	<i>Colwellia</i> (<i>Gammaproteobacteria</i>)	DNA	2.2%	0.3%	0.0%	0.4%	0.6%	0.1%	0.6%	0.4%	0.4%	0.1%	0.8%	1.1%	0.4%	0.0%
		RNA	0.2%	0.3%	n.d.	0.6%	0.4%	0.6%	0.8%	0.9%	0.9%	n.d.	0.6%	1.9%	0.4%	-0.5%
10263	<i>Desulfobulbus</i> (<i>Deltaproteobacteria</i>)	DNA	0.2%	0.4%	0.4%	0.3%	0.1%	0.8%	0.8%	0.1%	0.1%	0.3%	0.1%	0.1%	0.1%	-1.0%
		RNA	1.8%	2.9%	n.d.	1.7%	3.2%	3.4%	1.7%	4.0%	3.2%	n.d.	0.5%	1.9%	2.1%	-2.5%
11481	R76-B128 group (<i>Lentisphaerae</i>)	DNA	0.2%	0.2%	2.3%	0.2%	0.1%	0.1%	0.2%	0.1%	0.3%	0.0%	0.0%	0.0%	0.1%	-5.0%
		RNA	0.4%	0.3%	n.d.	0.5%	0.4%	0.5%	0.7%	0.3%	0.4%	n.d.	0.4%	0.4%	0.4%	
4319	<i>Cytophagales</i> (<i>Bacteroidetes</i>)	DNA	0.0%	0.0%	0.0%	0.0%	0.0%	0.0%	0.0%	0.0%	0.0%	0.0%	0.0%	0.0%	0.0%	p \leq 0.01
		RNA	0.2%	0.0%	n.d.	0.0%	0.0%	0.0%	0.0%	1.2%	0.0%	n.d.	0.3%	0.0%	0.0%	
8686	<i>Pelobacter</i> (<i>Deltaproteobacteria</i>)	DNA	0.1%	0.2%	0.0%	0.2%	0.1%	0.2%	1.3%	0.0%	0.0%	0.1%	0.1%	0.2%	1.3%	
		RNA	0.0%	0.0%	n.d.	0.1%	0.1%	0.6%	0.0%	0.0%	0.0%	n.d.	0.1%	0.0%	0.3%	
4144	Sva0485 group (<i>Deltaproteobacteria</i>)	DNA	0.1%	0.0%	1.1%	0.0%	0.0%	0.0%	0.1%	0.0%	0.0%	0.0%	0.0%	0.0%	0.0%	
		RNA	0.0%	0.0%	n.d.	0.0%	0.0%	0.0%	0.0%	0.0%	0.1%	n.d.	0.0%	0.0%	0.0%	
7873	Sh765B-TzT-29 (<i>Deltaproteobacteria</i>)	DNA	0.0%	0.1%	2.3%	0.0%	0.1%	0.0%	0.0%	0.0%	0.0%	0.0%	0.1%	0.1%	0.0%	
		RNA	0.0%	0.0%	n.d.	0.0%	0.0%	0.0%	0.1%	0.0%	0.2%	n.d.	0.0%	0.0%	0.0%	
3288	R76-B128 group (<i>Lentisphaerae</i>)	DNA	0.0%	0.0%	1.9%	0.0%	0.0%	0.0%	0.0%	0.0%	0.0%	0.0%	0.0%	0.0%	0.0%	
		RNA	0.0%	0.0%	n.d.	0.0%	0.0%	0.0%	0.0%	0.0%	0.0%	n.d.	0.0%	0.0%	0.0%	
10615	<i>Arcobacter</i> (<i>Epsilonproteobacteria</i>)	DNA	0.0%	0.4%	0.0%	0.3%	0.9%	1.9%	2.3%	2.3%	0.1%	0.8%	6.4%	6.7%	5.1%	
		RNA	0.0%	0.0%	n.d.	0.4%	0.7%	0.4%	3.4%	2.3%	0.0%	n.d.	5.9%	4.5%	5.9%	
8114	ML635J-21 (<i>Cyanobacteria</i>)	DNA	0.0%	0.0%	1.5%	0.0%	0.0%	0.0%	0.0%	0.0%	0.0%	0.0%	0.0%	0.0%	0.0%	
		RNA	0.0%	0.0%	n.d.	0.0%	0.0%	0.0%	0.0%	0.0%	0.0%	n.d.	0.0%	0.0%	0.0%	
10981	<i>Fibrobacteraceae</i> (<i>Fibrobacteres</i>)	DNA	0.0%	0.0%	1.1%	0.0%	0.0%	0.0%	0.0%	0.0%	0.0%	0.0%	0.0%	0.0%	0.0%	
		RNA	0.0%	0.1%	n.d.	0.0%	0.0%	0.0%	0.0%	0.1%	0.0%	n.d.	0.0%	0.0%	0.0%	
9401	<i>Planctomycetes</i>	DNA	0.0%	0.0%	2.7%	0.0%	0.0%	0.0%	0.0%	0.0%	0.0%	0.0%	0.0%	0.0%	0.2%	
		RNA	0.0%	0.0%	n.d.	0.0%	0.0%	0.0%	0.0%	0.0%	0.0%	n.d.	0.0%	0.0%	0.0%	
3289	<i>Oligosphaeria</i> (<i>Lentisphaerae</i>)	DNA	0.0%	0.0%	1.9%	0.0%	0.0%	0.0%	0.0%	0.0%	0.0%	0.0%	0.0%	0.0%	0.0%	
		RNA	0.0%	0.0%	n.d.	0.0%	0.0%	0.0%	0.0%	0.0%	0.0%	n.d.	0.0%	0.0%	0.0%	
5853	<i>Leptotrichiaceae</i> (<i>Fusobacteria</i>)	DNA	0.0%	0.0%	0.0%	0.0%	0.0%	0.0%	0.0%	0.0%	0.0%	0.0%	0.1%	0.0%	0.0%	
		RNA	0.0%	0.0%	n.d.	0.0%	0.2%	0.1%	0.0%	0.0%	0.0%	n.d.	1.4%	0.6%	0.0%	
10599	WCHB1-41 group (<i>Lentisphaerae</i>)	DNA	0.0%	0.0%	1.5%	0.0%	0.0%	0.0%	0.0%	0.0%	0.0%	0.0%	0.0%	0.0%	0.0%	
		RNA	0.0%	0.0%	n.d.	0.0%	0.0%	0.0%	0.0%	0.0%	0.0%	n.d.	0.0%	0.0%	0.0%	
9777	Candidate division OP11	DNA	0.0%	0.0%	2.3%	0.0%	0.0%	0.0%	0.0%	0.0%	0.0%	0.0%	0.0%	0.0%	0.0%	
		RNA	0.0%	0.0%	n.d.	0.0%	0.0%	0.0%	0.0%	0.0%	0.0%	n.d.	0.0%	0.0%	0.0%	

^a Phylotypes that were significantly enriched in both acetate and spirulina incubations are displayed in bold type.

^b Colors indicate absolute changes in relative abundance between labeled incubations and no substrate controls. Bordered values indicate statistically significant enrichment (p \leq 0.01).

^c n.d., no data due to an error in the barcode sequence

Table 2. Relative abundance of phylotypes that were significantly enriched following addition of spirulina^a compared to the no substrate control

OTU ID	Phylogenetic affiliation	sample type	d0	50 µg l ⁻¹ spirulina						1 mg l ⁻¹ spirulina						Legend ^b
				d8			d32			d8			d32			
				¹³ C	¹² C	¹³ C inh.	¹³ C	¹² C	¹³ C inh.	¹³ C	¹² C	¹³ C inh.	¹³ C	¹² C	¹³ C inh.	
2011	<i>Desulfobacteraceae</i> (<i>Deltaproteobacteria</i>)	DNA	1.3%	1.2%	1.3%	0.6%	1.4%	1.6%	1.0%	0.7%	1.5%	0.6%	0.5%	0.8%	0.1%	5.0%
		RNA	6.8%	8.2%	7.7%	2.9%	6.4%	6.3%	0.5%	3.3%	8.2%	1.1%	5.6%	10.6%	0.9%	2.5%
4400	<i>Marinifilum</i> (<i>Bacteroidetes</i>)	DNA	1.5%	2.1%	1.7%	2.1%	3.1%	2.9%	1.7%	6.7%	1.4%	5.1%	8.0%	1.3%	1.9%	1.0%
		RNA	2.7%	10.1%	3.2%	16.5%	4.5%	2.8%	2.4%	16.0%	2.4%	27.8%	10.8%	1.7%	5.4%	0.5%
11380	<i>Desulfobacteraceae</i> (<i>Deltaproteobacteria</i>)	DNA	1.1%	1.8%	1.7%	1.1%	0.7%	2.0%	1.1%	0.4%	1.1%	0.6%	0.5%	0.9%	0.1%	0.0%
		RNA	2.4%	2.9%	2.9%	1.1%	1.8%	2.0%	0.5%	1.5%	2.6%	0.5%	3.0%	3.5%	0.4%	-0.5%
4749	<i>Psychrilyobacter</i> (<i>Fusobacteria</i>)	DNA	1.7%	2.0%	2.3%	2.2%	2.4%	3.3%	2.3%	11.7%	7.5%	13.6%	10.6%	9.8%	12.0%	-1.0%
		RNA	1.1%	1.5%	1.0%	1.9%	1.7%	1.5%	2.9%	6.4%	4.9%	8.9%	5.3%	2.3%	13.5%	-2.5%
3714	<i>Desulfuromonas</i> (<i>Deltaproteobacteria</i>)	DNA	2.6%	3.2%	3.5%	3.2%	2.3%	2.4%	2.4%	1.4%	2.6%	1.4%	1.2%	1.8%	1.5%	-5.0%
		RNA	0.1%	0.0%	0.1%	0.2%	0.4%	0.1%	1.4%	0.1%	0.1%	0.1%	0.1%	0.0%	0.1%	
4982	<i>Desulfobulbaceae</i> (<i>Deltaproteobacteria</i>)	DNA	0.7%	1.1%	1.0%	0.4%	1.1%	1.3%	0.4%	0.5%	1.1%	0.4%	0.9%	0.6%	0.1%	p ≤ 0.01
		RNA	1.8%	6.1%	5.7%	0.9%	1.8%	3.2%	0.5%	7.0%	5.4%	0.5%	4.0%	3.7%	0.5%	
4270	BD2-2 (<i>Bacteroidetes</i>)	DNA	1.6%	1.7%	1.7%	1.2%	1.4%	1.4%	1.5%	0.4%	2.4%	0.6%	0.9%	2.3%	0.6%	
		RNA	0.8%	1.3%	0.7%	2.3%	0.8%	0.9%	1.4%	0.7%	1.0%	0.6%	0.4%	0.2%	0.3%	
7234	<i>Colwellia</i> (<i>Gammaproteobacteria</i>)	DNA	2.2%	0.4%	0.0%	0.2%	0.6%	0.9%	1.3%	0.2%	0.8%	0.4%	0.4%	1.1%	0.1%	
		RNA	0.2%	0.6%	0.6%	0.7%	0.3%	1.0%	0.0%	0.4%	0.9%	0.4%	0.2%	1.0%	1.6%	
10263	<i>Desulfobulbus</i> (<i>Deltaproteobacteria</i>)	DNA	0.2%	0.0%	0.0%	0.1%	0.0%	0.1%	0.0%	0.3%	0.5%	0.1%	0.0%	0.1%	0.0%	
		RNA	1.8%	0.4%	3.6%	0.3%	0.5%	1.6%	2.4%	1.2%	2.7%	0.5%	0.6%	0.9%	0.7%	
5414	<i>Marinilabiliaceae</i> (<i>Bacteroidetes</i>)	DNA	0.4%	0.2%	0.1%	0.4%	0.3%	0.5%	0.4%	0.1%	0.2%	0.1%	0.3%	0.5%	0.1%	
		RNA	0.9%	0.6%	0.4%	0.9%	0.3%	0.6%	1.9%	0.2%	0.8%	0.3%	0.9%	1.4%	0.6%	
7300	<i>Desulfobulbaceae</i> (<i>Deltaproteobacteria</i>)	DNA	0.6%	0.6%	1.0%	0.6%	0.8%	0.5%	0.7%	0.5%	0.7%	0.2%	0.4%	0.4%	0.1%	
		RNA	0.6%	0.7%	1.1%	0.2%	0.6%	0.7%	0.0%	1.5%	1.4%	0.2%	1.2%	0.7%	0.2%	
7435	<i>Psychromonas</i> (<i>Gammaproteobacteria</i>)	DNA	0.2%	0.4%	0.2%	0.5%	0.5%	0.3%	1.2%	30.6%	0.7%	32.5%	29.0%	1.0%	36.3%	
		RNA	0.1%	0.3%	0.1%	0.3%	0.0%	0.1%	1.0%	16.1%	0.5%	24.9%	6.4%	0.2%	30.1%	
3099	<i>Marinilabiliaceae</i> (<i>Bacteroidetes</i>)	DNA	0.1%	0.1%	0.0%	0.2%	0.2%	0.0%	0.3%	0.2%	0.0%	0.0%	0.2%	0.0%	0.0%	
		RNA	0.2%	0.4%	0.1%	0.8%	0.1%	0.1%	2.4%	0.3%	0.0%	0.4%	0.6%	0.1%	0.4%	
1797	<i>Marinilabiliaceae</i> (<i>Bacteroidetes</i>)	DNA	0.1%	0.0%	0.0%	0.0%	0.1%	0.1%	0.0%	0.1%	0.0%	0.0%	0.1%	0.0%	0.1%	
		RNA	0.1%	0.0%	0.2%	0.0%	0.0%	0.0%	2.9%	0.0%	0.2%	0.0%	0.0%	0.0%	0.0%	
1452	<i>Fusibacter</i> (<i>Firmicutes</i>)	DNA	0.2%	0.4%	0.7%	0.6%	0.6%	0.4%	0.9%	4.4%	2.0%	4.3%	4.6%	2.6%	4.3%	
		RNA	0.0%	0.1%	0.0%	0.2%	0.0%	0.0%	0.5%	0.8%	0.2%	0.7%	1.3%	0.2%	1.7%	
1656	<i>Fusibacter</i> (<i>Firmicutes</i>)	DNA	0.1%	0.0%	0.0%	0.0%	0.0%	0.0%	0.0%	1.4%	0.9%	2.2%	1.6%	0.9%	4.5%	
		RNA	0.0%	0.0%	0.0%	0.0%	0.0%	0.0%	0.0%	0.2%	0.1%	0.3%	0.2%	0.1%	0.7%	
8133	<i>Fusibacter</i> (<i>Firmicutes</i>)	DNA	0.1%	0.1%	0.0%	1.1%	0.2%	0.1%	1.1%	0.3%	0.5%	0.3%	0.3%	0.6%	0.3%	
		RNA	0.0%	0.0%	0.0%	0.1%	0.0%	0.0%	0.0%	0.1%	0.1%	0.0%	0.0%	0.0%	0.1%	
8686	<i>Pelobacter</i> (<i>Deltaproteobacteria</i>)	DNA	0.1%	0.1%	0.1%	0.1%	0.1%	0.1%	1.2%	0.1%	0.2%	0.2%	0.0%	0.0%	0.0%	
		RNA	0.0%	0.0%	0.0%	0.0%	0.0%	0.0%	0.0%	0.0%	0.0%	0.0%	0.1%	0.0%	0.1%	
9869	<i>Marinilabiliaceae</i> (<i>Bacteroidetes</i>)	DNA	0.0%	0.0%	0.0%	0.2%	0.3%	0.0%	0.1%	1.8%	0.0%	0.8%	2.0%	0.0%	0.4%	
		RNA	0.1%	0.3%	0.0%	2.0%	0.3%	0.1%	1.9%	9.1%	0.0%	6.0%	6.7%	0.0%	4.4%	
10369	<i>Spirochaeta</i> (<i>Spirochaetes</i>)	DNA	0.1%	0.3%	0.0%	0.4%	1.4%	0.1%	1.1%	0.5%	0.1%	0.2%	0.2%	0.1%	0.0%	
		RNA	0.0%	0.2%	0.0%	0.2%	0.0%	0.0%	0.0%	0.1%	0.0%	0.1%	0.0%	0.0%	0.0%	
6091	Candidate division BD1-5	DNA	0.0%	0.0%	0.0%	0.0%	0.0%	0.0%	0.0%	0.0%	0.0%	0.0%	0.0%	0.0%	0.0%	
		RNA	0.0%	0.0%	0.0%	0.0%	0.0%	0.0%	2.4%	0.0%	0.0%	0.0%	0.0%	0.0%	0.0%	
7997	Candidate division BRC1	DNA	0.0%	0.0%	0.0%	0.0%	0.0%	0.1%	0.0%	0.0%	0.0%	0.0%	0.0%	0.0%	0.0%	
		RNA	0.0%	0.1%	0.0%	0.1%	0.0%	0.2%	2.4%	0.0%	0.1%	0.0%	0.0%	0.1%	0.0%	
10246	<i>Phycisphaerales</i> (<i>Planctomycetes</i>)	DNA	0.0%	0.0%	0.0%	0.0%	0.0%	0.0%	0.1%	0.0%	0.0%	0.0%	0.0%	0.0%	0.0%	
		RNA	0.0%	0.0%	0.0%	0.0%	0.0%	0.0%	1.9%	0.0%	0.0%	0.0%	0.0%	0.0%	0.0%	
10615	<i>Arcobacter</i> (<i>Epsilonproteobacteria</i>)	DNA	0.0%	1.5%	0.5%	2.8%	3.0%	2.3%	9.3%	1.5%	2.9%	1.8%	4.7%	13.3%	5.6%	
		RNA	0.0%	0.4%	0.4%	0.7%	0.3%	0.4%	4.8%	0.3%	0.8%	1.6%	3.6%	2.7%	3.1%	

^a Phylotypes that were significantly enriched in both acetate and spirulina incubations are displayed in bold type.^b Colors indicate absolute changes in relative abundance between labeled incubations and no substrate controls. Bordered values indicate statistically significant enrichment (p ≤ 0.01).**Phylotypes associated with sulfate reduction**

In order to identify sulfate reduction-associated phylotypes we compared incubations where substrate was added against controls where sulfate reduction was inhibited. We could identify 12 phylotypes that were significantly enriched (p-value ≤ 0.01) in at least one of the incubation samples (Table 3). Phylogenetically these phylotypes were mostly (8 of 12 phylotypes) affiliated with the deltaproteobacterial families *Desulfobacteraceae* and *Desulfobulbaceae* that harbor many known SRM (Figure S1, Table 3). Additionally there were four phylotypes belonging to phyla with no known sulfate-reducing representatives: phylotypes

classified as *Arcobacter* (*Epsilonproteobacteria*), *Leptotrichiaceae* (*Fusobacteria*), *Marinifilum* (*Bacteroidetes*) and unclassified *Bacteroidetes*.

The highly abundant *Desulfobacteraceae* phylotype 2011 (1.3%/6.8% of all sequences at day 0 at DNA/RNA level) is significantly enriched compared to the inhibited control in most RNA samples, but not in DNA samples (Table 3), indicating that the inhibition of sulfate reduction merely decreased its activity but not its cell numbers. Phylogenetically it belongs, together with the also highly abundant phylotype 11380 (1.1% at DNA, 2.4% at RNA level; significantly enriched in 3 RNA samples), to the Sva0081 sediment group in the *Desulfobacteraceae* (Figure

S1). Of the other three sulfate reduction-associated phylotypes in the *Desulfobacteraceae*, phylotype 10184 (unclassified *Desulfobacteraceae*) is even more abundant at DNA level (1.4%), but less so at RNA level (1.2%), whereas *Desulfobacula*-related phylotype 5034 and phylotype 10183 (SEEP-SRB1) were less abundant (0.4%/0.2% and 0.0%/0.0% at DNA/RNA level, respectively).

Sulfate reduction-associated *Desulfobulbaceae* phylotypes were generally more abundant in RNA samples (0.6%-1.8%) than in DNA samples (0.3%-0.7%) from day 0 (Table 3). Phylotype 4982 (0.7% at DNA, 1.8% at RNA level) is related to unclassified *Desulfobulbaceae* sequences and is significantly enriched compared to the inhibited control in RNA samples from 5 incubation time points. Phylotype 7300 (0.6% abundance at DNA and RNA level; SEEP-SRB4 group) and phylotype 3944 (0.3% at DNA, 0.8% at RNA level; unclassified *Desulfobulbaceae*) are significantly enriched compared to the inhibited control in 1 and in 5 RNA samples, respectively (Table 3).

Marinifilum phylotype 4400 (*Bacteroidetes*) is highly abundant (1.5% at DNA, 2.7% at RNA level). It is significantly enriched compared to the inhibited control in the spirulina incubation at day 32 (DNA and RNA), but considerably more abundant in the

inhibited control at other time points, suggesting that it is not reliant on sulfate reduction, which is consistent with the fermentative metabolism of related *Marinifilum* species. *Marinilabiliaceae* phylotype 9869 (0.7% at DNA, 0.6% at RNA level) generally decreases in abundance in all but the high concentration spirulina incubations, where it is significantly enriched compared to the inhibited control in two samples (Table 3). *Leptotrichiaceae* phylotype 5853 is closely related to the genus *Leptotrichia* in the phylum *Fusobacteria* (Figure S1). In contrast to all other sulfate reduction associated phylotypes, most of its most closely related sequences do not derive from marine environments but from oral cavity samples. The phylotype could not be detected in day 0 samples and is thus not an organism that is likely to be relevant *in situ* and it is significantly enriched at only 1 incubation time point compared to the inhibited control. *Arcobacter* phylotype 10615 (*Epsilonproteobacteria*) is also only marginally abundant at time point zero (absent in DNA samples, 0.02% in RNA samples). It is significantly enriched at only 1 of 15 incubation time points. Furthermore, it is considerably more abundant in the inhibited control at multiple time points (Table 3) and therefore probably not a sulfate reducer.

Table 3. Relative abundance of sulfate-reduction associated phylotypes, i.e. phylotypes that were significantly enriched compared to the inhibited controls

OTU ID	Phylogenetic affiliation	sample type	d0	Acetate				Spirulina				Legend ^a :
				50 μ M		1 mM		50 μ g l ⁻¹		1 mg l ⁻¹		
				d8	d32	d8 ^b	d32	d8	d32	d8	d32	
2011	<i>Desulfobacteraceae</i> (<i>Deltaproteobacteria</i>)	DNA	1.3%	0.2%	1.2%	1.2%	1.0%	1.2%	1.4%	0.7%	0.5%	5.0%
		RNA	6.8%	7.3%	9.1%	9.4%	9.7%	8.2%	6.4%	3.3%	5.6%	2.5%
4400	<i>Marinifilum</i> (<i>Bacteroidetes</i>)	DNA	1.5%	0.8%	1.1%	1.7%	1.3%	2.1%	3.1%	6.7%	8.0%	1.0%
		RNA	2.7%	1.9%	1.3%	2.9%	1.5%	10.1%	4.5%	16.0%	10.8%	0.5%
11380	<i>Desulfobacteraceae</i> (<i>Deltaproteobacteria</i>)	DNA	1.1%	1.7%	2.1%	1.2%	1.5%	1.8%	0.7%	0.4%	0.5%	0.0%
		RNA	2.4%	3.2%	2.0%	2.4%	3.0%	2.9%	1.8%	1.5%	3.0%	-0.5%
10184	<i>Desulfobacteraceae</i> (<i>Deltaproteobacteria</i>)	DNA	1.4%	1.6%	1.2%	0.9%	1.2%	1.1%	0.9%	0.2%	0.4%	-1.0%
		RNA	1.2%	1.1%	2.2%	1.3%	2.0%	1.0%	0.6%	0.4%	0.7%	-2.5%
4982	<i>Desulfobulbaceae</i> (<i>Deltaproteobacteria</i>)	DNA	0.7%	0.7%	1.1%	0.8%	1.1%	1.1%	1.1%	0.5%	0.9%	-5.0%
		RNA	1.8%	3.0%	2.7%	2.5%	2.8%	6.1%	1.8%	7.0%	4.0%	
7300	<i>Desulfobulbaceae</i> (<i>Deltaproteobacteria</i>)	DNA	0.6%	0.6%	0.7%	0.9%	0.8%	0.6%	0.8%	0.5%	0.4%	
		RNA	0.6%	0.8%	0.9%	1.1%	0.7%	0.7%	0.6%	1.5%	1.2%	
9869	<i>Bacteroidetes</i>	DNA	0.7%	0.0%	0.1%	0.0%	0.0%	0.0%	0.3%	1.8%	2.0%	
		RNA	0.6%	0.0%	0.0%	0.0%	0.0%	0.3%	0.3%	9.1%	6.7%	
3944	<i>Desulfobulbaceae</i> (<i>Deltaproteobacteria</i>)	DNA	0.3%	0.5%	0.6%	0.5%	0.5%	0.7%	0.6%	0.5%	0.3%	
		RNA	0.8%	1.2%	0.4%	0.6%	1.5%	1.1%	0.6%	1.0%	1.2%	
5034	<i>Desulfobacteraceae</i> (<i>Deltaproteobacteria</i>)	DNA	0.4%	0.2%	0.2%	0.1%	0.3%	0.4%	0.5%	0.2%	0.4%	
		RNA	0.2%	0.1%	0.1%	0.4%	1.1%	0.4%	0.1%	0.1%	0.5%	
10183	<i>Desulfobacteraceae</i> (<i>Deltaproteobacteria</i>)	DNA	0.0%	0.5%	0.7%	0.5%	0.7%	0.6%	0.4%	0.3%	0.3%	
		RNA	0.1%	0.5%	1.2%	0.7%	1.3%	0.5%	0.2%	0.4%	0.4%	
5853	<i>Leptotrichiaceae</i> (<i>Fusobacteria</i>)	DNA	0.0%	0.0%	0.0%	0.0%	0.1%	0.0%	0.1%	0.0%	0.0%	
		RNA	0.0%	0.0%	0.2%	0.0%	1.4%	0.0%	0.6%	0.0%	0.1%	
10615	<i>Arcobacter</i> (<i>Epsilonproteobacteria</i>)	DNA	0.0%	0.4%	0.9%	2.3%	6.4%	1.5%	3.0%	1.5%	4.7%	
		RNA	0.0%	0.0%	0.7%	2.3%	5.9%	0.4%	0.3%	0.3%	3.6%	

$p \leq 0.01$

^a Colors indicate absolute changes in relative abundance between incubations with ¹³C-labeled substrate and inhibited controls. Bordered values indicate statistically significant enrichment ($p \leq 0.01$).

^b No inhibited control was available for the RNA sample of this time point.

Discussion

Mineralization of organic matter in Arctic marine sediments

Organic matter in anoxic marine sediments is degraded by the concerted activity of hydrolytic, fermentative and sulfate-reducing bacteria (Jørgensen, 1982). In order to investigate the carbon degradation cascade in Arctic marine sediments, we performed incubation experiments with sediment from the Arctic fjord Smeerenburgfjorden located on the northwest coast of Svalbard. Our results regarding the biogeochemistry of this sediment are in accordance with what was reported previously for this location (Finke *et al.*, 2007). Sulfate reduction rates in the no substrate control varied between 9 and 18 nmol cm⁻³ d⁻¹ (Figure 4), which is comparable to the 18-32 nmol cm⁻³ d⁻¹ measured previously for this sediment (Finke *et al.*, 2007) and lies within the range of sulfate reduction rates measured in Svalbard fjords (Sagemann *et al.*, 1998; Arnosti & Jørgensen, 2006). Of the measured VFAs (Figures 5 and 6), acetate occurred in the highest concentration (average of 12 µM in the no substrate controls), followed by formate (9 µM), succinate (5 µM), and lactate (4 µM).

16S rRNA sequence data from the day 0 time point of our incubations revealed a diverse association of bacteria with a composition similar to communities described by previous sequencing efforts at this site (Teske *et al.*, 2011). *Deltaproteobacteria*, *Bacteroidetes* and *Gammaproteobacteria* were the most abundant groups and together constituted over 60% of both DNA and RNA derived sequence reads in an otherwise very diverse microbial community (Figure 3A). We investigated the response of this community during the degradation of cyanobacterial biomass and acetate. We monitored biochemical processes by determining sulfate reduction rates and the turnover of VFAs and linked them to abundance changes of individual phylotypes over the course of substrate amended incubations. Organic matter that was introduced into the system was hydrolyzed and fermented and fermentation products were then consumed by SRM and phylotypes that were presumably responsible for these processes were identified (Figure 7).

Hydrolysis and fermentation

We used cyanobacterial biomass in the form of freeze-dried spirulina as a model for organic matter input. The fermentation products of spirulina degradation were primarily acetate, as well as formate and propionate, while the other measured VFAs did not change in response to spirulina addition (Figure 6). Phylotypes were considered putative

hydrolyzers or fermenters, if they (1) showed a clear growth or activity response to the addition of spirulina (significant relative increase in abundance in at least two 16S rRNA or at least two 16S cDNA amplicon libraries, respectively, from incubations where spirulina was added as a substrate compared to the respective no substrate control), (2) did not show such a response to the addition of acetate, and (3) were closely related to described species with hydrolytic or fermentative metabolic capabilities (Figure 7).

Three putative hydrolytic and fermentative phylotypes belonged to the phylum *Bacteroidetes*, members of which have been shown to be stimulated by cyanobacterial biomass input in marine sediment samples (Rosselló-Mora *et al.*, 1999). Even though especially *Flavobacteriaceae* have been shown to be remarkably responsive to phytoplankton availability (Pinhassi *et al.*, 2004; Abell & Bowman, 2005), none of the *Flavobacteriaceae* phylotypes detected in our study responded to the addition of spirulina. However, five phylotypes of the *Marinilabiliaceae* responded the addition of spirulina, especially *Marinifilum* phylotype 4400 (1.5%/2.7% of all sequences at day 0 on DNA/RNA level), phylotype 3099 (0.1%/0.2%) and phylotype 9869 (0%/0.1%) showed consistent enrichment in spirulina incubations. *Marinifilum* phylotype 4400 is closely related to *M. fragile* and *M. flexuosum* (Figure S1) that both possess hydrolytic activity and are able to ferment sugars to acetate and propionate (Na *et al.*, 2009; Ruvira *et al.*, 2013). Interestingly, *Marinifilum* phylotype 4400 (as well as several other phylotypes) responded mainly to addition of the ¹³C-spirulina substrate and not to ¹²C-spirulina. Together with the development of a distinct microbial community in ¹³C-spirulina incubations (Figure 2), divergent VFA production patterns (Figure 6) and clearly visible differences in color and homogeneity of the substrate solution, this provided further indication that these substrates were not equivalent despite the manufacturer's description.

Two gammaproteobacterial phylotypes showed a strong response to spirulina addition, *Colwellia* phylotype 7234 (2.2%/0.2% of all sequences at day 0 on DNA/RNA level) and *Psychromonas* phylotype 7435 (0.2%/0.1%). *Colwellia* phylotype 7234 was enriched in various samples from spirulina incubations at both low and high spirulina concentrations after 8 as well as after 32 days mainly, but not exclusively, in 16S cDNA libraries (Table 2). It was also significantly enriched at one incubation time point when acetate was added as a substrate (Table 1). *Colwellia* is a genus in the order *Alteromonadales* that contains several psychrophilic

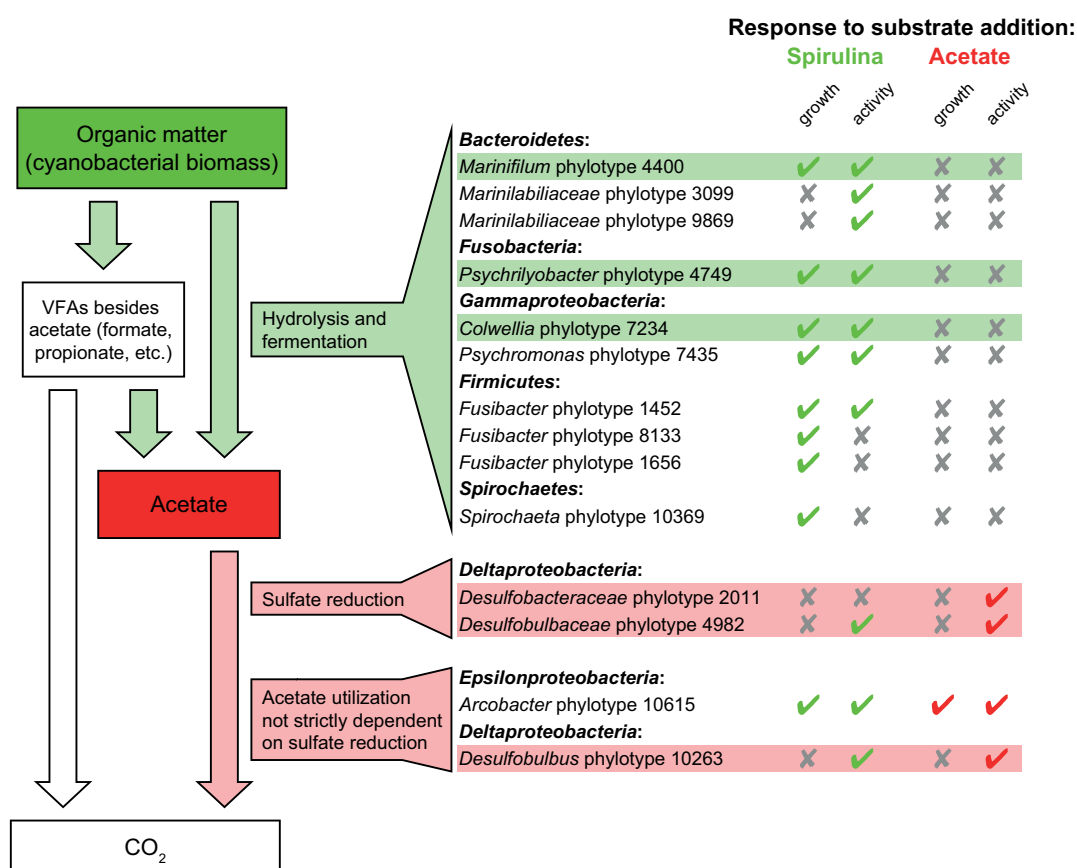


Figure 7. A model for cyanobacterial biomass degradation in Arctic marine sediments of Smeerenburgfjorden, Svalbard. Hydrolytic and fermentative bacteria utilize organic matter derived from cyanobacterial biomass and mainly form acetate, which is eventually consumed by SRM. Putative roles in carbon degradation are shown for all phylotypes that responded with significant relative increase in 16S rRNA gene abundance (possibly due to growth) or with significant relative increase in 16S cDNA abundance (possibly due to transcriptional activity) in at least two incubations samples relative to the respective no substrate controls. Phylotypes that are presumably abundant in the sediment (i.e. phylotypes with $\geq 1\%$ abundance in 16S rRNA gene or cDNA amplicon libraries at day 0) are highlighted in color.

fermentative and hydrolytic bacteria that were also shown to be able to use acetate (as well as several other VFAs) as sole carbon source (Bowman *et al.*, 1998). *Colwellia psychrerythraea*, for which the genome sequence is available (Methé *et al.*, 2005), has frequently been used as a model organism for studying cold adaptation in bacteria (e.g. Junge *et al.* (2003); Huston *et al.* (2004); Leiros *et al.* (2007); Marx *et al.* (2009)) and phylotypes classified as *Colwellia* have been implicated in biodegradation of petroleum hydrocarbons (Powell *et al.*, 2004). *Psychromonas* phylotype 7435 was less abundant at day 0 (0.2%/0.1% at DNA/RNA level) and showed the highest increase in abundance and sometimes provided more than a third of all reads in one sample (Table 2). The closest characterized relatives of *Psychromonas* phylotype 7435, *P. profunda* and *P.*

marina, are hydrolytic and fermentative nitrate reducers (Kawasaki *et al.*, 2002; Xu *et al.*, 2003).

Psychrilyobacter phylotype 4749 (1.7%/1.1%) of the phylum *Fusobacteria* was significantly enriched in all high concentration spirulina incubation samples with up to 2-14% of all 16S rRNA gene and cDNA sequences compared to 0.5-2% in the no substrate controls. Its response to high but not to low spirulina concentrations indicates that it is able to quickly take advantage of increased substrate concentrations. The genus *Psychrilyobacter* is so far represented by only one described species, *P. atlanticus*, a psychrotrophic member of the phylum *Fusobacteria* that ferments sugars and amino acids to H_2 and acetate (Zhao *et al.*, 2009). *P. atlanticus* was already shown to be one of the primary degraders of cyanobacterial biomass in an RNA-based stable-

isotope probing experiment with ^{13}C -labeled spirulina biomass (Graue *et al.*, 2012).

Three putative fermentative phylotypes in the phylum *Firmicutes* belonged to the genus *Fusibacter*. Related species, *F. paucivorans* and *F. tunisiensis*, ferment a limited number of carbohydrates and produce acetate among other fermentation products (Ravot *et al.*, 1999; Hania *et al.*, 2012). However, all three *Fusibacter* phylotypes are probably not very abundant in the sediment ($\leq 0.2\%$ of all 16S rRNA gene or cDNA sequences at day 0 of the incubation). Another putative fermenter that was present in low abundance at day 0 (0.2%/0.0%), *Spirochaeta* phylotype 10369, was closely related to *Spirochaeta perfilievii*, a carbohydrate fermenting member of the phylum Spirochaetes (Dubinina *et al.*, 2011).

Sulfate reduction

Sulfate reduction rates increased in response to addition of both acetate and spirulina compared to the no substrate controls (Figure 4), indicating that acetate as well as spirulina degradation products were utilized by SRM. The sulfate reduction response to spirulina addition was slightly delayed compared to the response to acetate, suggesting that the complex substrate required initial degradation before it was available to sulfate reducers. Substrate availability was probably not the rate limiting factor in the high concentration incubations, since a 20-fold higher substrate concentration resulted in only 38% and 55% increased sulfate reduction rates in acetate and spirulina incubations, respectively. In contrast to other incubation experiments with ^{13}C -labeled spirulina biomass (Graue *et al.*, 2012), sulfate was probably not depleted during the experiment as indicated by continually high sulfate reduction rates at day 39 after the start of the incubation (Figure 4). Since the acetate-stimulated putative SRM only increased in abundance in 16S cDNA but not in 16S rRNA gene amplicon libraries (Table 1), the SRM community present in the sediment likely operated at their peak metabolic rate in the high concentration incubations, but did not increase in cell numbers. The impact of sulfate reduction on carbon degradation in the substrate-amended sediment incubations were assessed by comparing them with the corresponding sulfate reduction-inhibited incubations. Accumulation in the inhibited controls was observed for acetate, butyrate, propionate, and valerate for both acetate and spirulina incubations and for formate and pyruvate in the spirulina incubations only (Figures 5 and 6), indicating that these VFAs were consumed by SRM during sulfate reduction in the uninhibited incubations.

In order to identify putative sulfate reducers, we compared the incubations with ^{13}C -labeled substrate

to the inhibited controls. It is important to keep in mind that enrichment in the ^{13}C -labeled incubation compared to the inhibited control does not necessarily mean that the enriched organism reduces sulfate, it is also possible that such enrichment is caused by an inhibiting effect of molybdate independent of sulfate reduction (Spain *et al.*, 2011; Zahedi *et al.*, 2013), stochastic biologic variation between incubation bottles or a syntrophic relationship of the organism with a sulfate reducer. Through these comparisons, we were able to identify 12 phylotypes that were significantly enriched in at least one sample from an incubation with ^{13}C -labeled substrate compared to the respective inhibited control (Table 3). Almost all such enrichments occurred in RNA samples, suggesting that the sulfate-reducing community is firmly established in this sediment and that SRM that are naturally abundant in this sediment react with increased activity to substrate input and that acetate and cyanobacterial biomass (which again is mainly degraded to acetate) are substrates likely to naturally occur in this sediment.

Most phylotypes that were associated with sulfate reduction belong to the *Deltaproteobacteria*. *Deltaproteobacteria* accounted for 28% and 31% of all 16S rRNA and cDNA sequences at day 0 and were mostly represented by phylotypes that were affiliated with sulfate-reducing bacteria of the families *Desulfobacteraceae* and *Desulfobulbaceae* (Table S2, Figure S1). *Desulfovibrionaceae* were almost completely absent, which is consistent with previous studies at this location (Ravenschlag *et al.*, 2000; Teske *et al.*, 2011), even though they were found to be the dominant group of SRM in other Svalbard fjord sediments (Sahm *et al.*, 1999). Some sulfate reduction-associated phylotypes belong to taxonomic groups for which the ability to reduce sulfate has not been shown so far, namely the *Bacteroidetes*, *Epsilonproteobacteria*, and *Fusobacteria*. However, *Marinilabiliaceae* phylotypes 4400 and 9869 (*Bacteroidetes*) and *Arcobacter* phylotype 10615 (*Epsilonproteobacteria*) did not show an enrichment pattern consistent with putative SRM as they were sometimes also significantly enriched in the inhibited control (compared to the uninhibited incubation as well as to the no substrate control) and *Leptotrichiaceae* phylotype 5853 (*Fusobacteria*) was only significantly enriched in one sample and present at very low abundance in all the others (Tables 2-4).

Of the other eight sulfate reduction-associated phylotypes, mainly *Desulfobacteraceae* phylotypes 2011 and 11380 and *Desulfobulbaceae* phylotypes 3944 and 4982 are probable candidates for putative active SRM, as they were significantly enriched in 3 or more time points and never significantly depleted

relative to the inhibited control (Table 3). Cultured members of the families *Desulfobacteraceae* and *Desulfobulbaceae* generally oxidize fermentation products like acetate and propionate using sulfate as electron acceptor (Widdel & Bak, 1992).

Desulfobacteraceae phylotype 2011 was one of the most abundant phylotypes accounting for 1.3% and 6.8% of sequences in DNA and RNA samples of day 0, respectively (Figure 2B). Phylogenetically it belongs to the Sva0081 sediment group (Figure S1). The Sva0081 sediment group is a key population of SRM in many coastal marine habitats ranging from polar to tropical sediments and is related to the highly diverse *Desulfosarcina/Desulfococcus*-group. The sequences most closely related to phylotype 2011 all derive from oil-polluted coastal sediments off the Spanish coast (Acosta-Gonzalez *et al.*, 2013), its closest cultivated relatives are *Desulfosarcina* species (Figure S1). *Desulfosarcina*-related phylotypes were shown to dominate the community of sulfate reducing bacteria in Smeerenburgfjorden sediments by fluorescence *in situ* hybridization and 16S rRNA slot blot hybridization (Ravenschlag *et al.*, 2000). Phylotype 2011 responded to the addition of acetate as well as spirulina and its activity (abundance in 16S cDNA libraries) is severely impacted by the inhibition of sulfate reduction (Tables 2-4). Closely related to phylotype 2011 and also a member of the Sva0081 sediment group is *Desulfobacteraceae* phylotype 11380. It was also relatively abundant at day 0 (1.1%/2.4% of all sequences on DNA/RNA level) and strongly associated with sulfate reduction.

Among the *Desulfobulbaceae*, phylotypes 4982 (0.7%/1.8% of all sequences at DNA/RNA level) and 3944 (0.3%/0.8%) were strongly associated with sulfate reduction (Table 3). *Desulfobulbaceae* phylotype 4982 showed a strong response to the addition of both acetate (Table 1) and spirulina (Table 2). It is related to sulfate-reducing members of the family *Desulfobulbaceae*, *Desulfobacterium catecholicum*, which can oxidize acetate (Szewzyk & Pfennig, 1987), and psychrophilic *Desulfotalea* species *D. psychrophila* and *D. arctica* that were isolated from Svalbard sediments and are able to use acetate as a carbon source (Knoblauch *et al.*, 1999). *Desulfobulbaceae* phylotype 3944 (0.3%/0.8%) is related to *Desulfofustis glycolicus*, a glycolate-oxidizing SRM (Friedrich *et al.*, 1996). Like their closest characterized relatives, these four phylotypes seem to be able to reduce sulfate, as is evident from their enrichment compared to the inhibited control (Tables 4). Putative sulfate reducing phylotypes 2011 and 4982 were also the two acetate-utilizing phylotypes that were most abundant at day 0 (Table 1).

Acetate utilization not strictly dependent on sulfate reduction

Most phylotypes that showed a response to acetate addition were either associated to sulfate reduction, or at least phylogenetically related to known sulfate reducers. The strongest response to acetate, however, was shown by epsilonproteobacterial phylotype 10615 (*Arcobacter*), which was only marginally abundant at day 0. It was also heavily enriched when spirulina was added as a substrate, and it was generally not affected by the addition of a sulfate reduction inhibitor. It is conceivable that its enrichment in the spirulina incubations was solely due to utilization of acetate produced from spirulina, but given the metabolic potential of *Arcobacter* species it is possibly able to utilize other spirulina degradation products as well. Described *Arcobacter* species are generally non-psychrophilic nitrate reducers (Vandamme *et al.*, 1991; Levican *et al.*, 2012; Levican *et al.*, 2013), but members of the genus have been identified as acetate-oxidizing manganese (Vandieken *et al.*, 2012; Vandieken & Thamdrup, 2013) and perchlorate/chlorate (Carlström *et al.*, 2013) reducers and exoelectrogens that can readily transfer electrons to an external solid electron acceptor with acetate as the sole carbon source (Fedorovich *et al.*, 2009). Due to its low abundance at day 0 it probably does not play a pivotal role in the biogeochemical processes in the sediment, but it shows the characteristic behavior of an r-strategist that is able to react to the sudden input of organic matter (e.g. in form of an algal bloom) and strongly benefit from the increased substrate availability, but might be outcompeted at lower substrate concentrations.

Desulfobulbus phylotype 10263 (0.2%/1.8% of all 16S rRNA gene/cDNA sequences at day 0) was also significantly enriched in response to both acetate and spirulina addition (Tables 2 and 3), but was not significantly less abundant in 16S cDNA libraries when sulfate reduction was inhibited. *Desulfobulbus* is a sulfate-reducing genus that typically produces acetate by incomplete reduction of VFAs like propionate (Sass *et al.*, 2002; Suzuki *et al.*, 2007; Sorokin *et al.*, 2012). However, it is quite possible that phylotype 10263 has an alternative means of energy generation when sulfate reduction is inhibited. *D. propionicus*, for example, can use oxygen, nitrite, nitrate, manganese or iron as electron acceptors and even reduce acetate plus CO₂ to propionate (Laanbroek *et al.*, 1982; Dannenberg *et al.*, 1992; Lovley & Phillips, 1994; Holmes *et al.*, 2004). Furthermore, it can ferment lactate, pyruvate, or ethanol in the absence of an electron acceptor (Laanbroek *et al.*, 1982; Widdel & Pfennig, 1982; Tasaki *et al.*, 1993).

Conclusion and perspectives

Based on our results and the assumption that phylotypes that are abundant at day 0 are the relevant performers of metabolic processes *in situ*, we propose a scenario regarding the carbon degradation cascade in this sediment (Figure 7): organic matter that comes into the system by sedimentation is utilized by putative hydrolytic and fermentative bacteria like *Marinifilum* phylotype 4400 (*Bacteroidetes*), *Psychrilyobacter* phylotype 4749 (*Fusobacteria*), and *Colwellia* phylotype 7234 (*Gammaproteobacteria*) to mainly acetate which is eventually consumed by putative SRM like *Desulfobacteraceae* phylotypes 2011 and *Desulfobulbaceae* phylotypes 4982 (both *Deltaproteobacteria*).

With the identification of these phylotypes it is now possible to show the incorporation of labeled substrate using fluorescence *in situ* hybridization in combination with Raman spectroscopy and directly investigate these organisms in follow-up experiments.

Acknowledgements

The authors would like to thank Laura Wehrmann for the excellent organization of the 2011 MPI Svalbard cruise, Kristian Lund (captain) and Klaus Ryberg (first mate) of the R/V Farm and cruise participants Carol Arnosti, Andy Canion, Patrick Chanton, and Kolja Kindler for their assistance with sample collection. This work was financially supported by the Austrian Science Fund (P25111-B22 to AL).

References

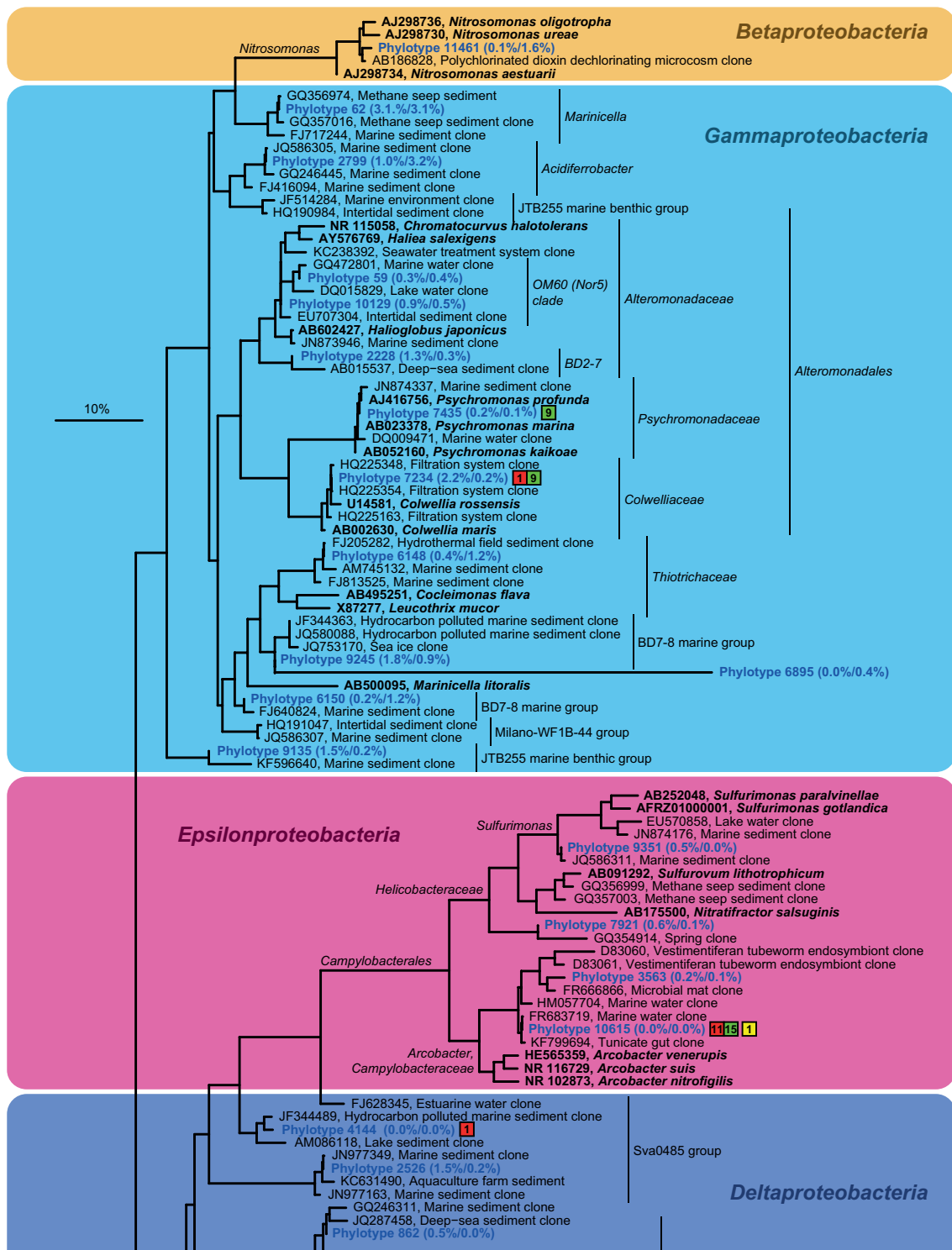
- Abell GC, Bowman JP. (2005). Ecological and biogeographic relationships of class Flavobacteria in the Southern Ocean. *FEMS Microbiol Ecol* **51**: 265-277.
- Acosta-Gonzalez A, Rossello-Mora R, Marques S. (2013). Characterization of the anaerobic microbial community in oil-polluted subtidal sediments: aromatic biodegradation potential after the Prestige oil spill. *Environ Microbiol* **15**: 77-92.
- Arndt S, Jørgensen BB, LaRowe DE, Middelburg JJ, Pancost RD, Regnier P. (2013). Quantifying the degradation of organic matter in marine sediments: A review and synthesis. *Earth-Sci Rev* **123**: 53-86.
- Arnosti C, Jørgensen BB, Sagemann J, Thamdrup B. (1998). Temperature dependence of microbial degradation of organic matter in marine sediments: polysaccharide hydrolysis, oxygen consumption, and sulfate reduction. *Mar Ecol Prog Ser* **165**: 59-70.
- Arnosti C, Jørgensen B. (2003). High activity and low temperature optima of extracellular enzymes in Arctic sediments: implications for carbon cycling by heterotrophic microbial communities. *Mar Ecol Prog Ser* **249**: 15-24.
- Arnosti C, Finke N, Larsen O, Ghobrial S. (2005). Anoxic carbon degradation in Arctic sediments: Microbial transformations of complex substrates. *Geochim Cosmochim Acta* **69**: 2309-2320.
- Arnosti C, Jørgensen BB. (2006). Organic carbon degradation in arctic marine sediments, Svalbard: A comparison of initial and terminal steps. *Geomicrobiol J* **23**: 551-563.
- Benjamini Y, Hochberg Y. (1995). Controlling the False Discovery Rate - a Practical and Powerful Approach to Multiple Testing. *J Roy Stat Soc B Met* **57**: 289-300.
- Berger SA, Krompass D, Stamatakis A. (2011). Performance, Accuracy, and Web Server for Evolutionary Placement of Short Sequence Reads under Maximum Likelihood. *Syst Biol* **60**: 291-302.
- Berry D, Mahfoudh KB, Wagner M, Loy A. (2011). Barcoded primers used in multiplex amplicon pyrosequencing bias amplification. *Appl Environ Microbiol* **77**: 7846-7849.
- Bowman JP, Gosink JJ, McCammon SA, Lewis TE, Nichols DS, Nichols PD *et al.* (1998). *Colwellia demingiae* sp. nov., *Colwellia hornerae* sp. nov., *Colwellia rossensis* sp. nov. and *Colwellia psychrotropica* sp. nov.: psychrophilic Antarctic species with the ability to synthesize docosahexaenoic acid (22:ω63). *Int J Syst Bacteriol* **48**: 1171-1180.
- Canfield DE. (1989). Sulfate reduction and oxic respiration in marine sediments: implications for organic carbon preservation in euxinic environments. *Deep Sea Res* **36**: 121-138.
- Caporaso JG, Kuczynski J, Stombaugh J, Bittinger K, Bushman FD, Costello EK *et al.* (2010). QIIME allows analysis of high-throughput community sequencing data. *Nat Methods* **7**: 335-336.
- Carlström CI, Wang OW, Melnyk RA, Bauer S, Lee J, Engelbrektson A *et al.* (2013). Physiological and Genetic Description of Dissimilatory Perchlorate Reduction by the Novel Marine Bacterium *Arcobacter* sp. Strain CAB. *Mbio* **4**: e00217-13.
- Dannenberg S, Kroder M, Dilling W, Cypionka H. (1992). Oxidation of H₂, organic compounds and inorganic sulfur compounds coupled to reduction of O₂ or nitrate by sulfate-reducing bacteria. *Arch Microbiol* **158**: 93-99.
- Deming JW. (2002). Psychrophiles and polar regions. *Curr Opin Microbiol* **5**: 301-309.

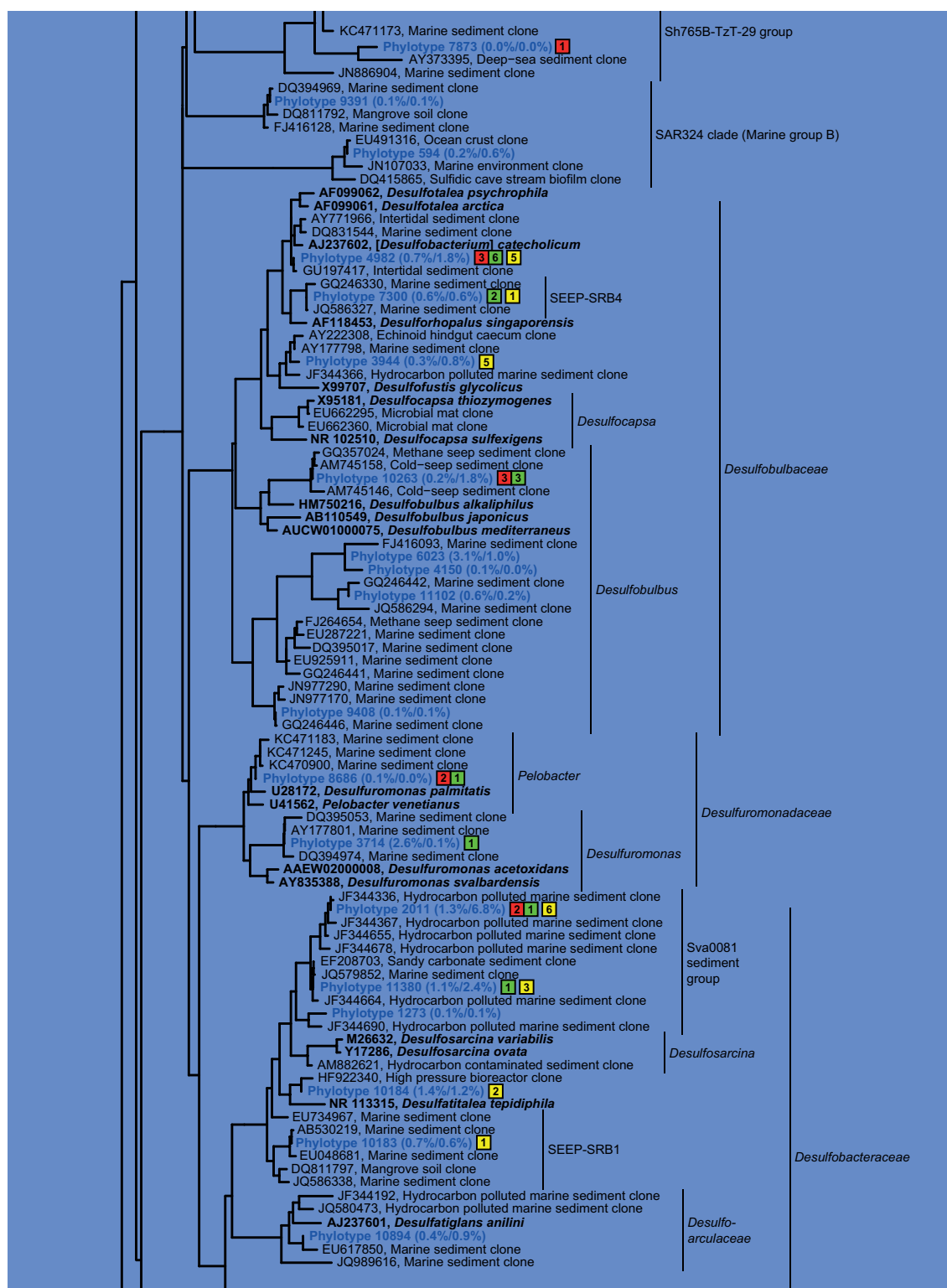
- Dubinina G, Grabovich M, Leshcheva N, Rainey FA, Gavrish E. (2011). *Spirochaeta perfilievii* sp. nov., an oxygen-tolerant, sulfide-oxidizing, sulfur- and thiosulfate-reducing spirochaete isolated from a saline spring. *Int J Syst Evol Microbiol* **61**: 110-117.
- Edgar RC. (2010). Search and clustering orders of magnitude faster than BLAST. *Bioinformatics* **26**: 2460-2461.
- Fedorovich V, Knighton MC, Pagaling E, Ward FB, Free A, Goryanin I. (2009). Novel Electrochemically Active Bacterium Phylogenetically Related to *Arcobacter butzleri*, Isolated from a Microbial Fuel Cell. *Appl Environ Microbiol* **75**: 7326-7334.
- Felsenstein J. (1989). PHYLIP-phylogeny inference package. *Cladistics* **5**: 163-166.
- Finke N, Vandieken V, Jørgensen BB. (2007). Acetate, lactate, propionate, and isobutyrate as electron donors for iron and sulfate reduction in Arctic marine sediments, Svalbard. *FEMS Microbiol Ecol* **59**: 10-22.
- Friedrich M, Springer N, Ludwig W, Schink B. (1996). Phylogenetic positions of *Desulfococcus glycolicus* gen. nov., sp. nov., and *Syntrophobacterium glycolicus* gen. nov., sp. nov., two new strict anaerobes growing with glycolic acid. *Int J Syst Bacteriol* **46**: 1065-1069.
- Glombitza C, Pedersen J, Røy H, Jørgensen BB. (2014). Direct analysis of volatile fatty acids in marine sediment porewater by two-dimensional ion chromatography-mass spectrometry. *Limnol Oceanogr-Meth* **12**: 455-468.
- Glud RN, Holby O, Hoffmann F, Canfield DE. (1998). Benthic mineralization and exchange in Arctic sediments (Svalbard, Norway). *Mar Ecol Prog Ser* **173**: 237-251.
- Graue J, Engelen B, Cypionka H. (2012). Degradation of cyanobacterial biomass in anoxic tidal-flat sediments: a microcosm study of metabolic processes and community changes. *ISME J* **6**: 660-669.
- Griffiths RI, Whiteley AS, O'Donnell AG, Bailey MJ. (2000). Rapid method for coextraction of DNA and RNA from natural environments for analysis of ribosomal DNA- and rRNA-based microbial community composition. *Appl Environ Microbiol* **66**: 5488-5491.
- Haas BJ, Gevers D, Earl AM, Feldgarden M, Ward DV, Giannoukos G et al. (2011). Chimeric 16S rRNA sequence formation and detection in Sanger and 454-pyrosequenced PCR amplicons. *Genome Res* **21**: 494-504.
- Hania WB, Fraj B, Postec A, Fadhlou K, Hamdi M, Ollivier B et al. (2012). *Fusibacter tunisiensis* sp. nov., isolated from an anaerobic reactor used to treat olive-mill wastewater. *Int J Syst Evol Microbiol* **62**: 1365-1368.
- Hansen JW, Thamdrup B, Jørgensen BB. (2000). Anoxic incubation of sediment in gas-tight plastic bags: a method for biogeochemical process studies. *Mar Ecol Prog Ser* **208**: 273-282.
- Henckel T, Friedrich M, Conrad R. (1999). Molecular analyses of the methane-oxidizing microbial community in rice field soil by targeting the genes of the 16S rRNA, particulate methane monooxygenase, and methanol dehydrogenase. *Appl Environ Microbiol* **65**: 1980-1990.
- Holmes DE, Bond DR, Lovley DR. (2004). Electron transfer by *Desulfobulbus propionicus* to Fe(III) and graphite electrodes. *Appl Environ Microbiol* **70**: 1234-1237.
- Huston AL, Methe B, Deming JW. (2004). Purification, characterization, and sequencing of an extracellular cold-active aminopeptidase produced by marine psychrophile *Colwellia psychrerythraea* strain 34H. *Appl Environ Microbiol* **70**: 3321-3328.
- Jørgensen BB. (1982). Mineralization of Organic-Matter in the Sea Bed - the Role of Sulfate Reduction. *Nature* **296**: 643-645.
- Junge K, Eicken H, Deming JW. (2003). Motility of *Colwellia psychrerythraea* strain 34H at subzero temperatures. *Appl Environ Microbiol* **69**: 4282-4284.
- Kallmeyer J, Ferdelman TG, Weber A, Fossing H, Jørgensen BB. (2004). A cold chromium distillation procedure for radiolabeled sulfide applied to sulfate reduction measurements. *Limnol Oceanogr-Meth* **2**: 171-180.
- Kanneworff E, Nicolaisen W. (1972). The "HAPS" a frame-supported bottom corer. *Ophelia* **10**: 119-128.
- Kawasaki K, Nogi Y, Hishinuma M, Nodasaka Y, Matsuyama H, Yumoto I. (2002). *Psychromonas marina* sp. nov., a novel halophilic, facultatively psychrophilic bacterium isolated from the coast of the Okhotsk Sea. *Int J Syst Evol Microbiol* **52**: 1455-1459.
- Knoblauch C, Sahm K, Jørgensen BB. (1999). Psychrophilic sulfate-reducing bacteria isolated from permanently cold arctic marine sediments: description of *Desulfofrigus oceanense* gen. nov., sp. nov., *Desulfofrigus fragile* sp. nov., *Desulfofaba gelida* gen. nov., sp. nov., *Desulfotalea psychrophila* gen. nov., sp. nov. and *Desulfotalea arctica* sp. nov. *Int J Syst Bacteriol* **49 Pt 4**: 1631-1643.
- Kostka JE, Thamdrup B, Glud RN, Canfield DE. (1999). Rates and pathways of carbon oxidation in permanently cold Arctic sediments. *Mar Ecol Prog Ser* **180**: 7-21.

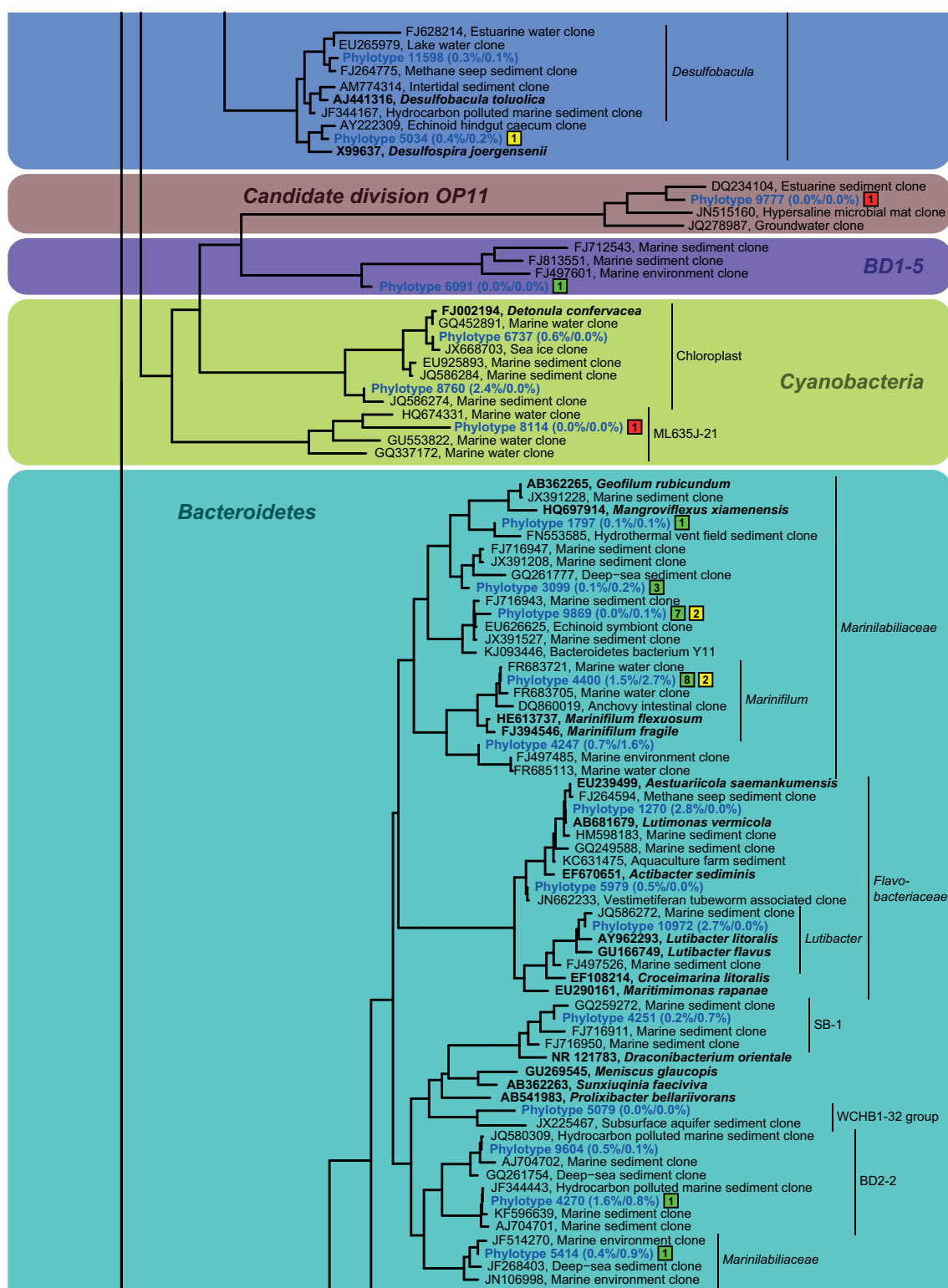
- Laanbroek HJ, Abee T, Voogd IL. (1982). Alcohol conversion by *Desulfobulbus propionicus* Lindhorst in the presence and absence of sulfate and hydrogen. *Arch Microbiol* **133**: 178-184.
- Leiros H-KS, Pey AL, Innselset M, Moe E, Leiros I, Steen IH *et al.* (2007). Structure of phenylalanine hydroxylase from *Colwellia psychrerythraea* 34H, a monomeric cold active enzyme with local flexibility around the active site and high overall stability. *J Biol Chem* **282**: 21973-21986.
- Letunic I, Bork P. (2007). Interactive Tree Of Life (iTOL): an online tool for phylogenetic tree display and annotation. *Bioinformatics* **23**: 127-128.
- Levican A, Collado L, Aguilar C, Yustes C, Dieguez AL, Romalde JL *et al.* (2012). *Arcobacter bivalviorum* sp nov and *Arcobacter venerupis* sp nov., new species isolated from shellfish. *Syst Appl Microbiol* **35**: 133-138.
- Levican A, Collado L, Figueras MJ. (2013). *Arcobacter cloacae* sp nov and *Arcobacter suis* sp nov., two new species isolated from food and sewage. *Syst Appl Microbiol* **36**: 22-27.
- Levitus S, Boyer T. (1994). World Ocean Atlas 1994. Volume 4. Temperature. National Environmental Satellite, Data, and Information Service, Washington, DC (United States).
- Lovley DR, Phillips EJ. (1994). Novel processes for anaerobic sulfate production from elemental sulfur by sulfate-reducing bacteria. *Appl Environ Microbiol* **60**: 2394-2399.
- Lozupone C, Lladser ME, Knights D, Stombaugh J, Knight R. (2011). UniFrac: an effective distance metric for microbial community comparison. *ISME J* **5**: 169-172.
- Ludwig W, Strunk O, Westram R, Richter L, Meier H, Yadhukumar *et al.* (2004). ARB: a software environment for sequence data. *Nucleic Acids Res* **32**: 1363-1371.
- Lueders T, Manefield M, Friedrich MW. (2004). Enhanced sensitivity of DNA- and rRNA-based stable isotope probing by fractionation and quantitative analysis of isopycnic centrifugation gradients. *Environ Microbiol* **6**: 73-78.
- Marx JG, Carpenter SD, Deming JW. (2009). Production of cryoprotectant extracellular polysaccharide substances (EPS) by the marine psychrophilic bacterium *Colwellia psychrerythraea* strain 34H under extreme conditions This article is one of a selection of papers in the Special Issue on Polar and Alpine Microbiology. *Can J Microbiol* **55**: 63-72.
- Méthé BA, Nelson KE, Deming JW, Momen B, Melamud E, Zhang X *et al.* (2005). The psychrophilic lifestyle as revealed by the genome sequence of *Colwellia psychrerythraea* 34H through genomic and proteomic analyses. *Proc Natl Acad Sci U S A* **102**: 10913-10918.
- Muyzer G, Stams AJ. (2008). The ecology and biotechnology of sulphate-reducing bacteria. *Nat Rev Microbiol* **6**: 441-454.
- Na H, Kim S, Moon EY, Chun J. (2009). *Marinifilum fragile* gen. nov., sp. nov., isolated from tidal flat sediment. *Int J Syst Evol Microbiol* **59**: 2241-2246.
- Nedwell DB, Walker TR, Ellis-Evans JC, Clarke A. (1993). Measurements of Seasonal Rates and Annual Budgets of Organic Carbon Fluxes in an Antarctic Coastal Environment at Signy Island, South Orkney Islands, Suggest a Broad Balance between Production and Decomposition. *Appl Environ Microbiol* **59**: 3989-3995.
- Park S-J, Park B-J, Jung M-Y, Kim S-J, Chae J-C, Roh Y *et al.* (2011). Influence of deglaciation on microbial communities in marine sediments off the coast of Svalbard, Arctic Circle. *Microb Ecol* **62**: 537-548.
- Pinhassi J, Sala MM, Havskum H, Peters F, Guadayol O, Malits A *et al.* (2004). Changes in bacterioplankton composition under different phytoplankton regimens. *Appl Environ Microbiol* **70**: 6753-6766.
- Powell S, Bowman J, Snape I. (2004). Degradation of nonane by bacteria from Antarctic marine sediment. *Polar Biol* **27**: 573-578.
- Pruesse E, Peplies J, Glockner FO. (2012). SINA: accurate high-throughput multiple sequence alignment of ribosomal RNA genes. *Bioinformatics* **28**: 1823-1829.
- Quast C, Pruesse E, Yilmaz P, Gerken J, Schweer T, Yarza P *et al.* (2013). The SILVA ribosomal RNA gene database project: improved data processing and web-based tools. *Nucleic Acids Res* **41**: D590-596.
- Quince C, Lanzen A, Curtis TP, Davenport RJ, Hall N, Head IM *et al.* (2009). Accurate determination of microbial diversity from 454 pyrosequencing data. *Nat Methods* **6**: 639-641.
- Ravenschlag K, Sahm K, Pernthaler J, Amann R. (1999). High bacterial diversity in permanently cold marine sediments. *Appl Environ Microbiol* **65**: 3982-3989.
- Ravenschlag K, Sahm K, Knoblauch C, Jørgensen BB, Amann R. (2000). Community structure, cellular rRNA content, and activity of sulfate-reducing bacteria in marine arctic sediments. *Appl Environ Microbiol* **66**: 3592-3602.
- Ravenschlag K, Sahm K, Amann R. (2001). Quantitative molecular analysis of the microbial community in marine arctic sediments (Svalbard). *Appl Environ Microbiol* **67**: 387-395.
- Ravot G, Magot M, Fardeau M-L, Patel BK, Thomas P, Garcia J-L *et al.* (1999). *Fusibacter paucivorans* gen. nov., sp. nov., an anaerobic, thiosulfate-

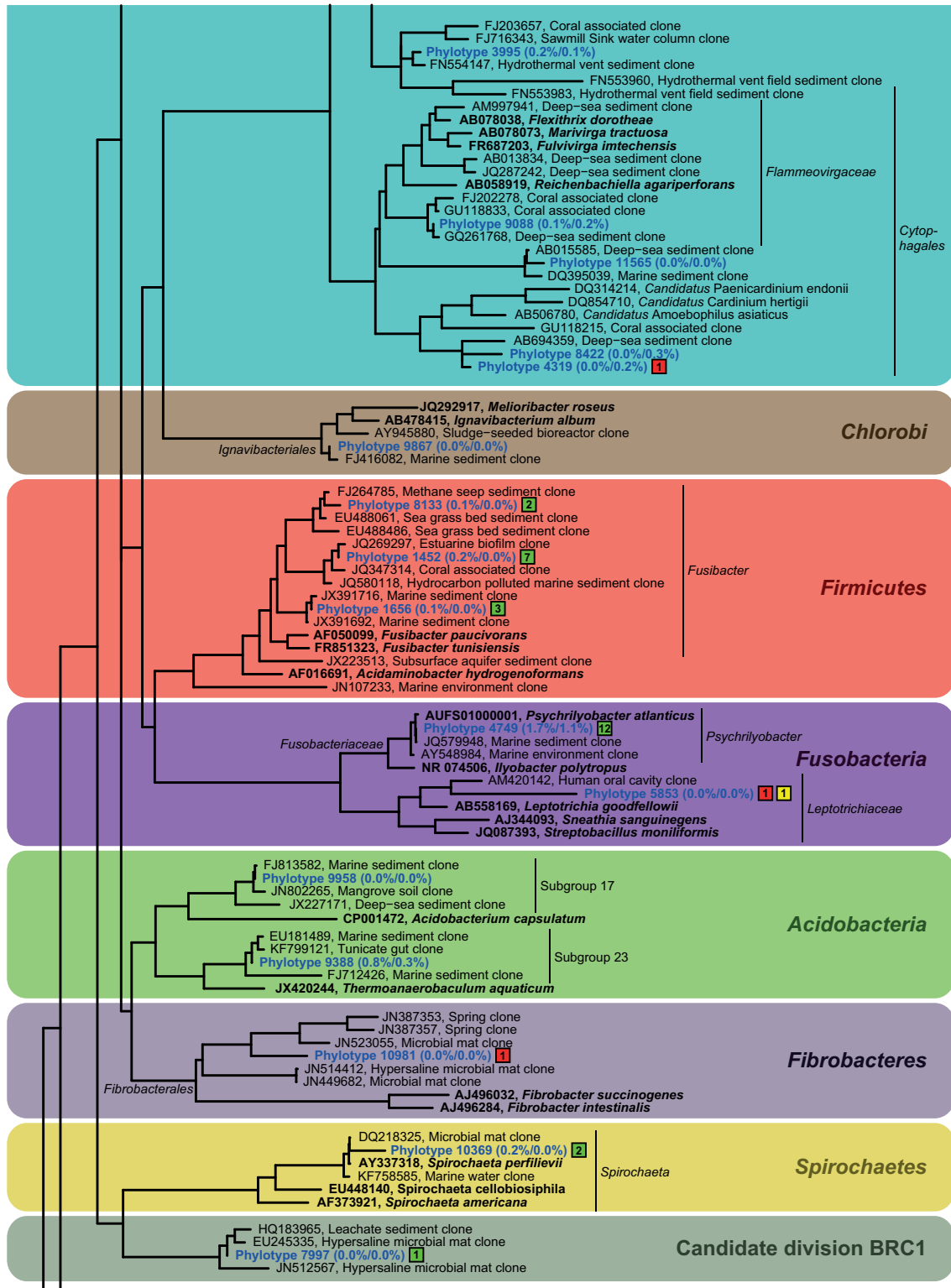
- reducing bacterium from an oil-producing well. *Int J Syst Bacteriol* **49**: 1141-1147.
- Rivkin RB, Anderson MR, Lajzerovic C. (1996). Microbial processes in cold oceans. I. Relationship between temperature and bacterial growth rate. *Aquat Microb Ecol*: 243-254.
- Rosselló-Mora R, Thamdrup B, Schäfer H, Weller R, Amann R. (1999). The response of the microbial community of marine sediments to organic carbon input under anaerobic conditions. *Syst Appl Microbiol* **22**: 237-248.
- Ruvira MA, Lucena T, Pujalte MJ, Arahall DR, Macian MC. (2013). *Marinifilum flexuosum* sp. nov., a new Bacteroidetes isolated from coastal Mediterranean Sea water and emended description of the genus *Marinifilum* Na et al., 2009. *Syst Appl Microbiol* **36**: 155-159.
- Rysgaard S, Glud RN, Risgaard-Petersen N, Dalsgaard T. (2004). Denitrification and anammox activity in Arctic marine sediments. *Limnol Oceanogr* **49**: 1493-1502.
- Sagemann J, Jorgensen BB, Greeff O. (1998). Temperature dependence and rates of sulfate reduction in cold sediments of Svalbard, Arctic Ocean. *Geomicrobiol J* **15**: 85-100.
- Sahm K, Berninger U. (1998). Abundance, vertical distribution, and community structure of benthic prokaryotes from permanently cold marine sediments (Svalbard, Arctic Ocean). *Mar Ecol- Prog Ser* **165**: 71-80.
- Sahm K, Knoblauch C, Amann R. (1999). Phylogenetic affiliation and quantification of psychrophilic sulfate-reducing isolates in marine arctic sediments. *Appl Environ Microbiol* **65**: 3976-3981.
- Sass A, Rutters H, Cypionka H, Sass H. (2002). *Desulfobulbus mediterraneus* sp nov., a sulfate-reducing bacterium growing on mono- and disaccharides. *Arch Microbiol* **177**: 468-474.
- Schloss PD, Westcott SL, Ryabin T, Hall JR, Hartmann M, Hollister EB et al. (2009). Introducing mothur: open-source, platform-independent, community-supported software for describing and comparing microbial communities. *Appl Environ Microbiol* **75**: 7537-7541.
- Sorokin DY, Tourova TP, Panteleeva AN, Muyzer G. (2012). *Desulfonatronobacter acidivorans* gen. nov., sp nov and *Desulfobulbus alkaliphilus* sp nov., haloalkaliphilic heterotrophic sulfate-reducing bacteria from soda lakes. *Int J Syst Evol Microbiol* **62**: 2107-2113.
- Spain AM, Peacock AD, Krumholz LR. (2011). Effects of microbial community structure, terminal electron accepting conditions, and molybdate on the extent of U(VI) reduction in landfill aquifer sediments. *Geomicrobiol J* **28**: 430-443.
- Stamatakis A. (2006). RAxML-VI-HPC: maximum likelihood-based phylogenetic analyses with thousands of taxa and mixed models. *Bioinformatics* **22**: 2688-2690.
- Suzuki D, Jeki A, Amaishi A, Ueki K. (2007). *Desulfobulbus japonicus* sp nov., a novel Gram-negative propionate-oxidizing, sulfate-reducing bacterium isolated from an estuarine sediment in Japan. *Int J Syst Evol Microbiol* **57**: 849-855.
- Szewzyk R, Pfennig N. (1987). Complete oxidation of catechol by the strictly anaerobic sulfate-reducing *Desulfobacterium catecholicum* sp. nov. *Arch Microbiol* **147**: 163-168.
- Tasaki M, Kamagata Y, Nakamura K, Okamura K, Minami K. (1993). Acetogenesis from pyruvate by *Desulfotomaculum thermobenzoicum* and differences in pyruvate metabolism among three sulfate-reducing bacteria in the absence of sulfate. *FEMS Microbiol Lett* **106**: 259-263.
- Tatusova T, Ciufo S, Fedorov B, O'Neill K, Tolstoy I. (2014). RefSeq microbial genomes database: new representation and annotation strategy. *Nucleic Acids Res* **42**: D553-559.
- Teske A, Durbin A, Ziervogel K, Cox C, Arnosti C. (2011). Microbial community composition and function in permanently cold seawater and sediments from an arctic fjord of svalbard. *Appl Environ Microbiol* **77**: 2008-2018.
- Vandamme P, Falsen E, Rossau R, Hoste B, Segers P, Tytgat R et al. (1991). Revision of *Campylobacter*, *Helicobacter*, and *Wolinella* Taxonomy - Emendation of Generic Descriptions and Proposal of *Arcobacter* gen. nov. *Int J Syst Bacteriol* **41**: 88-103.
- Vandieken V, Pester M, Finke N, Hyun JH, Friedrich MW, Loy A et al. (2012). Three manganese oxide-rich marine sediments harbor similar communities of acetate-oxidizing manganese-reducing bacteria. *ISME J* **6**: 2078-2090.
- Vandieken V, Thamdrup B. (2013). Identification of acetate-oxidizing bacteria in a coastal marine surface sediment by RNA-stable isotope probing in anoxic slurries and intact cores. *FEMS Microbiol Ecol* **84**: 373-386.
- Widdel F, Pfennig N. (1982). Studies on dissimilatory sulfate-reducing bacteria that decompose fatty acids II. Incomplete oxidation of propionate by *Desulfobulbus propionicus* gen. nov., sp. nov. *Arch Microbiol* **131**: 360-365.
- Widdel F, Bak F. (1992). Gram-negative mesophilic sulfate-reducing bacteria. In: Balows A, Trüper HG, Dworkin M, Harder W, Schleifer KH (eds). *The Prokaryotes*, 2nd edn. Springer Verlag: New York. pp 3352-3378.
- Xu Y, Nogi Y, Kato C, Liang Z, Ruger HJ, De Kegel D et al. (2003). *Psychromonas profunda* sp. nov., a psychropiezophilic bacterium from deep Atlantic sediments. *Int J Syst Evol Microbiol* **53**: 527-532.

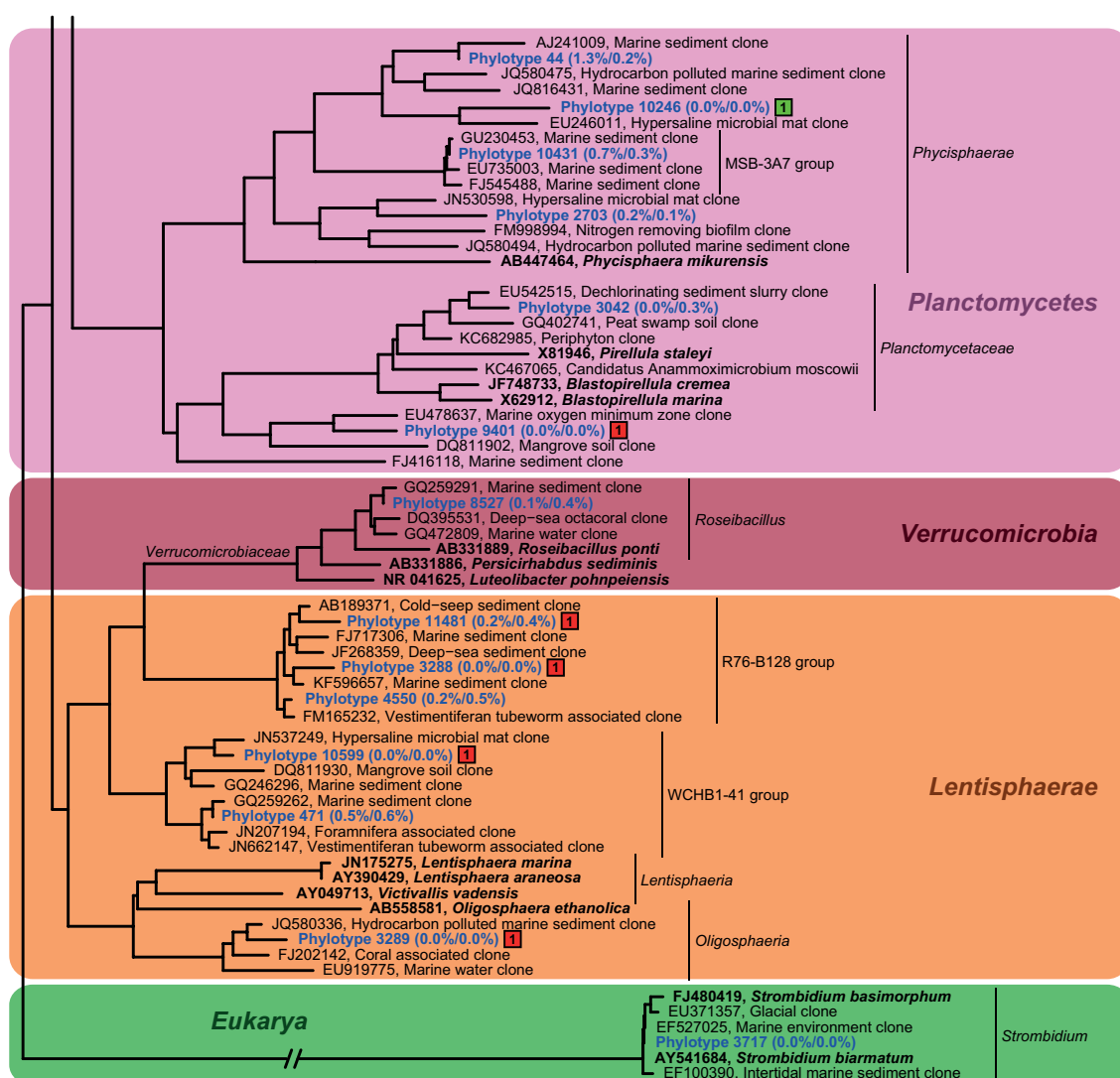
- Yilmaz P, Parfrey LW, Yarza P, Gerken J, Priesse E, Quast C *et al.* (2014). The SILVA and "All-species Living Tree Project (LTP)" taxonomic frameworks. *Nucleic Acids Res* **42**: D643-648.
- Zahedi S, Sales D, Romero LI, Solera R. (2013). Biomethanization from sulfate-containing municipal solid waste: effect of molybdate on microbial consortium. *J Chem Technol Biot* **89**: 1379-1387.
- Zhao JS, Manno D, Hawari J. (2009). *Psychrilyobacter atlanticus* gen. nov., sp. nov., a marine member of the phylum Fusobacteria that produces H₂ and degrades nitramine explosives under low temperature conditions. *Int J Syst Evol Microbiol* **59**: 491-497.











Supplementary Figure S1. Phylogeny of phylotypes present with $\geq 1\%$ of sequences in at least one incubation sample. A consensus tree (extended majority rule) was calculated from trees inferred by maximum likelihood, maximum parsimony and neighbor joining algorithms with the three closest relatives determined by SINA aligner for representative sequences of each phylotype as well as closely related cultivated organisms using a 50% conservation filter for bacteria covering 1222 nucleotide positions. The short amplicon sequences were subsequently added to this consensus tree without changing its topology using the EPA algorithm in RAXML-HPC 7.5.6. Environmental sequences were classified according to SILVA taxonomy. Scale bar indicates 10% sequence divergence. Numbers in parentheses indicate average abundance at day 0 (in DNA/RNA samples). Red and green squares indicate significant enrichment compared to the no substrate control ($p \geq 0.01$) following acetate and spirulina addition, respectively. Numbers within the squares indicate the number of samples (of 22 acetate and 24 spirulina incubation samples) in which the phylotype was significantly enriched. Yellow squares indicate sulfate reduction associated phylotypes, numbers in the square indicate numbers of samples (of 15) in which the phylotype was significantly enriched in the incubation with ^{13}C -labeled substrate compared to the inhibited control.

Supplementary Table S1. Read number, coverage, and alpha-diversity of bacterial 16S rRNA gene sequence libraries of incubation samples.

Incubation	Sample type	Number of high quality reads			Number of observed phylotypes (all seqs)			Good's coverage (all seqs)			Number of observed phylotypes (3250 seqs per library)			Chao1 richness (3250 seqs per library)			Simpson diversity index (3250 seqs per library)			Shannon diversity index (3250 seqs per library)			Equitability (3250 seqs per library)					
		day 0 ^a			day 8			day 32			day 0			day 8			day 32			day 0			day 8			day 32		
		day 0 ^a	day 8	day 32	day 0	day 8	day 32	day 0	day 8	day 32	day 0	day 8	day 32	day 0	day 8	day 32	day 0	day 8	day 32	day 0	day 8	day 32	day 0	day 8	day 32			
50 µM ¹³ C acetate Control (50 µM ¹² C acetate) Control (50 µM ¹³ C acetate + inhibitor) Control (No Substrate)	DNA	3770	4023		847	861	0.884	0.899	785	777	1447	1306	0.991	0.992	8.17	8.2	0.85	0.854										
	DNA	5523	262	4078	1083	853	0.899	0.898	818	759	1589	1364	0.991	0.991	8.17	8.1	0.844	0.846										
	DNA	4277	4468		949	891	0.884	0.901	820	759	1558	1384	0.991	0.991	8.21	8.08	0.848	0.845										
	DNA	4041	351		887	154	0.886	0.732	791	-	1494	-	0.991	-	8.18	-	0.849	-										
1 mM ¹³ C acetate Control (1 mM ¹² C acetate) Control (1 mM ¹³ C acetate + inhibitor) Control (No Substrate)	DNA	4281	3788		953	798	0.880	0.895	819	740	1631	1294	0.992	0.988	8.24	7.94	0.852	0.833										
	DNA	3282	4680	4360	643	853	0.903	0.907	640	737	1104	1313	0.969	0.991	0.988	7.18	7.94	0.85	0.834									
	DNA	4687	5687		934	1022	0.905	0.912	779	766	1375	1417	0.991	0.989	8.12	7.98	0.846	0.833										
	DNA	6035	4145		1151	910	0.903	0.894	827	805	1621	1373	0.991	0.992	8.07	8.27	0.847	0.857										
50 µg/l ¹³ C spirulina Control (50 µg/l ¹² C spirulina) Control (50 µg/l ¹³ C spirulina + inhibitor) Control (No Substrate)	DNA	5141	5073		1034	943	0.897	0.907	809	748	1554	1402	0.99	0.99	8.07	7.98	0.835	0.836										
	DNA	6013	1071	5181	1065	972	0.919	0.855	786	766	1395	-	0.989	-	8.04	-	0.836	-	0.839									
	DNA	5017	4510		947	817	0.909	0.912	762	692	1359	1215	0.99	0.983	8.05	7.63	0.84	0.809										
	DNA	4826	4992		980	996	0.897	0.895	792	791	1476	1552	0.989	0.99	8	8.04	0.831	0.836										
1 µM ¹³ C spirulina Control (1 µM ¹² C spirulina) Control (1 µM ¹³ C spirulina + inhibitor) Control (No Substrate)	DNA	5213	5984		600	597	0.940	0.949	466	428	909	856	0.883	0.892	5.46	5.36	0.616	0.613										
	DNA	4251	4342	5744	869	905	0.902	0.914	690	669	1321	1273	0.991	0.987	0.968	8.14	7.21	0.851	0.829	0.768								
	DNA	3802	4486		464	461	0.936	0.945	427	387	776	738	0.869	0.845	5.22	4.84	0.597	0.563										
	DNA	700	4873		259	973	0.794	0.898	-	790	-	1478	-	0.991	-	8.15	-	0.847	-									
50 µM ¹³ C acetate Control (50 µM ¹² C acetate) ^b Control (50 µM ¹³ C acetate + inhibitor) Control (No Substrate)	RNA	8826	4540		1283	967	0.935	0.892	790	813	1424	1478	0.985	0.985	7.91	8.04	0.822	0.832										
	RNA	5572	n.d.	5342	1057	967	0.912	n.d.	813	n.d.	1436	n.d.	0.989	n.d.	8.18	n.d.	0.846	n.d.	0.812									
	RNA	6351	4708		1266	979	0.907	0.903	906	818	1659	1414	0.992	0.991	8.54	8.27	0.869	0.855										
	RNA	5713	5386		1159	1090	0.904	0.902	872	845	1569	1541	0.99	0.991	8.33	8.29	0.852	0.852										
1 mM ¹³ C acetate Control (1 mM ¹² C acetate) Control (1 mM ¹³ C acetate + inhibitor) ^b Control (No Substrate)	RNA	5890	4102		1028	852	0.919	0.897	765	759	1377	1323	0.983	0.982	7.86	7.81	0.821	0.816										
	RNA	5940	6249	3298	1061	734	0.916	0.914	799	729	1400	1213	0.988	0.985	8.11	7.99	0.843	0.829	0.826									
	RNA	n.d.	4327		n.d.	819	n.d.	0.909	n.d.	712	n.d.	1240	n.d.	0.988	n.d.	7.88	n.d.	0.832	n.d.									
	RNA	6194	4552		1048	997	0.917	0.893	750	843	1387	1485	0.984	0.989	7.76	8.26	0.813	0.85										
50 µg/l ¹³ C spirulina Control (50 µg/l ¹² C spirulina) Control (50 µg/l ¹³ C spirulina + inhibitor) Control (No Substrate)	RNA	5489	1443		899	439	0.922	0.838	686	-	1257	-	0.973	-	7.29	-	0.774	-										
	RNA	7325	6405	5298	1141	1017	0.929	0.931	760	802	1238	1379	0.983	0.982	7.68	7.59	0.803	0.842										
	RNA	6797	210		1008	108	0.933	0.676	707	-	1249	-	0.965	-	7.34	-	0.776	-										
	RNA	5787	4317		1074	949	0.912	0.892	804	822	1448	1462	0.984	0.989	7.94	8.22	0.823	0.849										
1 µM ¹³ C spirulina Control (1 µM ¹² C spirulina) Control (1 µM ¹³ C spirulina + inhibitor) Control (No Substrate)	RNA	5901	4807		630	715	0.949	0.931	465	589	854	1013	0.928	0.968	5.68	6.86	0.641	0.745										
	RNA	4822	6835	5204	1013	1008	0.899	0.933	708	790	1469	1252	0.989	0.982	8.25	7.91	0.808	0.821										
	RNA	5820	3828		479	409	0.960	0.948	353	377	664	636	0.848	0.883	4.51	5.21	0.533	0.608										
	RNA	5431	5593		1035	1115	0.916	0.913	812	865	1355	1455	0.987	0.991	8.17	8.52	0.846	0.873										

^a DNA/RNA samples from day 0 were pooled prior to PCR amplification.^b n.d., no data due to an error in the barcode sequence

Supplementary Table S2. Phylotypes with average abundances of $\geq 1\%$ of all bacterial 16S rRNA sequences at day 0.

Phylotype	Taxonomy (phylum; class; order; family; genus)	DNA	RNA
4400	<i>Bacteroidetes; Bacteroidia; Bacteroidales; Marinilabiliaceae</i>	1.5%	2.7%
4247	<i>Bacteroidetes; Bacteroidia; Bacteroidales; Marinilabiliaceae</i>	0.7%	1.6%
4270	<i>Bacteroidetes; Bacteroidia; BD2-2</i>	1.6%	0.8%
10972	<i>Bacteroidetes; Flavobacteriia; Flavobacteriales; Flavobacteriaceae; Lutibacter</i>	2.7%	0.0%
1270	<i>Bacteroidetes; Flavobacteriia; Flavobacteriales; Flavobacteriaceae; Lutimonas</i>	2.8%	0.0%
8760	<i>Cyanobacteria; Chloroplast</i>	2.4%	0.0%
4749	<i>Fusobacteria; Fusobacteriia; Fusobacteriales; Fusobacteriaceae; Psychrilyobacter</i>	1.7%	1.1%
44	<i>Planctomycetes; Phycisphaerae; Phycisphaerales</i>	1.3%	0.2%
11461	<i>Proteobacteria; Betaproteobacteria; Nitrosomonadales; Nitrosomonadaceae; Nitrosomonas</i>	0.1%	1.6%
10184	<i>Proteobacteria; Deltaproteobacteria; Desulfobacterales; Desulfobacteraceae</i>	1.4%	1.2%
2011	<i>Proteobacteria; Deltaproteobacteria; Desulfobacterales; Desulfobacteraceae; Sva0081 sediment group</i>	1.3%	6.8%
11380	<i>Proteobacteria; Deltaproteobacteria; Desulfobacterales; Desulfobacteraceae; Sva0081 sediment group</i>	1.1%	2.4%
4982	<i>Proteobacteria; Deltaproteobacteria; Desulfobacterales; Desulfobacteraceae; Sva0081 sediment group</i>	0.7%	1.8%
6023	<i>Proteobacteria; Deltaproteobacteria; Desulfobacterales; Desulfobulbaceae; Desulfobulbus</i>	3.1%	1.0%
10263	<i>Proteobacteria; Deltaproteobacteria; Desulfobacterales; Desulfobulbaceae; Desulfobulbus</i>	0.2%	1.8%
3714	<i>Proteobacteria; Deltaproteobacteria; Desulfuromonadales; Desulfuromonadaceae; Desulfuromonas</i>	2.6%	0.1%
2526	<i>Proteobacteria; Deltaproteobacteria; Sva0485 group</i>	1.5%	0.2%
2228	<i>Proteobacteria; Gammaproteobacteria; Alteromonadales; Alteromonadaceae; BD2-7</i>	1.3%	0.3%
7234	<i>Proteobacteria; Gammaproteobacteria; Alteromonadales; Colwelliaceae; Colwellia</i>	2.2%	0.2%
9245	<i>Proteobacteria; Gammaproteobacteria; BD7-8 marine group</i>	1.8%	0.9%
6150	<i>Proteobacteria; Gammaproteobacteria; BD7-8 marine group</i>	0.2%	1.2%
2799	<i>Proteobacteria; Gammaproteobacteria; Chromatiales; Ectothiorhodospiraceae; Acidiferrobacter</i>	1.0%	3.2%
62	<i>Proteobacteria; Gammaproteobacteria; Order Incertae Sedis; Family Incertae Sedis; Marinicella</i>	3.1%	3.1%
6148	<i>Proteobacteria; Gammaproteobacteria; Thiotrichales; Thiotrichaceae</i>	0.4%	1.2%
9135	<i>Proteobacteria; Gammaproteobacteria; Xanthomonadales; JTB255 marine benthic group</i>	1.5%	0.2%

Chapter V

**Endospores of thermophilic bacteria as
tracers of microbial dispersal by ocean
currents**

ORIGINAL ARTICLE

Endospores of thermophilic bacteria as tracers of microbial dispersal by ocean currents

Albert Leopold Müller^{1,2}, Júlia Rosa de Rezende^{3,4}, Casey RJ Hubert⁴, Kasper Urup Kjeldsen³, Ilias Lagkouravdos¹, David Berry¹, Bo Barker Jørgensen³ and Alexander Loy^{1,2}

¹Division of Microbial Ecology, Department of Microbiology and Ecosystem Science, Faculty of Life Sciences, University of Vienna, Vienna, Austria; ²Austrian Polar Research Institute, Vienna, Austria; ³Center for Geomicrobiology, Department of Bioscience, Aarhus University, Aarhus, Denmark and ⁴School of Civil Engineering and Geosciences, Newcastle University, Newcastle Upon Tyne, UK

Microbial biogeography is influenced by the combined effects of passive dispersal and environmental selection, but the contribution of either factor can be difficult to discern. As thermophilic bacteria cannot grow in the cold seabed, their inactive spores are not subject to environmental selection. We therefore conducted a global experimental survey using thermophilic endospores that are passively deposited by sedimentation to the cold seafloor as tracers to study the effect of dispersal by ocean currents on the biogeography of marine microorganisms. Our analysis of 81 different marine sediments from around the world identified 146 species-level 16S rRNA phylotypes of endospore-forming, thermophilic *Firmicutes*. Phylotypes showed various patterns of spatial distribution in the world oceans and were dispersal-limited to different degrees. Co-occurrence of several phylotypes in locations separated by great distances (west of Svalbard, the Baltic Sea and the Gulf of California) demonstrated a widespread but not ubiquitous distribution. In contrast, Arctic regions with water masses that are relatively isolated from global ocean circulation (Baffin Bay and east of Svalbard) were characterized by low phylotype richness and different compositions of phylotypes. The observed distribution pattern of thermophilic endospores in marine sediments suggests that the impact of passive dispersal on marine microbial biogeography is controlled by the connectivity of local water masses to ocean circulation.

The ISME Journal (2014) 8, 1153–1165; doi:10.1038/ismej.2013.225; published online 19 December 2013

Subject Category: Microbial population and community ecology

Keywords: biogeography; endospores; marine microorganisms; ocean currents; thermophiles

Introduction

Microorganisms display distinct biogeographic patterns (reviewed in Foissner, 2006; Green and Bohannan, 2006; Martiny *et al.*, 2006; Ramette and Tiedje, 2007; Lindstrom and Langenheder, 2012), yet the mechanisms controlling their distribution in the environment are difficult to distinguish and thus not well understood. Four fundamental processes—selection, drift, dispersal and mutation—have been proposed for creating and maintaining microbial biogeographic patterns (Hanson *et al.*, 2012), updating the classical concept of dispersal, speciation and extinction as the main factors determining biogeography. Regardless of theoretical framework,

dispersal of microbial cells has a central role in shaping the spatial distribution of microbial biodiversity (Green and Bohannan, 2006; Fierer, 2008). In its strictest sense, microbial dispersal is defined as the physical movement of cells between two locations, but an extended definition additionally includes successful establishment—that is, physiological activity and growth of migrated cells—at the receiving location (Hanson *et al.*, 2012). The existence of physical dispersal barriers for microorganisms has traditionally been questioned. Under the Baas Becking paradigm of microbial cosmopolitanism—‘everything is everywhere, but, the environment selects’—it is hypothesized that microorganisms possess unlimited dispersal capabilities due to their large population sizes and short generation times. In this paradigm, environmental factors are the sole determinants of observed microbial distribution patterns (Baas Becking, 1934; Finlay, 2002; Fenchel and Finlay, 2004). More recently, multiple studies have put forward evidence for dispersal limitation among microorganisms (Papke *et al.*, 2003; Whitaker *et al.*, 2003; Green *et al.*, 2004; Reche *et al.*, 2005; Martiny *et al.*, 2006; Ghiglione *et al.*, 2012; Sul *et al.*,

Correspondence: CRJ Hubert, School of Civil Engineering and Geosciences, Newcastle University, Newcastle Upon Tyne, UK. E-mail: casey.hubert@newcastle.ac.uk

or A Loy, Division of Microbial Ecology, Department of Microbiology and Ecosystem Science, University of Vienna, Althanstrasse 14, Wien 1090, Austria. E-mail: loy@microbial-ecology.net

Received 12 September 2013; revised 7 November 2013; accepted 14 November 2013; published online 19 December 2013

2013). Controversy remains, however, partly due to differences in definitions of dispersal and the operational taxonomic units used to classify microorganisms (Hanson *et al.*, 2012), but mostly because the biogeography of free-living microorganisms is the result of a combination of various evolutionary and ecological processes that make it difficult to unravel the relative influence of passive transport (Martiny *et al.*, 2006; Ramette and Tiedje, 2007). We use the term dispersal here to describe physical movement by passive transport, but not colonization of the new location.

The presence of dormant endospores of thermophilic members of the bacterial phylum *Firmicutes* in cold marine sediments is the result of passive transport from warm environments and has been proposed as a natural model for selectively investigating the dispersal of microbial cells in the oceans (Bartholomew and Paik, 1966; Isaksen *et al.*, 1994; Hubert *et al.*, 2009; de Rezende *et al.*, 2013). The inactivity of these model organisms enables their biogeography to be investigated largely without any confounding influence of environmental selection. Therefore, any observed non-random spatial distribution patterns of these organisms should be directly attributable to the influence of dispersal limitation. Ocean currents and eventual sedimentation have been invoked as dispersal vectors for supplying thermophilic *Firmicutes* spores to Arctic fjord sediments off the coast of Svalbard at an estimated rate exceeding 10^8 spores per square meter per year (Hubert *et al.*, 2009). Once deposited in the cold sediment, these spores lie dormant as members of the rare biosphere and the 'microbial seed bank' (Pedros-Alio, 2012; Gibbons *et al.*, 2013), but they can be induced to germinate rapidly during sediment incubation experiments at high temperature (Hubert *et al.*, 2009).

Enrichment of thermophilic anaerobes from dormant spores in high-temperature incubation experiments enables selective focus on a specific, culturable part of the rare biosphere that is of exceptional interest for studying long-term and long-distance dispersal. Bacterial endospore dispersal represents an upper boundary for the dispersal capabilities of vegetative cells, as bacterial endospores are metabolically inert, highly stress resistant and able to survive unfavorable conditions for long periods (Nicholson *et al.*, 2000). For example, a half-life of up to 440 years was estimated for endospores of thermophilic sulfate-reducing bacteria deposited in Aarhus Bay in the Baltic Sea (de Rezende *et al.*, 2013); these viable endospores decreased in abundance with depth but were still detected at 6.5 m below seafloor in 4500-year-old sediment, suggesting a life span that could allow the global dispersal of spores through thermohaline circulation that fully connects the world oceans on a time scale of ~1000–2700 years (DeVries and Primeau, 2011). Diverse populations of dormant bacterial spores become active when sediment is heated (to 50–60 °C).

Once germinated, the vegetative cells catalyze the mineralization of organic matter via extracellular enzymatic hydrolysis, fermentation and sulfate reduction (Hubert *et al.*, 2010). So far, the phylogenetic composition of these dormant, thermophilic communities has only been studied in a few locations, that is, the sediments of West Svalbard fjords and Aarhus Bay. Even though these locations are ~3000 km apart, they share at least two thermophilic *Desulfotomaculum* phylotypes with identical 16S rRNA and dissimilatory (bi)sulfite reductase (*dsrAB*) gene sequences (de Rezende *et al.*, 2013). Although this is the first intriguing evidence for long-distance dispersal of these thermophilic endospores, their large-scale biogeography in the global ocean remains unexplored.

We thus analyzed the richness, phylogeny and distribution of endospores of thermophilic bacteria in marine sediments on global and regional scales to address the following questions: are thermophilic spores randomly distributed, which would be indicative of unlimited dispersal, or does the biogeography of thermophilic spores show signs of dispersal limitation? If these spores are not randomly distributed, how do local hydrography, sedimentation and major ocean currents impact their distribution? To investigate the biogeography of thermophilic spores, sediment samples from 81 locations around the world ocean, including regional Arctic samples from the Svalbard archipelago and the Baffin Bay that connect differently to global ocean circulation, were amended with organic substrates, pasteurized and incubated at 50 °C under anoxic conditions. Pasteurization kills the vegetative community of mesophilic or psychrophilic microorganisms. Shifts in microbial community activity and composition, owing to germination and growth of thermophilic endospores during the incubation, were then monitored by measuring sulfate reduction rates and by using multiplex pyrosequencing of bacterial 16S rRNA gene amplicons. Subsequently, the phylogeny and biogeography of enriched thermophilic phylotypes was analyzed.

Materials and methods

Marine sediment samples

The sample set comprised marine sediments from 81 locations around the world ocean, including two regional Arctic sample sets from Svalbard fjords and the Baffin Bay and samples from hydrothermally influenced sediments in the Guaymas Basin (43–150 °C, Gulf of California) that comprises potential source environments of endospore-forming thermophiles (Figure 1, Supplementary Table S1). Most sediment samples were collected from the seafloor surface (0–10 cm below seafloor) at coastal or deep sea, open ocean sites with *in situ* temperatures ranging from 0 to 30 °C. Samples were stored at 4 °C or frozen at –20 °C until germination experiments.

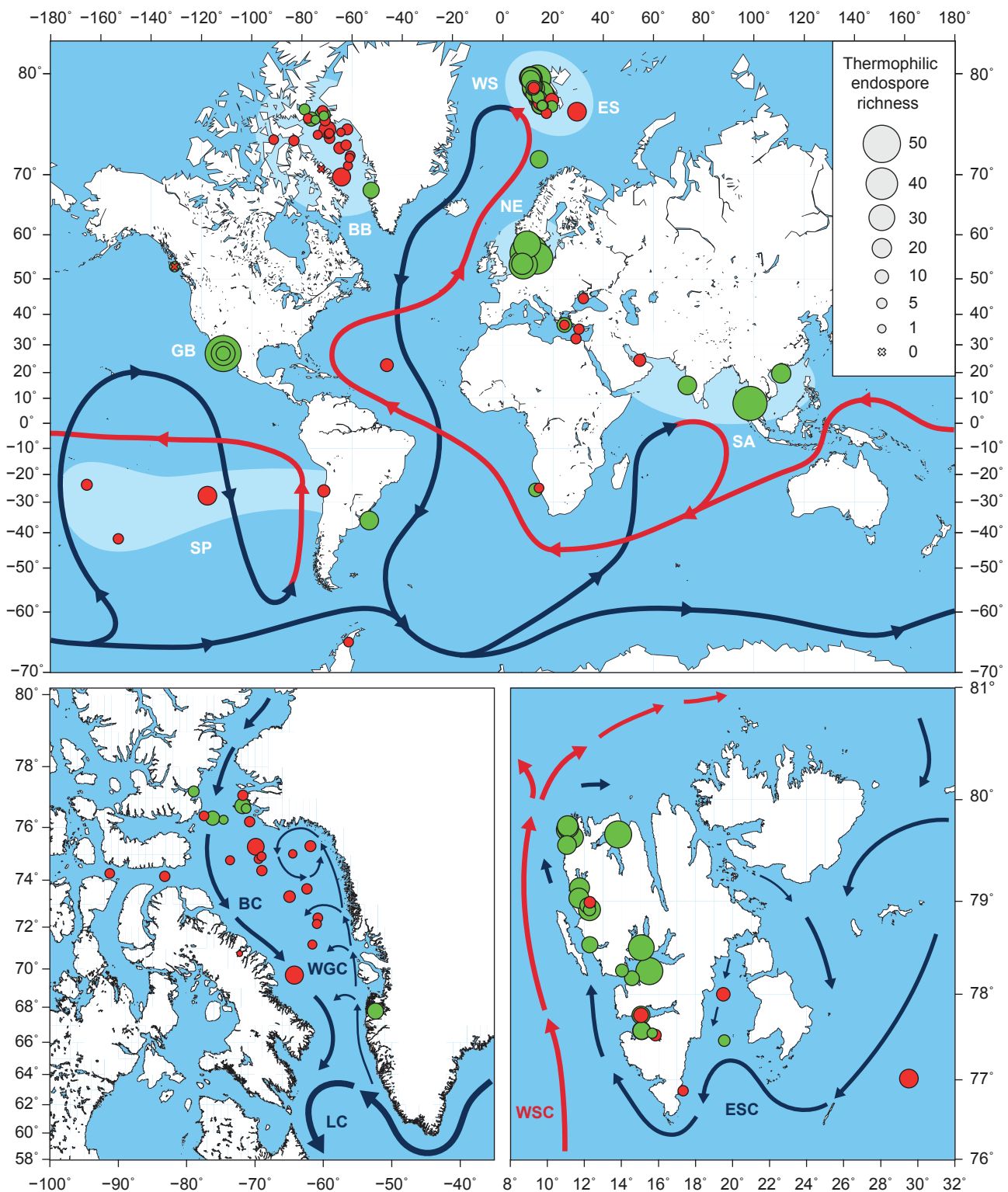


Figure 1 Global and regional maps show the sediment-sampling sites and selected major ocean currents. Circle sizes represent richness of thermophilic *Firmicutes* endospore phylotypes (crosses indicate a richness of 0). Symbol color indicates whether thermophilic sulfate reduction was detected during the high temperature incubation (green = positive, red = negative). Global map (top) shows the global thermohaline circulation (warm/surface currents in red, cold/deep water currents in blue; adapted and simplified from Rahmstorf (2002)). Broad geographic regions studied are highlighted in lighter blue (WS, West Svalbard; ES, East Svalbard; BB, Baffin Bay; NE, Northern Europe; GB, Guaymas Basin; SA, South Asia; SP, South Pacific). Map of Baffin Bay (bottom left): local currents reproduced from Lloyd *et al.* (2005); BC, Baffin Island Current; WGC, West Greenland Current; LC, Labrador Current. Map of Svalbard (bottom right): local currents reproduced from Knies *et al.* (2007); WSC, West Spitsbergen Current; ESC, East Spitsbergen Current.

Sediment incubation and sulfate reduction measurements

Sediment was homogenized and mixed with sterile anoxic synthetic seawater medium at a 1:2 (w/w) ratio under constant flow of N₂ gas. The sediment slurries were amended with organic substrates: formate, lactate, acetate, succinate, propionate, butyrate, ethanol (each to a final concentration of 0.5 mM) and/or with freeze-dried *Spirulina* cells (1.5 g l⁻¹). Two 12-ml aliquots of slurried sediment were transferred to Hungate tubes under constant flow of N₂ and pasteurized for 20 min at 80 °C and incubated in parallel at 50 °C. Before the incubation, one aliquot received ~720 kBq ³⁵S-labeled carrier-free sulfate tracer for sulfate reduction measurement. The incubations were sub-sampled by syringe-needle after 0, 56, 72 and/or 120 h. Aliquots of 3 ml from the ³⁵S-sulfate slurries were mixed with 6 ml 20% zinc acetate solution and stored at -20 °C until sulfate reduction was determined using a single-step cold chromium distillation method (Kallmeyer *et al.*, 2004). From the non-radioactive incubations, 2 ml subsamples were pelleted by centrifugation and frozen at -20 °C for subsequent DNA extraction.

Multiplex amplicon pyrosequencing

DNA was extracted from sediment slurries using the PowerSoil DNA isolation kit (MO BIO Laboratories, Inc., Carlsbad, CA, USA). Bacterial 16S rRNA gene amplicons were obtained and supplied with barcodes and pyrosequencing adaptors using a two-step PCR approach with low cycle numbers (20 + 5) and pooling of triplicate PCR reactions to reduce variability associated with barcoded pyrosequencing primers (Berry *et al.*, 2011). The PCR primers targeting most bacteria (909F: 5'-ACTCAAAKGAATWGACGG-3', 1492R: 5'-NTACCTTGTTACGACT-3') and conditions were described previously (Berry *et al.*, 2011). Final PCR products were purified using the Agencourt Ampure XP system (Beckman Coulter, Vienna, Austria) and the DNA concentration was determined using a Quant-iT PicoGreen dsDNA Assay (Invitrogen, Darmstadt, Germany). For better coverage of samples with higher expected bacterial diversity, amplicons were then pooled at a 2:1 ratio of 0 h and 120 h time points, respectively. Sequencing was performed on a GS FLX or GS FLX+ instrument using Titanium chemistry (Roche, Mannheim, Germany) by the Norwegian High-Throughput Sequencing Centre (Oslo, Norway) or by Eurofins MWG Operon (Ebersberg, Germany). In total, 1 493 577 reads with an average length of 567 nucleotides (nt) were received. Sequences were trimmed and erroneous sequencing reads removed using the PyroNoise implementation in mothur (Quince *et al.*, 2009; Schloss *et al.*, 2009) and sorted according to barcode using QIIME (Caporaso *et al.*, 2010), yielding a total of 1 196 847 usable reads with an

average length of 353 nt. A 97% identity threshold was used for clustering reads into phylotypes with UCLUST (Edgar, 2010). Representative sequences were aligned with mothur using the Needleman-Wunsch pairwise alignment method default settings (Schloss *et al.*, 2009). Chimeras were detected using Chimera Slayer (Haas *et al.*, 2011) and excluded from further analysis. Pyrosequencing data are archived at the NCBI Sequence Read Archive under accession SRP028774.

Identification of putative thermophilic endospore phylotypes

Two criteria were used to identify putative thermophilic endospore phylotypes. First, species-level phylotypes had to be significantly enriched in at least one sediment sample after incubation at high temperature. This criterion is based on the assumption that thermophilic endospores will survive the initial pasteurization and germinate and grow during the ensuing 50 °C incubation. Significant enrichment of phylotypes was determined using a two-proportion *T*-test and *P*-values were corrected for multiple comparisons using the false discovery rate method in R (Benjamini and Hochberg, 1995) to account for uncertainty due to sequence sampling depth. Corrected *P*-values ≤ 0.01 were considered significant. Second, phylotypes had to be affiliated with the phylum *Firmicutes*, to which all known endospore-forming bacteria belong (it was shown recently that endospore formation likely evolved only once at the base of the *Firmicutes* tree) (Abecasis *et al.*, 2013). This approach does not survey all inactive cells in the sampled environments, but hones in on a physiological subset of the rare biosphere (Lennon and Jones, 2011). The clear advantage of this strategy is that taxa that were active and subject to environmental selection *in situ* are excluded from the analysis, allowing passive dispersal to be evaluated in isolation. Representative sequences of enriched *Firmicutes* phylotypes were then automatically aligned using the web-based SINA aligner (Pruesse *et al.*, 2012) and imported into the ARB-SILVA database SSU Ref NR 111 (Quast *et al.*, 2013) using the ARB software package (Ludwig *et al.*, 2004). The alignment was manually curated and used to re-cluster the representative sequences into species-level phylotypes of ≥ 97% sequence similarity using the average neighbor algorithm in mothur. A phylotype was called present at a location if at least one sequence of this phylotype was detected before and/or after the 120 h incubation of sediment from this location.

Phylogeny

A maximum likelihood (RAxML) tree was calculated with almost full-length 16S rRNA sequences (≥ 1400 nt) of closely related reference bacteria or environmental clones based on 1222 alignment

positions by using a 50% sequence conservation filter for bacteria. Using the ARB Parsimony Interactive tool, the short amplicon pyrosequences were subsequently added to this tree one at a time by using the 50% sequence conservation filter and alignment filters covering the individual length of each representative phylotype sequence, without changing the overall tree topology. Trees were visualized using iTOL (Letunic and Bork, 2006).

Network analysis

Two different kinds of networks were built based on the phylotype presence/absence matrix. First, a network of phylotype co-occurrence was produced for phylotypes present in at least five sites and with a minimum Spearman correlation coefficient of 0.6 (and $P < 0.0001$ based on permutation testing) (Barberán *et al.*, 2012). Focus on phylotypes that occurred at multiple sites reduced network complexity and facilitated identification of the core thermophilic endospore community. Second, a network of sites based on phylotype diversity was produced based on Bray-Curtis similarity of at least 0.6. Networks were plotted using the 'network' package in R (Butts *et al.*, 2012).

Distance-decay analysis

Jaccard similarities were calculated from the phylotype presence/absence matrix using the 'vegan' package in R (Oksanen *et al.*, 2012). Distances were calculated from latitude and longitude coordinates of sampling sites using the Vincenty inverse formula for ellipsoids and World Geodetic System (WGS) 84 ellipsoid parameters and calculated using R (R Development Core Team, 2008). A linear model was fit to the data and the statistical significance of the resulting regression parameters was evaluated by analysis of variance in R. To determine which phylotypes were dispersal-limited, a permutation-testing approach was used. The geographical dispersal of each phylotype was calculated as the mean distance between sites at which it was found. A null distribution of mean distances was produced by randomly selecting from all sites an equally sized subset (e.g. if a phylotype was found at seven sites, then seven sites would be randomly selected). The mean distance between the random subsets was calculated, and this process was repeated for 10 000 re-samplings. The probability that the observed mean distance was due to chance was calculated and corrected for multiple comparisons and P -values ≤ 0.05 were considered significant.

Geographical maps were drawn using Generic Mapping Tools (Wessel and Smith, 1998).

Results and discussion

Non-uniform distribution of thermophilic Firmicutes endospores in marine sediments

We studied the biogeography of thermophilic endospores in Arctic and other permanently cold or temperate marine sediments, because longevity of endospores makes them ideal study objects for understanding the time-averaged impact of dispersal on marine microbial biogeography. While there might be differences in endospore survival between different bacteria (Nicholson *et al.*, 2000; McKenney *et al.*, 2013), results are interpreted under the assumption that differences in endospore distribution are dependent on dispersal and not on environmental selection.

Anoxic, high-temperature incubations of pasteurized marine sediment (mostly from the top few centimeters) (Supplementary Results and Discussion, Supplementary Figure S1) from 81 different locations (Supplementary Table S1) led generally to a reduction in bacterial alpha diversity due to germination and growth of thermophilic endospores combined with the death and DNA decay of vegetative cells (Supplementary Materials and Methods, Supplementary Table S2). Principle coordinate analysis of weighted UniFrac distances confirmed a shift in phylogenetic composition of bacterial 16S rRNA genes after the incubation of most, but not all, sediment samples (Supplementary Figure S2). In total, we identified 146 thermophilic endospore phylotypes (hereafter called 'thermospore phylotypes') across all high-temperature incubations (Supplementary Table S3). Thermospore phylotypes were detected in samples from almost all of the investigated locations ($n = 79/81$) (Figure 1). Most of the 146 thermospore phylotypes were affiliated with the orders *Clostridiales* (61.0%) and *Bacillales* (17.8%); the most represented families were *Clostridiaceae* (32.2%), *Peptococcaceae* (17.8%) and *Bacillaceae* (14.4%) (Supplementary Figure S3, Supplementary Table S3). The phylogenetic identity and potential physiology of thermospore phylotypes corroborate and greatly expand upon previous studies that investigated thermophilic endospores in marine sediments (Bartholomew and Paik, 1966; Isaksen *et al.*, 1994; Vandieken *et al.*, 2006; Hubert *et al.*, 2009, 2010; Ji *et al.*, 2012; de Rezende *et al.*, 2013) (Supplementary Results and Discussion). A screening of environmental amplicon databases showed that 16S rRNA gene sequences of the identified thermospore phylotypes are very rarely detected by environmental surveys in the marine environment (Supplementary Results and Discussion, Supplementary Table S4), which is likely consistent with the widespread occurrence of endospore taxa in low relative abundance in many habitats.

The different sampling locations showed considerable differences in thermospore phylotype richness, despite an absence of strict endemism of

phylotypes that occurred at multiple locations (that is, exclusive presence in only one geographic region). The number of detected thermospore phylotypes per site ranged from 0 to 51 (on average, 13.3 ± 11.6 (s.d.), $n = 81$) (Supplementary Table S1). Thermospore phylotype richness was generally higher in Northern Europe (36.4 ± 10.2 per site, $n = 5$), the Guaymas Basin (28.7 ± 18.6 per site, $n = 3$), West Svalbard (17.9 ± 8.3 per site, $n = 23$) and South Asia (22.8 ± 15.2 per site, $n = 4$), whereas sites in the Baffin Bay (5.4 ± 4.7 per site, $n = 25$), the South Pacific (9.5 ± 6.5 per site, $n = 4$), East Svalbard (10.3 ± 6.2 per site, $n = 4$) and other regions (7.2 ± 5.7 per site, $n = 13$) showed comparatively lower phylotype richness (Figure 1). These differences in site occupancy indicate non-random variation in the distribution of thermospore phylotypes across the investigated sites. Out of the 146 thermospore phylotypes, 21 were detected at more than 15 locations and were widely distributed across different oceanic regions ('cosmopolitan phylotypes', Figure 2, Supplementary Figures S4 and 5). This cosmopolitan distribution

of thermospore phylotypes suggests that these taxa (i) are globally dispersed by ocean circulation and/or (ii) derive from multiple, globally widespread source environments that support growth of similar communities of thermophilic, endospore-forming bacteria. The cosmopolitan thermospore phylotypes were related to *Bacillus* (TSP005, TSP010, TSP013, TSP021), the *Aeribacillus-Geobacillus* lineage (TSP003, TSP007, TSP016), *Desulfonisporea* (TSP014), *Desulfotomaculum* (TSP004, TSP006, TSP015), *Clostridium* (TSP018, TSP019, TSP020), the *Brassicibacter-Sporosolibacterium* lineage (TSP002, TSP009, TSP012), or were only assigned at the family or order level (*Clostridiales* Family XI. Incertae Sedis: TSP008; *Christensenellaceae*: TSP017; *Bacillales*: TSP001, TSP011) due to lack of close, cultivated relatives (Figure 2). In contrast, 82 thermospore phylotypes were found only at five or fewer locations (Supplementary Figures S3 and 4), indicating more restricted occurrence and/or low abundance below the detection limit of our approach.

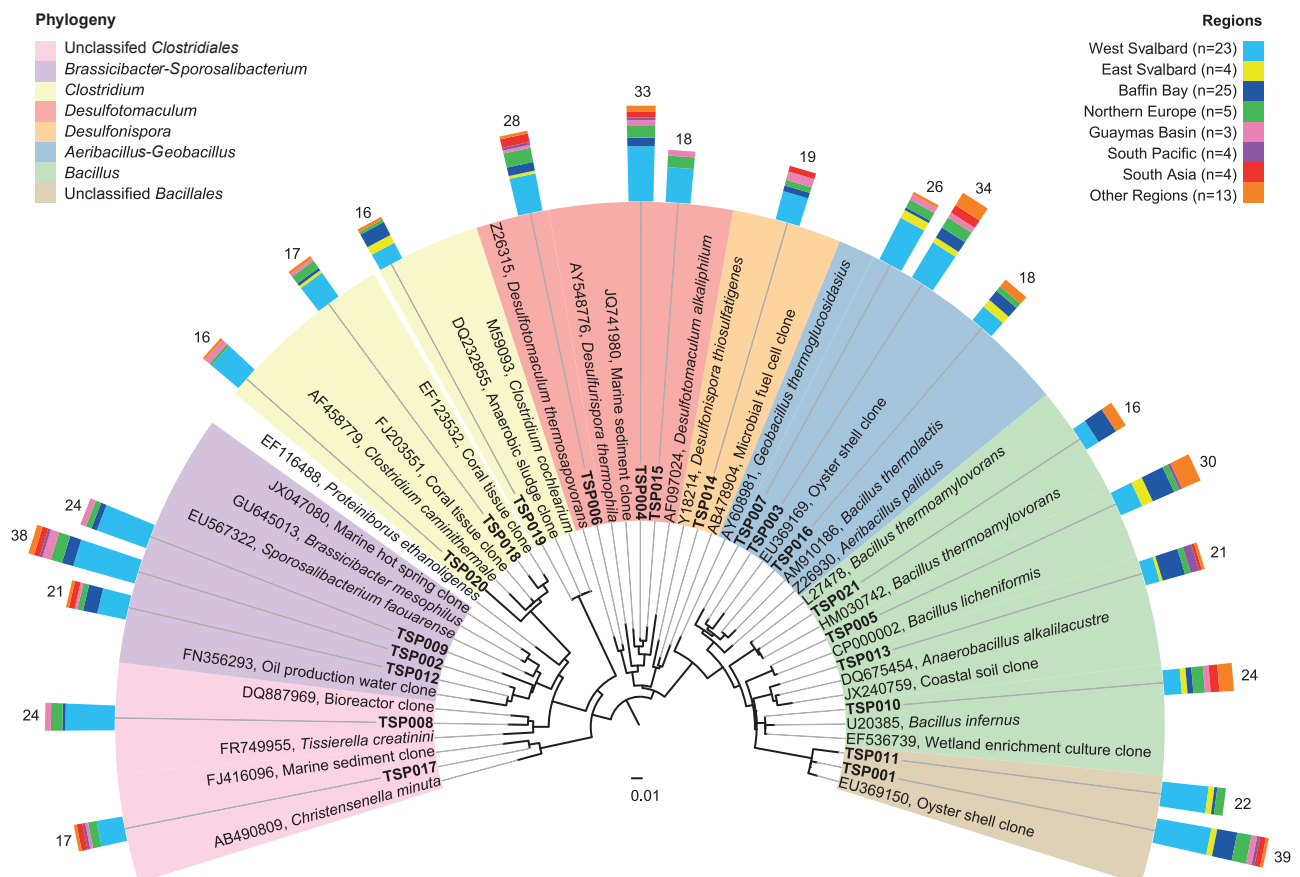


Figure 2 Phylogeny and geographic distribution of cosmopolitan thermophilic endospores. 16S rRNA-based phylogenetic tree of thermospore phylotypes (TSPs) that were detected at 15 or more sites. Scale bar indicates 1% sequence divergence as inferred from RAxML. Phylogenetic affiliations are highlighted in different colors. Colored bars indicate broad geographic regions where the thermospore phylotypes were present. Numbers indicate the number of sites at which a thermospore phylotype was detected, whereas the height of each bar color indicates the number of those phylotypes detected in each ocean region. TSP, thermospore phylotype. See Supplementary Figure S3 for an extended tree showing the phylogeny and geographic distribution of all 146 thermospore phylotypes.

Global biogeography patterns of thermophilic endospores show the influence of dispersal limitation

To analyze the relationship between geography and differences in endospore community structure, we plotted similarity between thermophilic endospore communities vs geographic distance for each location pair. This analysis revealed a significant, negative distance-decay curve (linear regression of log10-transformed variables with slope = -0.68177 , intercept = -0.09818 , $P < 0.001$) (Figure 3). This result shows that thermophilic endospore communities are non-randomly distributed, which suggests that dispersal limitation is influencing the beta-diversity of thermospore phylotypes. Alternatively, the shape of the distance-decay curve may be influenced by differences in the ability of endospore phylotypes to resist decay during dispersal (Nicholson *et al.*, 2000; McKenney *et al.*, 2013). To account for this, we investigated if the distribution of individual phylotypes, which should be less biased by within-phylotype variances in endospore survival, is significantly different from a random geographic distribution. Twelve of 146 thermospore phylotypes (TSP001, TSP007, TSP008, TSP009, TSP011, TSP015, TSP020, TSP027, TSP060, TSP061, TSP096, TSP111) were seemingly dispersal-limited because they had significantly geographically clustered occurrence; that is, the average geographic distance between the locations of each phylotype was significantly less than would be expected from its random occurrence at the same number of locations.

Correlation network analyses reveal a widely distributed core of frequently co-occurring thermophilic endospores
Network analysis was recently incorporated into microbial biogeography research to explore

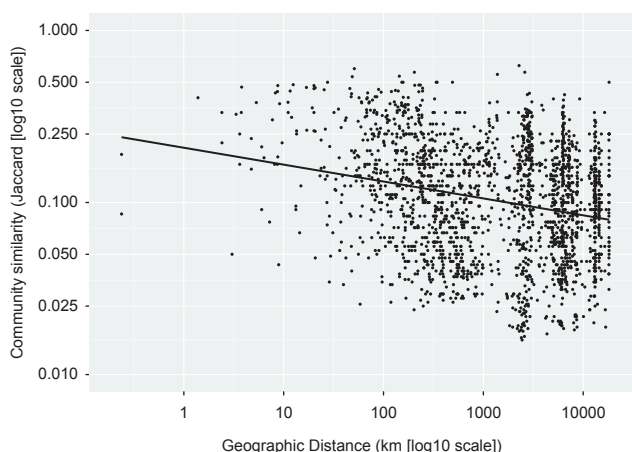


Figure 3 Distance decay of thermophilic endospore communities. The relationship between thermophilic endospore community similarity (Jaccard similarity, log10-transformed) and geographic distance (in kilometers, log10-transformed) is shown. The linear regression of log-transformed variables is significant ($P < 0.001$) and has a negative slope ($m = -0.68$) and shows that communities of thermophilic endospores are non-randomly distributed.

co-occurrence patterns of microbial taxa (Fuhrman, 2009; Barberán *et al.*, 2012). We used correlation network analysis to better describe the biogeography patterns of thermophilic endospores identified by the distance-decay curve and investigated which phylotypes tend to co-occur; that is, which phylotypes are found together at some sites and are commonly absent from others. The co-occurrence of thermospore phylotypes was calculated using non-parametric Spearman correlations of thermospore phylotype presence/absence across all sampling sites and, to explore groups of co-occurring phylotypes, network analysis was used for visualization. We identified eight small networks of different complexity, that is, numbers of nodes and edges (connections) (Supplementary Figure S6A). The largest network was characterized by four highly connected, central phylotypes (≥ 4 connections; TSP004, TSP008, TSP009, TSP015) and nine peripheral phylotypes that occurred at several locations (Figure 4a). Once we identified the most frequently co-occurring phylotypes, we explored similarities between thermospore phylotype communities by inferring association networks of sediment locations. The largest network contained 18 locations, of which many harbored several thermospore phylotypes (Figure 4b), whereas 10 other, much smaller networks were composed of ≤ 4 locations (Supplementary Figure S6B). The 18-location network was composed of most West Svalbard samples, but also samples that were geographically very distant from the Svalbard archipelago, namely two samples from the Baltic Sea (Aarhus Bay, Arkona Basin) and one sample from the Gulf of California (Guaymas Basin) (Figure 4b). This network contains a phylogenetically diverse core of co-occurring thermophilic endospores that are widely but not ubiquitously distributed in the oceans (for example, one of the phylotypes, TSP001, was detected in 39 sediments). This raises questions about whether certain thermospore phylotypes share common source environments from where they are disseminated in a non-random manner over long distances and along similar, as yet unidentified travel routes.

Hydrothermal sediments of the Guaymas Basin as potential source environments for endospore-forming thermophiles

Based on the identity, physiology and sedimentation rates of thermophilic spores in Svalbard and Aarhus Bay, we have previously postulated biogeochemical and geological characteristics of hypothetical source environments for these bacteria (Hubert *et al.*, 2009, 2010; de Rezende *et al.*, 2013). First, such anoxic marine environments must be warm enough to allow vegetative growth of the diverse community of anaerobic, endospore-forming thermophiles. Second, sufficiently strong fluxes (e.g., fluid transport) from these environments into the water column must physically transport cells into circulating seawater.

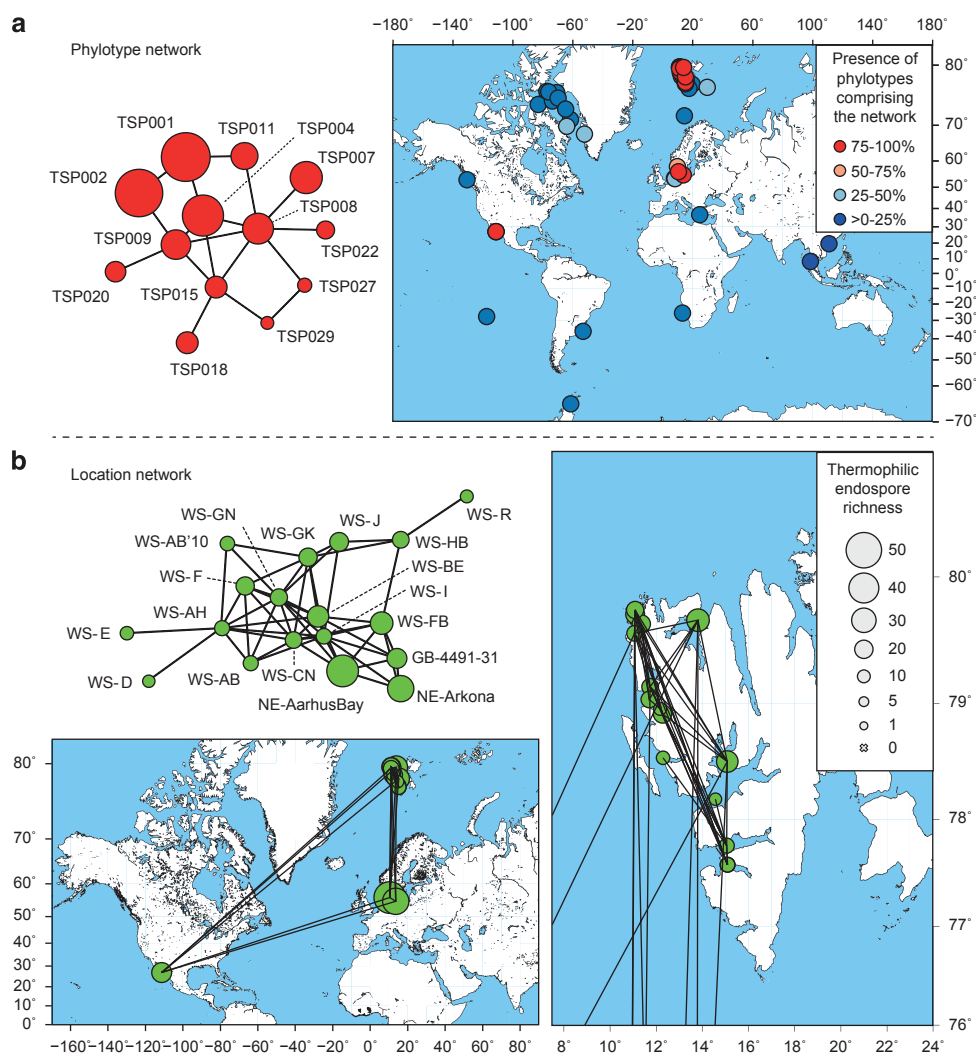


Figure 4 Network analysis of thermophilic endospore co-occurrence (a) and location (b). (a) Largest network of co-occurring thermospore phylotypes. Each node represents a thermospore phylotype (TSP). Presence of an edge between two nodes shows a strong correlation between these two phylotypes, which is indicative for co-occurrence. Circle size indicates site occupancy. Map shows locations where phylotypes of the network are present. The circle color indicates how many of the 13 phylotypes comprising the network are present at this site. (b) Largest location network. Each node represents a location. Presence of an edge between two nodes corresponds to a high Bray-Curtis similarity (≥ 0.6) between the endospore communities at these two locations. Circle size indicates thermospore phylotype richness. Maps show the global locations and correlations of these sites. The map on the right shows a magnification of Svalbard for enhanced resolution.

Consistent with this general description are, for example, pressurized gas or oil reservoirs in seabed sediments, and parts of oceanic spreading centers including hydrothermal vents and the sediments overlying them (Head *et al.*, 2003; Cowen, 2004; Brazelton *et al.*, 2006; Judd and Hovland, 2007; Hutnak *et al.*, 2008; Hubert and Judd, 2010). Anaerobic thermophiles in these hot sediment and ocean crust habitats are connected with the overlying cold ocean water via advection of seabed fluids such as hydrocarbons and recirculating water discharged from the ocean crust (Judd and Hovland, 2007; Hutnak *et al.*, 2008).

The hydrothermal surface sediments and the general geology and geography of Guaymas Basin satisfy these criteria (Supplementary Results and Discussion). Accordingly, a very large proportion

(44.5%) of all 146 thermospore phylotypes were detected overall in the three Guaymas Basin sediments investigated. Although surveys with much finer genetic resolution than offered by the 16S rRNA gene approach are required to prove that identical microorganisms co-occur at distant locations, it is intriguing that the Guaymas Basin sediment community comprised 15 of 25 cosmopolitan thermospore phylotypes and 8 of the 13 co-occurring phylotypes (including all four highly connected phylotypes in the largest network) (Figure 4a). High thermospore phylotype richness despite restricted access due to the geographic isolation of the semi-enclosed Gulf of California supports the hypothesis that environments in the Guaymas Basin are sources of thermophilic spores to the overlying water column. Thermohaline water

circulation in the Gulf of California is primarily influenced by wind, which alters directions and water transport between the gulf and the Pacific Ocean seasonally (Bray, 1988). It is conceivable that Guaymas Basin-derived spores embark on and survive long-distance travel to far away Svalbard and North Sea sediments via the global thermohaline circulation (Rahmstorf, 2000) (Figure 1). However, it may be more likely that these cold destinations are supplied with thermophilic spores from nearby warm environments that were not investigated in this study, and that dispersal barriers may prevent thermophilic endospores that escape the hot anoxic sediments in the Guaymas Basin from reaching far away water masses in the north Atlantic. Possible examples of potential source environments closer to Svalbard and the Baltic Sea could include systems such as the Lost City hydrothermal vent field associated with the mid-Atlantic ridge (Kelley *et al.*, 2005; Brazelton *et al.*, 2006) or the oil-bearing sediments in the North Sea (Gittel *et al.*, 2009), which both support thermophilic sulfate-reducing *Desulfotomaculum* species that are closely related to the thermospore phylotypes identified in this study. It is conceivable that thermophilic bacteria get distributed along the mid-oceanic ridges throughout the world oceans, as exemplified by hydrothermal vent animals and their symbionts (Petersen *et al.*, 2010; Vrijenhoek, 2010; Teixeira *et al.*, 2011), creating an extended series of source habitats from where thermophilic endospores may be further dispersed to the cold sediments tested in this study. The location network shown in Figure 4b, thus likely represents a fraction of a much larger network of warm sources and warm or cold destinations for dispersing thermophilic endospores that are interconnected through ocean currents.

Anthropogenic sources may also contribute to the presence of anaerobic thermophiles in marine sediments. North Sea oil production systems have been proposed as possible sources for thermophilic *Desulfotomaculum* species in Aarhus Bay sediments (de Rezende *et al.*, 2013) and close relatives to

thermospore phylotypes detected in the present study were found in oil production water (Gittel *et al.*, 2009). Close relatives were also detected in several anthropogenic, as well as natural terrestrial habitats such as bioreactors, activated sludge, compost and soil environments (Supplementary Tables S3 and 4). However, the phylotypes we have identified were enriched in artificial seawater, which is suggestive of a marine origin. Also, the presence of a widely distributed thermophilic *Desulfotomaculum alkaliphilum* phylotype (Figure 2) at depths corresponding to ~4500 years of sedimentation in Aarhus Bay (de Rezende *et al.*, 2013) indicates that there is a natural long-term dispersal of thermophilic endospores occurring in the marine environment that is independent of human activity.

Differences in thermophilic spore richness and phylogeny in Arctic regions correlate with connectivity of major water masses

The variable compositions of thermophilic endospore communities in Arctic sediments from the Baffin Bay and the east and west sides of the Svalbard archipelago suggest that thermospore phylotypes are not equally dispersed across these Arctic regions. Sediments from the Baffin Bay contained a significantly lower number of thermospore phylotypes than sediments from West Svalbard (Table 1). While sediments from only four locations on the East coast of Svalbard were available, we detected a similar yet not statistically significant trend of lower richness in East compared with West Svalbard sediments. Analysis of more samples from East Svalbard is required to confirm this trend. We additionally revealed a contrasting geographical distribution in the potential for thermophilic sulfate reduction that was generally consistent with the observed differences in thermospore phylotype richness (Figure 1). Thermophilic sulfate reduction was significantly more prevalent in West Svalbard than in East Svalbard and Baffin Bay sediments (Table 1).

The differences in thermophilic spore richness and metabolic potential were also reflected by the

Table 1 Comparison of thermospore phylotype richness, phylogenetic composition and prevalence of thermophilic sulfate reduction between Arctic regions

	West Svalbard (n = 23)	East Svalbard (n = 4)	Baffin Bay (n = 25)	West Svalbard vs Baffin Bay ^{a,b}	West Svalbard vs East Svalbard ^a	East Svalbard vs Baffin Bay ^a
Thermospore phylotype richness ^c	17.9 ± 8.3	10.3 ± 6.2	5.4 ± 4.7	P < 0.001	Not significant	Not significant
<i>Clostridiaceae</i> richness	6.0 ± 2.8	2.0 ± 1.8	1.5 ± 2.1	P < 0.001	P = 0.02	Not significant
<i>Peptococcaceae</i> richness	3.4 ± 2.9	2.0 ± 1.6	0.6 ± 0.9	P < 0.001	Not significant	Not significant
<i>Bacillaceae</i> richness	2.2 ± 1.9	3.0 ± 1.4	2.4 ± 1.4	Not significant	Not significant	Not significant
Thermophilic sulfate reduction (% of sites tested positive)	87	25	24	P < 0.001	P = 0.02	Not significant

^aSignificant differences between Arctic regions were determined by pairwise comparisons using the Mann–Whitney *U*-test for richness and Fisher's exact test for thermophilic sulfate reduction. *P*-values ≤ 0.05 were considered significant.

^bAll significant *P*-values in this column are also significant (*P* < 0.01) when only surface (0–10 cm, *n* = 13) or only deep (10–121 cm, *n* = 12) sediment samples are analyzed.

^cAll richness values are presented as mean ± s.d.

phylogenetic composition of thermophilic endospore communities in these Arctic regions (notwithstanding the aforementioned weak indications for strict endemism for any individual phylotypes). Of the three major families, West Svalbard sediments exhibit significantly more thermospore phylotypes belonging to the *Clostridiaceae* and the *Peptococcaceae* than Baffin Bay sediments, whereas *Bacillaceae* phylotypes were not differentially distributed between the Arctic regions (Table 1). Again, we observed a similar pattern between West Svalbard and East Svalbard, although differences were only significant for *Clostridiaceae* phylotypes (Table 1). No significant differences between East Svalbard and Baffin Bay sediments were found among these three taxonomic families (Table 1). Furthermore, frequently co-occurring thermospore phylotypes (e.g. TSP004, TSP008, TSP009, TSP015), as identified by network analysis (Figure 4), were almost exclusively limited to West Svalbard sediments. The observed distribution pattern is not impacted by the fact that 12 of 25 Baffin Bay sediment samples originate from a sediment depth below 10 cm (Supplementary Table S1). Restricting our analyses to only the shallow and deeper Baffin Bay sediments showed (i) no significant difference between them (e.g., thermospore phylotype richness: surface samples = 4.8 ± 4.7 , deeper samples = 6.1 ± 4.9) and (ii) that both had the same significant differences compared with West Svalbard regarding richness, phylogenetic composition and prevalence of thermophilic sulfate reduction (Table 1).

One dispersal-limiting factor that might be responsible for the different thermophilic endospore communities in Svalbard and Baffin Bay sediments is the rate at which spores are deposited to the seafloor. Based on sediment thickness and age, sedimentation rates in the Baffin Bay and off the coast of Svalbard are estimated to be in the same order of magnitude ($5\text{--}25\text{ cm ka}^{-1}$, Kallmeyer *et al.* (2012)). In contrast, reports for a few locations in these regions suggest that sedimentation rates are lower in the Baffin Bay (6.5 cm ka^{-1} , Simon *et al.* (2012)) than in Svalbard fjords (180 cm ka^{-1} , Hald *et al.* (2001); 190 cm ka^{-1} , Hubert *et al.* (2009)). However, it is currently unknown how efficient endospores in the water column are deposited to the sediment, that is, how the specific rate of spore sedimentation relates to the overall sedimentation rate. It is noteworthy that for most locations our enrichment inoculum derives from homogenized sediment from 0 to 10 cm depth and therefore integrates endospore communities that accumulated over 50 to 1500 years of deposition. Given the longevity of thermophilic spores (de Rezende *et al.*, 2013), our approach may diminish the impact of sedimentation rates on the recovered richness of thermophilic spore communities.

Besides the impact of local hydrography, sedimentation, and the possibility that unknown, local sources contribute to biogeography of thermophilic endospores, we hypothesized that dispersal-driven

distribution also depends on how local currents in the sampled regions are connected to global ocean circulation. The observed West–East difference in thermophilic endospore community structure in Svalbard appears to correlate with the regional hydrography of the archipelago, although the difference is not statistically significant in all parameters (Table 1). Two major ocean currents define the hydrography of Svalbard. The warm West Spitsbergen Current, which is an extension of the Gulf Stream, flows from the Atlantic Ocean northwards, whereas the East Spitsbergen Current transports cold water from the Arctic Ocean southwards (Loeng, 1991) (Figure 1). Although the core of the West Spitsbergen Current that flows along the continental slope is separated from the West Spitsbergen shelf waters by the Arctic Front, extensive cross-front exchange takes place below 50 m depth (Saloranta and Svendsen, 2001) and it has been shown that the West Spitsbergen Current extends its influence deep into the fjord system of West Svalbard (MacLachlan *et al.*, 2007).

The formation of deep and bottom water masses in the Baffin Bay are not fully understood (Tang *et al.*, 2004), but they are generally influenced by cold Arctic Ocean water via the Baffin Island Current in the north and by the Atlantic Ocean via the West Greenland Current (Figure 1). The low thermospore phylotype richness in the Arctic water-influenced sediments in the Baffin Bay suggests a lower influx of thermophiles derived from the Arctic Ocean. Reduced thermospore phylotype richness in the Arctic Ocean is possibly due to limited thermophile sources and lower connectivity to water masses from the rest of the world oceans where thermophile sources may be far more abundant.

Recent studies of vegetative microbial communities in the global ocean have suggested that hydrography and geographic isolation of the Arctic Ocean represents an effective dispersal barrier for microorganisms (Galand *et al.*, 2010; Ghiglione *et al.*, 2012; Hamdan *et al.*, 2013; Sul *et al.*, 2013). By tracking thermophilic endospores whose Arctic biogeography is only controlled by passive dispersal, our results demonstrate this dispersal limitation to be true. Importantly, evidence presented here suggests that this dispersal limitation even holds true for marine bacteria with enhanced survival capacities that are less prone to death during long-term and long-distance dispersal under unfavorable environmental conditions, that is, perhaps the most likely candidates to not be dispersal-limited. Different phylotypes of globally widespread thermophilic endospores co-occur at multiple distantly separated locations and thus could be simultaneously dispersed from common sources and/or along similar paths according to non-random mechanisms. Global dispersal routes and frequencies of marine microbial taxa are largely dependent on the degree of connectivity between major oceanic water masses. Dispersal barriers of this kind exert greater control on

the composition of marine microbial communities in water masses that participate minimally in global ocean circulation such as the Arctic Ocean.

Conflict of Interest

The authors declare no conflict of interest.

Acknowledgements

We gratefully acknowledge the provision of sediment samples by Jan Amend, Gail Lee Arnold, Carol Arnosti, Elisa Bayraktarov, Antje Boetius, Gerhard Bohrmann, Ellen Damm, Steve D'Hondt, Tim Ferdeman, Moritz Holtappels, Lars Holmkvist, Sabine Kasten, Martin Krüger, Connie Lovejoy, Maren Nickel, Aude Picard, Roy Price, Nils Risgaard-Petersen, Alberto Robador, Søren Rysgaard, Joanna Sawicka, Verona Vandieken, and Thorsten Wilhelm. We thank China Hanson for her valuable comments on a draft version of this paper. This work was financially supported by the Austrian Science Fund (FWF, P20185-B17 and P25111-B22 to AL).

References

- Abecasis AB, Serrano M, Alves R, Quintais L, Pereira-Leal JB, Henriques AO. (2013). A genomic signature and the identification of new sporulation genes. *J Bacteriol* **195**: 2101–2115.
- Baas Becking LGM. (1934). *Geobiologie of inleiding tot de milieukunde*. W.P. Van Stockum & Zoon: The Hague, The Netherlands.
- Barberán A, Bates ST, Casamayor EO, Fierer N. (2012). Using network analysis to explore co-occurrence patterns in soil microbial communities. *ISME J* **6**: 343–351.
- Bartholomew JW, Paik G. (1966). Isolation and identification of obligate thermophilic sporeforming bacilli from ocean basin cores. *J Bacteriol* **92**: 635–638.
- Benjamini Y, Hochberg Y. (1995). Controlling the false discovery rate - a practical and powerful approach to multiple testing. *J Roy Stat Soc B Met* **57**: 289–300.
- Berry D, Mahfoudh KB, Wagner M, Loy A. (2011). Barcoded primers used in multiplex amplicon pyrosequencing bias amplification. *Appl Environ Microbiol* **77**: 7846–7849.
- Bray NA. (1988). Thermohaline circulation in the Gulf of California. *J Geophys Res* **93**: 4993–5020.
- Brazelton WJ, Schrenk MO, Kelley DS, Baross JA. (2006). Methane- and sulfur-metabolizing microbial communities dominate the Lost City hydrothermal field ecosystem. *Appl Environ Microbiol* **72**: 6257–6270.
- Butts CT, Handcock MS, Hunter DR. (2012). Network: classes for relational data. R package version 1.7-1. <http://statnet.org/>.
- Caporaso JG, Kuczynski J, Stombaugh J, Bittinger K, Bushman FD, Costello EK *et al*. (2010). QIIME allows analysis of high-throughput community sequencing data. *Nat Methods* **7**: 335–336.
- Cowen JP. (2004). The microbial biosphere of sediment-buried oceanic basement. *Res Microbiol* **155**: 497–506.
- de Rezende JR, Kjeldsen KU, Hubert CR, Finster K, Loy A, Jorgensen BB. (2013). Dispersal of thermophilic Desulfotomaculum endospores into Baltic Sea sediments over thousands of years. *ISME J* **7**: 72–84.
- DeVries T, Primeau F. (2011). Dynamically and observationally constrained estimates of water-mass distributions and ages in the global ocean. *J Phys Oceanogr* **41**: 2381–2401.
- Edgar RC. (2010). Search and clustering orders of magnitude faster than BLAST. *Bioinformatics* **26**: 2460–2461.
- Fenchel T, Finlay BJ. (2004). The ubiquity of small species: Patterns of local and global diversity. *Bioscience* **54**: 777–784.
- Fierer N. (2008). Microbial biogeography: patterns in microbial diversity across space and time. In: Zengler K (ed.) *Accessing Uncultivated Microorganisms: From the Environment to Organisms and Genomes and Back*. ASM Press: Washington DC, pp 95–115.
- Finlay BJ. (2002). Global dispersal of free-living microbial eukaryote species. *Science* **296**: 1061–1063.
- Foissner W. (2006). Biogeography and dispersal of micro-organisms: a review emphasizing protists. *Acta Protozool* **45**: 111–136.
- Fuhrman JA. (2009). Microbial community structure and its functional implications. *Nature* **459**: 193–199.
- Galand PE, Potvin M, Casamayor EO, Lovejoy C. (2010). Hydrography shapes bacterial biogeography of the deep Arctic Ocean. *ISME J* **4**: 564–576.
- Ghiglione JF, Galand PE, Pommier T, Pedros-Alio C, Maas EW, Bakker K *et al*. (2012). Pole-to-pole biogeography of surface and deep marine bacterial communities. *Proc Natl Acad Sci USA* **109**: 17633–17638.
- Gibbons SM, Caporaso JG, Pirrung M, Field D, Knight R, Gilbert JA. (2013). Evidence for a persistent microbial seed bank throughout the global ocean. *Proc Natl Acad Sci USA* **110**: 4651–4655.
- Gittel A, Sørensen KB, Skovhus TL, Ingvorsen K, Schramm A. (2009). Prokaryotic community structure and sulfate reducer activity in water from high-temperature oil reservoirs with and without nitrate treatment. *Appl Environ Microbiol* **75**: 7086–7096.
- Green J, Bohannan BJ. (2006). Spatial scaling of microbial biodiversity. *Trends Ecol Evol* **21**: 501–507.
- Green JL, Holmes AJ, Westoby M, Oliver I, Briscoe D, Dangerfield M *et al*. (2004). Spatial scaling of microbial eukaryote diversity. *Nature* **432**: 747–750.
- Haas BJ, Gevers D, Earl AM, Feldgarden M, Ward DV, Giannoukos G *et al*. (2011). Chimeric 16S rRNA sequence formation and detection in Sanger and 454-pyrosequenced PCR amplicons. *Genome Res* **21**: 494–504.
- Hald M, Dahlgren T, Olsen T-E, Lebesbye E. (2001). Late Holocene palaeoceanography in Van Mijenfjorden, Svalbard. *Polar Res* **20**: 23–35.
- Hamdan LJ, Coffin RB, Sikaroodi M, Greinert J, Treude T, Gillevet PM. (2013). Ocean currents shape the microbiome of Arctic marine sediments. *ISME J* **7**: 685–696.
- Hanson CA, Fuhrman JA, Horner-Devine MC, Martiny JBH. (2012). Beyond biogeographic patterns: processes shaping the microbial landscape. *Nat Rev Microbiol* **10**: 497–506.
- Head IM, Jones DM, Larter SR. (2003). Biological activity in the deep subsurface and the origin of heavy oil. *Nature* **426**: 344–352.
- Hubert C, Loy A, Nickel M, Arnosti C, Baranyi C, Bruchert V *et al*. (2009). A constant flux of diverse thermophilic

- bacteria into the cold Arctic seabed. *Science* **325**: 1541–1544.
- Hubert C, Arnosti C, Bruchert V, Loy A, Vandieken V, Jorgensen BB. (2010). Thermophilic anaerobes in Arctic marine sediments induced to mineralize complex organic matter at high temperature. *Environ Microbiol* **12**: 1089–1104.
- Hubert C, Judd A. (2010). Using microorganisms as prospecting agents in oil and gas exploration. In: Timmis KN (ed.) *Handbook of Hydrocarbon and Lipid Microbiology*. Springer-Verlag: Berlin, Heidelberg, pp 2711–2725.
- Hutnak M, Fisher AT, Harris R, Stein C, Wang K, Spinelli G *et al.* (2008). Large heat and fluid fluxes driven through mid-plate outcrops on ocean crust. *Nat Geosci* **1**: 611–614.
- Isaksen MF, Bak F, Jorgensen BB. (1994). Thermophilic sulfate-reducing bacteria in cold marine sediment. *FEMS Microbiol Ecol* **14**: 1–8.
- Ji S, Wang S, Tan Y, Chen X, Schwarz W, Li F. (2012). An untapped bacterial cellulolytic community enriched from coastal marine sediment under anaerobic and thermophilic conditions. *FEMS Microbiol Lett* **335**: 39–46.
- Judd AG, Hovland M. (2007). *Seabed fluid flow: the impact of geology, biology and the marine environment*. Cambridge University Press: Cambridge.
- Kallmeyer J, Ferdelman TG, Weber A, Fossing H, Jorgensen BB. (2004). A cold chromium distillation procedure for radiolabeled sulfide applied to sulfate reduction measurements. *Limnol Oceanogr-Meth* **2**: 171–180.
- Kallmeyer J, Pockalny R, Adhikari RR, Smith DC, D'Hondt S. (2012). Global distribution of microbial abundance and biomass in subseafloor sediment. *Proc Natl Acad Sci USA* **109**: 16213–16216.
- Kelley DS, Karson JA, Früh-Green GL, Yoerger DR, Shank TM, Butterfield DA *et al.* (2005). A serpentinite-hosted ecosystem: the Lost City hydrothermal field. *Science* **307**: 1428–1434.
- Knies J, Brookes S, Schubert CJ. (2007). Re-assessing the nitrogen signal in continental margin sediments: New insights from the high northern latitudes. *Earth Planet Sc Lett* **253**: 471–484.
- Lennon JT, Jones SE. (2011). Microbial seed banks: the ecological and evolutionary implications of dormancy. *Nat Rev Microbiol* **9**: 119–130.
- Letunic I, Bork P. (2006). Interactive Tree Of Life (iTOL): an online tool for phylogenetic tree display and annotation. *Bioinformatics* **23**: 127–128.
- Lindstrom ES, Langenheder S. (2012). Local and regional factors influencing bacterial community assembly. *Env Microbiol Rep* **4**: 1–9.
- Lloyd JM, Park LA, Kuijpers B, Moros M. (2005). Early holocene palaeoceanography and deglacial chronology of Disko Bugt, West Greenland. *Quaternary Sci Rev* **24**: 1741–1755.
- Loeng H. (1991). Features of the physical oceanographic conditions of the Barents Sea. *Polar Res* **10**: 5–18.
- Ludwig W, Strunk O, Westram R, Richter L, Meier H, Yadhukumar *et al.* (2004). ARB: a software environment for sequence data. *Nucleic Acids Res* **32**: 1363–1371.
- MacLachlan SE, Cottier FR, Austin WE, Howe JA. (2007). The salinity: $\delta^{18}\text{O}$ water relationship in Kongsfjorden, western Spitsbergen. *Polar Res* **26**: 160–167.
- Martiny JBH, Bohannan BJM, Brown JH, Colwell RK, Fuhrman JA, Green JL *et al.* (2006). Microbial biogeography: putting microorganisms on the map. *Nat Rev Microbiol* **4**: 102–112.
- McKenney PT, Driks A, Eichenberger P. (2013). The *Bacillus subtilis* endospore: assembly and functions of the multilayered coat. *Nat Rev Microbiol* **11**: 33–44.
- Nicholson WL, Munakata N, Horneck G, Melosh HJ, Setlow P. (2000). Resistance of *Bacillus* endospores to extreme terrestrial and extraterrestrial environments. *Microbiol Mol Biol Rev* **64**: 548–572.
- Oksanen J, Blanchet FG, Kindt R, Legendre P, Minchin PR, O'Hara RB *et al.* (2012). *Vegan: community ecology package*. R package version 2.0-4. <http://CRAN.R-project.org/package=vegan>.
- Papke RT, Ramsing NB, Bateson MM, Ward DM. (2003). Geographical isolation in hot spring cyanobacteria. *Environ Microbiol* **5**: 650–659.
- Pedros-Alio C. (2012). The rare bacterial biosphere. *Ann Rev Mar Sci* **4**: 449–466.
- Petersen JM, Ramette A, Lott C, Cambon-Bonavita M-A, Zbinden M, Dubilier N. (2010). Dual symbiosis of the vent shrimp *Rimicaris exoculata* with filamentous gamma- and epsilonproteobacteria at four Mid-Atlantic Ridge hydrothermal vent fields. *Environ Microbiol* **12**: 2204–2218.
- Pruesse E, Peplies J, Glockner FO. (2012). SINA: accurate high-throughput multiple sequence alignment of ribosomal RNA genes. *Bioinformatics* **28**: 1823–1829.
- Quast C, Pruesse E, Yilmaz P, Gerken J, Schweer T, Yarza P *et al.* (2013). The SILVA ribosomal RNA gene database project: improved data processing and web-based tools. *Nucleic Acids Res* **41**: D590–D596.
- Quince C, Lanzen A, Curtis TP, Davenport RJ, Hall N, Head IM *et al.* (2009). Accurate determination of microbial diversity from 454 pyrosequencing data. *Nat Methods* **6**: 639–641.
- R Development Core Team (2008). *R: A language and environment for statistical computing*. R Foundation for Statistical Computing: Vienna, Austria.
- Rahmstorf S. (2000). The thermohaline ocean circulation: A system with dangerous thresholds? An editorial comment. *Climatic Change* **46**: 247–256.
- Rahmstorf S. (2002). Ocean circulation and climate during the past 120,000 years. *Nature* **419**: 207–214.
- Ramette A, Tiedje JM. (2007). Biogeography: an emerging cornerstone for understanding prokaryotic diversity, ecology, and evolution. *Microb Ecol* **53**: 197–207.
- Reche I, Pulido-Villena E, Morales-Baquero R, Casamayor EO. (2005). Does ecosystem size determine aquatic bacterial richness? *Ecology* **86**: 1715–1722.
- Saloranta TM, Svendsen H. (2001). Across the Arctic front west of Spitsbergen: high-resolution CTD sections from 1998–2000. *Polar Res* **20**: 177–184.
- Schloss PD, Westcott SL, Ryabin T, Hall JR, Hartmann M, Hollister EB *et al.* (2009). Introducing mothur: open-source, platform-independent, community-supported software for describing and comparing microbial communities. *Appl Environ Microbiol* **75**: 7537–7541.
- Simon Q, St-Onge G, Hillaire-Marcel C. (2012). Late Quaternary chronostratigraphic framework of deep Baffin Bay glaciomarine sediments from high-resolution paleomagnetic data. *Geochem Geophys Geosy* **13**: Q0A003.

- Sul WJ, Oliver TA, Ducklow HW, Amaral-Zettler LA, Sogin ML. (2013). Marine bacteria exhibit a bipolar distribution. *Proc Natl Acad Sci USA* **110**: 2342–2347.
- Tang CCL, Ross CK, Yao T, Petrie B, DeTracey BM, Dunlap E. (2004). The circulation, water masses and sea-ice of Baffin Bay. *Prog Oceanogr* **63**: 183–228.
- Teixeira S, Cambon-Bonavita M-A, Serrão EA, Desbruyères D, Arnaud-Haond S. (2011). Recent population expansion and connectivity in the hydrothermal shrimp *Rimicaris exoculata* along the Mid-Atlantic Ridge. *J Biogeogr* **38**: 564–574.
- Vandieken V, Knoblauch C, Jørgensen BB. (2006). *Desulfotomaculum arcticum* sp. nov., a novel spore-forming, moderately thermophilic, sulfate-reducing bacterium isolated from a permanently cold fjord sediment of Svalbard. *Int J Syst Evol Microbiol* **56**: 687–690.
- Vrijenhoek RC. (2010). Genetic diversity and connectivity of deep-sea hydrothermal vent metapopulations. *Mol Ecol* **19**: 4391–4411.
- Wessel P, Smith WHF. (1998). New, improved version of generic mapping tools released. *Eos* **79**: 579–579.
- Whitaker RJ, Grogan DW, Taylor JW. (2003). Geographic barriers isolate endemic populations of hyperthermophilic archaea. *Science* **301**: 976–978.



This work is licensed under a Creative Commons Attribution-NonCommercial-NoDerivs 3.0 Unported License. To view a copy of this license, visit <http://creativecommons.org/licenses/by-nc-nd/3.0/>

Supplementary Information accompanies this paper on The ISME Journal website (<http://www.nature.com/ismej>)

Supplementary Information

Supplementary Materials and Methods

Alpha and beta diversity

Alpha diversity metrics (observed phylotype richness, Chao1 richness, Shannon index, equitability index, and Simpson index), sampling coverage, and principal coordinates analysis of samples based on weighted UniFrac distances (Lozupone & Knight, 2005) were calculated using QIIME (Caporaso *et al.*, 2010) with re-sampling (bootstrapping and jackknifing: 1000 re-samples) at 800 reads to avoid sample size based artifacts (Lozupone *et al.*, 2011).

Environmental distribution of putative thermophilic endospore phylotypes

The Short Read Archive (SRA) database (Kodama *et al.*, 2012) was screened (May 2013) for metagenomic datasets containing 16S rRNA gene sequences obtained by PCR amplification and sequencing using the 454 platform. 226 amplicon metagenome files were downloaded and the sequences contained in them were extracted using fastq-dump (part of SRA tools freely available in SRA site) into environmental categories according to the NCBI taxonomic classification of their environmental origin (46 metagenomic categories). In addition, all datasets of the VAMPS database (<http://vamps.mbl.edu>) spanning variable regions V4 to V6 were downloaded (May 2013). Finally, using makeblastdb (available in the NCBI BLAST stand-alone distributions) those files were formatted into databases containing a total of 36,178,644 sequences. Since these datasets contain short amplicon sequences of different regions of the 16S rRNA gene, the use of representative thermospore phylotype sequences as BLAST queries only yield results in the subset database sequences from the same region. Thus to simultaneously access all datasets for the presence of thermospore phylotypes, we used proxy sequences of almost full length (>1400 nt) as queries. Proxy sequences were selected by BLAST searching [(Altschul *et al.*, 1990) megablast default options] representative sequences of thermospore phylotypes against the NCBI nucleotide database (Wheeler *et al.*, 2008) to identify, whenever possible, the closest, near full-length 16S rRNA sequences. Full-length sequences were only considered proxies of thermospore phylotypes if they shared more than 97% sequence identity across more than 80% of the query length. The BLAST hits for each proxy were quality filtered (longer than 300 nt with more than 97% identity across more than 80% of the amplicon length) and the results were normalized as relative abundance of the obtained sequences compared to the total number of sequences (longer than 300 nt) for each dataset. In addition, the L4-DeepSeq dataset (containing ~10 million 16S rRNA V6 reads from a deeply sequenced site in the English Channel) (Gibbons *et al.*, 2013) was downloaded from the European Nucleotide Archive (ENA accession: [PRJEB3249](https://www.ebi.ac.uk/ena/record/PRJEB3249)) and formatted to a database as described above. The full-length proxies of the thermospore phylotypes were then used as BLAST queries. Positive hits (>30 nt, ≥97% similarity, ≥80% coverage) were normalized against the 10,786,733 sequences longer than 30 nt in this dataset.

Supplementary Results and Discussion

Detecting thermophilic endospores as indicators for passive dispersal in the ocean

Direct identification of thermophilic endospores by DNA-based molecular methods is hampered by difficulties in (i) efficient DNA extraction from low abundant spores in marine sediments and (ii) distinguishing DNA from spores and vegetative cells in environmental nucleic acids extracts. Hence, an alternative means to identify thermophilic endospores is to record significant changes in community structure that are due to endospore germination and growth in incubations of pasteurized sediments at high temperature. We initially evaluated different incubation conditions and times (56 h, 72 h, and 120 h) to increase the recovery of thermospore phylotypes from sediments of Svalbard stations J and A, and/or Aarhus Bay station M5. The temperature was set to 50°C because previous studies have shown that maximal thermophilic sulfate reduction rates and numbers of endospore-forming, sulfate-reducing *Desulfotomaculum* phylotypes were obtained at incubation temperatures of about 50°C (de Rezende *et al.*, 2013; Hubert *et al.*, 2009). Amendment of sediment incubations with a mixture of formate, lactate, acetate, succinate, propionate, butyrate, and ethanol and/or freeze-dried *Spirulina* cells considerably increased the number of detected thermospore phylotypes compared to incubations without supplemental organic compounds (Supplementary Figure S1A). To confirm that *Spirulina* cells were free of viable thermophiles, they were incubated under the same conditions as the sediment samples and no growth/enrichment was observed. While there were some differences in the identity of the phylotypes detected after different incubation times, more thermospore phylotypes were detected after longer incubation (Supplementary Figure S1B) and thus all subsequent incubations were performed for 120 h. While still not all thermophilic endospores may germinate and grow under these incubation conditions, the amendment of incubations with organic compounds has a normalizing effect on endospore recovery by providing similar germination conditions in all sediments and thus allows comparative analysis of spore phylotype richness between different locations. Surveys of 16S rRNA gene sequence diversity are commonly used for studies of microbial biogeography (Chu *et al.*, 2010; Fierer *et al.*, 2009; Galand *et al.*, 2010; Horner-Devine *et al.*, 2004; Martiny *et al.*, 2011; Nemergut *et al.*, 2011), although the phylogenetic resolution of the 16S rRNA gene is limited to species-level phylotypes or higher order taxa and some microbial biogeography patterns only become apparent at the strain-level (Cho & Tiedje, 2000; García-Martínez & Rodríguez-Valera, 2000; Miller *et al.*, 2006; Papke *et al.*, 2003; Silva *et al.*, 2005; Whitaker *et al.*, 2003). Despite this acknowledged caveat, we used 16S rRNA as phylogenetic marker for our study also because the high sequence conservation renders this gene particularly advantageous for selective analysis of passive dispersal. Mutations in the 16S rRNA gene due to genetic drift are less likely to occur compared to mutations in other, more variable genetic markers.

Potential physiology of thermospore phylotypes

Previous analyses have shown that anoxic high temperature incubation resuscitates a diverse community of dormant *Firmicutes* that collectively catalyze the interdependent series of organic carbon degradation transformations i.e. hydrolysis, fermentation, and mineralization through sulfate respiration (Hubert *et al.*, 2010). The majority of thermospore phylotypes identified in this study belong to the class *Clostridia* (Supplementary Table S3, Supplementary Figure S3). *Clostridia* are anaerobic microorganisms that can ferment a wide range of organic compounds and produce a variety of metabolites (reviewed in Tracy *et al.*, 2012). In addition, they produce extracellular

enzymes to degrade large biological molecules into fermentable components. Thermospore phylotypes with $\geq 97\%$ 16S rRNA sequence similarity to e.g. *Anaerosalibacter bizertensis*, *Brassicibacter mesophilus*, *Caloranaerobacter azorensis*, *Clostridium* spp., *Sporosalibacterium faouarens* (Supplementary Table S3) were thus likely involved in hydrolysis and fermentation (Fang *et al.*, 2012; Rezgui *et al.*, 2011; Wery *et al.*, 2001; Wiegel *et al.*, 1989) of complex substrates present in the sediments and the supplied *Spirulina* cells. In contrast, thermospore phylotypes related to known sulfate reducers of the genus *Desulfotomaculum* (Fardeau *et al.*, 1995) and the iron reducer *Tepidimicrobium ferriphilum* (Slobodkin *et al.*, 2006) probably used the amended organic compounds and products from primary fermenters as electron donors for thermophilic reduction of sulfate and iron, respectively, in the anoxic, high-temperature incubations. Thermospore phylotypes belonging to the class *Bacilli* were mostly related to facultative (e.g. *Anoxybacillus flavithermus*, *Bacillus azotoformans*, *B. licheniformis*, *B. thermoamylovorans*, *B. thermolactis*, *Geobacillus thermoglucosidasius*, *Microaerobacter geothermalis*, *Virgibacillus proomii*) and obligate anaerobes (e.g. *Anaerobacillus alkalilustre*, *Bacillus infernus*, *Vulcanibacillus modesticaldus*) (Supplementary Table S3). The metabolic capabilities of these *Bacilli*-related phylotypes are presumably as diverse as those of their next cultivated relatives, which are capable of hydrolysis, fermentation, and/or anaerobic respiration with nitrate, iron, manganese or arsenate as electron acceptors (Boone *et al.*, 1995; Khelifi *et al.*, 2010; L'Haridon *et al.*, 2006; Voigt *et al.*, 2006; Zavarzina *et al.*, 2009).

Sequences belonging to thermophilic endospore-forming phylotypes are rare in available 16S rRNA sequence datasets

In order to gain insights into the general environmental distribution of thermospore phylotypes, we screened all available 16S rRNA amplicon datasets (that were deposited until May 2013 in the SRA database) for the presence of sequences with $\geq 97\%$ similarity to near full-length proxy sequences of thermospore phylotypes. The use of proxy sequences was necessary because different amplicon sequencing studies targeted different regions of the 16S rRNA gene. We obtained suitable proxy full-length sequences (>1400 nt, $\geq 97\%$ similarity, $>80\%$ coverage) for 78 of 146 thermospore phylotypes. Of over 36 million sequences analyzed in total only 0.005% were closely affiliated with thermospore phylotypes (Supplementary Table S4). Surprisingly, most of these hits were obtained with sequences from bioreactors and intestinal microbiomes. While these anoxic environments support presence of similar but not necessarily thermophilic bacteria, they are unlikely major sources of marine thermophilic endospores. In the datasets from marine environments (i.e., sediments, surface water, sponges, fish, hydrothermal vents, cold-seeps), sequences affiliated with thermospore phylotypes were only present at a very low relative abundance of 0.0003% ($n=363/1,132,627$). 93% of these hits ($n=338/363$) were derived from proxies of the cosmopolitan thermospore phylotypes TSP003, TSP005, TSP007, TSP010, TSP013, TSP016, TSP0017 or TSP021. We also analyzed the very deeply sequenced L4-DeepSeq dataset from the English Channel (Gibbons *et al.*, 2013) and found that only 213 of 10,786,733 reads longer than 30 nt showed $\geq 97\%$ similarity to 14 of our TSP proxy sequences. Under the premise that abundances of inactive spores will be underestimated in nucleic acids-based diversity surveys, the low prevalence of sequences affiliated with thermospore phylotypes in marine environments suggests that thermophilic spores are members of the rare biosphere in the oceans (Hubert *et al.*, 2009).

Guaymas Basin sediments exhibit characteristics of a source environment for thermophilic endospores

The Guaymas Basin spreading center is the largest in the Gulf of California and harbors a unique hydrothermal vent system at a water depth of about 2000 m (Weber & Jørgensen, 2002). Unlike other deep-sea vent sites, the hydrothermal fluids in this basin are driven by deeply buried magmatic intrusions and rise up to the surface through a sediment cover that has a mean thickness of >100 m (Curry *et al.*, 1982; Fisher & Becker, 1991). Hydrothermal fluid flow supplies oil compounds (Didyk & Simoneit, 1989), methane, and small organic compounds to the anaerobic microbial communities close to the sediment surface. These hydrothermal sediments are anoxic and temperatures at the hot spots increase rapidly with depth from 3°C to above 100°C within the uppermost 30-40 cm and thus provide ideal environments for a variety of anaerobic thermophiles (Martens, 1990; Meyer *et al.*, 2013). Consequently, organisms related to sulfate-reducing *Desulfotomaculum* spp. (*Clostridiales*) (Dhillon *et al.*, 2003; Kniemeyer *et al.*, 2007) (which could contribute to the high thermophilic sulfate reduction rates measured in situ (Weber & Jørgensen, 2002)), members of the genus *Bacillus* (*Bacillales*) (Dick *et al.*, 2006; Marteinsson *et al.*, 1996), and other thermophilic, endospore-forming bacteria were previously detected in these sediments (Biddle *et al.*, 2012; Lakhal *et al.*, 2013; Phelps *et al.*, 1998). The considerable flux of hydrothermal fluids emanating from hydrothermal mounds, chimneys and sediments (Campbell & Gieskes, 1984) could expel large amounts of thermophilic spores into the water column.

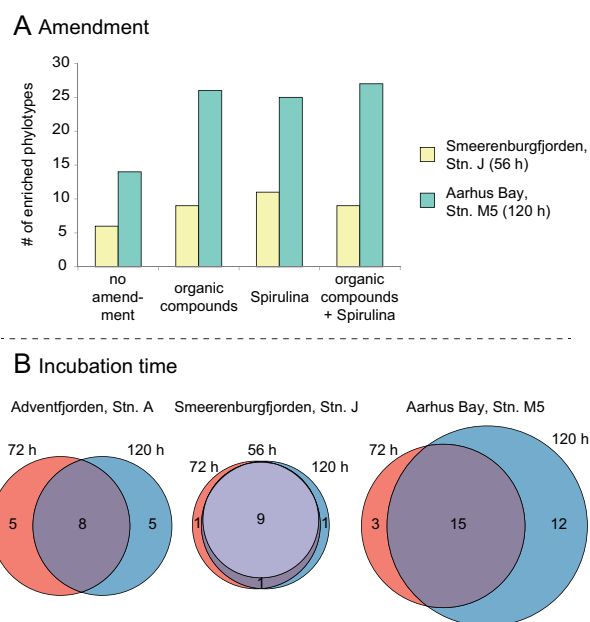
References

- Altschul SF, Gish W, Miller W, Myers EW, Lipman DJ. (1990). Basic Local Alignment Search Tool. *J Mol Biol* **215**: 403-410.
- Biddle JF, Cardman Z, Mendlovitz H, Albert DB, Lloyd KG, Boetius A *et al.*. (2012). Anaerobic oxidation of methane at different temperature regimes in Guaymas Basin hydrothermal sediments. *ISME J* **6**: 1018-1031.
- Boone DR, Liu Y, Zhao Z-J, Balkwill DL, Drake GR, Stevens TO *et al.*. (1995). *Bacillus infernus* sp. nov., an Fe(III)- and Mn(IV)-Reducing Anaerobe from the Deep Terrestrial Subsurface. *Int J Syst Evol Microbiol* **45**: 441-448.
- Campbell AC, Gieskes JM. (1984). Water column anomalies associated with hydrothermal activity in the Guaymas Basin, Gulf of California. *Earth Planet Sc Lett* **68**: 57-72.
- Caporaso JG, Kuczynski J, Stombaugh J, Bittinger K, Bushman FD, Costello EK *et al.*. (2010). QIIME allows analysis of high-throughput community sequencing data. *Nat Methods* **7**: 335-336.
- Cho J-C, Tiedje JM. (2000). Biogeography and degree of endemism of fluorescent *Pseudomonas* strains in soil. *Appl Environ Microbiol* **66**: 5448-5456.
- Chu H, Fierer N, Lauber CL, Caporaso JG, Knight R, Grogan P. (2010). Soil bacterial diversity in the Arctic is not fundamentally different from that found in other biomes. *Environ Microbiol* **12**: 2998-3006.
- Curry J, Moore D, Aguayo J, Aubry M, Einsele G, Fornari D *et al.*. (1982). *Initial Rep Deep Sea, Parts I and II, US Govt Printing Office*: 1314pp.
- de Rezende JR, Kjeldsen KU, Hubert CR, Finster K, Loy A, Jørgensen BB. (2013). Dispersal of thermophilic *Desulfotomaculum* endospores into Baltic Sea sediments over thousands of years. *ISME J* **7**: 72-84.

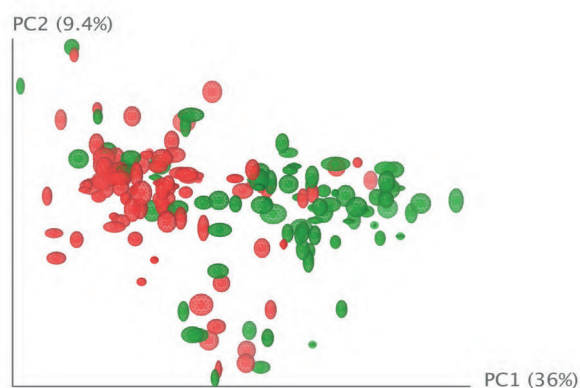
- Dhillon A, Teske A, Dillon J, Stahl DA, Sogin ML. (2003). Molecular characterization of sulfate-reducing bacteria in the Guaymas Basin. *Appl Environ Microbiol* **69**: 2765-2772.
- Dick GJ, Lee YE, Tebo BM. (2006). Manganese(II)-oxidizing *Bacillus* spores in Guaymas Basin hydrothermal sediments and plumes. *Appl Environ Microbiol* **72**: 3184-3190.
- Didyk BM, Simoneit BRT. (1989). Hydrothermal oil of Guaymas Basin and implications for petroleum formation mechanisms. *Nature* **342**: 65-69.
- Fang M-X, Zhang W-W, Zhang Y-Z, Tan H-Q, Zhang X-Q, Wu M *et al.*. (2012). *Brassicibacter mesophilus* gen. nov., sp. nov., a strictly anaerobic bacterium isolated from food industry wastewater. *Int J Syst Evol Microbiol* **62**: 3018-3023.
- Fardeau M-L, Ollivier B, Patel BKC, Dwivedi P, Ragot M, Garcia J-L. (1995). Isolation and Characterization of a Thermophilic Sulfate-Reducing Bacterium, *Desulfotomaculum thermosapovorans* sp. nov. *Int J Syst Bacteriol* **45**: 218-221.
- Fierer N, Carney KM, Horner-Devine MC, Megonigal JP. (2009). The biogeography of ammonia-oxidizing bacterial communities in soil. *Microb Ecol* **58**: 435-445.
- Fisher AT, Becker K. (1991). Heat flow, hydrothermal circulation and basalt intrusions in the Guaymas Basin, Gulf of California. *Earth Planet Sc Lett* **103**: 84-99.
- Galand PE, Potvin M, Casamayor EO, Lovejoy C. (2010). Hydrography shapes bacterial biogeography of the deep Arctic Ocean. *ISME J* **4**: 564-576.
- García-Martínez J, Rodríguez-Valera F. (2000). Microdiversity of uncultured marine prokaryotes: the SAR11 cluster and the marine Archaea of Group I. *Mol Ecol* **9**: 935-948.
- Gibbons SM, Caporaso JG, Pirrung M, Field D, Knight R, Gilbert JA. (2013). Evidence for a persistent microbial seed bank throughout the global ocean. *Proc Natl Acad Sci U S A* **110**: 4651-4655.
- Horner-Devine MC, Lage M, Hughes JB, Bohannan BJM. (2004). A taxa-area relationship for bacteria. *Nature* **432**: 750-753.
- Hubert C, Loy A, Nickel M, Arnosti C, Baranyi C, Bruchert V *et al.*. (2009). A Constant Flux of Diverse Thermophilic Bacteria into the Cold Arctic Seabed. *Science* **325**: 1541-1544.
- Hubert C, Arnosti C, Bruchert V, Loy A, Vandieken V, Jorgensen BB. (2010). Thermophilic anaerobes in Arctic marine sediments induced to mineralize complex organic matter at high temperature. *Environ Microbiol* **12**: 1089-1104.
- Khelifi N, Ben Romdhane E, Hedi A, Postec A, Fardeau M-L, Hamdi M *et al.*. (2010). Characterization of *Microaerobacter geothermalis* gen. nov., sp. nov., a novel microaerophilic, nitrate- and nitrite-reducing thermophilic bacterium isolated from a terrestrial hot spring in Tunisia. *Extremophiles* **14**: 297-304.
- Kniemeyer O, Musat F, Sievert SM, Knittel K, Wilkes H, Blumenberg M *et al.*. (2007). Anaerobic oxidation of short-chain hydrocarbons by marine sulphate-reducing bacteria. *Nature* **449**: 898-901.
- Kodama Y, Shumway M, Leinonen R, C INSD. (2012). The sequence read archive: explosive growth of sequencing data. *Nucleic Acids Res* **40**: D54-D56.
- L'Haridon S, Miroshnichenko ML, Kostrikina NA, Tindall BJ, Spring S, Schumann P *et al.*. (2006). *Vulcanibacillus modesticaldus* gen. nov., sp. nov., a strictly anaerobic, nitrate-reducing bacterium from deep-sea hydrothermal vents. *Int J Syst Evol Microbiol* **56**: 1047-1053.
- Lakhal R, Pradel N, Postec A, Hamdi M, Ollivier B, Godfroy A *et al.*. (2013). Characterization of *Vallitalea guaymasensis* gen. nov., sp. nov., a novel marine bacterium, isolated from sediments of Guaymas basin. *Int J Syst Evol Microbiol*.

- Lozupone C, Knight R. (2005). UniFrac: a new phylogenetic method for comparing microbial communities. *Appl Environ Microbiol* **71**: 8228-8235.
- Lozupone C, Lladser ME, Knights D, Stombaugh J, Knight R. (2011). UniFrac: an effective distance metric for microbial community comparison. *ISME J* **5**: 169-172.
- Marteinsson V, Birrien J-L, Jeanthon C, Prieur D. (1996). Numerical taxonomic study of thermophilic *Bacillus* isolated from three geographically separated deep-sea hydrothermal vents. *FEMS Microbiol Ecol* **21**: 255-266.
- Martens CS. (1990). Generation of short chain acid anions in hydrothermally altered sediments of the Guaymas Basin, Gulf of California. *Appl Geoch* **5**: 71-76.
- Martiny JB, Eisen JA, Penn K, Allison SD, Horner-Devine MC. (2011). Drivers of bacterial beta-diversity depend on spatial scale. *Proc Natl Acad Sci U S A* **108**: 7850-7854.
- Meyer S, Wegener G, Lloyd KG, Teske A, Boetius A, Ramette A. (2013). Microbial habitat connectivity across spatial scales and hydrothermal temperature gradients at Guaymas Basin. *Front Microbiol* **4**.
- Miller SR, Purugganan MD, Curtis SE. (2006). Molecular population genetics and phenotypic diversification of two populations of the thermophilic cyanobacterium *Mastigocladus laminosus*. *Appl Environ Microbiol* **72**: 2793-2800.
- Nemergut DR, Costello EK, Hamady M, Lozupone C, Jiang L, Schmidt SK *et al.* (2011). Global patterns in the biogeography of bacterial taxa. *Environ Microbiol* **13**: 135-144.
- Papke RT, Ramsing NB, Bateson MM, Ward DM. (2003). Geographical isolation in hot spring cyanobacteria. *Environ Microbiol* **5**: 650-659.
- Phelps CD, Kerkhof LJ, Young LY. (1998). Molecular characterization of a sulfate-reducing consortium which mineralizes benzene. *FEMS Microbiol Ecol* **27**: 269-279.
- Rezgui R, Ben Ali Gam Z, Ben Hamed S, Fardeau M-L, Cayol J-L, Maaroufi A *et al.* (2011). *Sporosolibacterium faouarensense* gen. nov., sp. nov., a moderately halophilic bacterium isolated from oil-contaminated soil. *Int J Syst Evol Microbiol* **61**: 99-104.
- Silva C, Vinuesa P, Eguiarte LE, Souza V, MARTÍNEZ-ROMERO E. (2005). Evolutionary genetics and biogeographic structure of *Rhizobium gallicum sensu lato*, a widely distributed bacterial symbiont of diverse legumes. *Mol Ecol* **14**: 4033-4050.
- Slobodkin AI, Tourova TP, Kostrikin NA, Lysenko AM, German KE, Bonch-Osmolovskaya EA *et al.* (2006). *Tepidimicrobium ferriphilum* gen. nov., sp. nov., a novel moderately thermophilic, Fe(III)-reducing bacterium of the order Clostridiales. *Int J Syst Evol Microbiol* **56**: 369-372.
- Tracy BP, Jones SW, Fast AG, Indurthi DC, Papoutsakis ET. (2012). Clostridia: the importance of their exceptional substrate and metabolite diversity for biofuel and biorefinery applications. *Curr Opin Biotechnol* **23**: 364-381.
- Voigt B, Schweder T, Sibbald MJB, Albrecht D, Ehrenreich A, Bernhardt J *et al.* (2006). The extracellular proteome of *Bacillus licheniformis* grown in different media and under different nutrient starvation conditions. *Proteomics* **6**: 268-281.
- Weber A, Jørgensen BB. (2002). Bacterial sulfate reduction in hydrothermal sediments of the Guaymas Basin, Gulf of California, Mexico. *Deep-Sea Res Part I: Oceanographic Research Papers* **49**: 827-841.
- Wery N, Moricet JM, Cueff V, Jean J, Pignet P, Lesongeur F *et al.* (2001). *Caloranaerobacter azorensis* gen. nov., sp. nov., an anaerobic thermophilic bacterium isolated from a deep-sea hydrothermal vent. *Int J Syst Evol Microbiol* **51**: 1789-1796.

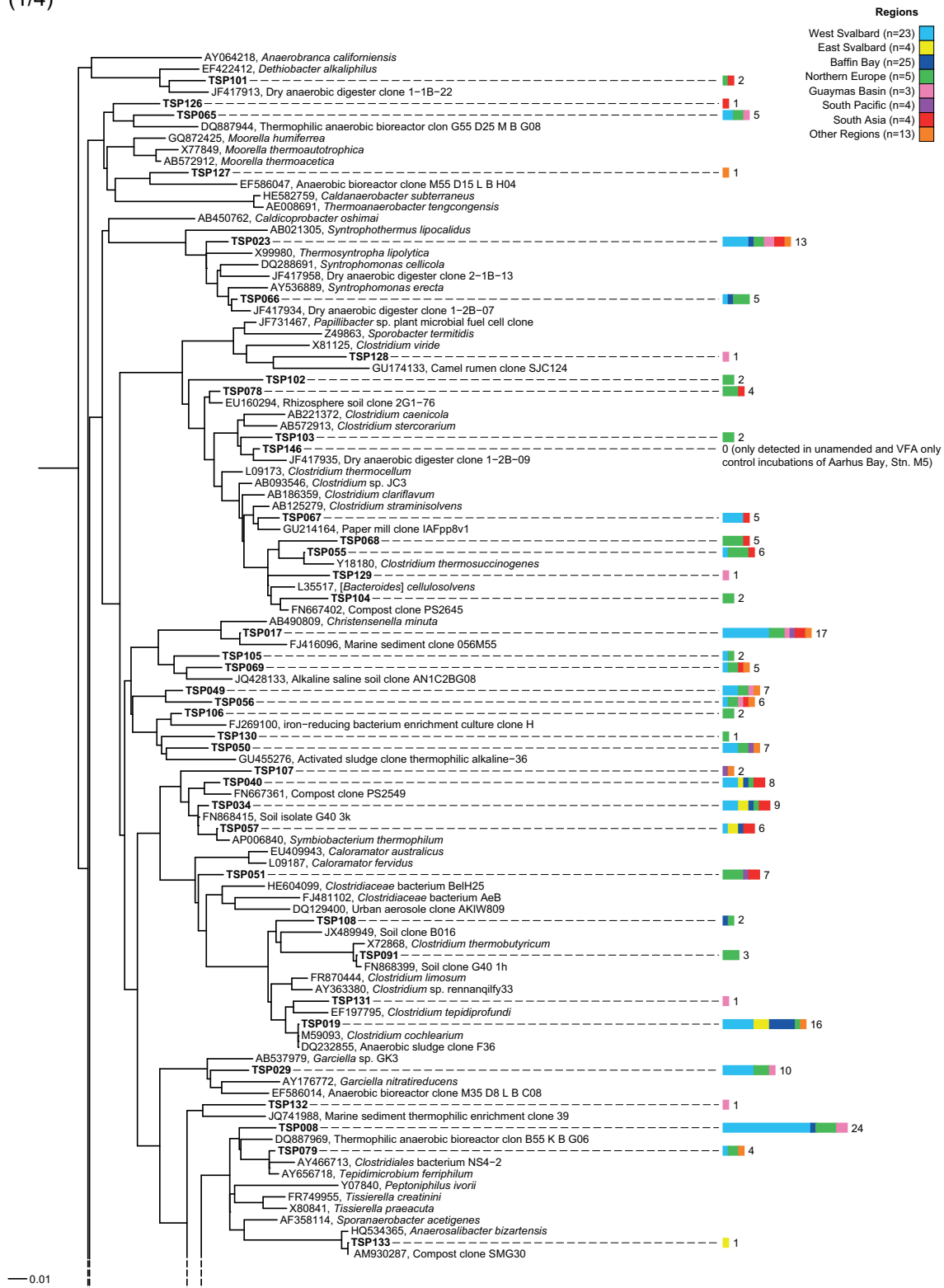
- Wheeler DL, Barrett T, Benson DA, Bryant SH, Canese K, Chetvernin V *et al.*. (2008). Database resources of the national center for biotechnology information. *Nucleic Acids Res* **36**: D13-D21.
- Whitaker RJ, Grogan DW, Taylor JW. (2003). Geographic barriers isolate endemic populations of hyperthermophilic archaea. *Science* **301**: 976-978.
- Wiegel J, Kuk S-U, Kohring GW. (1989). *Clostridium thermobutyricum* sp. nov., a Moderate Thermophile Isolated from a Cellulolytic Culture, That Produces Butyrate as the Major Product. *Int J Syst Bacteriol* **39**: 199-204.
- Zavarzina D, Tourova T, Kolganova T, Boulygina E, Zhilina T. (2009). Description of *Anaerobacillus alkalilacustre* gen. nov., sp. nov.—Strictly anaerobic diazotrophic bacillus isolated from soda lake and transfer of *Bacillus arseniciselenatis*, *Bacillus macyae*, and *Bacillus alkalidiazotrophicus* to *Anaerobacillus* as the new combinations *A. arseniciselenatis* comb. nov., *A. macyae* comb. nov., and *A. alkalidiazotrophicus* comb. nov. *Microbiology* **78**: 723-731.

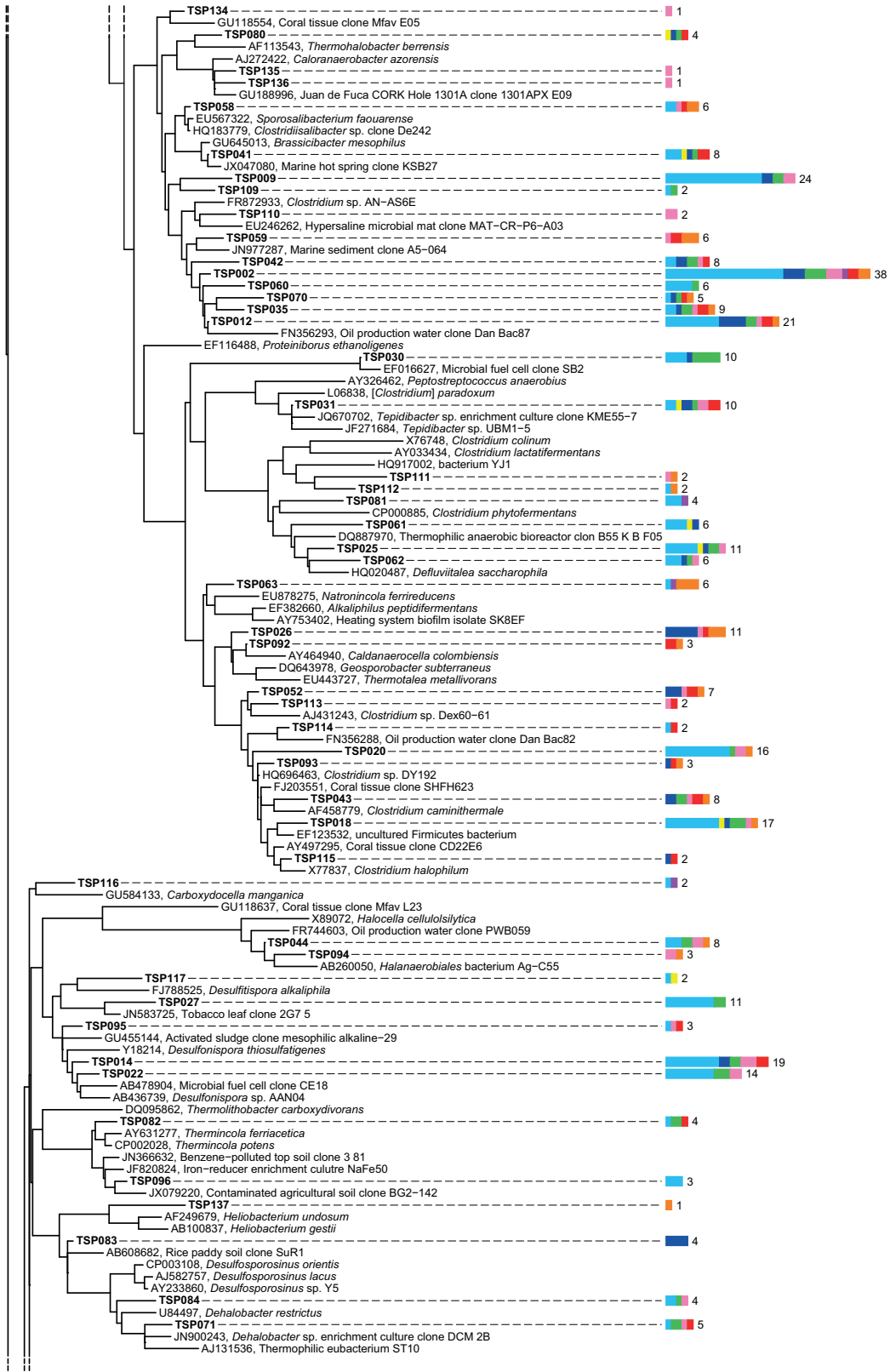


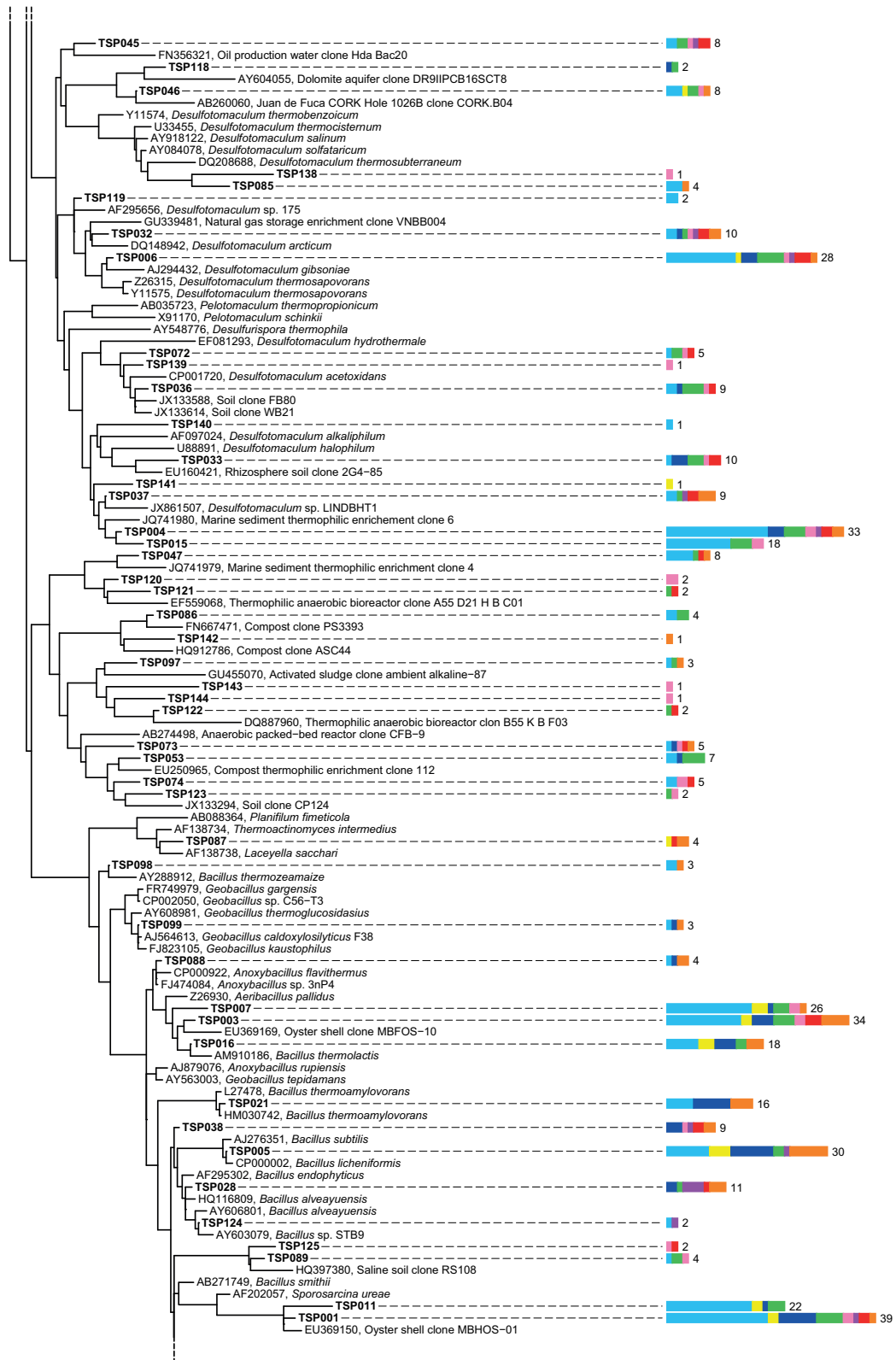
Supplementary Figure S1. Maximizing detection of thermophile spores. Impact of different incubation conditions (A, amendment type; B, incubation time) on the number of thermospore phylotypes detected during germination experiments.



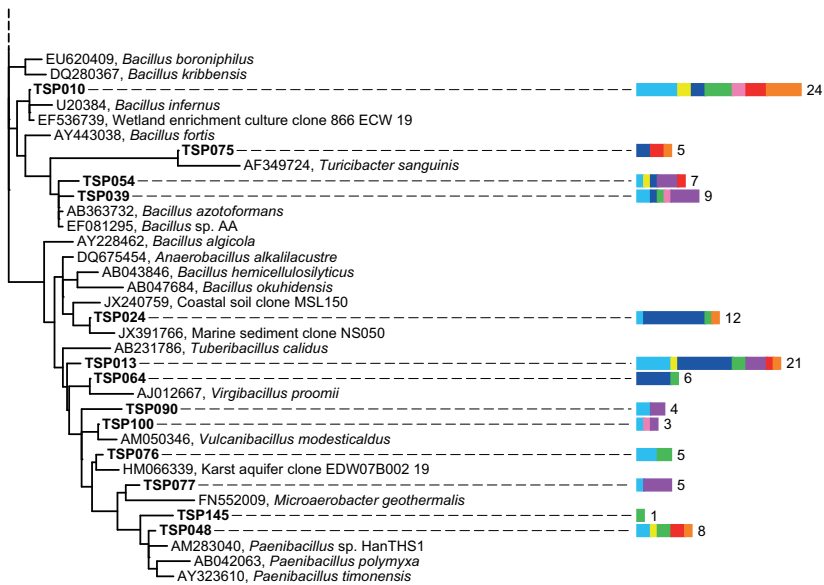
Supplementary Figure S2. Beta-diversity analysis (PCoA of weighted UniFrac distances) of bacterial communities before and after incubation of pasteurized marine sediments at 50°C. Analysis was performed at 800 reads per library. Sphere sizes and shapes indicate 95% confidence intervals based on 1000 re-samplings. Red spheres indicate starting samples (T=0 h) and green spheres indicate after incubation (T=120 h).

Supplementary Figure S3
(1/4)

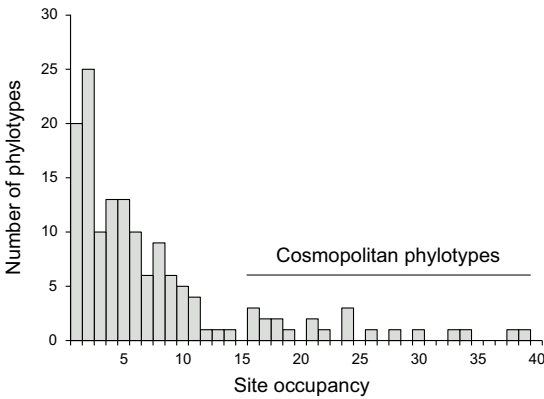
Supplementary Figure S3
(2/4)

Supplementary Figure S3
(3/4)

Supplementary Figure S3
(4/4)

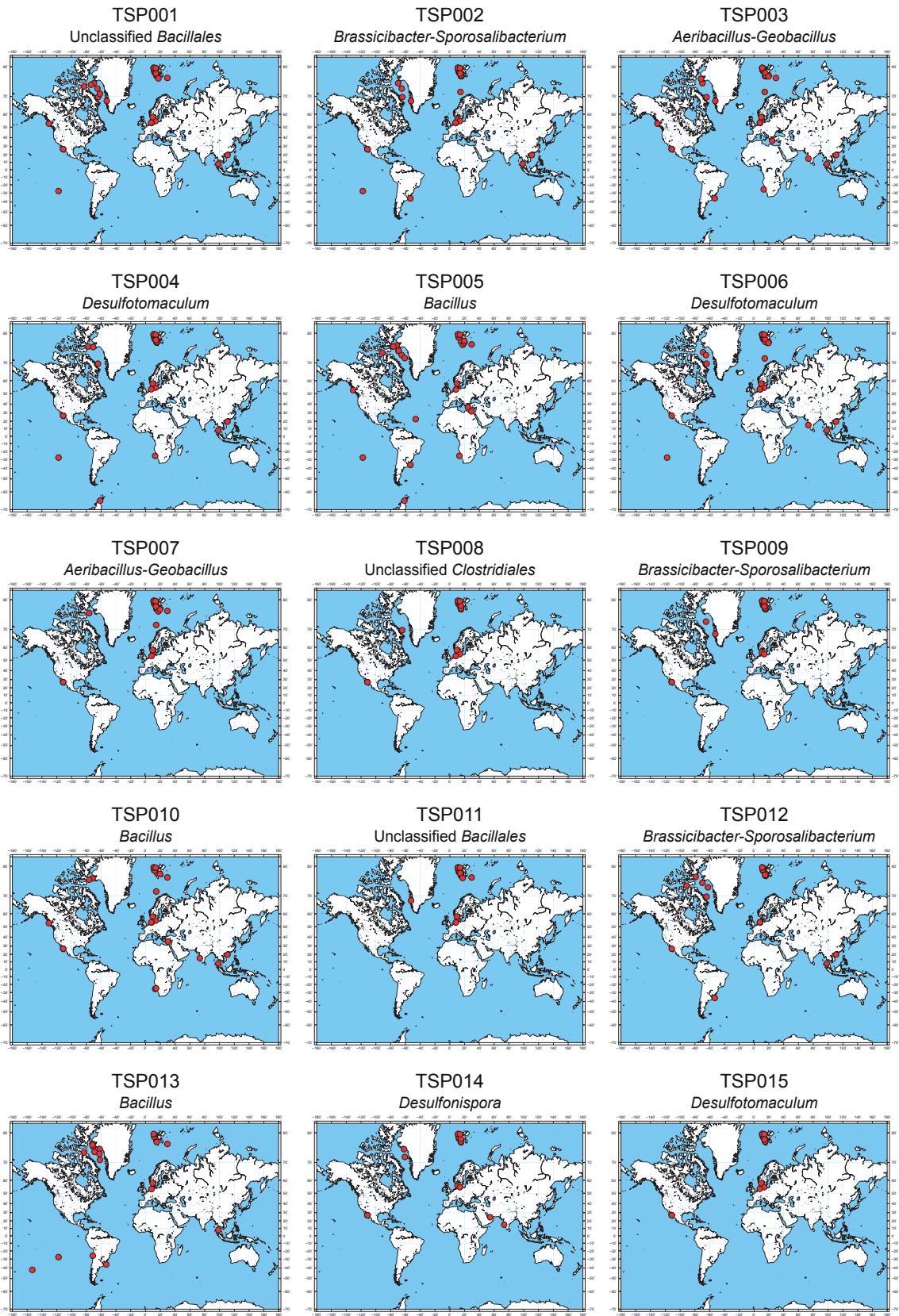


Supplementary Figure S3. Phylogeny and geographic distribution of all 146 *Firmicutes* thermospore phylotypes. Scale bar indicates 1% sequence divergence as inferred from RAXML. Colored bars indicate broad geographic regions where the thermospore phylotypes were present. Numbers indicate the number of sites at which a thermospore phylotype was detected.

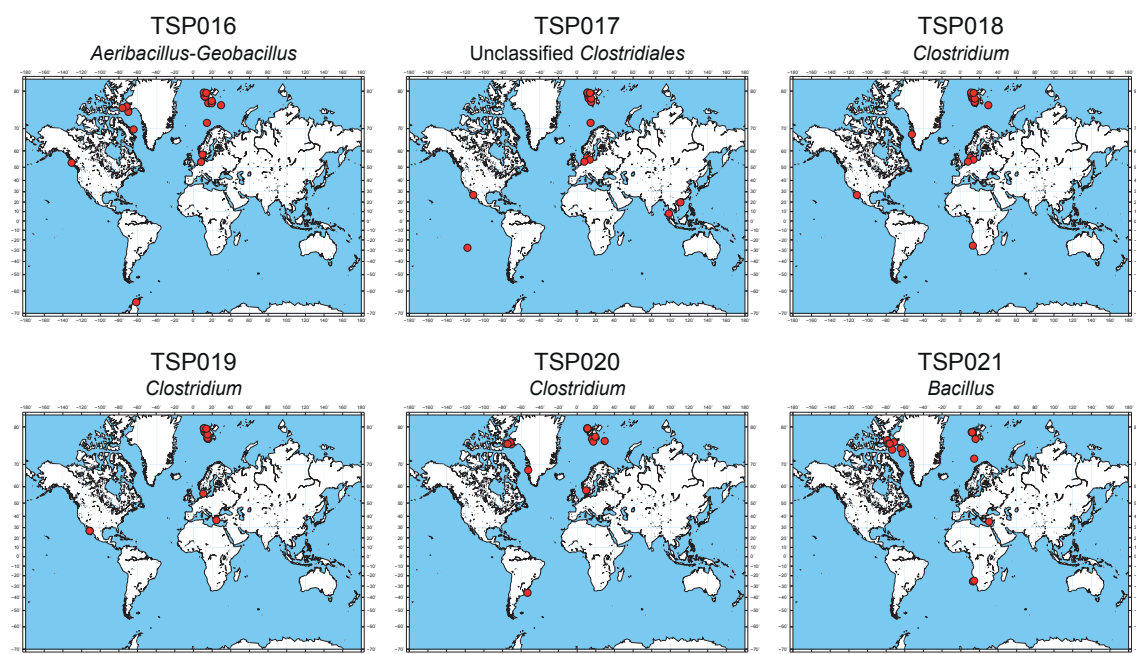


Supplementary Figure S4. Site occupancy of thermophilic endospore phylotypes. Graph shows the number of phylotypes versus the number of sites at which each phylotype was detected. The majority of the 146 thermospore phylotypes is present at 5 sites or less, while 21 phylotypes were present at 15 or more locations (arbitrarily designated as 'cosmopolitan phylotypes').

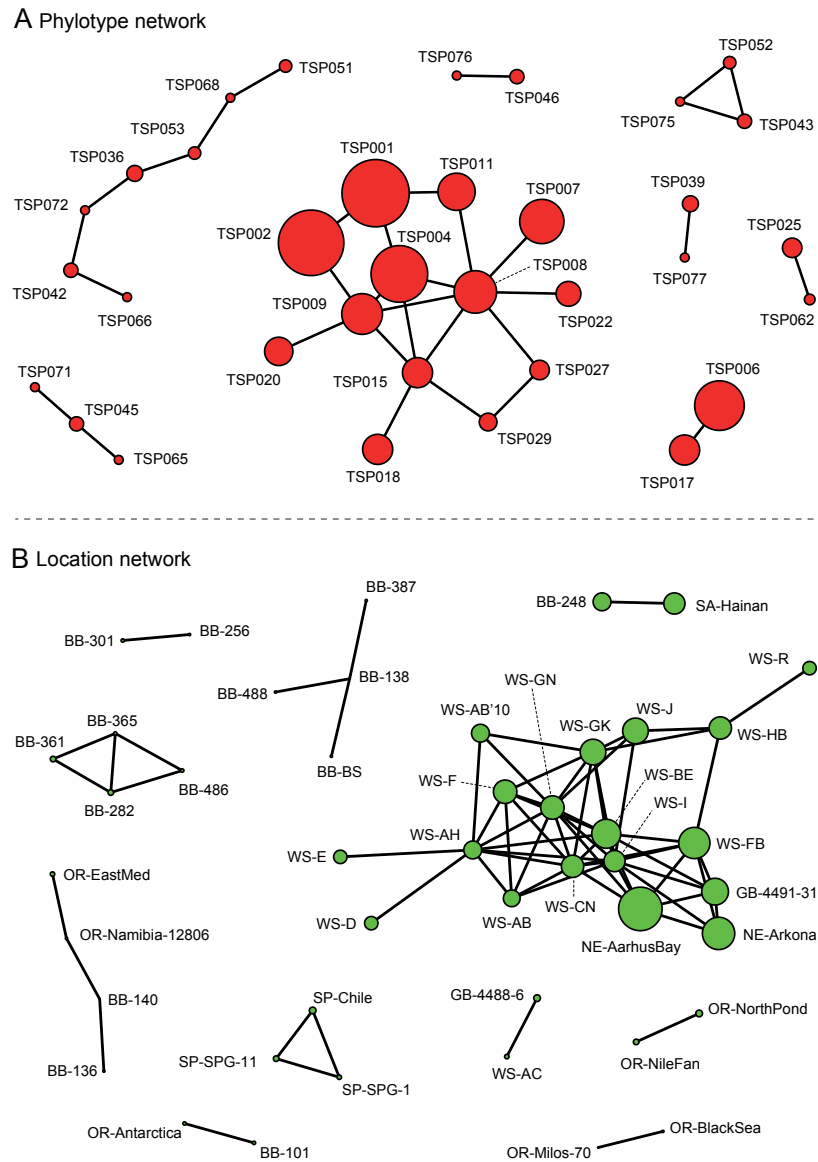
Supplementary Figure S5
(1/2)



Supplementary Figure S5
(2/2)



Supplementary Figure S5. Geographic distribution of each cosmopolitan thermospore phylotype. Red circles show the locations where a phylotype was detected.



Supplementary Figure S6. Network analysis of thermophile spore co-occurrence **(A)** and location **(B)**. **A**, Networks of co-occurring thermospore phylotypes. Each node represents a thermospore phylotype. Presence of an edge between two nodes shows a strong correlation between these two phylotypes, which is indicative for co-occurrence. Circle size indicates site occupancy. **B**, Location networks. Each node represents a location, presence of an edge between two nodes corresponds to a high Bray Curtis similarity (≥ 0.6) between the endospore communities at these two locations. Circle size indicates thermospore phylotype richness.

Supplementary Tables S1-S4 are not included in the print/pdf version of this thesis due to size and formatting constraints. However, they are available online under following links:

Table S1. Marine sediment sample description, sediment incubation conditions, thermospore phylotype richness, and thermophilic sulfate reduction rates.

<http://www.nature.com/ismej/journal/v8/n6/extref/ismej2013225x2.xls>

Table S2. Read number, coverage, and alpha-diversity of bacterial 16S rRNA gene sequence libraries of pasteurized marine sediments before and after incubation at 50°C.

<http://www.nature.com/ismej/journal/v8/n6/extref/ismej2013225x3.xls>

Table S3. Site occupancy, next relatives, presence/absence at sampling locations and representative 16S rRNA gene sequences of putative thermophilic *Firmicutes* endospore phylotypes

<http://www.nature.com/ismej/journal/v8/n6/extref/ismej2013225x4.xls>

Table S4. Prevalence of proxy sequences of thermospore phylotypes in publically available 16S rRNA amplicon pyrosequencing datasets from various environments.

<http://www.nature.com/ismej/journal/v8/n6/extref/ismej2013225x5.xls>

Chapter VI

**Activity and community structures of
sulfate-reducing microorganisms in polar,
temperate and tropical marine sediments**

Activity and community structures of sulfate-reducing microorganisms in polar, temperate and tropical marine sediments

Alberto Robador^{1,*}, Albert L. Müller², Joanna E. Sawicka³, David Berry², Casey Hubert⁴, Alexander Loy^{2,6}, Bo Barker Jørgensen⁵, Volker Brüchert³

¹Department of Biogeochemistry, Max Planck Institute for Marine Microbiology, Celsiusstr.1, 28359 Bremen, Germany; ²Department of Microbiology and Ecosystem Science, University of Vienna, Division of Microbial Ecology, Althanstr. 14, A-1090 Wien, Austria; ³Department of Geological Sciences and Bolin Centre for Climate Research, Stockholm University, 10691 Stockholm, Sweden; ⁴School of Civil Engineering and Geosciences, Newcastle University, Newcastle upon Tyne NE1 7RU UK; ⁵Department of Bioscience, Center for Geomicrobiology, Aarhus University, Ny Munkegade 116, 8000 Aarhus C, Denmark; ⁶Austrian Polar Research Institute, Vienna, Austria; *Present address: University of Southern California, Los Angeles 90089, USA

Temperature has a fundamental impact on the metabolic rates of microorganisms and strongly influences microbial ecology and biogeochemical cycling in the environment. In this study, we examined the thermal metabolic response of natural communities of sulfate-reducing microorganisms (SRM) in polar, temperate, and tropical marine sediments. In short-term sediment incubation experiments with ³⁵S-sulfate, we found that the temperature characteristics of sulfate reduction rates correlated with mean annual sediment temperatures, indicating specific thermal adaptations of the dominant SRM in each of the investigated ecosystems. The community structure of putative SRM in the sediments, as revealed by pyrosequencing of bacterial 16S rRNA gene amplicons and phylogenetic assignment to known SRM taxa, consistently correlated with *in situ* temperatures, but not with sediment organic carbon concentrations or C:N ratios of organic matter. Additionally, several species-level SRM phylotypes of the class *Deltaproteobacteria* tended to co-occur at sites with similar mean annual temperatures, regardless of geographic distance. The observed temperature adaptations of SRM imply that environmental temperature is the major controlling variable for physiological selection and ecological and evolutionary differentiation of microbial communities.

Introduction

Microorganisms in the natural environment cope with changing and sometimes hostile conditions that require a wide range of metabolic adaptations (Neidhardt *et al.*, 1990). Microorganisms that are physiologically best adapted to exploit prevailing physical, chemical and biological factors will predominate, which can lead to varying patterns of microbial diversity over different temporal and spatial scales (Prosser *et al.*, 2007). The convergence of ecological and evolutionary timescales is substantiated by the observation of biogeographic patterns in microbial diversity (Hanson *et al.*, 2012). For example, latitudinal gradients of microbial diversity associated to temperature have been observed in marine free-living microbial taxa (Fuhrman, 2009). However, it is not well known whether the same applies to microorganisms in benthic environments. The data

available on marine sediments is scarce and the correlation of the expression of microbial metabolism and co-occurrence of microbial taxa with environmental temperatures is largely unknown.

Over short, seasonal time scales, the rates of microbial sulfate reduction strongly correlate with changes in sediment temperature (Aller and Yingst, 1980; Jørgensen, 1977; Kristensen *et al.*, 2000; Moeslund *et al.*, 1994), indicating a response of the metabolic activity of the sulfate-reducing community to ambient temperatures. It has been observed that organic matter limitation has a regulating effect on the temperature dependence of sulfate reduction in marine sediments, as the availability of reactive organic matter becomes the overriding limiting factor (Kostka *et al.*, 1999; Sawicka *et al.*, 2012). However, recent studies support the notion that the thermal response of sulfate reduction is related to the metabolic

temperature adaptations of the individual sulfate-reducing microbial populations (Robador *et al.*, 2009; Sawicka *et al.*, 2012).

Studies on the temperature dependence of sulfate reduction in different climatic regions have shown that sulfate-reducing microorganisms (SRM) at high latitudes, i.e., in Arctic and Antarctic marine sediments, are predominantly psychrophilic (Isaksen and Jørgensen, 1996; Sagemann *et al.*, 1998), while SRM in temperate sediments at lower latitudes are mostly mesophilic (Isaksen *et al.*, 1994). Yet, the available phylogenetic data on sedimentary SRM communities (e.g. Leloup *et al.*, 2007; Leloup *et al.*, 2009; Ravensschlag *et al.*, 1999) has been insufficient to reveal diversity distribution patterns that would associate with different temperature regimes.

In this study, we explored how temperature controls the respiration rate of natural communities of SRM by means of short-term incubation experiments with ^{35}S -sulfate in a thermal gradient using sediment samples from a wide range of geographic regions that differ with respect to the prevailing temperature. Furthermore, we studied the *in situ* diversity of the corresponding SRM communities by analyzing bacterial 16S rRNA gene amplicon pyrosequencing libraries for the presence of sequences of known sulfate-reducing lineages. We found distinct patterns of metabolic

adaptations to environmental temperatures that coincided with the presence of specific SRM populations at sites with similar mean annual temperatures.

Material and Methods

Study sites

Marine sediment samples for the present work ranged from polar regions to temperate and tropical latitudes. Brief descriptions of the study sites are provided in Table 1. Samples were obtained from the upper 15 cm of sediment from each site, which generally corresponds to the depth range where bacterial sulfate reduction peaks in shelf sediments (Jørgensen, 1982). After sampling, sediments were kept under anoxic conditions at *in situ* temperatures until further processing in the lab, which occurred within one week of sampling.

Index properties and elemental analysis

Wet-bulk density and porosity were calculated from one sediment sample, taken at each sampling site. Measurements were based on the ratio between the wet and dry masses and density of the sample.

Elemental analyses were performed on triplicate samples of 20-100 mg of freeze-dried and ground sediment. Total carbon (TC) and total nitrogen (TN)

Table 1. Sampling site descriptions

Study sites	Coordinates	Sampling date	Sampling device	Water depth (m)	Average environmental temperature (°C)	Salinity (‰)	Wet Density (g/cm ³)	Porosity	C/N	TOC (%)	Sediment description
Southern Ocean (Weddell Sea)	65° 26' S 61° 26' W	Sep-07	Multi core	850	0 ^a	34 ^a	1.5	0.7	7	0.3	Permanently cold sediment situated near a methane-venting cold seep, consisting of light-grey stiff clay.
Arctic Ocean (Ymerbukta, Svalbard)	78° 16' N 14° 02' E	Jul-05	Push core	Subtidal	0 ^a	27-30 ^a	1.5	0.6	13	2.9	Seasonally freezing-thawing sediment located at the tidal-dominated fringe of a glacier moraine and consisting of black coarse-grained sand.
Arctic Ocean (Smeerenburgfjord, Svalbard)	79° 42' N 11° 05' E	Aug-07	HAPS core	215	0 ^a	33-34 ^a	1.7	0.6	11	1.6	Permanently cold sediment with abundant worm burrows, soft brown clay grading to mottled dark grey-black at depth.
North Sea (Wadden Sea, German Bight)	53° 27' N 08° 07' E	May-07	Push core	Intertidal	12 ^b	22-30 ^b	1.3	0.7	13	3.0	Estuary subjected to large seasonal temperature changes with abundant meio- and macrofauna, light-brown sandy mud changing to black at depth.
Baltic Sea (Arkona Basin)	54° 46' N 13° 48' E	Jun-07	Multi core	9	8 ^b	8-9 ^b	1.2	0.7	9	6.1	Sediment subjected to small seasonal temperature changes, dark-brown and black mud.
Arabian Sea (off the coast of Goa, India)	15° 6' N 73° 24' E	Apr-07	Multi core	60	26 ^a	34-35 ^a	1.2	0.8	14	3.0	Permanently warm sediment from an upwelling system, green soft fine-grained and watery mud.
Arabian Sea (Sadayat island, United Arab Emirates)	24° 31' N 54° 26' E	Sep-07	Push core	Intertidal	30 ^a	200 ^a	1.4	0.7	106	1.4	Permanently warm hypersaline sediment covered by a 0.5 cm-thick microbial mat, fine-grained sand, yellow with grey-black streaks.
Andaman Sea (Phuket Island, Thailand)	08° 03' N 98° 25' E	Aug-07	Push core	Intertidal	28 ^a	28-34 ^a	1.3	0.6	30	3.6	Permanently warm tide-dominated mangrove forest, brown coarse-grained sand.
South China Sea (Hainan Island, China)	19° 35' N 110° 48' E	Sep-07	Push core	Intertidal	30 ^a	15-25 ^a	1.8	0.4	10	0.2	Permanently warm sediment with abundant worm burrows, dark-brown sand.

a) *In situ* measurements

b) Measurements from closest automated monitoring station

content were determined using a Fisons NA 1500 (Series 2) elemental analyzer. Freeze-dried material was combusted with vanadium pentoxide catalyst at 900-1000°C in a stream of oxygen and the produced gases were separated by gas chromatography and quantified with a thermal conductivity detector.

Total inorganic carbon (TIC) was determined by coulometry using a CM5240 TIC acidification module attached to a CM5014 CO₂ analyzer (UIC, Inc.), which measures CO₂ evolved from sample acidification. Total organic carbon (TOC) in the sediments was determined from the difference between TC and TIC.

Temperature-gradient experiments

Sediment slurries were prepared by diluting sediment 1:1 (vol/vol) with anoxic artificial seawater prepared as described by Widdel and Bak 1992. Slurries were prepared under N₂, and 5 ml of slurry was transferred into each Hungate tube. Hungate tubes were flushed with N₂ according to the Hungate technique (Bryant, 1972) and sealed with butyl rubber stoppers. Sediment slurries in Hungate tubes were incubated in an aluminum temperature-gradient block heated electrically at one end and cooled at the other end with a refrigerated and thermostated water bath. Hungate tubes were pre-incubated for at least 5 hours to allow them to reach thermal equilibrium. Triplicate samples were incubated in parallel (at the same temperature) at several points along the temperature gradient block in order to confirm the reproducibility of SRR. The temperature span was from 0° to +50°C to cover the potential physiological temperature range of the active microorganisms. The incubation temperature gradient for the Arctic Ocean (Ymerbukta, Svalbard), North Sea and Baltic Sea sites (Table 1) was extended to -10°C in order to explore the physiological limits of microorganisms at temperatures below the freezing point.

Measurements of bacterial sulfate reduction were performed using ³⁵S-sulfate according to Kallmeyer *et al.*, 2004 and Roy *et al.*, 2014. In order to minimize bacterial growth and re-oxidation of radiolabeled sulfate during the experiment, the incubation time with the radiotracer was restricted to 24 hours. Growth of SRM in marine sediments is too slow to generate significant changes in the community during the short pre-incubation (Hoehler and Jørgensen, 2013).

Temperature dependence

The Arrhenius equation (Arrhenius, 1908) was applied to model the temperature dependence of SRR. The slope of the linear range obtained from plotting the natural logarithm of the reaction rate against the reciprocal of the absolute temperature is a measure of the activation energy (E_a) of a chemical reaction. In a biochemical context, E_a estimated from the slope of the linear temperature ranges are commonly interpreted to reflect the temperature response of the rate-limiting step in a physiological process, e.g., membrane transport or enzymatic catalytic conversion. The catalysis of a chemical reaction by an efficient enzyme with low temperature dependence will yield a low E_a (D'Amico *et al.*, 2002; Marx *et al.*, 2007). For naturally occurring microbial communities, E_a values are not activation energies of a single sulfate-reducing population, but are a “temperature characteristic” and reflect the combined response of a complex SRM community (e.g., Figure 1). Despite this complexity, Knoblauch and Jørgensen 1999 found that calculated E_a values for pure cultures of SRM were similar to those estimated for the natural SRM communities in the marine sediments from which these cultures were derived. Coincident E_a values indicate that SRM have similar responses to increasing temperatures in pure cultures and in natural sediments. E_a is therefore a useful parameter to describe the temperature sensitivity of SRM communities in sediments from different temperature regions. The temperature dependence can also be described by the temperature coefficient (Q_{10}), which describes the factor by which rate increases in response to a temperature increase of 10°C.

Arrhenius curves were obtained from temperature-gradient incubation data and represent the metabolic rate as a function of temperature as follows:

$$\ln(k) = \ln(A) + \left(\frac{-E_a}{R} \cdot \frac{1}{T} \right),$$

where E_a is the activation energy (J mol⁻¹), k is the rate of sulfate reduction (nmol cm⁻³ day⁻¹), A is the Arrhenius constant, R is the gas constant (8.314 J K⁻¹ mol⁻¹), and T is the absolute temperature (K).

Q_{10} values were calculated for the 10°C interval 20-30 °C in the linear temperature range of Arrhenius plots according to:

$$Q_{10} = \exp \left[\frac{E_a \cdot 10}{RT(T+10)} \right].$$

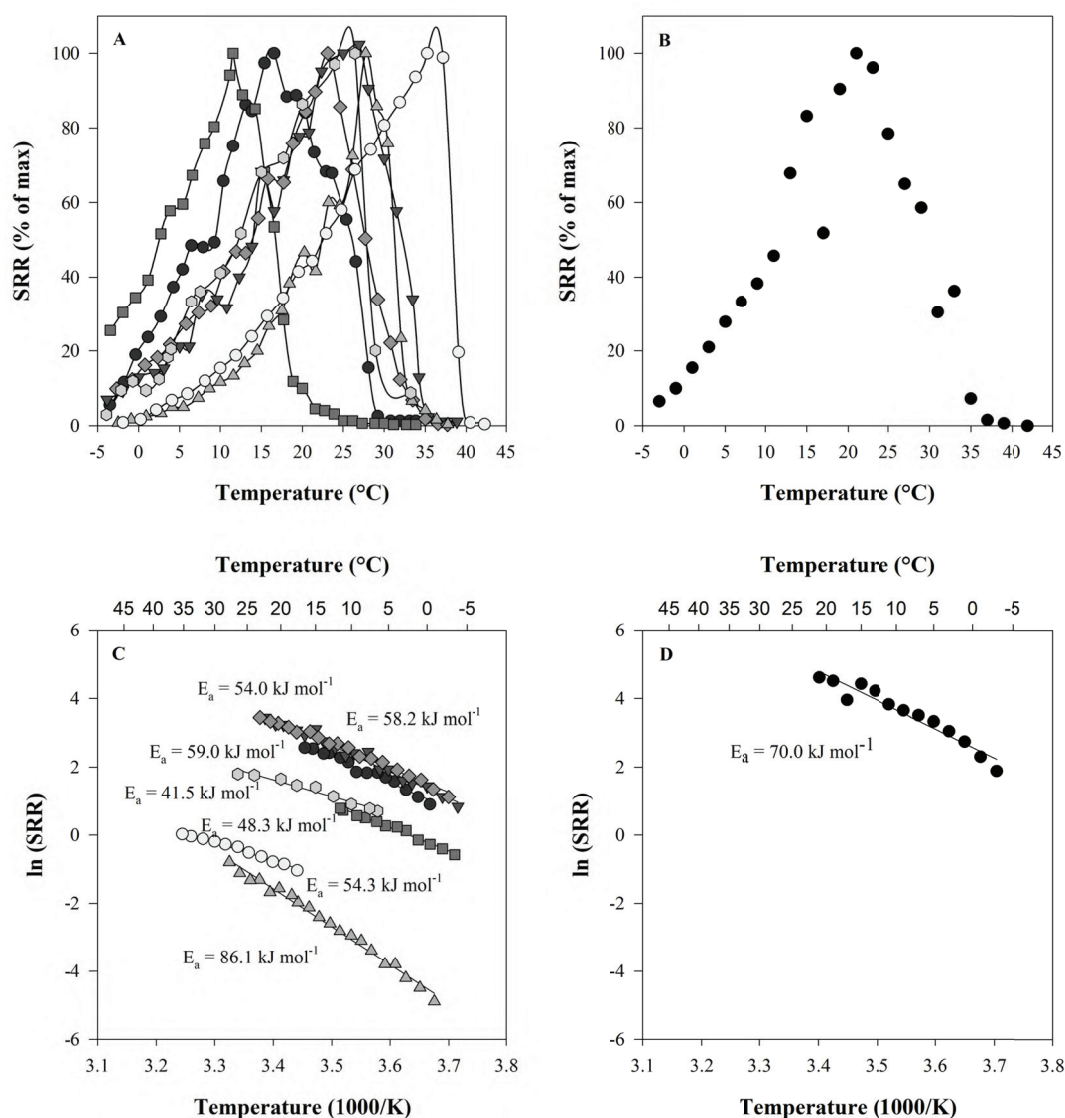


Figure 1. (A) SRR of seven pure cultures of sulfate-reducing bacteria measured in temperature-gradient incubation experiments. Data from Isaksen and Jørgensen (1996), Knoblauch and Jørgensen (1999), Tarpgaard *et al.*, (2005). (B) Sum of SRR of the seven strains from panel A, calculated at 2°C temperature intervals. Equal weight is given to each SRM strain in (A) to illustrate the cumulative effect of a mixed SRM community. The temperature dependence of individual isolates and summed SRRs is presented as Arrhenius plots in (C) and (D), respectively.

Sequence analysis and phylogenetic identification of putative sulfate reducing bacteria

Bacterial 16S rRNA gene libraries from the same sediment samples used in this study (Antarctica, Goa, Sadeyat, Phuket, Hainan) and from samples obtained from the same sampling locations (Ymerbukta, Smeerenburgfjorden, Dangast, Arkona) were constructed as part of a previous study (Muller *et al.*, 2014) (NCBI Sequence Read Archive accession number SRP028774). These libraries were

re-analyzed here focusing on the presence of sequences affiliated with known lineages of SRM. Amplicon pyrosequencing reads were clustered into phylotypes using a 97% identity threshold with UCLUST (Edgar, 2010). Representative sequences were aligned with mothur using the Needleman-Wunsch pairwise alignment method default settings (Schloss *et al.*, 2009). Chimeras were detected using Chimera Slayer (Haas *et al.*, 2011) and excluded from further analysis, resulting in 6,935 phylotypes

across the nine locations. Taxonomy was automatically assigned using the RDP classifier (Wang *et al.*, 2007). In addition, the web-based SINA aligner (Pruesse *et al.*, 2012) was used to automatically align representative phylotype sequences and to determine the most closely related sequences that were then imported into the SILVA SSU Ref NR 111 database (Quast *et al.*, 2013) for phylogenetic analysis in ARB (Ludwig *et al.*, 2004). Short amplicon sequences were added to the SILVA reference tree using the ARB Parsimony Interactive tool. Phylotypes were defined as candidate SRM phylotypes if they clustered phylogenetically with known SRM lineages and/or were assigned to known SRM lineages by the RDP classifier. The alignment of candidate SRM phylotype sequences was manually curated and used to re-cluster the representative sequences into species-level phylotypes of $\geq 97\%$ sequence similarity based on the average neighbor algorithm in mothur (Schloss *et al.*, 2009). A maximum likelihood (RAxML) tree was calculated with almost full-length 16S rRNA sequences (≥ 1400 nt) of known SRM ($n=167$) and most closely related sequences ($n=328$) based on 1,222 alignment positions by using a 50% sequence conservation filter for bacteria. The candidate SRM phylotype sequences from the amplicon libraries were then added to the tree without changing the overall tree topology using the ARB Parsimony Interactive tool and applying the 50% conservation filter. This resulted in 384 putative SRM phylotypes that clustered phylogenetically with known SRM lineages and shared $\geq 90\%$ sequence similarity with described SRM species.

Bacterial community analysis

Pyrosequencing libraries, which contained a median of 5,190 reads (min/max: 1,024/10,082) and a median of 1,028 reads assigned to putative SRM (min/max: 117/2,323), were rarefied to the smallest library for all analyses (i.e. 1,024 reads for total communities and 117 reads for SRM). Principal coordinates analysis (PCoA) was performed based on a Bray-Curtis dissimilarity matrix (using presence-absence as well as relative abundance data) using the package 'vegan' in R (Oksanen *et al.*, 2012). The significance of environmental factors affecting community composition was assessed using the non-parametric permutational multivariate analysis of variance (perMANOVA) test (Anderson, 2001). To assess co-occurrence of SRM phylotypes in multiple sediments, a correlation network was produced from SRM phylotype relative abundance across the nine sites. Briefly, pairwise Pearson correlation coefficients (r) were calculated for phylotypes. The statistical significance of r was

determined by generating a null distribution for r by randomly permuting relative abundances across the nine sites for 1,000 iterations and calculating the P-value of the observed r from the null distribution. P-values were corrected for multiple testing using the False Discovery Rate approach (Benjamini and Hochberg, 1995) and corrected P-values with a value of ≤ 0.05 were used to create a correlation network that was visualized in Cytoscape (Saito *et al.*, 2012). The site occupancy of a phylotype was calculated as the number of sample locations at which the phylotype was detected. The mean temperature at which each phylotype was enriched was calculated by multiplying its relative abundance at each site by the mean temperature at the site, summing these products, and dividing by the sum of abundances over all nine sites. This produced a weighted value signifying the temperature at which the phylotype was most abundant. All calculations were done in R (R Development Core Team, 2011).

Results

Sulfate reduction rates

SRR as a function of temperature were determined for all nine sediments (Figure 2). Sulfate reduction was detected within the studied temperature range (0° to $+50^\circ\text{C}$) for all sediments, including temperatures well outside the *in situ* range corresponding to the sampled environments. The lowest SRR, $0.1\text{--}0.5\text{ nmol cm}^{-3}\text{ d}^{-1}$, were measured in the sediment with the greatest water depth in the Southern Ocean, Weddell Sea (Figure 2a and Table 1) while the highest rates, $230\text{--}2200\text{ nmol cm}^{-3}\text{ d}^{-1}$, were observed in a shallow Arctic Ocean intertidal lagoon, Ymerbukta on Svalbard, characterized by a relatively higher content of organic matter derived from decomposing macrophytes (Figure 2b and Table 1).

The temperature curves for SRR all show a distinct peak corresponding to the optimal temperature (T_{opt}) i.e., the temperature at which the rates are highest. Arctic and Antarctic sediments showed T_{opt} for sulfate reduction of $24\text{--}26^\circ\text{C}$ (Figure 2a-c), which is 25°C above the *in situ* temperatures in these sediments. Temperate sediments have broader *in situ* temperature ranges than polar sediments, and in these samples sulfate reduction was detected from below 0°C up to T_{opt} at 35°C (Figure 2d, e). The thermal optimum for sulfate reduction in tropical sediments was shifted towards $38\text{--}44^\circ\text{C}$ (Figure 2f-i).

SRR measured in polar sediments at *in situ* temperatures of ca. 0°C were 9–20 % of the maximal rates (Figure 2a-c and Table 1 and 2). In temperate sediments, SRR at the mean *in situ* temperatures of

ca. 12°C were 9-13% of maximal rates (Figure 2d, e and Table 1 and 2) while in tropical sediments, SRR at corresponding *in situ* temperatures were 23-76 % of maximal rates (Figure 2f-i and Table 1 and 2).

Several of the studied sediments, irrespective of their *in situ* temperature, displayed an increase in SRR at temperatures exceeding 40-45°C, well above the psychrophilic or mesophilic T_{opt} (Figure 2a, 2c-h). This indicates the presence of spores of thermophilic SRM that germinated at these high temperatures, even though the study sites would

not support *in situ* growth at their ambient temperatures. Thermophilic spore-forming bacteria, among them SRM, have been reported from a variety of marine environments ranging from high Arctic to temperate environments (Isaksen *et al.*, 1994; Hubert *et al.*, 2009; de Rezende *et al.*, 2013; Müller *et al.*, 2014). Their distribution patterns can be linked to a combination of dispersal by ocean currents, regional hydrography and local geological factors.

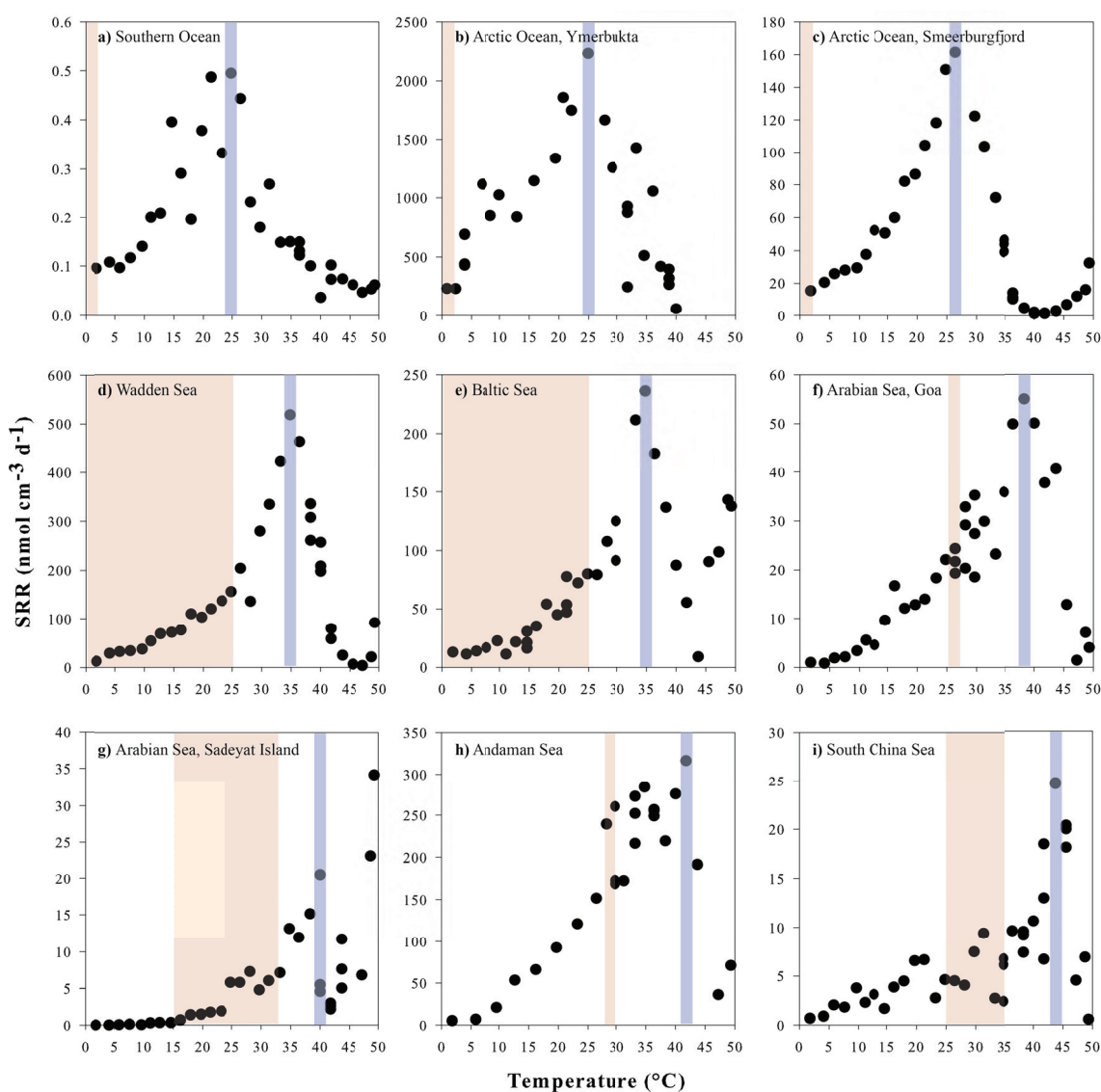


Figure 2. SRR measured in temperature-gradient incubation experiments of sediment slurries from all sampling sites. *In situ* temperature range is indicated by the area shaded in red, always to the left of the band shaded in blue indicating the T_{opt} for sulfate reduction.

Table 2. Summary of temperature gradient experiments based on data from Figure 2

Study sites	Sulfate reduction		Sulfate reduction rates (nmol cm ⁻³ day ⁻¹)				<i>E_a</i> (kJ mol ⁻¹)	<i>Q</i> ₁₀ ^c
	<i>T</i> _{opt} (°C)	<i>T</i> _{crit} (°C)	At 0°C	At <i>T</i> _{opt}	0°C vs <i>T</i> _{opt} (%) ^a	Range of linearity ^b (°C)		
Southern Ocean (Weddell Sea)	21.3	N/A	0.1	0.5	20	0, +21	51.2 ± 8.0	2.0
Arctic Ocean (Ymerbukta, Svalbard)	24.9	N/A	232	2233	10	0, +25	54.9 ± 6.9	2.1
Arctic Ocean (Smeerenburgfjord, Svalbard)	26.4	N/A	15	161	9	0, +26	64.5 ± 1.7	2.4
North Sea (Wadden Sea, German Bight)	34.8	N/A	12	518	2	+4, +35	63.7 ± 3.2	2.4
Baltic Sea (Arkona Basin)	34.8	N/A	13	236	5	0, +35	67.0 ± 3.9	2.5
Arabian Sea (off the coast of Goa, India)	38.3	11	1	55	2	+11, +38	55.7 ± 5.7	2.1
Arabian Sea (Sadayat island, UAE)	40	18	0.02	21	0.1	+18, +40	97.4 ± 11.9	3.7
Andaman Sea (Phuket Island, Thailand)	41.8	13	5	316	2	+13, +42	44.6 ± 4.8	1.8
South China Sea (Hainan Island, China)	43.7	8	1	25	3	+6, +44	36.0 ± 5.0	1.6

a) Percentage of SRR at 0°C of maximum SRR at *T*_{opt};

b) The term "Range of linearity" refers to the linear part of the Arrhenius plot;

c) The temperature interval for the calculation of *Q*₁₀ is +20°C to +30°C.**Temperature characterization of sulfate reduction**

The Arrhenius plots are characterized by a range of linear slopes, mostly extending below and above the respective environmental temperature ranges (Figure 3). Apparent *E_a* values in all sediments ranged between 36 and 97 kJ mol⁻¹. *Q*₁₀ values ranged from 1.6-3.7 in the temperature range of 20-30 °C (Table 2, Figure 3). In polar and temperate sediments the linear range of sulfate reduction extended below 0°C (Figure 3a,b). The SRR-temperature relationship was linear down to -4°C to -6°C (Figure 4), which is at the freezing range for the sediment slurries. Rates thus dropped off steeply below this temperature range. By contrast, in sediments from tropical latitudes, with the exception of the South China Sea, *E_a* remained constant over a linear range that extended from the *T*_{opt} down to an apparent transition between +4°C and +18°C (Figure 3d, 3f-i). Below these temperatures the slope changed sharply to higher *E_a* values of 130-234 kJ mol⁻¹ (*Q*₁₀, 5.7-23). The temperature at which the *E_a* values changed was estimated by calculating the best-fit line for the experimental data using linear regression analysis. The temperature at the intersection of the two lines is here defined as the critical temperature (*T*_{crit}).

The existence of a critical temperature (*T*_{crit}) (Lamanna *et al.*, 1973) has been proposed for bacterial growth at low temperatures to explain the transition between optimal and sub-optimal thermal activity ranges (Guillou and Guespin-Michel, 1996). A *T*_{crit} has also been described for

thermophilic, mesophilic, and psychrotolerant microorganisms (Harder and Veldkamp, 1968; Mohr and Krawiec, 1980; Reichardt and Morita, 1982). The biochemical basis for *T*_{crit} remains uncertain, but this temperature is likely the result of the uncoupling of DNA synthesis rate and growth rate at low temperatures (Bakermans and Neelson, 2004). Although a *T*_{crit} has been described for pure isolates of sulfate-reducing bacteria (Targgaard *et al.*, 2006), there have been no reports for natural communities of sulfate-reducing microorganisms in marine sediments.

Diversity and co-localization of SRM phylotypes in marine sediments

All but one of the 384 putative SRM phylotypes were affiliated with the class *Deltaproteobacteria* and accounted for 9.7% to 25.9% of the total bacterial 16S rRNA gene sequences from the nine marine sediment samples (Figure 5 and Supplementary Figure S1). SRM phylotype diversity in all nine samples was dominated by members of the *Desulfobacteraceae*, *Desulfobulbaceae*, and *Desulfatiglans anilini* lineages (Figure 5A, B and Supplementary Figure S2). A slight exception to this pattern is the sediment sample from Sadayat, which contained less *Desulfobulbaceae* but a substantial fraction of *Desulfobulbiaceae*, a family that comprises many halophilic SRM species (Kjeldsen *et al.*, 2007), which is consistent with the higher salinity of this sediment.

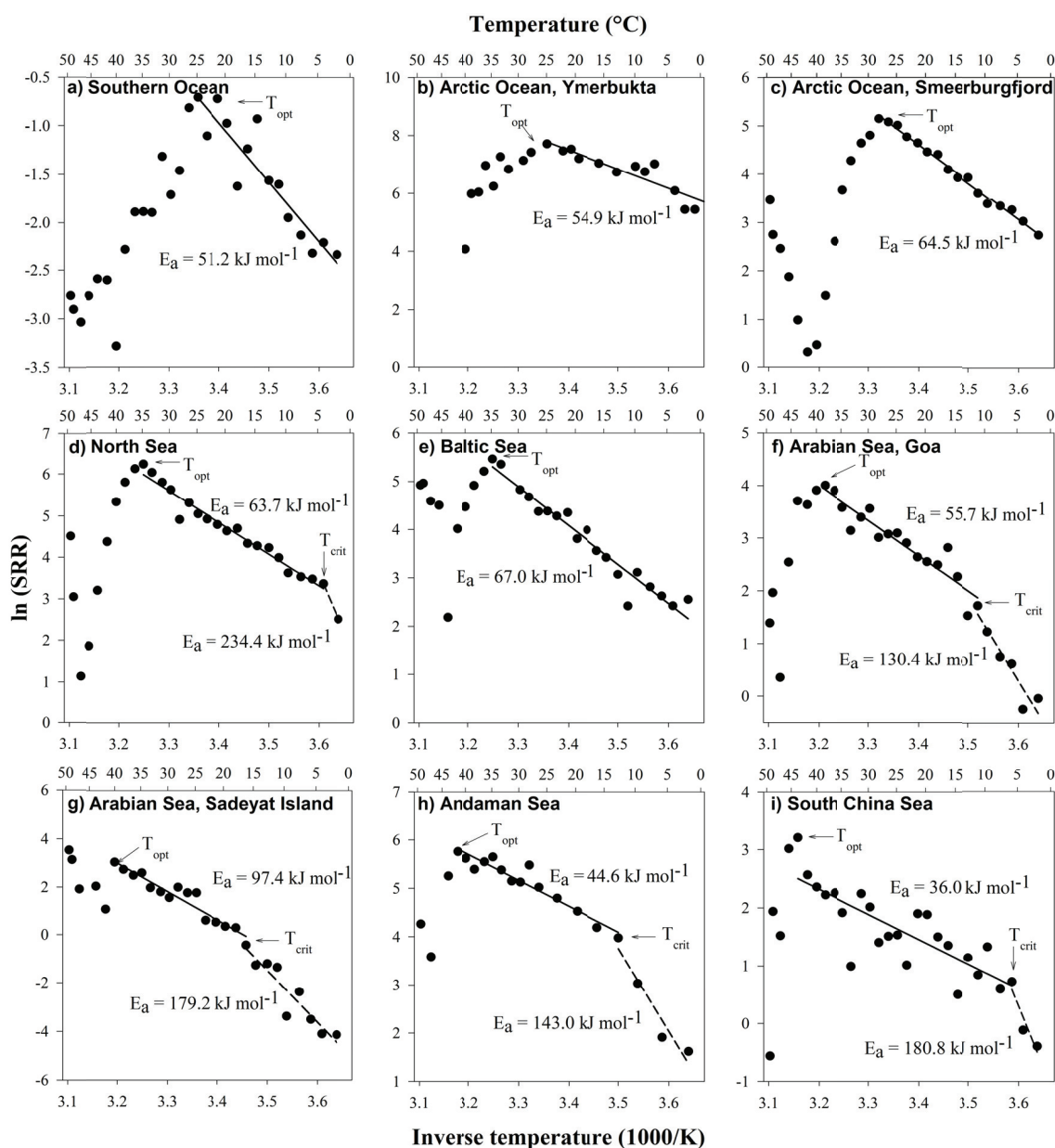


Figure 3. Arrhenius plots of data from Figure 1. Corresponding E_a values are shown.

PCoA of total bacterial communities using the Bray-Curtis metric revealed clustering of sites by mean temperature, when either presence/absence or relative abundance was used to calculate sulfate-reducing and total community dissimilarities between locations (Supplementary Figure S3). The one exception to this tight clustering by temperature was the saline Sadayat sediment sample. To evaluate which environmental parameters were important in shaping the community compositions, a non-parametric

permutational analysis of variance (perMANOVA) was applied to test the significance of temperature, salinity, C:N ratio, total organic carbon, and activation energy for sulfate reduction. Temperature and salinity, but not the other factors, were significantly associated with SRM community composition (perMANOVA, $p < 0.001$, Table S1).

In order to evaluate co-localization of individual SRM phylotypes across the nine sites, a correlation network based on the abundance of SRM phylotypes relative to the entire SRM community

was developed. Strong clustering of phylotypes into nine modules, that is, clusters of co-occurring phylotypes, was observed (Figure 6). Many phylotypes associated with each module were enriched at only one site. Consistent with the PCoA, phylotype modules clustered in the overall network according to mean temperature. Several phylotypes detected at multiple sites (i.e. site occupancy >1) were correlated with other phylotypes in multiple modules (i.e., phylotypes that represent links between modules in the network), and these correlations were predominantly between modules associated with sites having similar mean temperatures. Some module-connecting phylotypes (e.g., *Desulfobulbaceae* phylotypes 195, 1511 and 2651; *Desulfatiglans anilini* lineage phylotypes 5671 and 4726) were characteristic of sediments with cold temperatures, while others (*Desulfobacteraceae* phylotypes 134, 1263, and 5726; *Desulfobulbaceae* phylotypes 2510 and 6454; *Desulfoarculus baarsii* lineage phylotype 1201; *Desulfobacca acetoxidans* lineage phylotype 5807) were characteristic of sediments with warmer temperatures. The phylotype module associated with the warm and high-salinity site, Sadeyat, was unique and disconnected from all other sites. No trend was observed with respect to taxonomic affiliation and co-occurrence of phylotypes (data not shown).

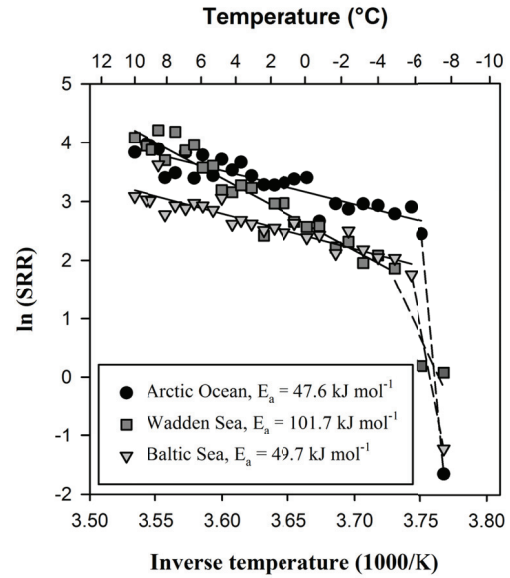
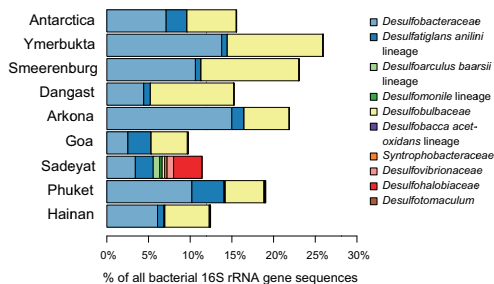


Figure 4. Arrhenius plots of SRR ($\text{nmol cm}^{-3} \text{d}^{-1}$) measured in temperature-gradient incubation experiments down to -10°C of sediment slurries from sampling sites at the Arctic Ocean (Smeerenburgfjord, Svalbard), Wadden Sea, and Baltic Sea.

A Relative abundance



B Number of phylotypes

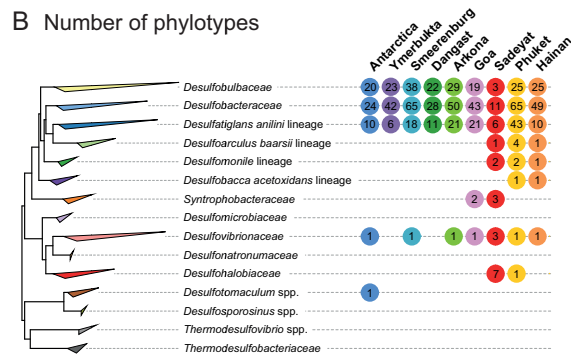


Figure 5. A) Relative abundance of 16S rRNA gene sequences of putative SRM, which were inferred from phylogenetic relationships to known SRM; B) Maximum likelihood (RAxML) tree of SRM. Taxa and lineages of known SRM are clustered and the numbers of associated phylotypes present at each location are shown.

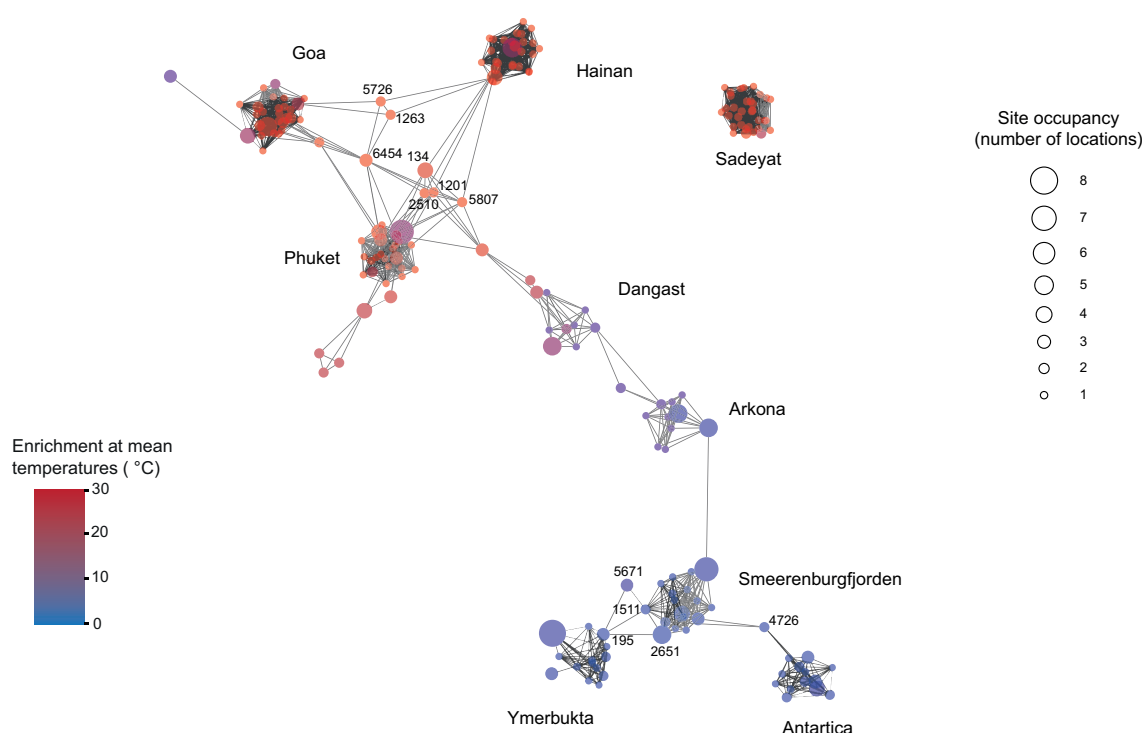


Figure 6. Correlation network analysis using the abundance of SRM phylotypes relative to the entire SRM community. Each node (i.e. circle) represents a phylotype and each edge (i.e. grey line) represents a statistically significant positive correlation between two nodes. Nodes were colored according to the mean sediment temperature at which each phylotype was enriched and their size was scaled according to site occupancy. Aside from a single *Desulfotomaculum* phylotype from Antarctica, all SRM were affiliated with the class *Deltaproteobacteria*.

Discussion

Temperature response and diversity of SRM are site-specific

The temperature response of microbial respiration and growth has commonly been determined in temperature-gradient incubation experiments (Battley, 1964) where the thermal response of an individual organism can be described using three cardinal temperatures (Neidhardt *et al.*, 1990). The minimum temperature (T_{\min}) and maximum temperature (T_{\max}) delimit the range of growth, while the optimum temperature (T_{opt}) denotes the temperature at which growth rate is highest. On the basis of these defining cardinal parameters, microorganisms are frequently divided into broad classes: psychrophilic ($T_{\min} < 0^{\circ}\text{C}$, $T_{\text{opt}} \leq 15^{\circ}\text{C}$, $T_{\max} \leq 20^{\circ}\text{C}$), psychrotolerant ($T_{\min} \leq 0^{\circ}\text{C}$, $T_{\text{opt}} \leq 25^{\circ}\text{C}$, $T_{\max} \leq 35^{\circ}\text{C}$), mesophilic ($T_{\text{opt}} \sim 25$ to 40°C , T_{\max} is ~ 35 to 45°C), and thermophilic ($> 45^{\circ}\text{C}$) (Morita, 1975). In the case of complex SRM communities in marine sediments, their temperature response can be interpreted as the combination of SRR of many different SRM populations, each with a given set of

cardinal temperatures. Such a mixed community response is illustrated in Figure 1, where the SRR of different psychrophilic, psychrotolerant, and mesophilic sulfate-reducing strains (Figure 1A) are summed to give a theoretical temperature response of a mixed SRM community (Figure 1B). As an example, a hypothetical mixture of SRM (Figure 1B), each with characteristic temperature ranges but predominantly psychrophilic, results in a relatively broad temperature response similar to that observed for many natural communities in cold sediments (Isaksen and Jørgensen, 1996; Sagemann *et al.*, 1998). The composite of the temperature responses of these organisms (Figure 1C) translates into a temperature characteristic with an average E_a of 70 kJ mol^{-1} (Figure 1D), corresponding to a Q_{10} of 2.6. These values fall within the range for active SRM (Isaksen and Jørgensen, 1996; Sagemann *et al.*, 1998) as well as other heterotrophic bacterial communities (Pomeroy and Wiebe, 2001). Accordingly, the regulation of T_{opt} for sulfate reduction by mean ambient temperatures (Figure 2) denotes the dominant temperature sensitivities of the active SRM community in the studied

environments and is indicative of the enrichment of particular SRM. Our observations extend previous findings (e.g. Arnosti *et al.*, 1998; Isaksen and Jørgensen, 1996; Sagemann *et al.*, 1998) that suggested temperature-dependent adaptations of SRM communities based on whole-community SRR and reveal that the environment selects organisms that are physiologically best adapted to the prevailing temperature.

SRR measured at the *in situ* temperature in polar sediments (0°C) were 9-20% of the maximal rates at T_{opt} (Figure 2a-c and Table 2). By comparison, in temperate sediments, the relative SRR at 0 °C were only 2-5 % of the rates at T_{opt} (Figure 2d, e and Table 2). Relatively high metabolic rates at temperatures near the freezing point are characteristic of microorganisms adapted to cold habitats (Harder and Veldkamp, 1968). The SRR at 0°C relative to T_{opt} in the polar sediments are in the range previously described for psychrophilic sulfate-reducing microbial communities in cold polar marine sediments (Isaksen and Jørgensen, 1996; Robador *et al.*, 2009). This shows a distinct adaptation of SRM to the low temperature in the polar region. Of the three polar environments, the Antarctic sediment had the highest relative SRR at low temperatures (20% of SRR at T_{opt} ; Figure 2 and Table 2). Arctic sediments collected from Smeerenburgfjorden and Ymerbukta on the west coast of Svalbard are influenced by the slightly higher temperatures of the North Atlantic Water compared to Antarctic waters (Walczowski and Piechura 2007), which may explain the broader temperature range to which the Arctic SRM communities are adapted to. Similar response patterns to water temperatures have been observed in permanently but moderately cold sediments from temperate regions, where sulfate reduction showed a mesophilic temperature response (Isaksen and Jørgensen, 1996). Sediments with seasonally changing temperatures are only exposed to low temperature during winter while the psychrotolerant and mesophilic community develops primarily in summer when temperatures are warmer and the influx of organic matter is greater. Psychrophiles may be better adapted during winter but, with a mean cell turnover time of about one year (Hoehler and Jørgensen, 2013), probably grow too slowly for a 'winter community' to develop. Therefore, the psychrotolerants and mesophiles predominate in temperate habitats even at low temperatures during winter (Robador *et al.*, 2009). In tropical sediments, high SRR at *in situ* temperatures relative to T_{opt} (23-76%; Figure 2 and Table 2) suggest that a mesophilic SRM community dominates these environments with an optimal activity close to the ambient temperature.

The permanently warm conditions in these environments select for a community adapted to temperatures that remain above 10-15°C and are generally 25-30°C.

The distinct physiological differentiation of SRM communities in polar, temperate, and tropical regions (Figures 2-4) is consistent with differences in phylotype composition among the nine study sites (Figure 5 and 6). While the phylotype composition of the SRM communities is unique at each site, certain phylotypes were specific to warm or cold regions (Figure 6 and Supplementary Figure S2). Notable, geographically distant sediments from the Arctic and Antarctic hosted a microbial community that was more similar to each other than to low-latitude sediments from, e.g., the Arabian Sea (Goa) or the southern North Sea (Dangast) (Figure 6) indicating that the prevailing ambient temperature is a major environmental driver of microbial community composition in the studied sediments.

Respiration rates and community composition of SRM is determined by temperature

In the studied sediments, the temperature dependence of the short-term SRR indicated a linear response extending from the lower temperature limit of sulfate reduction, which varied according to the observed T_{crit} , up to the T_{opt} (Figures 3 and 4). The E_o of 36-97 kJ mol⁻¹ (Figure 3 and Table 2) are within the range of apparent E_o estimated in seasonal studies of shallow coastal marine sediments, 36-132 kJ mol⁻¹ (Westrich and Berner, 1988). Below the T_{crit} , SRR decreased abruptly exhibiting a stronger temperature dependency, i.e. higher E_a values (Figure 3). This can be attributed to a different physiological temperature regulation of sulfate reduction below the T_{crit} and shows that some SRM were stressed below the temperature range to which they are adapted. In polar and temperate sediments, the linear temperature dependence of SRR down to -10°C showed no evidence of a low temperature threshold for microbial activity (Figure 4). Thus, the observed T_{crit} was very low and likely reflected the physico-chemical constraints (i.e., ice crystallization, high salinity, low nutrient availability) imposed by sediment freezing (Figure 4). Our results show that sulfate-reducing communities in these cold habitats can tolerate temperatures down to or below the freezing point of seawater, which may permit survival and recovery after temporary freezing of the sediment. Studies of Arctic sediments show that sulfate reduction decreases strongly during freezing, yet SRM may exhibit relatively high metabolic rates immediately upon thawing, even after repeated freeze-thaw cycles (Sawicka *et al.*,

2010). Unfrozen water at subfreezing temperatures on mineral surfaces and in liquid veins in ice can provide adequate habitats for active microbial populations (Bowman *et al.*, 2012; Ewert and Deming, 2014; Price, 2007). Moreover, there is no evidence of a minimum temperature for metabolism even at temperatures as low as -20°C (Rivkina *et al.*, 2000). In addition to psychrophily, cryotolerance (e.g., D'Amico *et al.*, 2006) may be an important characteristic of SRM for survival in polar coastal environments with constant low temperatures and that freeze during winter. By contrast, T_{crit} was much higher in tropical sediments and a narrower thermal range was observed, close to the respective *in situ* temperatures (Figure 3). The larger difference between the T_{opt} and T_{crit} in the polar and temperate habitats shows that the active SRM consist of a mixture of divergent temperature adaptations that may include psychrophiles, psychrotolerants, and mesophiles, whereas in the tropical habitats a more narrowly adapted mesophilic community is present.

Conclusions

The combination of our respiration rate measurements with phylogenetic community analysis provides new evidence that the observed temperature response of the SRM is a trait of the temperature adaptation of the sulfate-reducing community. Metabolic theory suggests that it is the metabolic rate, affected largely by temperature, that controls ecological processes at all levels of organization from individual to population interactions, and ecosystem processes (Brown *et al.*, 2004). Our work is consistent with metabolic theory showing that physiological temperature adaptations allow certain SRM to capitalize on the environmental thermal range linking the performance of individual organisms and the ecology of populations, communities, and ecosystems. Previous studies have shown that rates of carbon mineralization by SRM are mainly controlled by the availability of suitable electron donors rather than by *in situ* temperature (Arnosti *et al.*, 1998; Finke and Jørgensen, 2008). Our results indicate that temperature selects for different SRM and structures community diversity, but has little effect on overall rates of carbon mineralization. This implies significant functional redundancy of seabed microbial communities at all temperatures. An intriguing implication is therefore that changes in microbial community composition due to higher *in-situ* temperatures may not result in higher carbon mineralization rates, because the adaptation of the microbial community already accounts for environmental temperature effects.

Acknowledgements

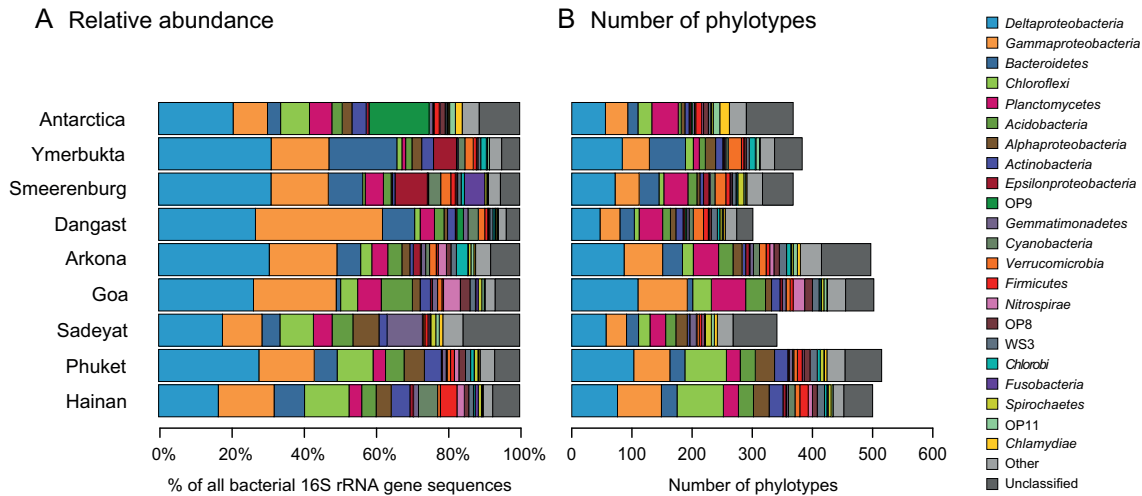
We thank Mohammad Al-Najjar, Naik Hema, Moritz Holtappels, Erik Kristensen, Uwe Krumme, S.W.A. Naqvi and Helge Niemann for sediment samples, and Kirsten Imhoff, Anna Kaufmann, Susanne Schwarz and Katharina Zyromski for assistance in the lab. This work was supported through the DFG Priority Program 1162 'The impact of climate variability on aquatic ecosystems (Aquashift)' (grants BR-2174-1.1 and BR 2174-1.2 to VB), the Austrian Science Fund (FWF project P25111-B22 to AL), and the Max Planck Society.

References

- Aller RC, Yingst JY (1980). Relationships between microbial distributions and the anaerobic decomposition of organic-matter in surface sediments of Long-Island Sound, USA. *Mar Biol* **56**: 29-42.
- Anderson MJ (2001). A new method for non-parametric multivariate analysis of variance. *Austral Ecol* **26**: 32-46.
- Arnosti C, Jørgensen BB, Sagemann J, Thamdrup B (1998). Temperature dependence of microbial degradation of organic matter in marine sediments: polysaccharide hydrolysis, oxygen consumption, and sulfate reduction. *Mar Ecol- Prog Ser* **165**: 59-70.
- Arrhenius S (1908). Immunochemie. *Ergebnisse der Physiologie* **7**: 480-551.
- Bakermans C, Nealson KH (2004). Relationship of critical temperature to macromolecular synthesis and growth yield in *Psychrobacter cryopegella*. *J Bacteriol* **186**: 2340-2345.
- Battley EH (1964). Thermal-gradient block for determination of temperature relationships in microorganisms. *Anton Van Lee J M S* **30**: 81-&.
- Benjamini Y, Hochberg Y (1995). Controlling the false discovery rate – a practical and powerful approach to multiple testing. *J R Stat Soc Ser B-Methodol* **57**: 289-300.
- Bowman JS, Rasmussen S, Blom N, Deming JW, Rysgaard S, Sicheritz-Ponten T (2012). Microbial community structure of Arctic multiyear sea ice and surface seawater by 454 sequencing of the 16S RNA gene. *ISME J* **6**: 11-20.
- Brown JH, Gillooly JF, Allen AP, Savage VM, West GB (2004). Toward a metabolic theory of ecology. *Ecology* **85**: 1771-1789.
- Bryant MP (1972). Commentary on hungate technique for culture of anaerobic bacteria. *Am J Clin Nutr* **25**: 1324-1328.

- D'Amico S, Claverie P, Collins T, Georlette D, Gratia E, Hoyoux A *et al.*, (2002). Molecular basis of cold adaptation. *Phil Trans R Soc B* **357**: 917-925.
- D'Amico S, Collins T, Marx JC, Feller G, Gerday C (2006). Psychrophilic microorganisms: challenges for life. *EMBO Rep* **7**: 385-389.
- Edgar RC (2010). Search and clustering orders of magnitude faster than BLAST. *Bioinformatics* **26**: 2460-2461.
- Ewert M, Deming JW (2014). Bacterial responses to fluctuations and extremes in temperature and brine salinity at the surface of Arctic winter sea ice. *FEMS Microbiol Ecol* **89**: 476-489.
- Finke N, Jørgensen BB (2008). Response of fermentation and sulfate reduction to experimental temperature changes in temperate and Arctic marine sediments. *ISME J* **2**: 815-829.
- Fuhrman JA (2009). Microbial community structure and its functional implications. *Nature* **459**: 193-199.
- Guillou C, Guespin-Michel JF (1996). Evidence for two domains of growth temperature for the psychrotrophic bacterium *Pseudomonas fluorescens* MF0. *Appl Environ Microbiol* **62**: 3319-3324.
- Haas BJ, Gevers D, Earl AM, Feldgarden M, Ward DV, Giannoukos G *et al.*, (2011). Chimeric 16S rRNA sequence formation and detection in Sanger and 454-pyrosequenced PCR amplicons. *Genome Res* **21**: 494-504.
- Hanson CA, Fuhrman JA, Horner-Devine MC, Martiny JBH (2012). Beyond biogeographic patterns: processes shaping the microbial landscape. *Nat Rev Micro* **10**: 497-506.
- Harder W, Veldkamp H (1968). Physiology of an obligately psychrophilic marine pseudomonas species. *J Appl Bacteriol* **31**: 12-8.
- Hoehler TM, Jørgensen BB (2013). Microbial life under extreme energy limitation. *Nature Reviews Microbiology* **11**: 83-94.
- Isaksen MF, Bak F, Jørgensen BB (1994). Thermophilic sulfate-reducing bacteria in cold marine sediment. *FEMS Microbiol Ecol* **14**: 1-8.
- Isaksen MF, Jørgensen BB (1996). Adaptation of psychrophilic and psychrotrophic sulfate-reducing bacteria to permanently cold marine environments. *Appl Environ Microbiol* **62**: 408-414.
- Jørgensen BB (1977). Sulfur cycle of a coastal marine sediment (Limfjorden, Denmark). *Limnol Oceanogr* **22**: 814-832.
- Jørgensen BB (1982). Mineralization of organic matter in the sea bed - the role of sulphate reduction. *Nature* **296**: 643-645.
- Kallmeyer J, Ferdelman TG, Weber A, Fossing H, Jørgensen BB (2004). A cold chromium distillation procedure for radiolabeled sulfide applied to sulfate reduction measurements. *Limnol Oceanogr Meth* **2**: 171-180.
- Kjeldsen KU, Loy A, Jakobsen TF, Thomsen TR, Wagner M, Ingvorsen K (2007). Diversity of sulfate-reducing bacteria from an extreme hypersaline sediment, Great Salt Lake (Utah). *FEMS Microbiol Ecol* **60**: 287-298.
- Knoblauch C, Jørgensen BB (1999). Effect of temperature on sulphate reduction, growth rate and growth yield in five psychrophilic sulphate-reducing bacteria from Arctic sediments. *Environ Microbiol* **1**: 457-467.
- Kostka JE, Thamdrup B, Glud RN, Canfield DE (1999). Rates and pathways of carbon oxidation in permanently cold Arctic sediments. *Mar Ecol-Prog Ser* **180**: 7-21.
- Kristensen E, Bodenbender J, Jensen MH, Rennenberg H, Jensen KM (2000). Sulfur cycling of intertidal Wadden Sea sediments (Konigshafen, Island of Sylt, Germany): sulfate reduction and sulfur gas emission. *J Sea Res* **43**: 93-104.
- Lamanna C, Mallette MF, Zimmerman LN (1973). *Basic Bacteriology Its Biological and Chemical Background 4th ed.* Williams & Wilkins, Baltimore, MD.
- Leloup J, Loy A, Knab NJ, Borowski C, Wagner M, Jørgensen BB (2007). Diversity and abundance of sulfate-reducing microorganisms in the sulfate and methane zones of a marine sediment, Black Sea. *Environ Microbiol* **9**: 131-142.
- Leloup J, Fossing H, Kohls K, Holmkvist L, Borowski C, Jørgensen BB (2009). Sulfate-reducing bacteria in marine sediment (Aarhus Bay, Denmark): abundance and diversity related to geochemical zonation. *Environ Microbiol* **11**: 1278-1291.
- Ludwig W, Strunk O, Westram R, Richter L, Meier H, Yadhukumar *et al.*, (2004). ARB: a software environment for sequence data. *Nucleic Acids Res* **32**: 1363-1371.
- Marx JC, Collins T, D'Amico S, Feller G, Gerday C (2007). Cold-adapted enzymes from marine antarctic microorganisms. *Mar Biotechnol* **9**: 293-304.
- Moeslund L, Thamdrup B, Jørgensen BB (1994). Sulfur and iron cycling in a coastal sediment: Radiotracer studies and seasonal dynamics. *Biogeochemistry* **27**: 129-152.
- Mohr PW, Krawiec S (1980). Temperature characteristics and Arrhenius plots for nominal psychrophiles, mesophiles and thermophiles. *Microbiology* **121**: 311-317.
- Morita RY (1975). Psychrophilic bacteria. *Bacteriol Rev* **39**: 144-167.

- Müller AL, de Rezende JR, Hubert CRJ, Kjeldsen KU, Lagkouvardos I, Berry D *et al.*, (2014). Endospores of thermophilic bacteria as tracers of microbial dispersal by ocean currents. *ISME J* **8**: 1153-1165.
- Neidhardt FC, Ingraham J., M. S (1990). *Physiology of the Bacterial Cell: A Molecular Approach*. Sinauer Associates: Sunderland, MA.
- Oksanen J, Blanchet FG, Kindt R, Legendre P, Minchin PR, O'Hara RB *et al.*, (2012). Vegan: Community Ecology Package. R package version 2.0-3.
- Pomeroy LR, Wiebe WJ (2001). Temperature and substrates as interactive limiting factors for marine heterotrophic bacteria. *Aquat Microb Ecol* **23**: 187-204.
- Price PB (2007). Microbial life in glacial ice and implications for a cold origin of life *FEMS Microbiol Ecol* **59**: 217-231.
- Prosser JI, Bohannan BJM, Curtis TP, Ellis RJ, Firestone MK, Freckleton RP *et al.*, (2007). The role of ecological theory in microbial ecology. *Nature Rev Microbiol* **5**: 384-392.
- Pruesse E, Peplies J, Glöckner FO (2012). SINA: Accurate high-throughput multiple sequence alignment of ribosomal RNA genes. *Bioinformatics* **28**: 1823-1829.
- Quast C, Pruesse E, Yilmaz P, Gerken J, Schweer T, Yarza P *et al.*, (2013). The SILVA ribosomal RNA gene database project: improved data processing and web-based tools. *Nucleic Acids Res* **41**: D590-D596.
- Ravenschlag K, Sahn K, Pernthaler J, Amann R (1999). High bacterial diversity in permanently cold marine sediments. *Appl Environ Microbiol* **65**: 3982-3989.
- Reichardt W, Morita RY (1982). Temperature Characteristics of Psychrotrophic and Psychrophilic Bacteria. *J Gen Microbiol* **128**: 565-568.
- Rivkina EM, Friedmann EI, McKay CP, Gilichinsky DA (2000). Metabolic activity of permafrost bacteria below the freezing point. *Appl Environ Microbiol* **66**: 3230-3233.
- Robador A, Brüchert V, Jørgensen BB (2009). The impact of temperature change on the activity and community composition of sulfate-reducing bacteria in arctic versus temperate marine sediments. *Environ Microbiol* **11**: 1692-1703.
- Roy H, Weber HS, Tarpgaard IH, Ferdelman TG, Jørgensen BB (2014). Determination of dissimilatory sulfate reduction rates in marine sediment via radioactive S-35 tracer. *Limnol Oceanogr Meth* **12**: 196-211.
- Sagemann J, Jørgensen BB, Greeff O (1998). Temperature dependence and rates of sulfate reduction in cold sediments of Svalbard, Arctic Ocean. *Geomicrobiol J* **15**: 85-100.
- Saito R, Smoot ME, Ono K, Ruscheinski J, Wang PL, Lotia S *et al.*, (2012). A travel guide to Cytoscape plugins. *Nat Methods* **9**: 1069-1076.
- Sawicka JE, Robador A, Hubert C, Jørgensen BB, Brüchert V (2010). Effects of freeze-thaw cycles on anaerobic microbial processes in an Arctic intertidal mud flat. *ISME J* **4**: 585-594.
- Sawicka JE, Jørgensen BB, Brüchert V (2012). Temperature characteristics of bacterial sulfate reduction in continental shelf and slope sediments. *Biogeosciences* **9**: 3425-3435.
- Schloss PD, Westcott SL, Ryabin T, Hall JR, Hartmann M, Hollister EB *et al.*, (2009). Introducing mothur: Open-Source, platform-independent, community-supported software for describing and comparing microbial communities. *Appl Environ Microbiol* **75**: 7537-7541.
- Tarpgaard IH, Boetius A, Finster K (2006). *Desulfobacter psychrotolerans* sp. nov., a new psychrotolerant sulfate-reducing bacterium and descriptions of its physiological response to temperature changes. *Anton Van Lee J M S* **89**: 109-124.
- R Development Core Team (2011). R: A language and environment for statistical computing. Vienna, Austria : the R Foundation for Statistical Computing.
- Walczowski W, Piechura J (2007). Pathways of the Greenland Sea warming. *Geophys Res Lett* **34**: L10608.
- Wang Q, Garrity GM, Tiedje JM, Cole JR (2007). Naive Bayesian classifier for rapid assignment of rRNA sequences into the new bacterial taxonomy. *Appl Environ Microbiol* **73**: 5261-5267.
- Westrich JT, Berner RA (1988). The effect of temperature on rates of sulfate reduction in marine sediments. *Geomicrobiol J* **6**: 99-117.
- Widdel F, Bak F (1992). Gram-negative mesophilic sulfate-reducing bacteria. Balows A, Trüper, H.G., Dworking, M., Harder, W. and Schleifer, K.-H. (ed). In: *The Prokaryotes 2nd edn*. Springer: New York.



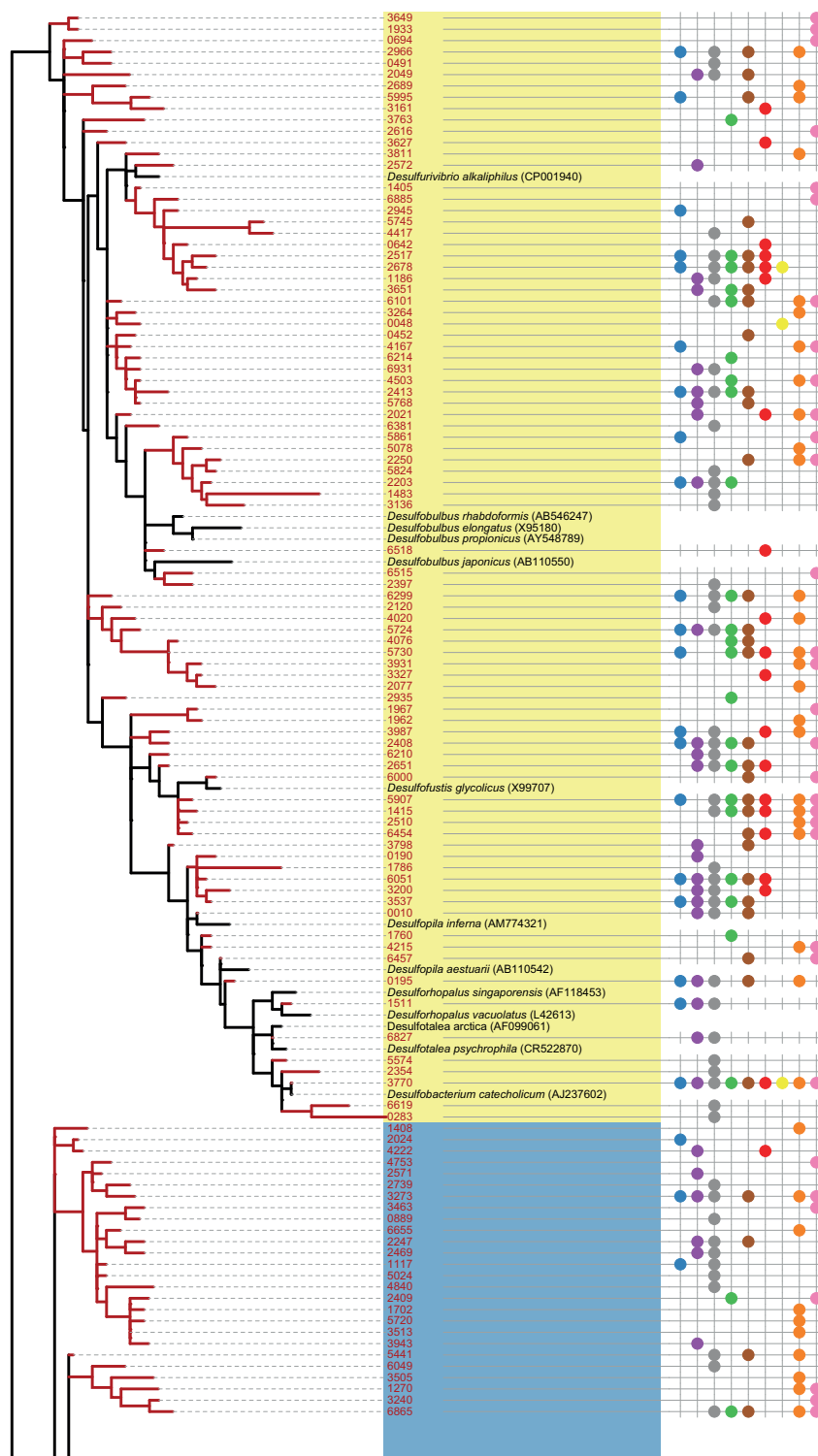
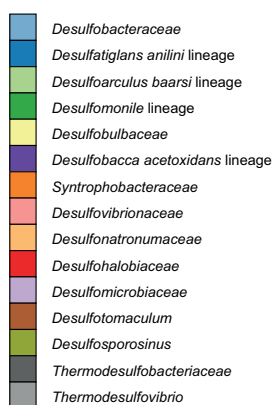
Supplementary Figure S1. Community composition of the entire bacterial community as determined by 16S rRNA gene amplicon pyrosequencing.

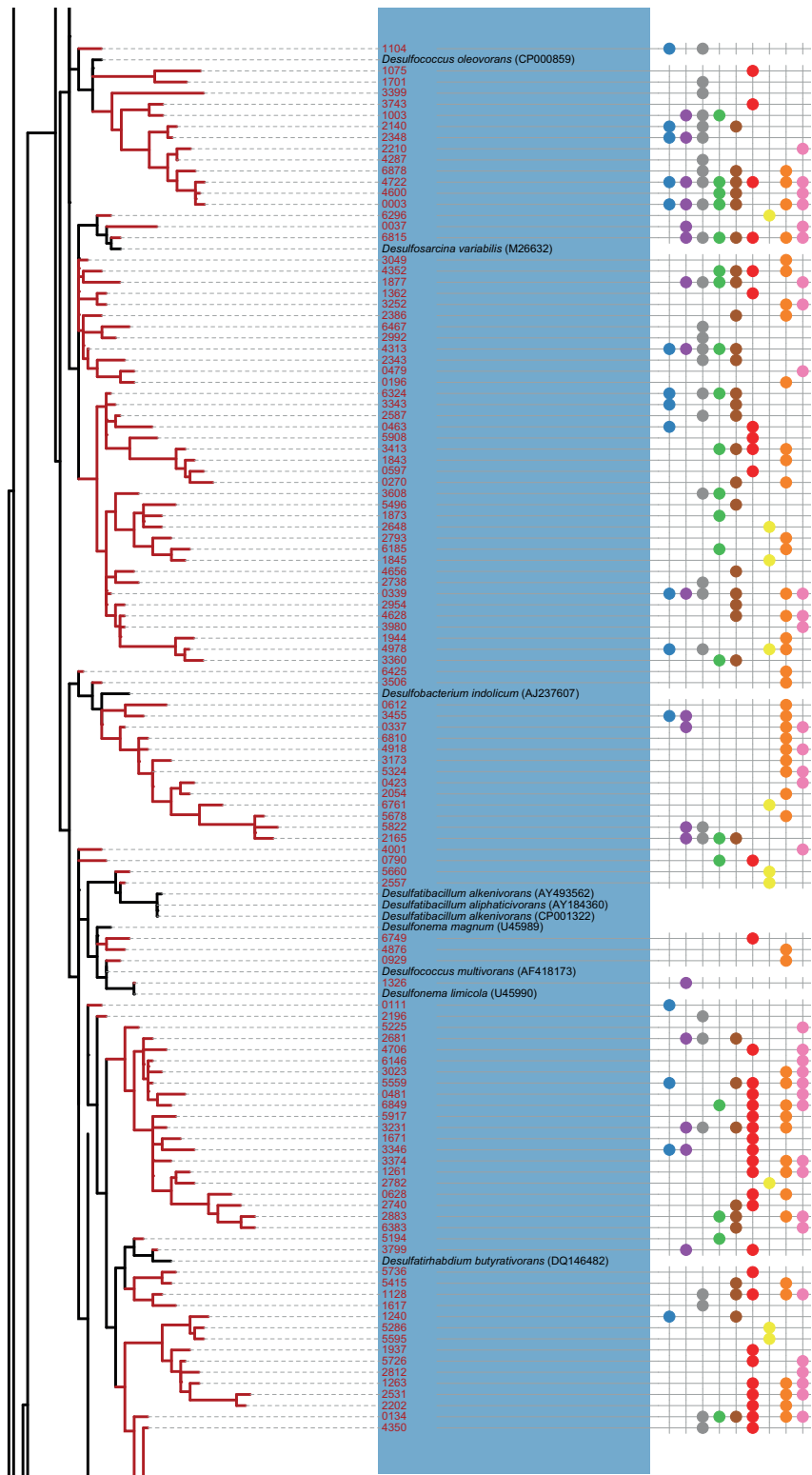
Location:

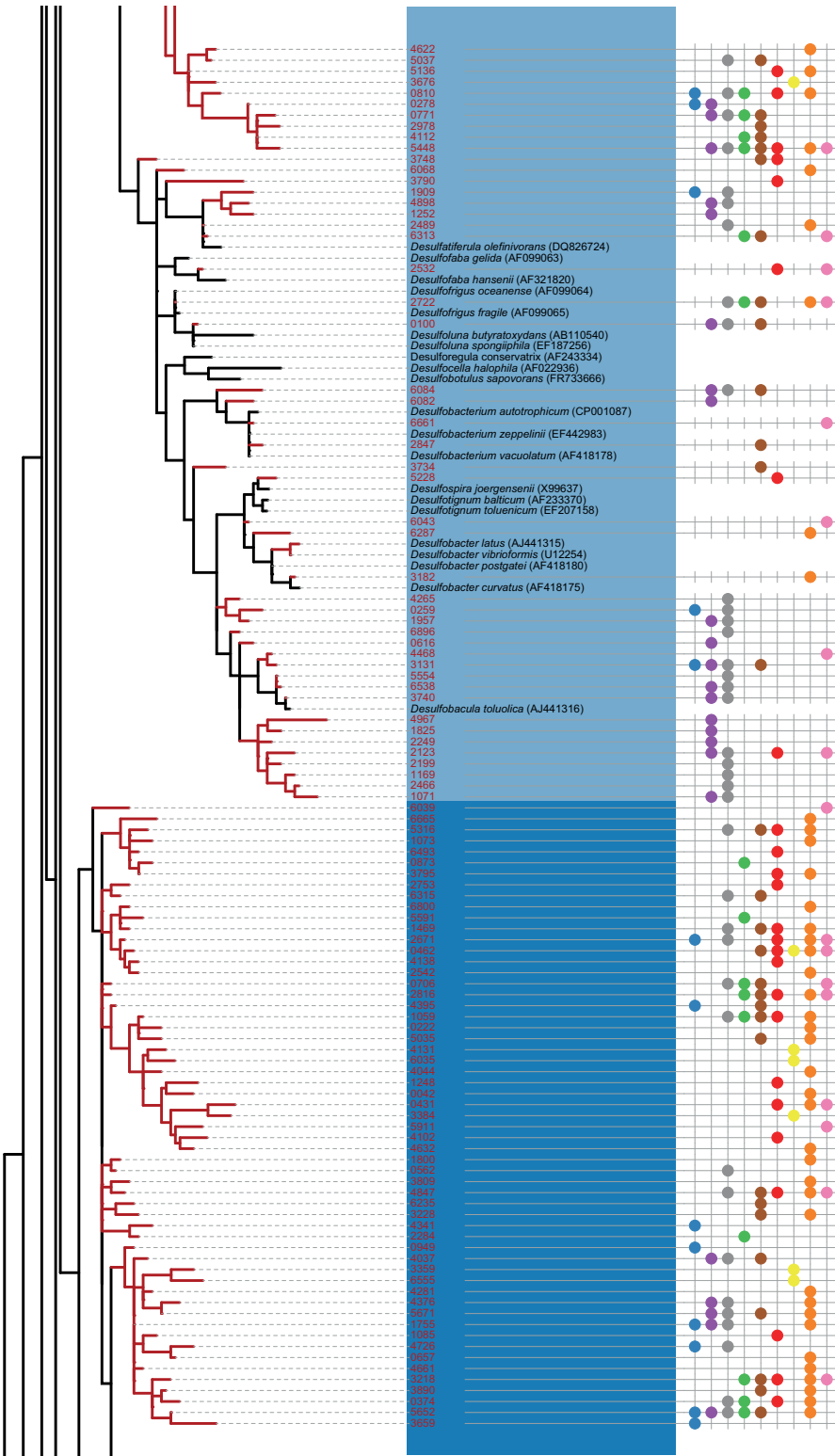
Colored dot on the right side indicates presence of phylotype.

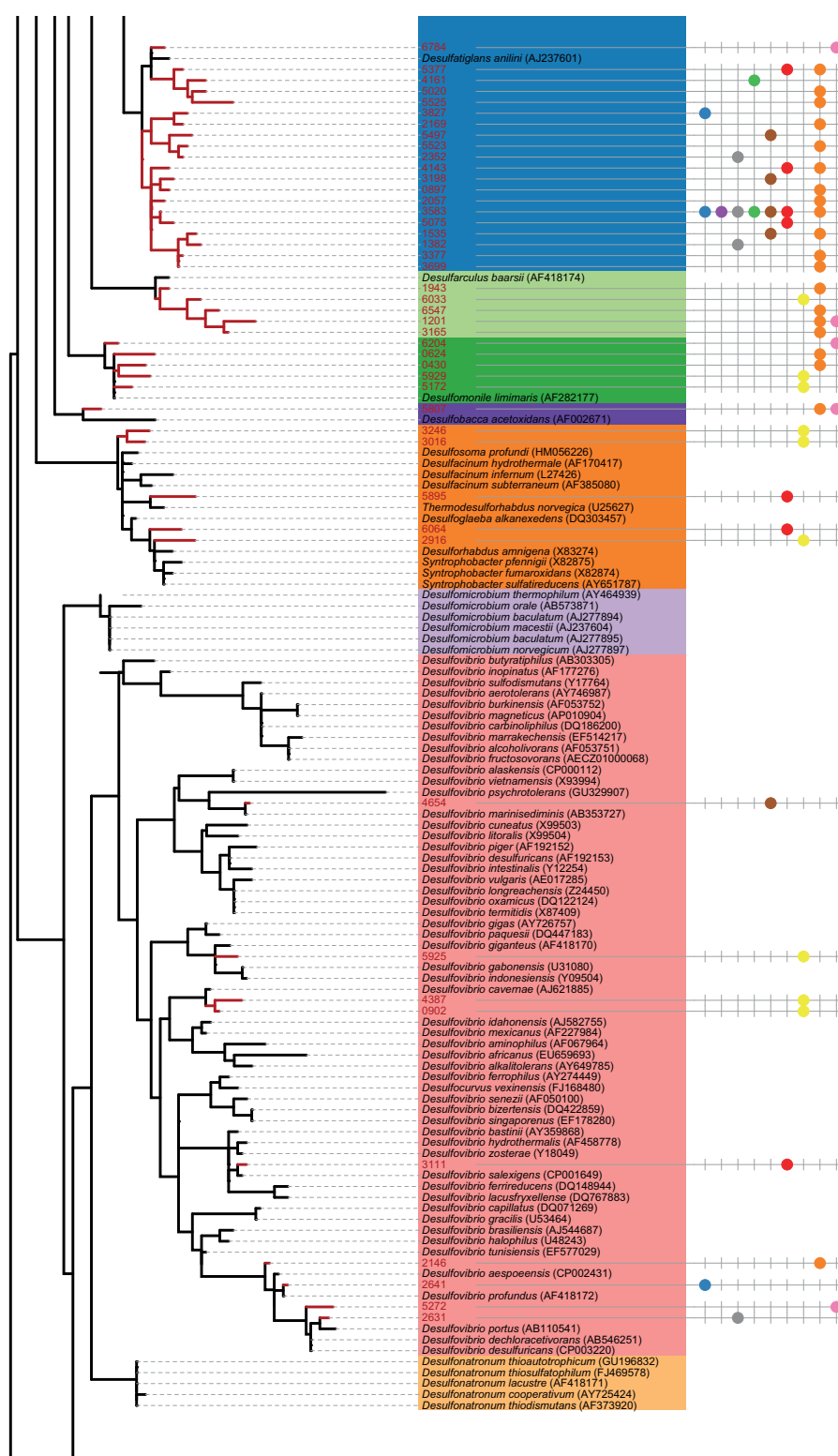
**Phylogeny:**

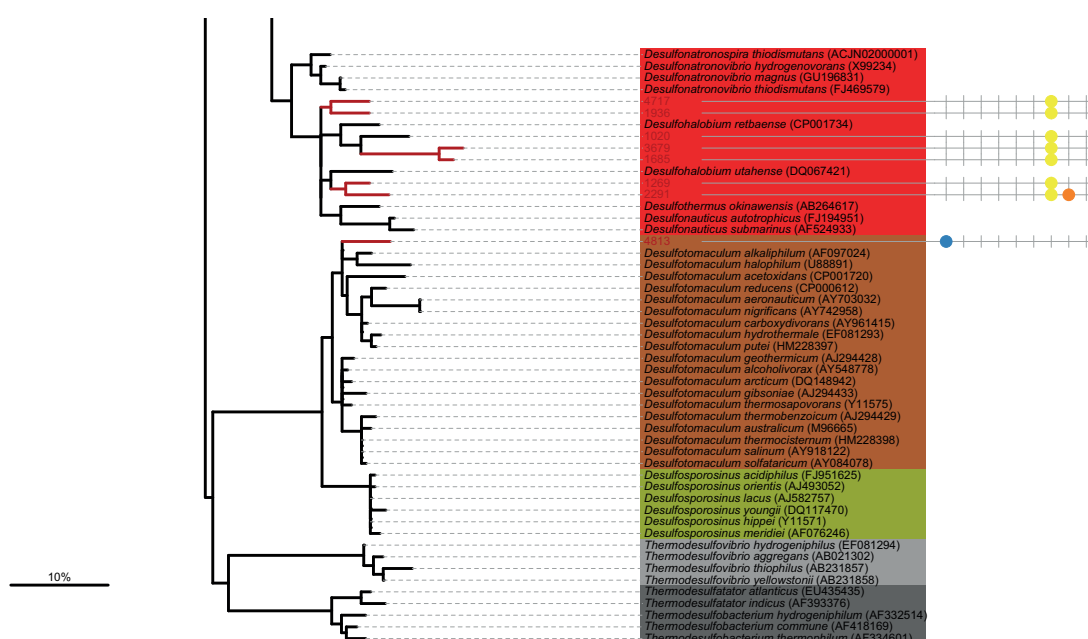
Background color indicates affiliation to family level lineage of known SRM.



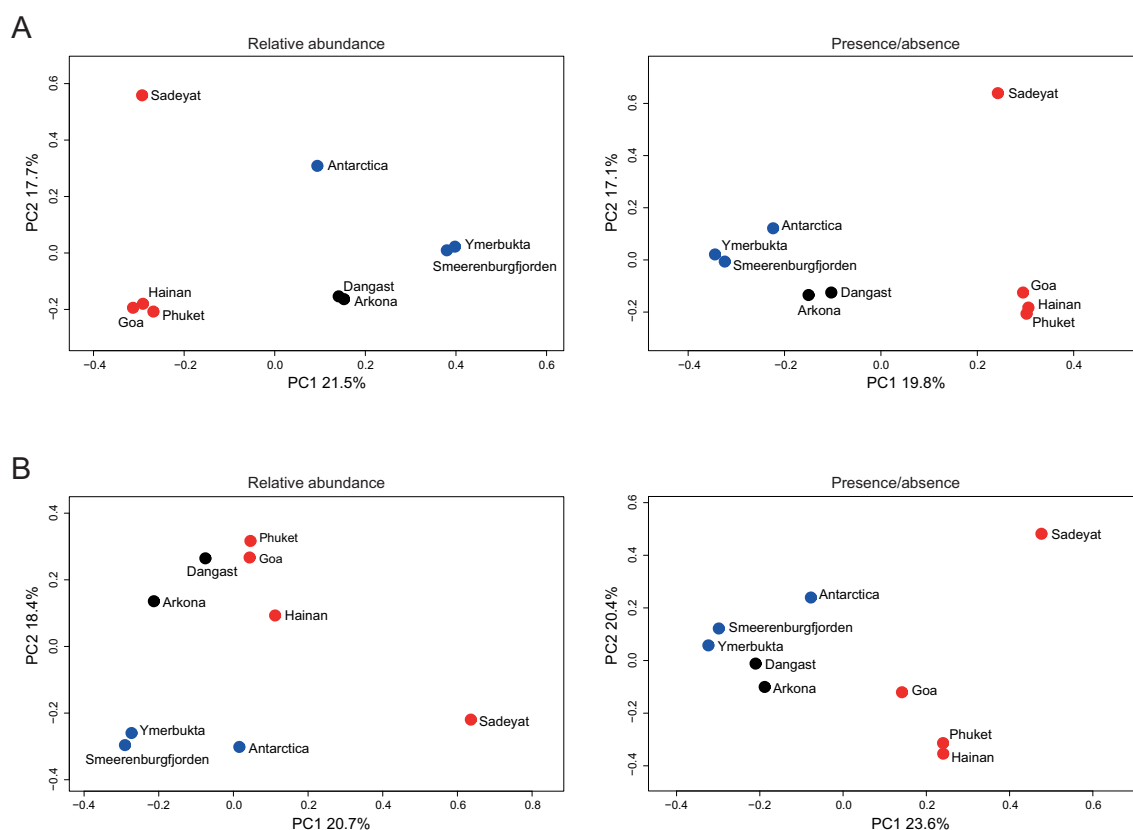








Supplementary Figure S2. 16S rRNA tree showing the affiliation of putative SRM phylotypes. The Maximum likelihood (RAxML) tree was calculated using 167 full-length sequences of described SRM species and further 328 full-length sequences of environmental clones that were most closely related to the sequences of putative SRM phylotypes analyzed in this study. Short sequences of 384 putative SRM are shown in red. Sequences of described SRM are shown in black. Phylogenetic association to a known SRM taxa or lineages is shown by background color. Presence/absence of putative SRM phylotypes at the nine locations is shown by colored dots.



Supplementary Figure S3. Principal coordinates analysis (PCoA) of putative SRM communities (A) and total bacterial communities (B) at each sediment site based on the Bray-Curtis distance metric (both relative abundance and presence-absence variants of the metric). Sites are colored by sampling region into polar (blue), temperate (black), and tropical (red) regions.

Table S1. The significance of environmental factors on community composition was tested using the non-parametric permutational multivariate analysis of variance (perMANOVA).

Significance of variables: Total community

	Df	Sums of Sqs	Mean Sqs	F.Model	R2	Pr(> F)
Temperature	1	0.65578	0.65578	2.429	0.22033	0.001 * **
Salinity	1	0.5768	0.5768	2.1365	0.19379	0.001 * **
C:N ratio	1	0.35262	0.35262	1.3061	0.11847	0.17 3
T:O:C ratio	1	0.31127	0.31127	1.1529	0.10458	0.31 0
Residuals	4	1.07991	0.26998	0.36283		
Total	8	2.97637	1.00000			

Significance of variables: Putative SRM

	Df	Sums of Sqs	Mean Sqs	F.Model	R2	Pr(> F)
Temperature	1	0.63801	0.63801	2.3075	0.21086	0.001 * **
Salinity	1	0.58541	0.58541	2.1173	0.19348	0.001 * **
C:N ratio	1	0.37165	0.37165	1.3442	0.12283	0.098
T:O:C ratio	1	0.32467	0.32467	1.1743	0.10731	0.24 1
Residuals	4	1.10595	0.27649	0.36552		
Total	8	3.0257	1.00000			

Chapter VII

Concluding discussion

Concluding discussion

Sulfate-reducing microorganisms (SRM) are a guild of microbes that is highly relevant for biochemical processes in anoxic ecosystems and has important biotechnological applications, e.g. in bioremediation (Muyzer & Stams, 2008). In my thesis, I used the functional guild of SRM as a starting point to tackle important topics in modern microbial ecology, ranging from the biogeography of microorganisms to biochemical degradation of organic matter and temperature adaptation of microbial communities in marine sediments. The advent of next generation sequencing techniques has brought about a plethora of opportunities for studying the ecology of microorganisms by largely bypassing the need for cultivation and dramatically accelerating ecological and environmental research (Shokralla *et al.*, 2012). The universally present 16S rRNA gene is commonly used as a phylogenetic marker and environmental 16S rRNA gene sequences can be classified based on comparisons to known 16S rRNA gene sequences in databases. Massively parallel sequencing of PCR amplicons of 16S rRNA genes obtained with general bacterial primers allows for phylogenetic characterization of bacterial communities across multiple samples (Huse *et al.*, 2008). It is thus possible to monitor differences in microbial community composition across time and space or in response to changes in environmental conditions at previously unamenable analytical scale and sample throughput. During this thesis, bacterial 16S rRNA gene amplicon pyrosequencing was employed to (i) identify endospores of thermophilic bacteria in marine sediments in hot temperature incubation experiments in order to study the effect of dispersal on marine microbial biogeography, (ii) characterize the response of members of the bacterial community in Arctic marine sediments to substrate addition in order to identify bacteria carrying out specific processes in anoxic psychrophilic carbon degradation, and (iii) identify putative sulfate reducers in order to compare SRM community structure in polar, temperate and tropical marine sediments. However, using only the 16S rRNA gene is inadequate when studying a group of organisms like SRM, who are defined by an ecological function rather than by evolutionary relationship. SRM are phylogenetically heterogeneous and can be found in at least four bacterial and two archaeal phyla. In many of these phyla, SRM are closely related to non-SRM and do not share 16S rRNA sequence homologies that clearly differentiate them from non-SRM. Therefore, it is difficult to identify SRM in environmental samples with 16S rRNA-based approaches, as there is no 16S rRNA-targeting probe or primer available that allows detection of all members of this guild by hybridization or PCR-based techniques. Even with highly multiplexed methods, such as a microarray specifically developed for detection of SRM in the environment (Loy *et al.*, 2002), it is still not possible to identify novel SRM in the environment. However, most SRM share a common pathway for sulfate reduction and genes involved in this pathway, most importantly *dsrAB*, can be used as functional marker genes for SRM (Wagner *et al.*, 2005).

Cloning-based environmental studies targeting *dsrAB* and metagenomic studies have produced a great amount of environmental *dsrAB* sequence data. Yet so far, next generation sequencing methods have not been used for large-scale *dsrAB* amplicon sequencing. For high throughput sequencing of *dsrAB* genes to be viable, a comprehensive *dsrAB* reference database is required in order to provide a phylogenetic framework and classification system that enables quick interpretation of the large amount of obtained sequence data using established bioinformatics pipelines (Schloss *et al.*, 2009; Caporaso *et al.*, 2010; Pester *et al.*, 2012b; Pester *et al.*, 2013). Therefore, within the framework of an extensive *dsrAB* diversity survey (Müller *et al.*, 2014b), we

compiled a reference database containing 7956 full length and partial *dsrAB* sequences of high quality and sufficient length (at least 300 nucleotides of sequence information in the region used for phylogenetic inference). We established a robust DsrAB phylogeny by constructing a phylogenetic consensus tree based on different methods of phylogeny reconstruction, ranging from maximum likelihood and maximum parsimony to neighbor joining. Also, we developed a hierarchical operational classification system for *dsrAB* sequences by combining the taxonomic information from cultivated and/or genome sequenced organisms with newly developed operational taxonomic units (OTUs) for environmental sequences. The classification system encompasses multiple phylogenetic levels for categorizing *dsrAB* sequences, ranging from DsrAB enzyme families that reflect reductive or oxidative DsrAB types of bacterial or archaeal origin over superclusters to family-level DsrAB lineages. The publication of a comprehensive *dsrAB*/DsrAB reference database (available for download at www.microbial-ecology.net/download) containing all publicly available *dsrAB* nucleotide and inferred DsrAB amino acid sequences that were manually aligned, phylogenetically classified and environmentally annotated now allows researchers to easily classify obtained *dsrAB* sequences and integrate them into the consensus phylogeny. Together with a set of recommended primers based on *in silico* evaluation of all published *dsrAB*-targeted primers and the accessibility of the reference database via the probeCheck webserver (www.microbial-ecology.net/probecheck), which allows for straightforward *in silico* testing of primer specificity and coverage, this provides a solid foundation for future studies assessing *dsrAB* diversity.

We categorized the known *dsrAB* diversity present in our database. A large proportion (35%) of reductive bacterial type DsrAB sequences are not affiliated with known taxa (i.e. families, genera) represented by cultured organisms. The number of proposed uncultured DsrAB lineages (i.e. family-level lineages that contain no cultivated representatives) (Pester *et al.*, 2012a) was expanded to 13 and now 90% of reductive bacterial type DsrAB sequences are affiliated with described taxonomic families or these uncultured family-level lineages. The minimum number of *dsrAB*-containing species that is represented by this dataset was estimated by determining a species-level *dsrAB* sequence identity cutoff of 90% that is equivalent to the frequently used 99% sequence identity threshold on 16S rRNA level (Stackebrandt & Ebers, 2006). This demonstrated that a large fraction of putative SRM species is still unidentified as reductive bacterial type DsrAB sequences represent at least 647 species-level OTUs, which is almost three times the number of species of SRM currently present in the List of Bacterial Names with Standing in Nomenclature (Euzéby, 1997). Sequences were also assigned to broad environmental categories based on environmental origin (marine, estuarine, freshwater, soil, and industrial) or microbial lifestyle (thermophilic, alkali-/halophilic, and symbiotic) in order to provide insight into the environmental distribution of the major phylogenetic DsrAB lineages. Most members of these lineages are widely distributed among different environments, yet a few showed signs of environmental preference. Most notably, sequences of uncultured family-level lineages 2, 3 and 4 are almost exclusively derived from marine environments, whereas *Desulfohalobiaceae* and *Desulfonatronumaceae* sequences predominantly originated from high-salt and/or high-pH environments.

Furthermore, we used the database to reanalyze the evolutionary history of *dsrAB*. Paralogous rooting analysis added support to the proposed early evolution of DsrAB as a reductive enzyme (Wagner *et al.*, 1998) by showing that the reductive archaeal type DsrAB family and the unusual second DsrAB copy of *Moorella thermoacetica* represent the deepest branches in the DsrAB tree,

whereas the separation of the oxidative bacterial type DsrAB family (containing mostly DsrAB of sulfur-oxidizing bacteria) from the reductive bacterial DsrAB family (containing mostly but not exclusively DsrAB from SRM) occurred later in evolution. Construction of a robust consensus phylogeny with an up-to-date dataset created an overarching phylogenetic framework of reductive bacterial, oxidative bacterial, and reductive archaeal type DsrAB sequences and integrated, for the first time, novel DsrAB sequences from phyla previously not known to contain *dsrAB* genes, namely *Actinobacteria*, *Aigarchaeota*, and *Caldiserica*. These novel sequences were shown to be part of the *Firmicutes* group *sensu lato*, a diverse and phylogenetically relatively unstable group containing the non-laterally acquired DsrAB sequences of *Firmicutes* and a large number of uncultured and unclassified environmental DsrAB sequences. The recently published DsrAB sequence of *Candidatus Magnetobacterium casensis* (Lin *et al.*, 2014) was placed together with DsrAB of closely related *Thermodesulfovibrio* species (both belong to the family *Nitrospiraceae*) into the same supercluster, which was hence renamed from *Thermodesulfovibrio* supercluster (Pester *et al.*, 2012a) to *Nitrospirae* supercluster. Lateral acquisition of *dsrAB* has already been documented for members of the genus *Archaeoglobus*, the phylum *Thermodesulfobacteria*, and a group of *Firmicutes* (Klein *et al.*, 2001; Zverlov *et al.*, 2005). Evidence for further possible lateral gene transfer was obtained from phylogenetic analyses that indicated that members of the phyla *Actinobacteria*, *Aigarchaeota*, and *Caldiserica* could have acquired their *dsrAB* copies laterally. It remains to be seen, whether more members of these phyla carry reductive type *dsrAB* genes and whether these organisms employ DsrAB for sulfate reduction. If the latter is the case, it would convincingly demonstrate the power of *dsrAB* as functional marker to uncover novel SRM in the environment. If not, it might be necessary to re-evaluate our understanding of the functionality of DsrAB. In this context, cultivation and subsequent physiological characterization will still be a valuable source of information. In the future, more and more microbial genomes will become available. This will indubitably lead to the phylogenetic identification of those *dsrAB* lineages that are so far only represented by environmental sequences and will thereby further increase the value of *dsrAB* as a functional marker for assessing the diversity of SRM and sulfur-oxidizing bacteria in the environment.

Even though the use of functional markers like *dsrAB* is tremendously useful for assessing the environmental diversity of a functional group like SRM, the approach has some inherent limitations. The presence of specific genes does not provide information about the activity of a certain organism and it is not possible to reliably determine ecological function by sequencing efforts alone. Linking metabolic function to phylogenetic identity is one of the major challenges in microbial ecology. A technique commonly used for linking the identity of microorganisms to their function is stable isotope probing, which relies on the incorporation of a substrate labeled with a stable isotope, such as ^{13}C , by active microorganisms. These microorganisms can then be identified by selective recovery and analysis of isotope-enriched biomarkers, such as DNA or rRNA (reviewed in Radajewski *et al.* (2003), Dumont & Murrell (2005), Friedrich (2006), and Neufeld *et al.* (2007)). We employed stable isotope probing in order to link identity and function of bacteria involved in carbon degradation in Arctic marine sediments. So far, several psychrophiles from Arctic marine sediments have been cultivated and metabolically characterized (Knoblauch *et al.*, 1999; Knittel *et al.*, 2005; Vandieken *et al.*, 2006). However, these cultured organisms may not necessarily be the important drivers of biochemical nutrient cycling *in situ*. A few 16S rRNA based studies have characterized bacterial communities in Arctic marine sediments (Ravenschlag *et al.*, 1999; Ravenschlag *et al.*, 2001; Li *et al.*, 2009; Teske *et al.*, 2011; Hamdan *et al.*, 2013), but linking microbial identities to specific functions

has so far only been attempted for SRM (Sahm *et al.*, 1999; Ravenschlag *et al.*, 2000). We incubated samples of an Arctic marine sediment with ^{13}C -labeled acetate and whole cell cyanobacterial biomass (spirulina) in order to directly identify microorganisms that are involved in the cascade of complex carbon degradation in these sediments (Müller *et al.*, manuscript in preparation). Experiments demonstrating the incorporation of ^{13}C into biomass with a combination of fluorescence *in situ* hybridization with Raman spectroscopy or high-resolution secondary ion mass spectrometry (NanoSIMS) are still ongoing. Nevertheless, biochemical and sequencing data obtained over the course of these incubations already provided valuable insights into the response of the psychrophilic bacterial community to the addition of specific substrates. Measuring the concentration of volatile fatty acids and sulfate reduction rates revealed that acetate, formate, and propionate were the major fermentation products during the degradation of cyanobacterial biomass and that acetate, propionate, butyrate, and valerate were the main substrates preferred by the SRM community. The response of individual bacterial phylotypes to the addition of substrate was tracked by 16S rRNA gene and cDNA amplicon sequencing over the course of the incubations, which provided an important starting point for understanding the microbial dynamics during carbon degradation in Arctic marine sediments. Comparisons between the labeled incubations with the corresponding time points from the unlabeled, sulfate reduction-inhibited and no substrate controls led to the identification of the primary degraders of acetate and cyanobacterial biomass and the putative sulfate reducers that are active in this sediment. Phylotypes classified as *Psychrilyobacter* (*Fusobacteria*), *Colwellia* (*Gammaproteobacteria*), *Marinifilum* (*Bacteroidetes*), and *Psychromonas* (*Gammaproteobacteria*) were likely the primary degraders of cyanobacterial biomass that was added in the form of freeze-dried spirulina and phylotypes classified as *Desulfobacteraceae*, *Desulfobulbaceae*, and *Arcobacter* were the primary degraders of acetate. Most sulfate reduction-associated phylotypes belonged to the families *Desulfobacteraceae* and *Desulfobulbaceae*. Identification of these phylotypes now enables the design of specific probes targeting their 16S rRNA to confirm substrate incorporation by these organisms by combining fluorescence *in situ* hybridization with Raman spectroscopy or NanoSIMS and thereby provides a solid basis for directly linking identity and function of carbon degrading bacteria in these sediments.

Overall carbon mineralization rates in Arctic marine sediments are mainly controlled by substrate availability rather than by *in situ* temperature (Arnosti *et al.*, 1998; Finke & Jørgensen, 2008), suggesting that microbial communities in marine sediments are well adapted to the prevailing temperatures. We investigated natural sulfate-reducing communities of polar, temperate, and tropical marine sediments by combining respiration rate measurements with phylogenetic community analysis (Robador *et al.*, manuscript in preparation) and could show that the observed thermal response of SRM is a trait of the temperature adaptation of the sulfate-reducing community. The optimal temperature for sulfate reduction was regulated by mean ambient temperature and the community structure of putative SRM correlated of with mean annual temperature, but not with sediment organic carbon concentrations or C:N ratios of organic matter, indicating that temperature structures the sulfate-reducing community by selecting for different SRM that are best adapted to the prevailing temperatures.

Changes in environmental conditions like substrate input and temperature lead to changes in microbial community composition, as microorganisms that are better adapted to take advantage of the new conditions will be more successful. However, in order to be able to be selected for by the

environmental conditions, microorganisms must first be able to arrive in a given habitat. Thus, environmental selection and passive dispersal work in concert to create biogeographic patterns of microorganisms (Martiny *et al.*, 2006; Ramette & Tiedje, 2007; Hanson *et al.*, 2012). Endospores of thermophilic bacteria are not influenced by environmental selection in cold and temperate marine sediments, therefore they represent ideal model organism for studying the effect of passive dispersal on the distribution of microorganisms in the oceans. A biogeography study (Müller *et al.*, 2014a) of such endospores revealed widespread but not ubiquitous distribution of these dormant members of the rare biosphere. The non-uniform distribution patterns of thermophilic endospore phylotypes (“thermospore phylotypes”) provided, for the first time, evidence of dispersal limitation affecting the biogeography of bacterial endospores. This is particularly noteworthy considering that they are, based on their inherent properties of high durability and longevity, much less likely to be dispersal limited than vegetative cells. Analysis of global biogeography patterns of thermospore phylotypes in marine sediments suggested that relative isolation from global ocean circulation negatively influences thermospore phylotype richness and highlighted possible global dispersal routes of marine microorganisms. Passive dispersal was shown to be influenced by the connectivity of local water masses to ocean circulation. Focus on two Arctic regional sample sets from the Baffin Bay and the archipelago of Svalbard showed that local hydrography shapes the distribution of thermospore phylotypes. These findings corroborate recent studies of vegetative microbial communities that have suggested that hydrography and comparably increased geographic isolation of the Arctic Ocean represent an effective dispersal barrier for microorganisms (Galand *et al.*, 2010; Ghiglione *et al.*, 2012; Hamdan *et al.*, 2013; Sul *et al.*, 2013). A widely distributed core of frequently co-occurring thermospore phylotypes was identified that possibly shares common sources and/or travel routes in the oceans. Previously, the diversity of endospores of thermophilic bacteria in marine sediments was only studied at a few selected sites and was thought to mainly consist of members of the families *Peptococcaceae* and *Clostridiaceae* (Hubert *et al.*, 2009; Hubert *et al.*, 2010; Ji *et al.*, 2012; de Rezende *et al.*, 2013). We characterized the communities of thermophilic endospore-forming bacteria at 81 different marine locations and showed that thermospore phylotypes are widely but not ubiquitously distributed. Thereby, we greatly increased the knowledge about their diversity and showed that also members of the family *Bacillaceae* were frequently a significant component of these communities. In addition, hydrothermal sediments of the Guaymas Basin were identified as a possible source environment. Not only do they exhibit all the biogeochemical and geological characteristics that were proposed for a potential source environment of marine thermophiles (Hubert *et al.*, 2009; Hubert *et al.*, 2010; de Rezende *et al.*, 2013) – sufficiently high temperature to allow vegetative growth and sufficiently strong fluxes from these environments into the water column for physical transport of cells into the circulating seawater - but they also contain a high richness of thermospore phylotypes and a high number of cosmopolitan phylotypes despite relative geographic isolation. Future research on thermophilic endospores in marine sediments promises further elucidation of microbial distribution pathways in the world oceans and they can be used to test further biogeographical hypotheses. The discovery of the actual source environments of these spores remains a most intriguing challenge. If endospores of thermophilic bacteria are released into the water column via fluid flow from the hot subsurface, they could potentially be used as bioindicators for deep deposits of oil and gas and might thus serve as prospecting agents in oil and gas exploration (Hubert & Judd, 2010).

Altogether, the research presented in this thesis contributes to the knowledge about the phylogenetic and environmental diversity of SRM and other *dsrAB*-containing microorganisms, elucidates structure and function of bacterial communities in Arctic marine sediments, and provides new perspectives on how passive dispersal and temperature shape microbial biogeography.

References

- Arnosti C, Jørgensen BB, Sagemann J, Thamdrup B. (1998). Temperature dependence of microbial degradation of organic matter in marine sediments: polysaccharide hydrolysis, oxygen consumption, and sulfate reduction. *Mar Ecol Prog Ser* **165**: 59-70.
- Caporaso JG, Kuczynski J, Stombaugh J, Bittinger K, Bushman FD, Costello EK *et al.* (2010). QIIME allows analysis of high-throughput community sequencing data. *Nat Methods* **7**: 335-336.
- de Rezende JR, Kjeldsen KU, Hubert CRJ, Finster K, Loy A, Jørgensen BB. (2013). Dispersal of thermophilic *Desulfotomaculum* endospores into Baltic Sea sediments over thousands of years. *ISME J* **7**: 72-84.
- Dumont MG, Murrell JC. (2005). Stable isotope probing - linking microbial identity to function. *Nat Rev Microbiol* **3**: 499-504.
- Euzéby JP. (1997). List of Bacterial Names with Standing in Nomenclature: a folder available on the Internet. *Int J Syst Bacteriol* **47**: 590-592.
- Finke N, Jørgensen BB. (2008). Response of fermentation and sulfate reduction to experimental temperature changes in temperate and Arctic marine sediments. *ISME J* **2**: 815-829.
- Friedrich MW. (2006). Stable-isotope probing of DNA: insights into the function of uncultivated microorganisms from isotopically labeled metagenomes. *Curr Opin Biotech* **17**: 59-66.
- Galand PE, Potvin M, Casamayor EO, Lovejoy C. (2010). Hydrography shapes bacterial biogeography of the deep Arctic Ocean. *ISME J* **4**: 564-576.
- Ghiglione JF, Galand PE, Pommier T, Pedrós-Alió C, Maas EW, Bakker K *et al.* (2012). Pole-to-pole biogeography of surface and deep marine bacterial communities. *Proc Natl Acad Sci U S A* **109**: 17633-17638.
- Hamdan LJ, Coffin RB, Sikaroodi M, Greinert J, Treude T, Gillevet PM. (2013). Ocean currents shape the microbiome of Arctic marine sediments. *ISME J* **7**: 685-696.
- Hanson CA, Fuhrman JA, Horner-Devine MC, Martiny JBH. (2012). Beyond biogeographic patterns: processes shaping the microbial landscape. *Nat Rev Microbiol* **10**: 497-506.
- Hubert C, Loy A, Nickel M, Arnosti C, Baranyi C, Brüchert V *et al.* (2009). A Constant Flux of Diverse Thermophilic Bacteria into the Cold Arctic Seabed. *Science* **325**: 1541-1544.
- Hubert C, Arnosti C, Brüchert V, Loy A, Vandieken V, Jørgensen BB. (2010). Thermophilic anaerobes in Arctic marine sediments induced to mineralize complex organic matter at high temperature. *Environmental microbiology* **12**: 1089-1104.
- Hubert C, Judd A. (2010). Using microorganisms as prospecting agents in oil and gas exploration. *Handbook of Hydrocarbon and Lipid Microbiology Springer-Verlag: Berlin, Heidelberg*.
- Huse SM, Dethlefsen L, Huber JA, Welch DM, Relman DA, Sogin ML. (2008). Exploring microbial diversity and taxonomy using SSU rRNA hypervariable tag sequencing. *PLoS Genet* **4**: e1000255.
- Ji S, Wang S, Tan Y, Chen X, Schwarz W, Li F. (2012). An untapped bacterial cellulolytic community enriched from coastal marine sediment under anaerobic and thermophilic conditions. *FEMS Microbiol Lett* **335**: 39-46.
- Klein M, Friedrich M, Roger AJ, Hugenholtz P, Fishbain S, Abicht H *et al.* (2001). Multiple lateral transfers of dissimilatory sulfite reductase genes between major lineages of sulfate-reducing prokaryotes. *J Bacteriol* **183**: 6028-6035.
- Knittel K, Kuever J, Meyerdierks A, Meinke R, Amann R, Brinkhoff T. (2005). *Thiomicrospira arctica* sp. nov. and *Thiomicrospira psychrophila* sp. nov., psychrophilic, obligately chemolithoautotrophic, sulfur-oxidizing bacteria isolated from marine Arctic sediments. *Int J Syst Evol Microbiol* **55**: 781-786.
- Knoblauch C, Sahm K, Jørgensen BB. (1999). Psychrophilic sulfate-reducing bacteria isolated from permanently cold arctic marine sediments: description of *Desulfofrigus oceanense* gen. nov., sp. nov., *Desulfofrigus fragile* sp. nov., *Desulfofaba gelida* gen. nov., sp. nov., *Desulfotalea psychrophila* gen. nov., sp. nov. and *Desulfotalea arctica* sp. nov. *Int J Syst Bacteriol* **49 Pt 4**: 1631-1643.

- Li H, Yu Y, Luo W, Zeng Y, Chen B. (2009). Bacterial diversity in surface sediments from the Pacific Arctic Ocean. *Extremophiles* **13**: 233-246.
- Lin W, Deng A, Wang Z, Li Y, Wen T, Wu LF *et al.* (2014). Genomic insights into the uncultured genus 'Candidatus Magnetobacterium' in the phylum Nitrospirae. *ISME J* **8**: 2463-2477.
- Loy A, Lehner A, Lee N, Adamczyk J, Meier H, Ernst J *et al.* (2002). Oligonucleotide microarray for 16S rRNA gene-based detection of all recognized lineages of sulfate-reducing prokaryotes in the environment. *Appl Environ Microbiol* **68**: 5064-5081.
- Martiny JBH, Bohannan BJM, Brown JH, Colwell RK, Fuhrman JA, Green JL *et al.* (2006). Microbial biogeography: putting microorganisms on the map. *Nat Rev Microbiol* **4**: 102-112.
- Müller AL, de Rezende JR, Hubert C, Kjeldsen KU, Lagkourados I, Berry D *et al.* (2014a). Endospores of thermophilic bacteria as tracers of microbial dispersal by ocean currents. *ISME J* **8**: 1153-1165.
- Müller AL, Kjeldsen KU, Rattei T, Pester M, Loy A. (2014b). Phylogenetic and environmental diversity of DsrAB-type dissimilatory (bi)sulfite reductases. *ISME J*.
- Müller AL, de Rezende JR, Putz M, Kjeldsen KU, Jørgensen BB, Loy A. Bacterial community response during degradation of cyanobacterial biomass and acetate in a sulfate-reducing Arctic fjord sediment. Manuscript in preparation.
- Muyzer G, Stams AJ. (2008). The ecology and biotechnology of sulphate-reducing bacteria. *Nat Rev Microbiol* **6**: 441-454.
- Neufeld JD, Wagner M, Murrell JC. (2007). Who eats what, where and when? Isotope-labelling experiments are coming of age. *ISME J* **1**: 103-110.
- Pester M, Knorr KH, Friedrich MW, Wagner M, Loy A. (2012a). Sulfate-reducing microorganisms in wetlands - fameless actors in carbon cycling and climate change. *Front Microbiol* **3**: 72.
- Pester M, Rattei T, Flechl S, Gröngroft A, Richter A, Overmann J *et al.* (2012b). amoA-based consensus phylogeny of ammonia-oxidizing archaea and deep sequencing of amoA genes from soils of four different geographic regions. *Environ Microbiol* **14**: 525-539.
- Pester M, Maixner F, Berry D, Rattei T, Koch H, Lüscher S *et al.* (2013). NxrB encoding the beta subunit of nitrite oxidoreductase as functional and phylogenetic marker for nitrite-oxidizing Nitrospira. *Environ Microbiol* **16**: 3055-71.
- Radajewski S, McDonald IR, Murrell JC. (2003). Stable-isotope probing of nucleic acids: a window to the function of uncultured microorganisms. *Curr Opin Biotech* **14**: 296-302.
- Ramette A, Tiedje JM. (2007). Biogeography: an emerging cornerstone for understanding prokaryotic diversity, ecology, and evolution. *Microb Ecol* **53**: 197-207.
- Ravenschlag K, Sahm K, Pernthaler J, Amann R. (1999). High bacterial diversity in permanently cold marine sediments. *Appl Environ Microbiol* **65**: 3982-3989.
- Ravenschlag K, Sahm K, Knöblach C, Jørgensen BB, Amann R. (2000). Community structure, cellular rRNA content, and activity of sulfate-reducing bacteria in marine arctic sediments. *Appl Environ Microbiol* **66**: 3592-3602.
- Ravenschlag K, Sahm K, Amann R. (2001). Quantitative molecular analysis of the microbial community in marine arctic sediments (Svalbard). *Appl Environ Microbiol* **67**: 387-395.
- Robador A, Müller AL, Sawicka JE, Berry D, Hubert C, Loy A *et al.* Activity and community structures of sulfate-reducing microorganisms in polar, temperate and tropical marine sediments. Manuscript in preparation.
- Sahm K, Knöblach C, Amann R. (1999). Phylogenetic affiliation and quantification of psychrophilic sulfate-reducing isolates in marine arctic sediments. *Appl Environ Microbiol* **65**: 3976-3981.
- Schloss PD, Westcott SL, Ryabin T, Hall JR, Hartmann M, Hollister EB *et al.* (2009). Introducing mothur: open-source, platform-independent, community-supported software for describing and comparing microbial communities. *Appl Environ Microbiol* **75**: 7537-7541.
- Shokralla S, Spall JL, Gibson JF, Hajibabaei M. (2012). Next-generation sequencing technologies for environmental DNA research. *Mol Ecol* **21**: 1794-1805.
- Stackebrandt E, Ebers J. (2006). Taxonomic parameters revisited: tarnished gold standards. *Microbiology Today* **33**: 152.
- Sul WJ, Oliver TA, Ducklow HW, Amaral-Zettler LA, Sogin ML. (2013). Marine bacteria exhibit a bipolar distribution. *Proc Natl Acad Sci U S A* **110**: 2342-2347.
- Teske A, Durbin A, Zieveling K, Cox C, Arnosti C. (2011). Microbial community composition and function in permanently cold seawater and sediments from an arctic fjord of svalbard. *Appl Environ Microbiol* **77**: 2008-2018.

- Vandieken V, Mussmann M, Niemann H, Jørgensen BB. (2006). *Desulfuromonas svalbardensis* sp. nov. and *Desulfuromusa ferrireducens* sp. nov., psychrophilic, Fe(III)-reducing bacteria isolated from Arctic sediments, Svalbard. *Int J Syst Evol Microbiol* **56**: 1133-1139.
- Wagner M, Roger AJ, Flax JL, Brusseau GA, Stahl DA. (1998). Phylogeny of dissimilatory sulfite reductases supports an early origin of sulfate respiration. *J Bacteriol* **180**: 2975-2982.
- Wagner M, Loy A, Klein M, Lee N, Ramsing NB, Stahl DA *et al.* (2005). Functional marker genes for identification of sulfate-reducing prokaryotes. *Method Enzymol* **397**: 469-489.
- Zverlov V, Klein M, Lucker S, Friedrich MW, Kellermann J, Stahl DA *et al.* (2005). Lateral gene transfer of dissimilatory (bi)sulfite reductase revisited. *J Bacteriol* **187**: 2203-2208.

Chapter VIII

Summary & Zusammenfassung

Summary

Sulfate-reducing microorganisms (SRM) are ubiquitous in anoxic habitats, where they fulfill an important role in the biochemical cycling of sulfur and carbon by using sulfate as terminal electron acceptor in the degradation of organic compounds. In this thesis, I focused on SRM and used them in my research as model organisms to study the ecophysiology and biogeography of microorganisms in marine sediments.

The last and main energy-conserving step during sulfate respiration is the reduction of sulfite to sulfide. It is catalyzed by the dissimilatory (bi)sulfite reductase (DsrAB), which can also perform the reverse reaction in some sulfur-oxidizing bacteria. DsrAB genes are commonly used as functional markers for SRM and sulfur-oxidizing bacteria and an extensive amount of largely uncharacterized *dsrAB* sequence data has thus accumulated in public databases. In order to establish a foundation for large-scale *dsrAB* ecology studies with next-generation sequencing methods, we compiled a comprehensive, manually curated *dsrAB*/DsrAB reference database. We used this database to construct a robust DsrAB consensus phylogeny and to evaluate the coverage of all published *dsrAB*-targeted primers. Furthermore, we systematically categorized all environmental *dsrAB* sequences according to a new operational classification system at multiple taxonomic and phylogenetic levels. Environmental *dsrAB* sequences constituted at least 13 stable family-level lineages without any cultivated representatives, suggesting that major SRM taxa have not yet been identified. Additionally, we investigated the environmental distribution of the major phylogenetic DsrAB lineages by assigning *dsrAB* sequences to broad categories based on environmental origin or lifestyle. Most sequences are derived from marine environments (31%), followed by freshwater (24%), industrial (16%) and soil environments (11%). Members of most major DsrAB lineages are widely distributed among various different environments with a few exceptions that are indicative of environmental preference. Most notably, sequences of uncultured DsrAB family-level lineages 2, 3 and 4 were almost exclusively of marine origin, whereas sequences assigned to the deltaproteobacterial families *Desulfohalobiaceae* and *Desulfonatronumaceae* derive predominantly from high-salt and/or high-pH environments. Furthermore, we reanalyzed the evolutionary history of *dsrAB*. We obtained evidence for possible lateral gene transfer of *dsrAB* in members of phyla in which *dsrAB* has only recently been discovered, namely *Actinobacteria*, *Aigarchaeota*, and *Caldiserica*, and provided support for the proposed early evolution of DsrAB as a reductive enzyme.

We investigated the degradation of organic matter in anoxic Arctic marine sediments, during which SRM perform a crucial role by catalyzing the terminal carbon mineralization step. Incubations were amended with cyanobacterial biomass as a model substrate mixture for complex organic matter input and acetate as a typical degradation intermediate and the response of the microbial community was monitored by 16S rRNA gene and cDNA amplicon pyrosequencing. The main fermentation products of cyanobacterial biomass were acetate, formate, and propionate and the consumption of acetate, propionate, butyrate, and valerate was selectively impacted by SRM. Bacterial 16S rRNA phylotype dynamics suggested that phylotypes classified as *Psychrilyobacter*, *Colwellia*, *Marinifilum*, and *Psychromonas* were the primary degraders of cyanobacterial biomass while acetate was mainly utilized by phylotypes classified as *Desulfobacteraceae*, *Desulfobulbaceae*, and *Arcobacter*. Additionally, several putative sulfate-reducing phylotypes were identified among the deltaproteobacterial families *Desulfobacteraceae* and *Desulfobulbaceae*. Identification of these

phylotypes provides a foundation for directly linking identity and function of carbon degrading bacteria in these sediments by enabling the design of specific probes to confirm substrate incorporation by combining fluorescence *in situ* hybridization with Raman spectroscopy or NanoSIMS.

Cold marine sediments frequently harbor endospores of thermophilic bacteria in addition to the vegetative microbial community. These seemingly misplaced organisms, which are dormant and not subject to environmental selection, were used to selectively investigate the contribution of passive dispersal to microbial biogeography. We conducted a global experimental survey of thermophilic endospores in 81 different marine sediments. We could show that they are widely but not ubiquitously distributed and identified 146 species-level 16S rRNA phylotypes. Non-uniform spatial distribution patterns of these phylotypes provided evidence of dispersal limitation in bacterial endospores, which are, based on their inherent properties like high durability and longevity, much less likely to be dispersal limited than vegetative cells. Possible global dispersal routes of marine microorganisms were highlighted by using network analysis to identify frequently co-occurring phylotypes that were widely distributed across great distances. Oceanic regions with increased isolation from global ocean currents were characterized by lower thermophilic endospore richness, suggesting that the impact of passive dispersal on marine microbial biogeography is controlled by the connectivity of local water masses to ocean circulation. Closer investigation of two Arctic regions, the Svalbard archipelago and the Baffin Bay, showed that local hydrography shapes the distribution of thermophilic endospores.

The biogeographic patterns of vegetative cells, in contrast to those of endospores, are in large part due to environmental factors, such as temperature. In order to gain an understanding of the temperature-dependent distribution and diversity of microorganisms in marine ecosystems, we investigated the thermal response of SRM communities in polar, temperate, and tropical marine sediments. We could show that the optimal temperature for sulfate reduction was regulated by the mean ambient temperature and that the community structure of putative SRM correlated with mean annual temperature, but not with sediment organic carbon concentrations or C:N ratios of organic matter. This indicates that temperature structures the sulfate-reducing community by selecting for different SRM that are best adapted to the prevailing temperatures and implies that temperature is a major determinant of microbial community composition in marine sediments.

In summary, the research presented in this thesis comprises an encompassing analysis of environmental diversity and phylogeny of SRM and other *dsrAB*-containing organisms, begins linking the identity of members of the bacterial community in Arctic marine sediments to their role during the degradation of organic matter, and provides new perspectives on how passive dispersal and temperature shape microbial community composition in the sea floor.

Zusammenfassung

Sulfatreduzierende Mikroorganismen (SRM) findet man in nahezu allen anoxischen Lebensräumen. Dort verwenden sie Sulfat als Elektronenakzeptor beim Abbau von organischen Verbindungen und tragen damit entscheidend zu den biochemischen Kreisläufen von Schwefel und Kohlenstoff bei. In dieser Dissertation beschäftigte ich mich hauptsächlich mit SRM und verwendete diese funktionelle Gruppe als Modellorganismen, um mehr über die generelle Ökophysiologie und Biogeographie von Mikroorganismen in marinen Sedimenten herauszufinden.

Der letzte und energiekonservierende Schritt während der Reduktion von Sulfat durch SRM ist die Reduktion von Sulfit zu Sulfid. Katalysiert wird er durch ein Enzym namens Dissimilatorische (Bi-) Sulfitreduktase (DsrAB), einem Protein das in manchen schwefeloxidierenden Bakterien auch die umgekehrte Reaktion durchführen kann. DsrAB Gene werden häufig als funktionelle Marker für SRM und schwefeloxidierende Bakterien verwendet, was zur Anhäufung einer umfangreichen Menge an größtenteils uncharakterisierten *dsrAB* Sequenzen in öffentlichen Datenbanken geführt hat. Um eine Grundlage für großangelegte, *dsrAB*-basierte Ökologiestudien mit Hilfe moderner Sequenzierungsmethoden zu schaffen, erstellten wir eine umfassende, manuell kuratierte *dsrAB*/DsrAB Referenzdatenbank. Diese Datenbank verwendeten wir zur Erstellung einer stabilen DsrAB Konsensusphylogenie und zur Evaluierung der Abdeckung aller publizierten, *dsrAB*-spezifischen Primer. Außerdem konnten wir mit Hilfe eines neuentwickelten, mehrstufigen Klassifikationssystems erstmals alle *dsrAB*-Umweltsequenzen systematisch mehreren taxonomischen und/oder phylogenetischen Gruppen zuordnen. Mindestens 13 stabile phylogenetische Linien im Rang einer Familie beinhalteten keine *dsrAB* Sequenzen von bekannten, kultivierten Organismen, sondern ausschließlich Umweltsequenzen, was darauf hindeutet, dass bedeutende SRM-Taxa bislang noch nicht identifiziert wurden. Darüber hinaus wurden alle *dsrAB*-Sequenzen in weitgefaste Kategorien basierend auf ihrer ökologischen Herkunft oder Lebensweise eingeteilt und die Verbreitung der größeren phylogenetischen DsrAB-Linien in der Umwelt untersucht. Die meisten *dsrAB* Sequenzen stammen aus marinen Lebensräumen (31%), gefolgt von Sequenzen aus Süßwasser (24%), Industrie (16%) und Boden (11%). In den meisten größeren phylogenetischen Linien finden sich Vertreter aus vielen unterschiedlichen Habitaten, es gibt allerdings auch einige Ausnahmen, die auf eine Bevorzugung bestimmter Lebensräume hindeuten. Vor allem Sequenzen der DsrAB-Umweltlinien 2, 3 und 4 sind fast ausschließlich marinen Ursprungs, während Sequenzen der deltaproteobakteriellen Familien *Desulfobacteriaceae* und *Desulfonatronumaceae* in erster Linie aus Lebensräumen mit erhöhter Salzkonzentration bzw. erhöhtem pH-Wert stammen. Weiterführende, evolutionäre Analysen der *dsrAB*-Gene brachten unter anderem Hinweise auf möglichen lateralen Gentransfer von *dsrAB* in Phyla, in denen diese Gene erst kürzlich entdeckt wurden, nämlich in Vertretern der *Actinobacteria*, *Aigarchaeota* und *Caldiserica*.

Wir untersuchten den Abbau von organischem Material in anoxischen, arktischen Meeressedimenten, wo SRM eine entscheidende Rolle spielen, indem sie den terminalen Mineralisierungsschritt beim Abbau von Kohlenstoffverbindungen katalysieren. In Inkubationsexperimenten simulierten wir den Eintrag an komplexem organischen Material durch cyanobakterielle Biomasse oder setzten mit Azetat ein typisches Abbauzwischenprodukt zu. Anschließend beobachteten wir den Einfluss dieser Substratzugabe auf die Zusammensetzung der mikrobielle Gemeinschaft durch Pyrosequenzierung von 16S rRNA Gen- und cDNA Amplikons. Die cyanobakterielle Biomasse wurde hauptsächlich zu Azetat, Format und Propionat fermentiert und der Verbrauch von Azetat, Propionat, Butyrat und Valerat wurde selektiv von SRM beeinflusst. Die Dynamik bakterieller 16S rRNA Phylotypen deutete darauf hin, dass die cyanobakterielle Biomasse primär von als *Psychrilyobacter*, *Colwellia*, *Marinifilum* und *Psychromonas* klassifizierte Phylotypen abgebaut wurden, während Azetat hauptsächlich von als *Desulfobacteraceae*, *Desulfobulbaceae* und *Arcobacter* klassifizierten Phylotypen genutzt wurde. Außerdem konnten wir einige mutmaßliche

sulfatreduzierende Phylotypen unter den deltaproteobakteriellen Familien *Desulfobacteraceae* und *Desulfobulbaceae* identifizieren. Die Identifikation dieser Phylotypen liefert die Grundlage, um eine direkte Verbindung zwischen Identität und Funktion von im Kohlenstoffabbau involvierten Bakterien in diesen Sedimenten herzustellen. Nun können spezifischen Sonden designed werden, mit deren Hilfe der Einbau des Substrats durch Kombination von Fluoreszenz-in-situ-Hybridisierung mit Raman-Spektroskopie oder NanoSIMS gezeigt werden kann.

Kalte Meeressedimente beherbergen häufig zusätzlich zur vegetativen mikrobiellen Gemeinschaft auch Sporen thermophiler Bakterien. Wir verwendeten diese scheinbar deplatzierten Organismen, die sich in einem Ruhestadium befinden und nicht der Selektion durch Umwelteinflüsse unterliegen, um selektiv den Beitrag der passiven Verbreitung auf die Biogeographie von Mikroorganismen zu erforschen. Eine globale Biogeographiestudie von thermophilen Endosporen in 81 verschiedenen marinen Sedimenten zeigte, dass diese weit, aber nicht ubiquitär verbreitet sind und identifizierte insgesamt 146 16S rRNA Phylotypen auf Speziesebene. Die ungleichmäßigen räumlichen Verbreitungsmuster dieser Phylotypen lieferten erstmals Beweise für eine eingeschränkte Verbreitung bakterieller Endosporen, welche auf Grund ihrer Eigenschaften – hohe Widerstandsfähigkeit und Langlebigkeit – wesentlich weniger in ihrer Verbreitung eingeschränkt sein dürften als vegetative Zellen. Wir konnten mögliche globale Verbreitungswege von marinen Mikroorganismen aufzeigen, indem wir mit Hilfe von Netzwerkanalysen eine Reihe häufig gleichzeitig auftretender und über große Distanzen verbreiteter Phylotypen identifizieren konnten. Regionen, die relative isoliert von den globalen Meereströmung sind, zeichneten sich durch einen geringeren Artenreichtum an thermophilen Endosporen aus. Das deutet darauf hin, dass die Auswirkung von passiver Verbreitung auf die mikrobielle Biogeographie in marinen Sedimenten von der Konnektivität der lokalen Wassermassen zur globalen Meereszirkulation gesteuert wird. Eine eingehendere Untersuchung von zwei arktischen Regionen, der Inselgruppen Svalbard und der Baffin Bay, zeigte den Einfluss der lokale Hydrographie auf die Verbreitung thermophiler Endosporen.

Die biogeographischen Verbreitungsmuster von vegetativen Zellen, im Gegensatz zu jenen von Endosporen, kommen größtenteils durch Umweltfaktoren, wie beispielsweise Temperatur, zustande. Um die temperaturabhängige Verbreitung und Diversität von Mikroorganismen in marinen Ökosystemen zu verstehen, untersuchten wir die Reaktion von SRM-Gemeinschaften in polaren, gemäßigten und tropischen Meeressedimenten auf Temperaturänderung und konnten zeigen, dass die optimale Temperatur für Sulfatreduktion durch die mittlere Umgebungstemperatur reguliert wurde. Außerdem korrelierte die Zusammensetzung der mikrobiellen Gemeinschaft der mutmaßlichen Sulfatreduzierer mit den Jahresmitteltemperaturen, nicht aber mit der Konzentration des organischen Kohlenstoffs in den Sedimenten oder dem C:N Verhältnis des organischen Materials. Das deutet darauf hin, dass die vorherrschende Umgebungstemperatur die Zusammensetzung der sulfatreduzierenden mikrobiellen Gemeinschaft maßgeblich bestimmt, in dem sie auf jene SRM selektiert, die am besten an die herrschenden Temperaturen angepasst sind und impliziert, dass Temperatur ein wesentlicher, bestimmender Faktor für die Zusammensetzung mikrobieller Gemeinschaften in marinen Sedimenten ist.

Die in dieser Dissertation präsentierte Forschung beinhaltet eine umfassende Analyse der Umweltdiversität und Phylogenie der SRM und anderen *dsrAB*-enthaltenden Organismen, beginnt die Identität von Mitgliedern der mikrobiellen Gemeinschaft in arktischen Meeressedimenten mit ihrer Rolle während des Abbaus organischer Verbindungen zu verknüpfen und bietet neue Perspektiven auf den Einfluss von passiver Verbreitung und Temperatur auf die Zusammensetzung mikrobieller Gemeinschaften im Meeresboden.

Appendix

Acknowledgements

First and foremost I would like to thank Alex Loy. You were a very supportive and well-organized PhD supervisor, which made my PhD an enjoyable experience throughout. I learned a lot from you about doing science and I am particularly grateful for your assistance in writing the publications. You helped me to shape my first writing attempts into something I can now legitimately be proud of. I am also thankful that you let me participate in two research expeditions to Svalbard. Those were an awesome experience, even though I am still deeply envious that you saw the polar bear cubs and I didn't (I'm still crying inside when thinking about it).

A lot of thanks also go to all my collaboration partners. Working with you was delightful! Thanks to Júlia, you took great care of me each time I visited Aarhus, and of course to Bo, you made me feel very welcome there (I still fondly remember crafting Christmas decorations at your place). Casey and Kasper, you are great scientists and it was a pleasure working with you! I would also like to thank the organizers and participants of the 2010 and 2011 Svalbard cruises for the good times up North.

Furthermore, my thanks go to ...

... Karin, you were easily my favorite DoMiE and I am lucky that I can still call you my friend.

... the other members of "our generation" of PhD students, Hanna, Chrissy, and Lena. You are great people and I respect you a lot! It was a pleasure doing my PhD alongside you (at this point also a small shout-out to The Roast and the late Al Dente for providing much needed nourishment).

... my collaborators at the department, David, Micha, Ilias and Thomas. The time and effort you spent on my projects is greatly appreciated!

... my diploma student Martina, for all the help in the lab. You were a model student and I still feel bad that your project was not as successful as you would have deserved.

... Bela and the Daryl for going out of their way to help me with bioinformatic analyses and bioinformatic problems (two things that are synonymous most of the time anyway).

... my fellow sulfur groupies, for the occasional bowling, hiking or beers.

... Martina, for being a super helpful technician and for always trying (against overwhelming odds) to make the DoME a better place.

... all dwellers of the oval office for the nice time that I had down there, even though it was freezing cold, both in winter (open windows) and in summer (air conditioning).

... the inhabitants of the upstairs office, where I peacefully spent my last days at DoME, for making me (almost) regret finishing my thesis.

If you are a DoMiE reading this and you do not find your name in this section, I'm truly sorry, but there were SO MANY of you during my time here. But don't worry, I would like to thank you too – you were all great 😊!

Special thanks to Andrea, for making life outside of work EVEN MORE fun than doing a PhD at DoME!

And finally, I would like to thank my family for their unconditional support of me doing this cryptic work that serves no apparent purpose and doesn't even pay well either.

Curriculum Vitae

Personal information

Albert Leopold Müller

Born on June 21st, 1983 in Feldkirch, Austria



Education

since 10/2009	PhD thesis at the Department of Microbiology and Ecosystem Science, University of Vienna; Supervisor: Alexander Loy; Title: "Microbial biogeography, carbon degradation, and temperature adaptation: Insights from ecological studies of sulfate-reducing microorganisms in marine sediments"
06/2008 – 08/2009	Diploma thesis at the Department of Microbial Ecology, University of Vienna; Supervisor: Matthias Horn; Title: "Optimization of a DNA microarray for global transcription analysis of <i>Protochlamydia amoebophila</i> "
10/2003 – 08/2009	Master in biology (Diplomstudium Biologie) at the University of Vienna with focus on microbiology and genetics (Studienzweig Mikrobiologie und Genetik)
10/2002 – 09/2003	Civilian service at the Department of Radiation Therapy at the Landeskrankenhaus Feldkirch, Austria
09/1994 – 06/2002	Austrian A-levels (Matura), Bundesgymnasium Feldkirch Rebberggasse, Austria

Research stays

11-12/2009 and 07-08/2011	Research stay at the Center of Geomicrobiology, Aarhus University
08-09/2010 and 08-09/2011	Research cruise on R/V Farm to Svalbard fjords and research stay at Kings Bay Marinlaboratorium, Ny Ålesund, Svalbard

Teaching

09/2009, 07/2010, and 07/2011	Organization and tutoring of the practical course "DNA Microarrays – highly parallel molecular analysis of microorganisms" of the Department of Microbial Ecology, University of Vienna
-------------------------------	---

Publications in peer-reviewed journals

Raman microspectroscopy reveals long-term extracellular activity of chlamydiae

Haider S, Wagner M, Schmid MC, Sixt BS, Christian JG, Häcker G, Pichler P, Mechtler K, **Müller A**, Baranyi C, Toenshoff ER, Montanaro J, Horn M.

Molecular Microbiology (2010); 77(3): p. 687-700

Endospores of thermophilic bacteria as tracers of microbial dispersal by ocean currents

Müller AL, de Rezende JR, Hubert C, Kjeldsen KU, Lagkouvardos I, Berry D, Jørgensen BB, Loy A.

The ISME Journal (2014) 8, 1153-1165

Phylogenetic and environmental diversity of DsrAB-type dissimilatory (bi)sulfite reductases

Müller AL, Kjeldsen KU, Rattei T, Pester M, Loy A.

The ISME Journal (2014)

Activity and community structures of sulfate-reducing microorganisms in polar, temperate and tropical marine sediments

Robador A, **Müller AL**, Sawicka JE, Berry D, Huber C, Loy A, Jørgensen BB, Brüchert V.

Submitted to The ISME Journal

Presentations at international conferences

08/2010 Poster at the **13th International Symposium on Microbial Ecology (ISME13)**,
Seattle, WA, USA

Müller AL, de Rezende JR, Huber C, Kjeldsen KU, Wagner M, Jørgensen BB, Loy A.

Tracking heat-lovers in the cold: Towards a global phylogeography of thermophilic sporeforming bacteria in marine sediments

10/2011 Oral presentation at the **8th International Workshop on New Techniques in Microbial Ecology (INTIME-8)**, Slettestrand, Denmark

Müller AL, de Rezende JR, Huber C, Kjeldsen KU, Berry D, Wagner M, Jørgensen BB, Loy A.

Towards a global phylogeography of thermophilic sporeforming bacteria in marine sediments

08/2012 Poster presentation at the **14th International Symposium on Microbial Ecology (ISME14)**, Copenhagen, Denmark

Müller AL, de Rezende JR, Hubert C, Kjeldsen KU, Berry D, Wagner M, Jørgensen BB, Loy A.

Phylogeography of thermophilic bacterial spores in marine sediments: Bioindicators for dispersal in the oceans

10/2013 Oral presentation at the **9th International Workshop on New Techniques in Microbial Ecology (INTIME-9)**, Aarhus, Denmark

Müller AL, de Rezende JR, Hubert C, Kjeldsen KU, Lagkouvardos I, Berry D, Jørgensen BB, Loy A.

Endospores of thermophilic bacteria as tracers of microbial dispersal by ocean currents

Awards and grants

03/2011	Award for the best oral presentation given by a PhD student at the Science Day of the Faculty Center of Ecology, University of Vienna
01/2014	PhD Completion Grant of the Faculty of Life Sciences, University of Vienna